THE BLUE CRAB

Callinectes sapidus

Edited by

Victor S. Kennedy

and

L. Eugene Cronin

A Maryland Sea Grant Book
College Park, Maryland

Published by the Maryland Sea Grant College.

Publication of this book is supported by grant #NA06OAR4171042 from the National Oceanic and Atmospheric Administration to the Maryland Sea Grant College.

Printed in China through Four Colour Imports, Ltd., Louisville, Kentucky

Book and cover design by Sandy Rodgers.
Cover art by Sandy Rodgers.
Photograph on page xxvi, McGaw and Reiber (2002). For description of image, see page 174.

Maryland Sea Grant College
Publication UM-SG-TS-2007-01

Library of Congress Cataloging-in-Publication Data

The blue crab : Callinectes sapidus / edited by Victor S. Kennedy, L. Eugene Cronin.
p. cm.
Includes bibliographical references and index.
ISBN-13: 978-0-943676-67-8 (alk. paper)
ISBN-10: 0-943676-67-3 (alk. paper)
1. Blue crab. I. Kennedy, Victor S. II. Cronin, L. Eugene (Lewis Eugene), 1917-
QL444.M33B68 2007
595.3'86—dc22 2006039259

16 chapters

For information on Maryland Sea Grant books, write:

Maryland Sea Grant College
University of Maryland
4321 Hartwick Road, Suite 300
College Park, Maryland 20740

or visit our web site:

www.mdsg.umd.edu

Chapter 4

Muscles and Neurons

C.K. GOVIND

INTRODUCTION

Crustaceans have provided several premier model preparations for the study of key concepts in neuroscience, specifically in the areas of synaptic transmission, sensory transduction, and muscle fiber typing. Their attractiveness for such research is the relative simplicity of the nervous system compared to vertebrates, as crustaceans have considerably fewer neurons, many of which are large and individually identifiable. The nerves and muscles are also accessible to experimentation. A few crustaceans, such as lobsters and crabs, are commercially important and therefore readily available and attractive for study. The blue crab, *Callinectes sapidus* Rathbun, has all these attributes as well as some unique adaptations, including its euryhaline life, swimming behavior, and courtship behavior.

Driven by these attributes, neuroscience research in blue crabs is marked by scattered oases of intense study in an otherwise largely unexplored desert. A conceptual framework in which to review these disparate studies is to focus on the neural control of behavior. Within this framework the two major and readily identifiable themes would be the muscles and neurons. Such a thematic subdivision is also useful in pointing out obvious gaps in our knowledge and directions for future research.

MUSCLES

Organization

Movements of the appendages are brought about by striated muscles that originate and insert on specific parts of the exoskeleton. They occur in functional groups that usually operate as antagonists. This is also the case with movements of the viscera and especially of the foregut (Fig. 1). Muscles of the hindgut and heart and its major vessels have a slightly different organization, lacking distinct insertion points for movement, but organized into circular bands that serve to alter the diameter of these structures.

Blue crab muscle has a basic structure similar to that of striated muscle in other crustaceans (Atwood 1973; Chapple 1982). The two major structural proteins, myosin and actin, occur as filaments that are grouped into bundles of various diameters termed myofibrils. Within the myofibrils the filaments occur in a highly organized linear manner that repeats itself and is symbolized by the sarcomere (Fig. 2) (Jahromi and Govind 1976). In longitudinal view the sarcomere is delimited by adjacent Z-lines. The thin actin filaments project from the Z-line towards the middle of the sarcomere and surround the centrally-located thick myosin filaments. This gives rise to a central dark band (A-band) comprised of the

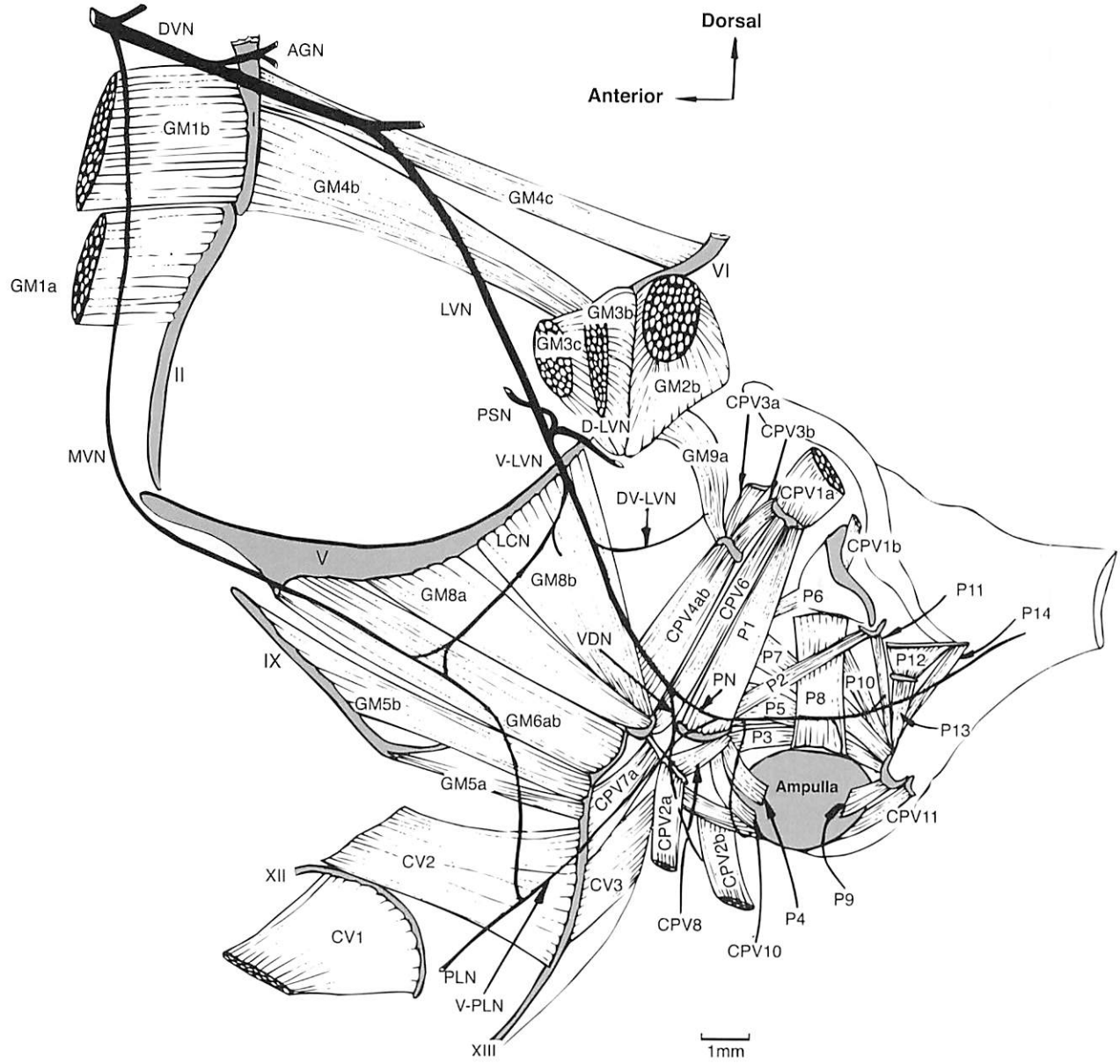

Figure 1. Lateral view of the left half of the blue crab stomach showing the muscles, principal nerves (black lines), and ossicles (grey). The muscles are divisible into intrinsic muscles with both ends attached to stomach ossicles and extrinsic muscles with one end attached to the ossicles and the other to the exoskeleton (shown here as the cut end). The muscle nomenclature follows that given in Table 1, which deals only with the intrinsic muscles. The principal nerve branches are as follows: anterior gastric [AGN]; dorsal ventricular [DVN]; dorsal branch of lateral ventricular [D-LVN]; dorsal branch of ventral lateral ventricular [DV-LVN]; lateral cardiac [LCN]; lateral ventricular [LVN]; median ventricular [MVN]; postero-lateral [PLN]; posterior stomach [PSN]; pyloric [PN]; ventral dilator [VDN]; ventral branch of lateral ventricular [V-LVN]; ventral branch of postero-lateral [V-PLN]. The stomach ossicles are numbered as follows: I mesocardiac; II pterocardiac; V zygocardiac; VI propyloric; IX prepectineal; XII posterior lateral cardiac; XIII inferior lateral cardiac. From Govind et al. (1975).

overlapping actin and myosin filaments and on either side a light band (I-band) with only actin filaments. The overlapping arrangement of thin and thick filaments in the A-band shows each thick filament surrounded by several thin filaments. The middle of the A-band where only myosin filaments prevail is not as dark as the rest of the A-band and is referred to as the H-band. In the middle of the H-band a dark M-line is visible where the myosin filaments attach to each other.

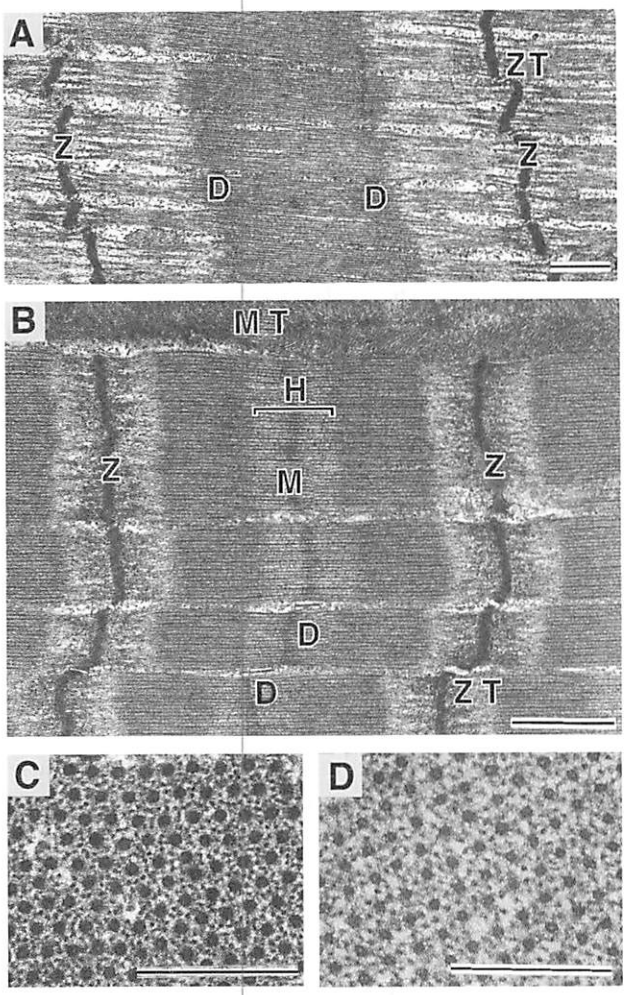

Figure 2. Fine structure of fast and slow myofibrils from the blue crab gastric mill muscles. (A) gm8a. (B) and (D) gm8b. (C) gm9a. Slow myofibrils have long sarcomeres, thick wavy Z-lines (A), and a high thin-to-thick filament ratio (C). Fast myofibrils have short sarcomeres, narrow straight Z-lines (B), and a low thin-to-thick filament ratio (D). The longitudinal views of sarcomeres in (A) and (B) show diads [D], H-band [H], M-line [M]), mitochondria [MT], Z-line [Z], Z-line tubules [ZT]. Bars: 2 μm in (A), (B); 0.2 μm in (C), (D). From Jahromi and Govind (1976).

Surrounding each myofibril in the form of a collar is a fenestrated system of tubules forming the sarcoplasmic reticulum. At points along the myofibril, elements of the transverse tubular system are found, closely juxtaposed to the sarcoplasmic reticulum and thus forming diads or triads (Fig. 2). The myofibrils are congregated into a fiber that also contains granular sarcoplasm, mitochondria, and nuclei, as well as a delimiting sheath of connective tissue. Muscle fibers, however, subdivide and branch extensively and are electrically connected, forming functional units of several fibers (Govind et al. 1975). In rare instances the Z-line appears to be split with an interspersed sarcomere, suggesting a method for adding sarcomeres in the maxilliped flagellum abductor muscle (Jahromi and Charlton 1979).

Differentiation of Fiber Types

Speed of contraction varies widely in crustacean muscle fibers and forms the basis for categorization into fast and slow types. Fast fibers respond to depolarization with a quick rise to peak tension where tension is maintained for the duration of the stimulus. Slow fibers, on the other hand, show a continual increase in tension for the duration of the stimulus. These two responses represent the two ends of a continuous spectrum and are both seen in blue crabs. The fast type response is seen in the maxilliped flagellum abductor muscle (Charlton 1971) and the slow type in the stomach muscles (Govind et al. 1975). Among the slow-type stomach muscles, the contractile behavior of fibers in the gastric mill muscles reveals that tension develops relatively slowly and does not follow rapid changes in the membrane potential (Fig. 3) (Jahromi and Govind 1976). Some fibers are slower than others, judging from differences in the rise and relaxation times (compare examples in Fig. 3). Electrical interconnections amongst fibers in the various muscles are also observed during tension recordings. Not only does the individual fiber that is being depolarized contract, but usually two to three

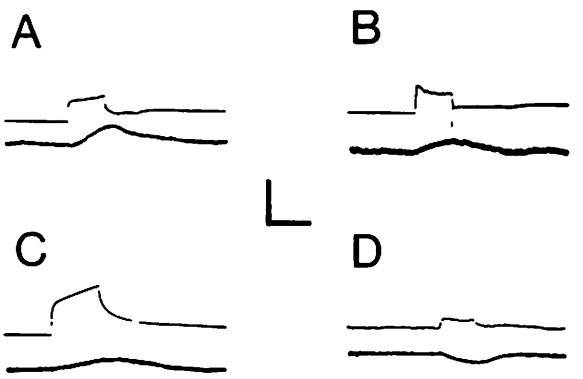

Figure 3. Contractile responses of the single muscle fibers (lower traces) to depolarizing pulses (upper traces) from blue crab gastric mill muscles. (A) gm8b. (B) gm9a. (C) gm5. (D) gm5a. Tension does not follow the rapid depolarizing changes but develops and relaxes more slowly. Horizontal bar: upper traces – 20 mV; lower traces – 30 mg in (A), (C), (D) and 16 mg in (B). Vertical bar: 1 sec in (A), (B), (D) and 2 sec in (C). (A) from Jahromi and Govind (1976).

adjacent fibers contract as well. Moreover, the contractile force developed by these muscle fibers is largely independent of temperature (Blundon 1989).

The contractile behavior of crustacean muscle fibers is regulated by several intrinsic factors such as sarcomere length, number of thin filaments surrounding a thick one, and activity of myofibrillar ATPase and mitochondrial NADH-diaphorase enzymes. Among the intrinsic factors governing contractile behavior, sarcomere length is perhaps the most influential in guiding speed of contraction. Other factors being equal, a fiber with more sarcomeres per unit length will contract more rapidly than one with fewer sarcomeres (Jahromi and Atwood 1969; Josephson 1975). Vertebrate muscles have fairly uniform sarcomere lengths of 2 to 4 μm, whereas invertebrates and most notably crustaceans have a wide range of sarcomere lengths ranging from 2 to 20 μm. This diversity is unparalleled in the animal kingdom (Hoyle 1983). The wide range in sarcomere length permits an equally wide range in contractile speed, but for simplicity, crustacean sarcomeres are broadly classified into fast (<6 μm) and slow (>6 μm) types (Govind and Atwood 1982; Govind 1992). Accordingly, sarcomeres of blue crab muscles ranging from 2 to 15 μm, thus indicating a wide continuum, are broadly divisible into fast and slow types.

The assemblage of myofilaments within a myofibril has a characteristic pattern: a thick filament is surrounded by several thin filaments and in crustacean muscle there are two basic patterns reflecting fast and slow fiber types (Govind and Atwood 1982). The thick filament is surrounded by 6 thin filaments in fast fibers and by 10 to 12 in slow fibers. Both patterns are seen in the stomach muscles of blue crabs (Fig. 2), where the fast pattern is associated with shorter sarcomeres and the slow pattern with longer sarcomeres, in keeping with the typical crustacean fast and slow fiber types.

Differentiation of muscle fibers is also seen in the activity levels of their myofibrillar ATPase enzyme. Histochemical detection of this enzyme reveals much more intense staining in uniformly fast muscle compared to slow muscle, as in the deep and superficial abdominal flexor muscles of crayfish *Procambarus clarkii* and lobster *Homarus americanus* (Ogonowski and Lang 1979). The difference in staining intensity reflects the 2- to 3-fold difference in their activity profiles (Hajek et al. 1973). Both types of histochemically differentiated fibers are found in blue crab muscles. The exopodite abductor muscle of the maxilliped flagellum shows uniformly intense staining for ATPase, denoting fast muscle (Silverman and Charlton 1980) that is in keeping with the short 2 to 3 μm sarcomere lengths (Jahromi and Charlton 1979). On the other hand, muscles at the base of the swimming paddle (Fig. 4) reveal distinct differences in ATPase staining (Tse et al. 1983). For instance, one of the two branches of the dual-branched levator muscle shows uniformly intense staining indicative of fast fibers whereas the other branch shows intense staining around the periphery and much less intense staining indicative of slow fibers in the core (Fig. 5). However, sarcomere lengths between 4 to 5 μm, indicative of fast fibers, are found across the levator muscle, including those regions that stain weakly for ATPase activity, suggesting independent expression of these two properties.

Mitochondria are intrinsic to muscle fibers and serve as powerhouses for fueling contraction. Their

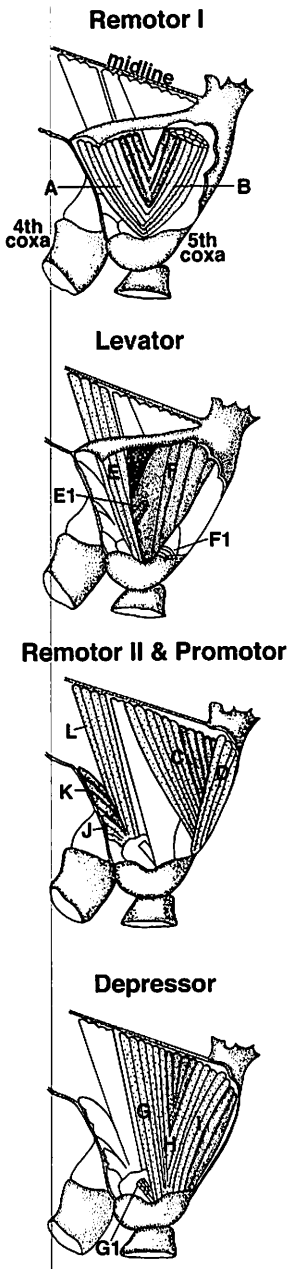

Figure 4. Basal muscles of the swimming paddle of blue crab showing the four major groups in successive stages of dissection from the outermost to the innermost (midline) layers. Branches composing each of the muscle groups are denoted alphabetically and are as follows: [A, B] for remotor I; [E, E1, F, F1] for levator; [C, D] for remotor II; [J, K, L] for promotor; [G, G1, H, I] for depressor. In freshly dissected preparations, muscles appear colored as white, light pink, and dark pink and these are denoted by light, medium, and heavy stippling. From Tse et al. (1983).

density varies, and histochemical staining for the mitochondrial enzyme NADH-diaphorase provides a measure of this variation. Fast fibers classified according to ATPase activity in the swimming muscles show a relatively low density of mitochondria that are restricted to the periphery while slow fibers show a much higher density of mitochondria that criss-cross the cross-sectional area of the fiber (Fig. 5) (Tse et al. 1983). An exception to this pattern is the fast flagellum abductor muscle of the maxilliped that has a thick cortex of mitochondria surrounding each fiber, making it a highly oxidative muscle (Silverman and Charlton 1980).

In summary, blue crab muscle is differentiated into fast and slow fiber types on a structural basis (sarcomere length and actin:myosin ratio). However, some structurally fast fibers may express differential enzyme activities for ATPase and NADH-diaphorase reminiscent of fast and slow fibers, indicating that not all muscle properties are locked into these categories. Such independence in phenotype requires further study, as does biochemical analysis of the structural and regulatory proteins and their isoforms involved in assembling fiber types such as those for lobster muscles (Mykles 1985).

Fiber Composition of Muscles

Muscles in the foregut (Table 1) and appendages (Table 2), based on their sarcomere lengths, are either fast or slow. Among these, the claw closer muscles and the swimming paddle muscles deserve further consideration because of their large size and functional prominence.

The paired chelipeds of blue crabs are unusual in that they show a marked morphological bilateral asymmetry consisting of a large major (crusher) chela with molar-like dentition, and a relatively smaller minor (cutter) chela with incisor-like dentition (Fig. 6). In most blue crabs the crusher appears on the right side and the cutter on the left side (Hamilton et al. 1976). The closing behavior of the dactyl during feeding is correspondingly asymmetric; the crusher cracks mollusc shells while the cutter tears at the exposed flesh (Hamilton 1976; Blundon and Kennedy 1982). This behavior creates the dis-

tinct impression of the crusher as a slow-acting but very powerful claw and the cutter as a relatively faster-acting more agile claw. Differences in closing speed are due, in part, to the fact that motoneurons to the cutter are more effective at a lower firing frequency than their crusher homologs (Fig. 6) (Govind and Blundon 1985). Twitch-type contractions are seen only in the cutter claw whereas tonic contractions are seen in cutter and crusher claws. Differences in closing strength are due, in part, to the larger size and greater mechanical advantage of the crusher compared to the cutter. Surprisingly, the

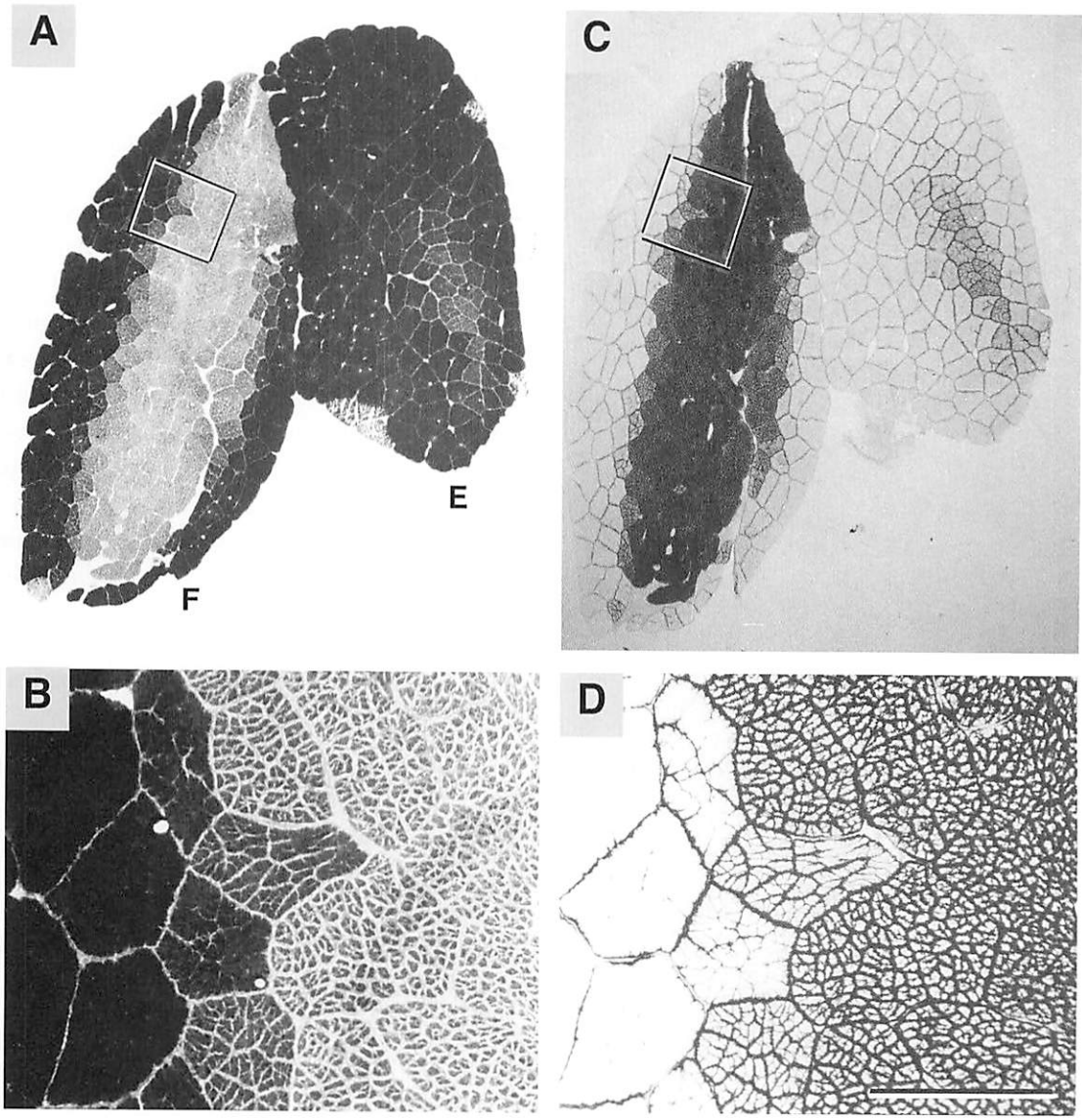

Figure 5. Cross-sections of the basal levator muscle of the swimming paddle of blue crab stained for myofibrillar ATPase. (A) Shows fast (dark staining) and slow (light staining) components in bundle [F] and purely fast in bundle [E]. (C) An adjacent section stained for NADH-diaphorase showing mitochondrial density that is high (dark staining) and low (light staining) in the core and periphery, respectively, of bundle [F] and uniformly low in muscle bundle [E]. (B) and (D) High power views of the boxed-in areas in (A) and (C) show not only the two distinct intensities of staining but also an intermediate level. Bar in (D): 1 mm for (A), (C); 250 μm for (B), (D). From Tse et al. (1983).

Table 1. Structural features of the intrinsic stomach muscles in blue crabs, their motoneuron supply, and physiological features of their neuromuscular synapses. Muscles are named according to regions of the stomach (see Fig. 1). Sharing of single excitor motoneurons is indicated by letters of the alphabet. Facilitation of the excitatory post-synaptic potential (EPSP) is a ratio of its amplitude at 10 Hz compared to 1 Hz. From Govind et al. (1975); Jahromi and Govind (1976); Atwood et al. (1977, 1978).

Name	Muscle		Motoneuron		Neuromuscular synapse	
	Sarcomere length (μm)	Thin: thick filaments	Inhibitor	Excitor (shared)	EPSP (mv)	Facilitation (10/1 Hz)
Gastric mill (gm)						
gm4b	6	-	-	1	5-15	1.1
gm4c	8	-	-	1	5	1.8
gm5a	4	6:1	-	1 (a)	5-9	2.1
gm5b	8	10-12:1	-	1 (b)	6-26	1.3
gm6ab	9	10-12:1	-	1 (b)	6-15	1.9
gm8a	8	10-12:1	-	1 (b)	6-18	2.3
gm8b	4	6:1	-	1 (c)	7-12	2.8
gm9a	5	12:1	-	1 (c)	7-20	2.1
Ventral cardiac (cv)						
cv2	4	6:1	-	1 (a)	18-33	1.1
cv3	3	6:1	-	1 (a)	14-22	1.5
Cardio-pyloric valve (cpv)						
cpv3a	10	-	-	1 (d)	0.4	2.0
cpv3b	4	-	-	1 (d)	2	4.5
cpv4ab	5	-	-	1 (d)	5.6	3.9
cpv6	5	-	-	1 (d)	1.2	4.5
cpv7a	6	-	-	1 (a)	2-10	1.5
cpv8	5	-	-	1	2	4.4
cpv10	5	-	-	2 (1e)	-	-
cpv11	5	-	-	2 (1e)	-	-
Pyloric (p)						
p1	4	-	-	1 (d)	0.7	12.6
p2	9	-	-	3 (1f)	-	-
p3	4	-	-	3 (1g)	-	-
p4	4	-	-	1	-	-
p5	5	-	-	-	-	-
p6	6	-	-	1	-	-
p7	7	-	-	2 (g)	-	-
p8	4	-	-	3 (1f)	-	-
p9	5	-	-	2 (1e)	-	-
p10	6	-	-	1 (f)	2.5	-
p11	8	12:1	1	1 (h)	0.5	5
p12	8	12:1	1	1 (h)	3	-
p13	8	12:1	1	1 (h)	33	0.9
p14	8	12:1	1	2 (1h)	-	-

Table 2. Sarcomere lengths and the number and type of motoneurons innervating muscles in the appendages of blue crabs.

Appendage and muscle	Sarcomere length (μm)	Excitor	Inhibitor	Reference
Antennule				
m26	-	2 (fast, slow)	-	Roye 1994
m27	-	1	-	Roye 1994
m28	-	1	-	Roye 1994
m30	-	1	-	Roye 1994
Maxilliped				
flagellum abductor	2-3	2 (fast)	-	Charlton 1971; Jahromi and Charlton 1979
Pereopods				
claw closer	7-14	2 (fast, slow)	1 (common)	Govind and Blundon 1985
accessory flexor:				
proximal head	-	1	1 (common)	Govind and Wiens 1985
distal head	7-10	4	1 (common)	Govind et al. 1978; Govind and Wiens 1985; Wiens and Govind 1985
swimming paddle:				
remotor	-	2	2	White and Spirito 1973
promotor	4-5	2-7	1	Tse et al. 1983; White and Spirito 1973; Blight and Llinas 1980
levator	-	1	1	White and Spirito 1973
depressor	-	2	1	White and Spirito 1973
opener	6-12	1	1	Honsa and Govind 2002

fiber composition of the paired closer muscles is not asymmetric; both muscles are uniformly slow, with sarcomere lengths ranging from 6 to 15 μm (Fig. 6). Moreover, the frequency distribution of the sarcomere lengths is also similar between the paired claws, as are the activities of their myofibrillar ATPase and mitochondrial NADH-diaphorase enzymes. This similarity in fiber composition of the paired muscles is present in the usual cheliped configuration of right crusher-left cutter, as well as in the unusual configurations of right cutter-left crusher or right cutter-left cutter. These unusual configurations may arise because of a tendency to regenerate a cutter following loss of either claw, and transformation of the existing cutter into a crusher (Hamilton et al. 1976). A similar mechanism for reversing claw bilateral asymmetry exists in snapping shrimps where loss of the major snapper claw triggers transformation of the existing minor pincer into a snapper and regeneration of a new pincer at the old snapper site (Young et al. 1994; Read and Govind 1997a, b).

Modification of the fifth pereopods into swim-

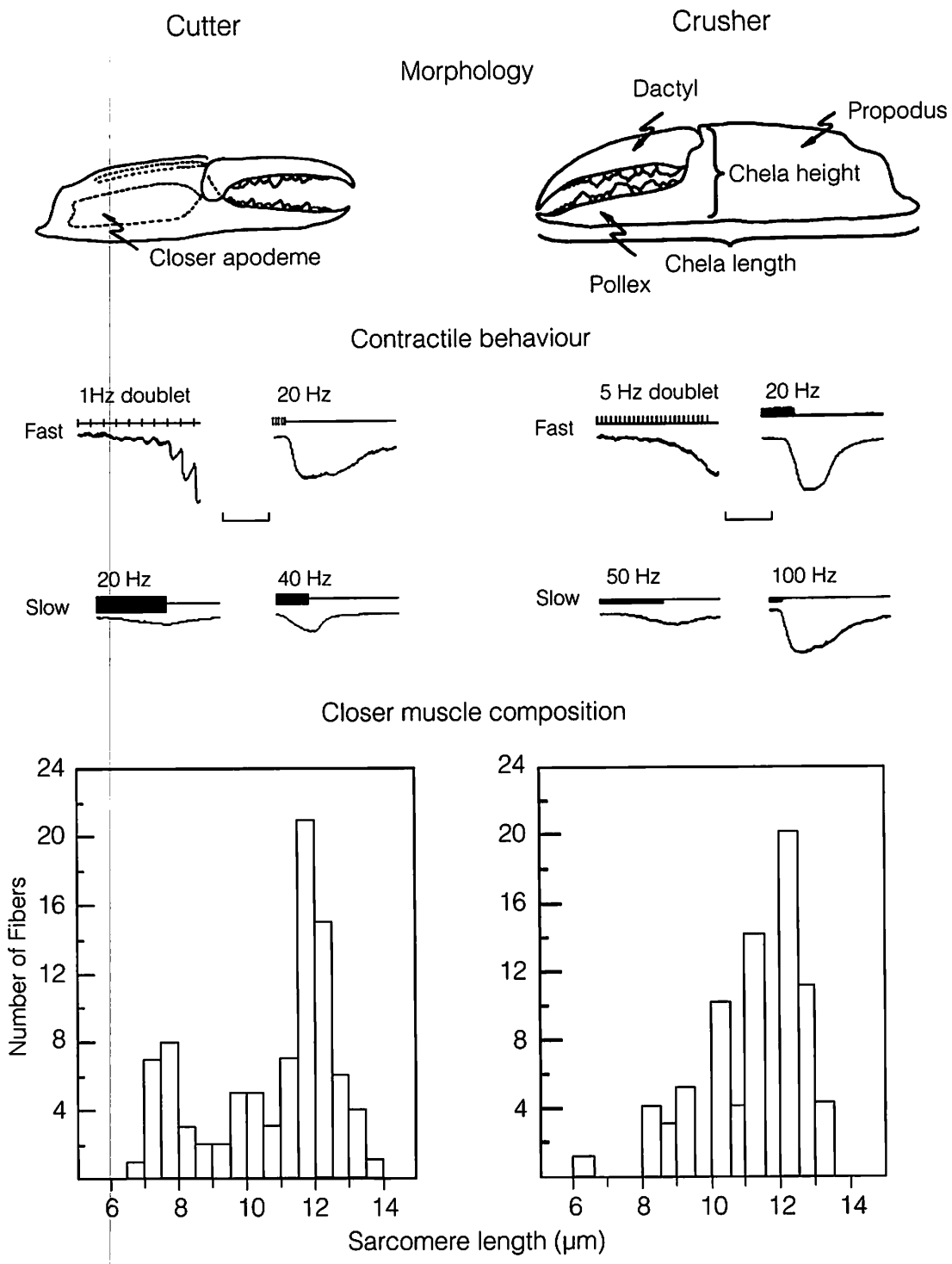

Figure 6. Bilateral asymmetry of the paired chelae in blue crabs. In external morphology, the cutter is smaller, slender, and has incisor-like dentition compared to the crusher which is larger, stouter, and has molar-like dentition. The contractile behavior of the closer muscle is monitored by recording movements of the dactyl (lower trace) in response to varying frequencies of stimulation of either fast or slow axons (upper trace). Both axons evoke contraction more readily and rapidly and with fewer stimuli in the cutter claw compared to the crusher claw. The fiber composition of the closer muscle based on sarcomere length is similar between cutter and crusher claws, with a wide range of slow (>6 μm sarcomere lengths) fibers in both claws; 90 fibers were sampled in each muscle. Bars: Cutter, fast 0.2 sec, slow 0.5 sec; Crusher, fast 0.5 sec, slow 0.2 sec. From Govind and Blundon (1985).

ming paddles in blue crabs has resulted in the evolution of extremely hypertrophied basal muscles, each consisting of two to four distinct bundles with a common insertion but separate origins (Fig. 4) (Cochran 1935; Hartnoll 1971; White and Spirito 1973). Up and down movement of the paddle is brought about by a pair of antagonistic muscles, the depressor and levator, which generate the power and return strokes, respectively. Sculling action of the paddle during the up and down motion is effected by a second pair of antagonistic muscles, the remotor and promotor. The swimming muscles have fast and slow fibers as shown by enzyme histochemical detection of myofibrillar ATPase activity (Tse et al. 1983; Houlihan et al. 1985). Discrete branches in each muscle group are either homogenously fast, or a regionalized mixture of fast and slow, either with fast fibers on the periphery and slow in the core (Fig. 5), or adjacent to each other. Corresponding differentiation in sarcomere lengths, however, is not obvious, as 4 to 7 μm sarcomere lengths are seen in both types of branches. Based on limited evidence, sarcomere length and ATPase appear to be independently expressed in these basal muscles. On the other hand, expression of mitochondrial density is closely linked to myofibrillar ATPase activity. Thus fast and slow fibers, based on ATPase activity, show weak and intense staining for mitochondrial NADH-diaphorase, denoting respectively low and high densities of mitochondria (Fig. 5). This high level of differentiation subserves the muscles' role in swimming, both sideways and backwards (Spirito 1972), and in courtship display by male blue crabs (Wood and Derby 1995).

MOTONEURONS

Organization

Crustacean muscles are supplied by both excitatory and inhibitory motoneurons (Wiersma 1961; Atwood 1976; Govind and Atwood 1982). Most excitatory neurons have glutamate as their neurotransmitter, although a few contain acetylcholine; both transmitters depolarize the muscle membrane and elicit contraction (Atwood 1976). Inhibitory neurons with gamma-aminobutyric acid (GABA) as their neurotransmitter serve to stabilize or hyperpolarize the muscle membrane and prevent contraction. This general classification of motoneurons would apply to blue crabs as well, although there are relatively few confirmatory reports. For instance, motoneurons to the intrinsic muscles in the blue crab stomach are glutamatergic, while those to the extrinsic muscles are cholinergic based on the sensitivity of muscle fibers to applied neurotransmitters (Atwood et al. 1977; Lingle 1980). There are also relatively few data on the morphology and physiology of blue crab motoneurons except those to the muscles of the antennule (Fig. 7) (Roye 1989, 1994; Roye and Bashor 1991) and swimming paddle (Blight and Llinas 1980). Motoneuron cell bodies are located in the ganglia where they give rise to a single primary neurite from which arise higher order branches including dendrites to form the neuropilar segment (Fig. 8). At its distal end, the neurite leaves the ganglion as an axon that travels to the target muscle. Synaptic input from sensory neurons and interneurons activates the integrating segment of the neurite and generates action potentials that travel in the axon to the target muscle (Fig. 7). Among the antennular motoneurons, apart from activating individual motoneurons or a functional group, there is also evidence for interaction between neurons with different functions, such as reciprocal inhibition between flick and withdrawal neurons (Fig. 7).

In the swimming paddle promotor muscle, four motoneurons are most likely fired by synaptic connections to the stretch receptor neuron (Fig. 8) (Blight and Llinas 1980). Current pulses in this sensory fiber gives rise to excitatory post-synaptic potentials (EPSPs) in the motoneurons which at threshold give rise to action potentials. Those cells with larger somata and axons are likely involved in more phasic activity such as swimming, whereas the smaller cells are involved with more tonic activity such as maintaining posture. Electrical coupling among dendrites of some motoneurons may permit them to operate as a group. There may also be differences in the spike-generating mechanism among this group of motoneurons, the phasic ones having a higher threshold for spiking than the tonic ones,

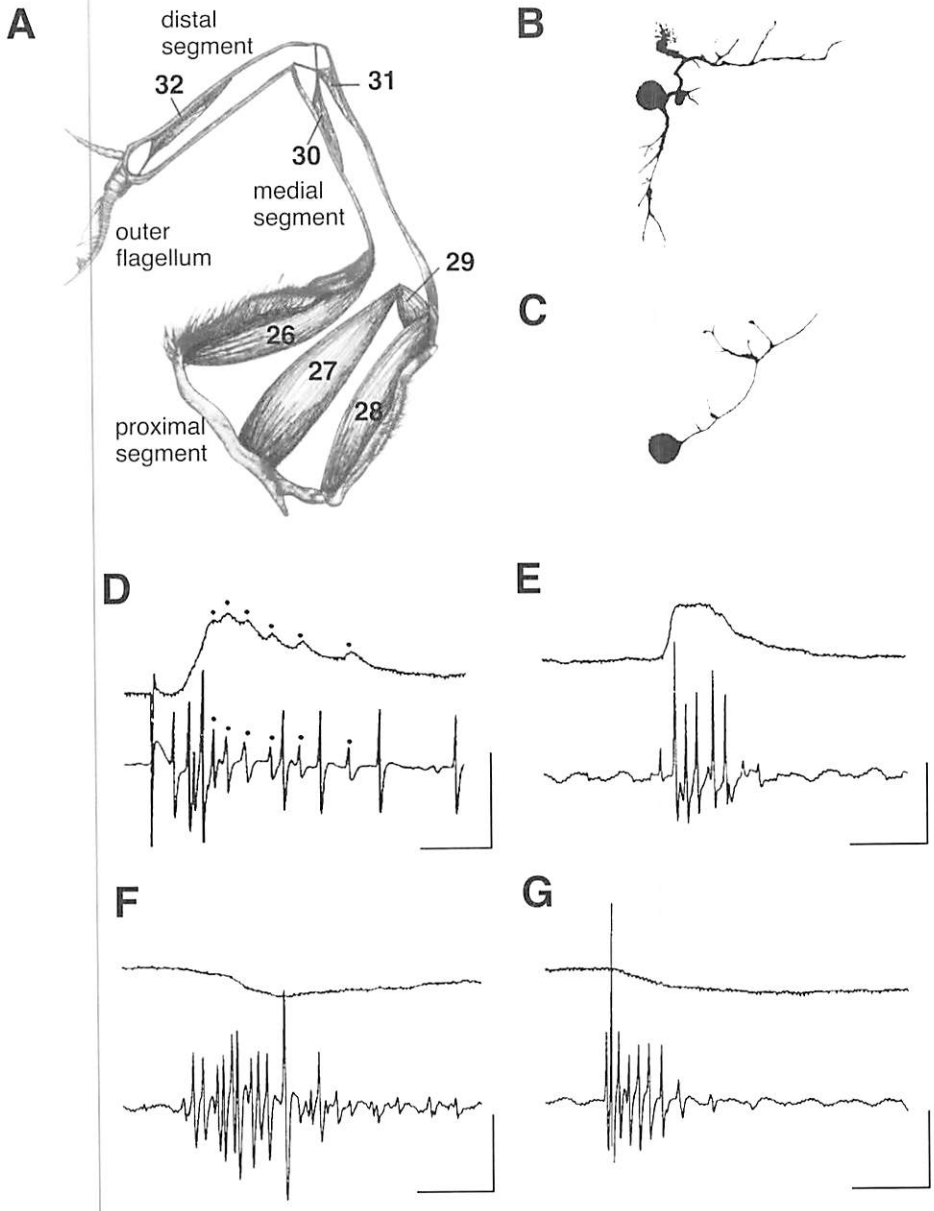

Figure 7. (A) Muscles in the segmented antennule of the blue crab. Four muscles [26 to 29] in the proximal segment control movement of the medial segment and are innervated by at least 5 motoneurons. The muscle pair [30, 31] in the medial segment control movements of the distal segment, and a single muscle [32] controls the outer flagellum. (B) Morphology of one of two motoneurons to muscle [26] showing a prominent soma and extensive branching of secondary and tertiary neurites. (C) Morphology of a motoneuron to muscle [31] showing a prominent soma with a primary neurite that gives rise to a number of secondary neurites before exiting as an axon. (D) Identification of motoneuron to muscle [26] in the cerebral ganglion seen by stimulating sensory nerve IIIc and recording intracellular junctional potentials in its neurite (dots in upper trace) with corresponding extracellular spikes in its axon in nerve 1A (dots in lower trace). (E) Spontaneous depolarization in neurite of antennular motoneuron to muscle [31] (upper trace) with corresponding burst of spikes in motor nerve 1A (lower trace); such spontaneity is typical of the repetitive flicking of the distal segment and outer flagellum in the intact animal. (F) and (G) Evidence for reciprocal inhibition between flicking and withdrawal motoneurons, respectively, as seen by sustained hyperpolarization in neurite of a flick or withdrawal motoneuron (upper traces) during firing of a withdrawal or flick axon in the motor nerve (lower traces). Vertical bars: 5 mV in (D); 10 mV in (E), (F), (G). Horizontal bars: 10 msec. From Roye and Bashor (1991); Roye (1994).

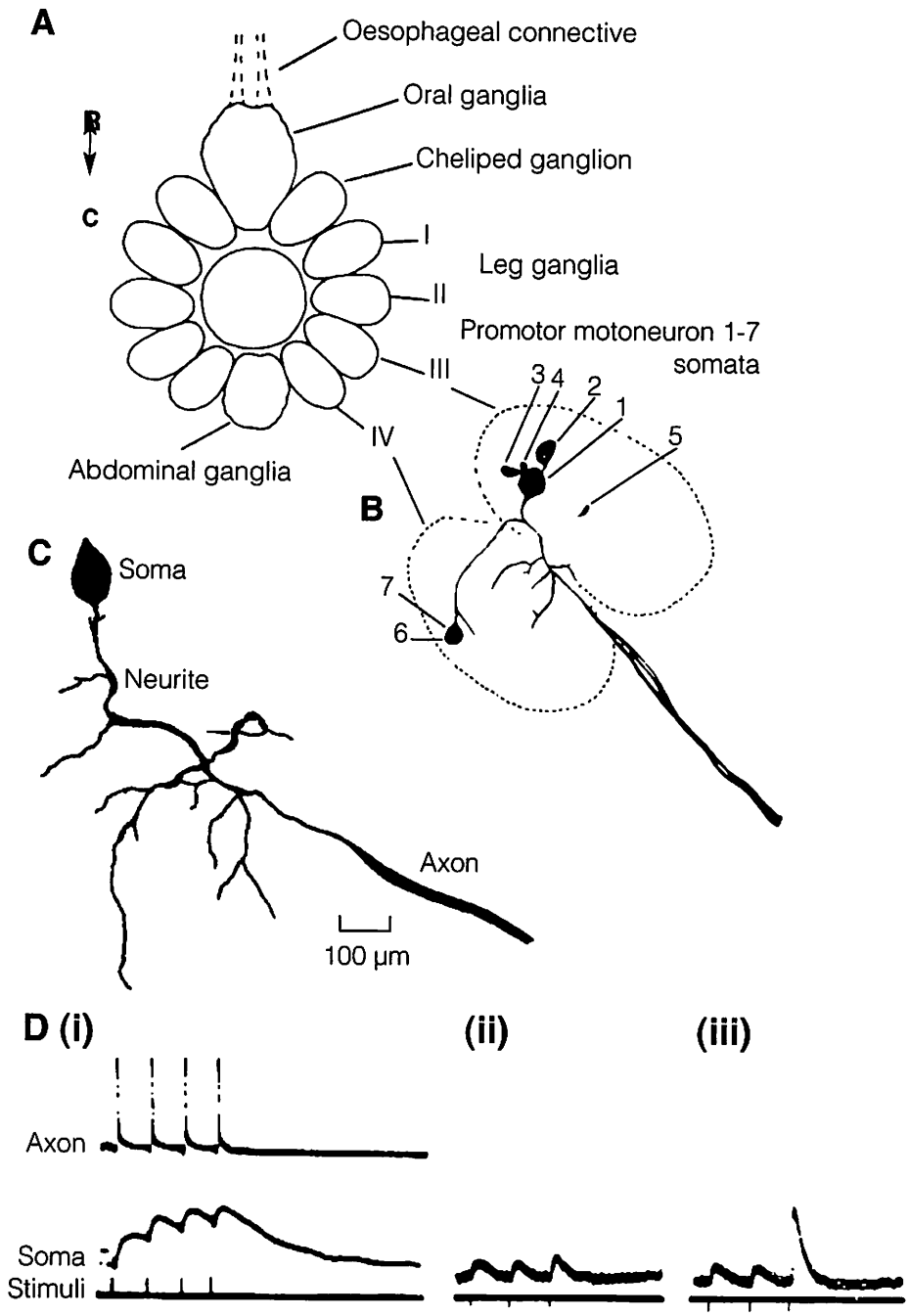

Figure 8. Motoneurons of the levator swimming muscle in blue crab. (A) The central nervous system comprises the cerebral ganglion (not shown) connected via the oesophageal connective to a fused ventral nerve cord in which the segmentally arranged rostral to caudal [R-C] neuropils are distinct. These consist of the oral ganglia, cheliped ganglia, walking leg ganglia [I, II, III, IV], and abdominal ganglia. (B) The seven levator motoneuron somata [1-7] located in the fused thoracic ganglia have their neurites in the neuropil of walking legs [III] and [IV]. (C) Morphology of one of these levator motoneurons with a single primary neurite arising from its soma and giving rise to other neurites before exiting as a single axon. (D) (i) Stimulation of the promotor nerve gives antidromic spikes in the axon and summating potentials in the soma, and with increasing stimulus intensity (ii, iii) shows two sizes of potentials in the soma. From Blight and Llinas (1980).

ensuring responsiveness to a wide range of movements of the receptor muscle.

Firing of individual motoneurons ranges from single spikes to bursts that vary in duration and degree of patterning. For instance, promotor and remotor motoneurons fire in reciprocal bursts to bring about spontaneous movements of the proximal segment of the antennule (Roye 1979). More complex firing patterns characterize motoneurons to the swimming paddle muscles to effect sideways and backward swimming and courtship display in males (Wood and Derby 1995).

The cardiac ganglion situated in the heart is located outside the nervous system, with four to five small (20 μm) pacemaker cells and five large (80 μm) follower cells (Hawkins and Howse 1978). Nerve terminals in the neuropil show synaptic contacts and have several vesicle types, including the conventional clear, small (30-60 nm) round or elliptical vesicles that are indicative of excitatory and inhibitory connections. Larger vesicles (70-100 nm) indicative of neuromodulatory action, either clear or dense, are also present.

Although details of central synaptic connections are sketchy due to the technically challenging task of recording from the neuropil, more is known about neuromuscular synaptic connections of the motoneuron because recordings from the muscle fibers are much easier to make. In blue crabs, the fine structure of motor nerve terminals has been extensively examined in muscles of the stomach (Govind and Lingle 1987) and the swimming paddle (Honsa and Govind 2002). The primary axon and its branches are encased in glial tissue, supported internally by neurotubules, and populated with mitochondria. Individual motor axons branch extensively over the muscle and over individual muscle fibers. From the muscle surface, the axonal branches dip below the muscle fiber connective tissue and continue branching as preterminal or subterminal axons still sheathed in glial cells (Fig. 9). When these branches contact muscle membrane, they lose their glial covering and form nerve terminals that are often varicose in form. Synaptic contacts with the muscle membrane in the area of muscle granular sarcoplasm are made intermittently along the length of these nerve terminals. Mitochondria and glycogen granules continue to populate the synaptic terminals as do at least two classes of vesicles: small clear synaptic vesicles and larger dense or dense-core vesicles. The final endings of nerve terminals are synaptic contacts.

The small clear synaptic vesicles are the predominant class and assume a characteristic shape when treated with aldehyde fixatives: round for excitor axons (Fig. 9) and elliptical for inhibitor axons (Tisdale and Nakajima 1976). The defining feature of nerve terminals is synaptic contacts that are recognized by densely-stained presynaptic and postsynaptic membranes, aligned in a very regular manner and separated by a synaptic gap (Fig. 9). Often there is a filamentous substructure within the synaptic gap. Synapses tend to be delimited by glial fingers that insinuate themselves in the muscle granular sarcoplasm.

Dense bars occur on the presynaptic membrane (Fig. 9). These bars are T-shaped structures with synaptic vesicles aligned on either side under the transverse arms and in contact with the presynaptic membrane. This gives the impression that dense bars are docking sites for synaptic vesicles poised for release. The impression is confirmed with the observation of Ω-shaped figures denoting exocytosis where vesicles have fused with the presynaptic membrane along the dense bar. Clearly, transmitter release occurs preferentially along these dense bars or active zones.

Apart from being more densely stained, the postsynaptic membrane appears relatively unspecialized (Fig. 9). Occasionally, the muscle sarcoplasm immediately adjacent to this membrane has a fine granular appearance and stains more intensely than the surrounding tissue, denoting the postsynaptic receptor area.

Differentiation of Motor Axons

Crustacean motoneurons fall into at least two classes, viz., excitatory and inhibitory (Atwood 1976, 1982; Govind and Atwood 1982), and a possible third neuromodulatory type (Sharman et al. 2000). This differentiation permits fine control of muscle contraction, enabling exquisite functioning

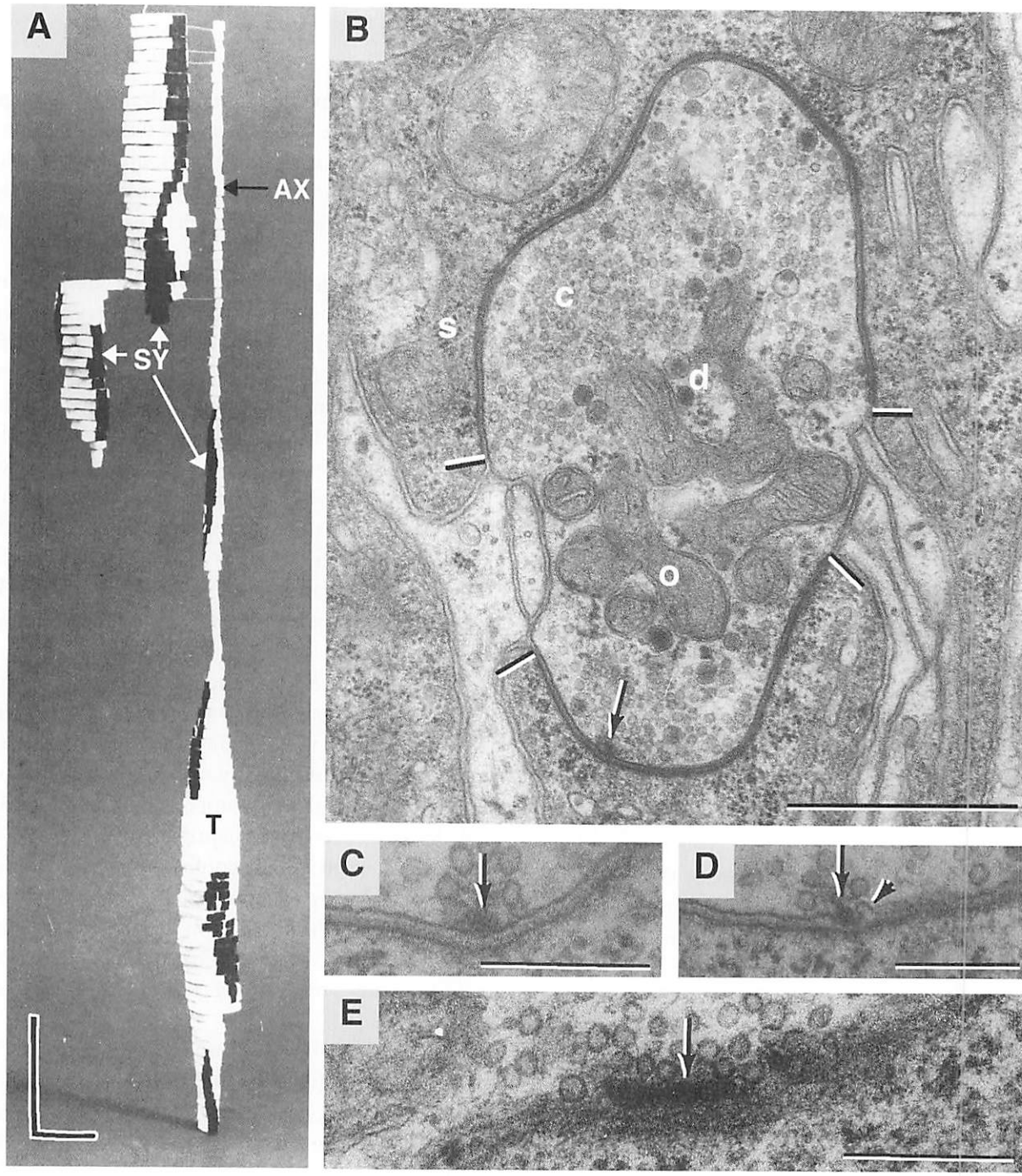

Figure 9. (A)Three-dimensional reconstruction of excitatory innervation to the blue crab gastric mill muscle, gm8b, showing nerve terminals [T] connected by a thin axonal branch [AX], both of which contain synapses [SY]. (B) Cross-section of excitatory nerve terminal populated with many small, clear spherical synaptic vesicles [c], a few larger dense core vesicles [d], and mitochondria [o]. Two long synaptic contacts (between bars) are made with the muscle membrane adjacent to granular sarcoplasm [s]. One synapse has a presynaptic dense bar (arrow) with clustered synaptic vesicles indicative of an active zone. (C) and (D) Cross-section view of presynaptic dense bar (arrows) with clustered synaptic vesicles, and an omega-shaped profile depicting exocytosis of a synaptic vesicle (arrowhead). (E) Longitudinal view of presynaptic dense bar (arrow) emphasizing its elongate nature and the docking of clear synaptic vesicles poised for release. Horizontal and vertical bars: 1 μm in (A). Horizontal bars: 1 μm in (B), 0.25 μm in (C), (D),(E). From Atwood et al. (1977); Patel and Govind (1997a, b).

with relatively few motoneurons. The most studied excitor shows differentiation between neurons such as fast and slow as well as differentation within single individual neurons. These various levels of differentiation allow a single or a small number of motoneurons to extend the functional range of the muscle, particularly as the degree of contraction of a muscle fiber is dependent on the extent to which it is depolarized (Atwood 1973, 1976). Each class of motoneuron will be dealt with separately below with particular attention to the differentiation within excitor motoneurons as this is best studied.

Excitatory Axon

Differentiation into Fast and Slow Axons. Fast and slow axons are the two extremes in a range of crustacean motoneurons and are best exemplified in the claw closer muscles of lobsters and crayfish where they are used for fast and slow contractions (Atwood and Wojtowicz 1986; Lnenicka 1991; Govind 1992). In blue crabs, the claw closer muscle also receives fast and slow excitors that give rise respectively to twitch and tonic type contractions (Fig. 6) (Govind and Blundon 1985). These contractile differences presumably arise largely from differences in the properties of neuromuscular synapses of the respective axons, although this observation has not been verified for blue crabs as it has for lobsters and crayfish.

Differentiation of Slow Axons. A defining feature of crustacean excitor axons is the wide variation in the amount of transmitter released at their numerous synapses (Atwood 1976, 1982; Atwood and Wojtowicz 1986; Atwood and Cooper 1996). Excitor axons in the blue crab are no exception. The relatively few that have been studied are of the slow type because they are fatigue-resistant and have a substantial population of mitochondria (Patel and Govind 1997a) and glycogen granules (Honsa and Govind 2002). Among the slow axons, synaptic differentiation is seen primarily in the amplitude of the excitatory post-synaptic potential (EPSP), but also in the structural characteristics of their synapses and active zones. Both these features will be reviewed to highlight differentiation within a single target muscle, as well as among several separate target muscles.

Within Muscles. Stimulation of the single excitor axon generates EPSPs that vary from 2- to 5-fold among individual fibers as seen in the stomach muscles (Fig. 10) (Table 1) and in the limb accessory flexor muscle (Wiens and Govind 1985). Repetitive stimulation generally increases the amplitude of the EPSP, due to increased output of neurotransmitter, which is referred to as synaptic facilitation. The degree of facilitation varies among individual axons, although initially-small EPSPs tend to facilitate more than initially-large EPSPs (Table 1). A unique feature of synaptic facilitation among some stomach muscles (gm8b, gm9a, p1) is that it is very long-lasting, so that EPSPs 10 sec apart still show this phenomenon (Fig. 10). Although most synapses of slow axons facilitate, a notable exception is seen in p13 muscle where the repetitive EPSPs are slightly depressed, but subsequent unitary EPSPs are almost twice as large, demonstrating a robust form of post-tetanic potentiation.

The physiological differentiation of synapses of individual motor axons is underlined by a morphological differentiation regarding synapses and their presynaptic dense bars or active zones. Synapse size, measured as surface area, varies from 20- to 25-fold among single axons to the stomach muscles (Atwood et al. 1978). Thus, for instance, synapses in the pyloric muscle, p1, have a spread from 0.5 to 10 μm and those in gastric mill muscles, gm8b and gm9a, vary from 0.2 to 3 μm. This is an unusually large variation because in other neuromuscular systems in crustacean limb muscle, for which most information is available, synapse size may vary 5- to 10-fold (Walrond et al. 1993; Govind et al. 1994). Presynaptic dense bars are found in most synapses in the blue crab stomach muscles, although a few are without (Atwood et al. 1977, 1978; Patel and Govind 1997a, b). Twice as many synapses have a single active zone compared to synapses with two or more, and the latter enhances transmitter release (Patel and Govind 1997a).

Another feature of these excitatory axons is the differentiation in vesicle species. Apart from the

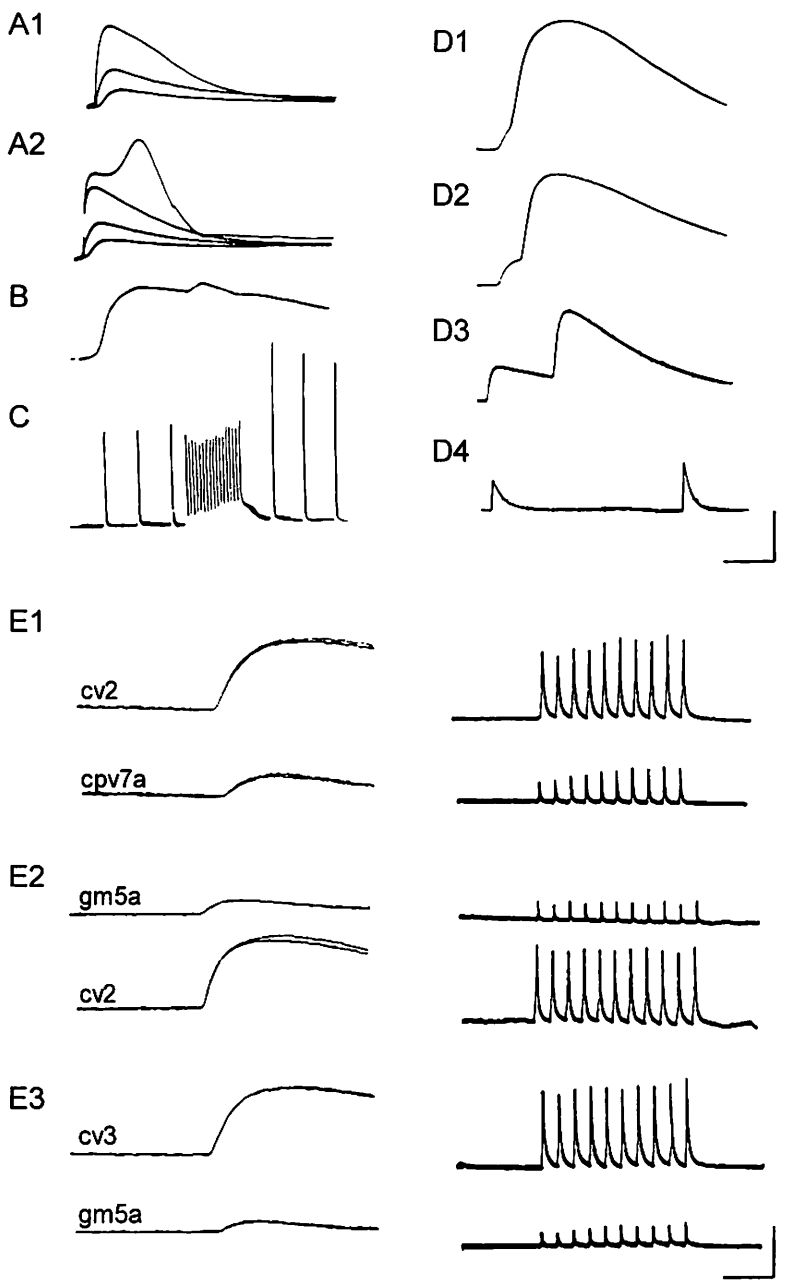

Figure 10. Representative excitatory post-synaptic potentials (EPSPs) from intrinsic stomach muscles in blue crabs in response to nerve stimulation. [A1] Three sizes of EPSPs in muscle p2 at increasing stimulus intensities, denoting triple innervation; [A2] in the same preparation, stimulation of all three axons simultaneously evoked a larger EPSP with an active reponse; [B] stimulation of a single axon to muscle p1 often gave a biphasic EPSP suggesting differences in synaptic performance along the muscle fiber; [C] stimulation at 1 Hz of the single axon to muscle p13 gave large, non-facilitating EPSPs at 1 Hz or during a brief 10 Hz burst. However, following the burst, stimulation at 1 Hz evoked two-fold larger EPSPs, demonstrating marked post-tetanic potentiation; [D1 to D4] twin-pulse stimulation of the single axon to muscle gm8b shows facilitation of EPSPs with increasingly longer interpulse intervals of 10, 20, 250 and 400 msec respectively; [E] individual stimuli to a single axon (left panels) show sharing among four muscles in which [cpv7a] and [gm5a] have small EPSPs, while [cv2] and [cv3] have larger EPSPs. Stimulation at 10 Hz (right panels) evokes little facilitation in either small or large EPSPs. Vertical bars: 5 mV in [A]; 4 mV in [B]; 20 mV in [C, D, E]. Horizontal bars: 40 msec in [A, D]; 30 msec in [B]; 2 sec in [C]; 20 msec in [E] left traces and 2 sec in [E] right traces. From Govind et al. (1975); Atwood et al. (1977); Patel and Govind (1997a).

usual small 40 to 50 nm, clear, spherical vesicles that contain the fast neurotransmitter (most likely glutamate), there is a second species of vesicle, consisting of larger 70 to 80 nm dense or dense-core vesicles, that presumably stores a slow neurotransmitter or neuromodulator (Figs. 9, 11) (Patel and Govind 1997b; Sharman et al. 2000). There is also evidence that these neurotransmitters are released not only extrasynaptically, as has been shown at other invertebrate synapses (Golding and Bayraktaroglu 1984; Schurmann et al. 1991), but also at the synapses in these blue crab stomach muscles (Figs. 11, 12).

Among Muscles. Single motoneurons innervate single muscles, although occasionally a single motoneuron innervates two or more muscles with different roles. Blue crab stomach muscles offer several excellent examples of this complex type of motor unit (Table 1). For instance, the inferior cardiac motoneuron innervates four separate muscles, gm5a, cpv7a, cv2 and cv3 (Fig.1), which have disparate roles in chewing and filtering food (Claiborne and Ayers 1987). To accomplish these varied roles, synapse differentiation is imposed among muscles, over and above that imposed within muscles. Thus, motor nerve terminals to two of the muscles (cpv7a and gm5a) release small amounts of transmitter (low-output) while those to the other two muscles (cv2 and cv3) release 3- to 5-fold greater amounts (high-output) (Fig. 10) (Govind et al. 1975; Patel and Govind 1997a).

Structural features underlying the disparity in synaptic strength were analysed with thin serial-section electron microscopy (Patel and Govind 1997a). Nerve terminals are similar in their volume percent of mitochondria (17%), clear vesicles (27%), and dense core vesicles (3%) among the four muscles. This is also the case for the number and size of synaptic contacts. However, presynaptic dense bars representing active zones are significantly longer and occur more frequently at high-output synapses than at low-output ones (Fig. 13). High-output synapses are also characterized by the close spacing of adjacent active zone dense bars. The longer and more closely spaced dense bars at high-output synapses would be factors in the generation of larger synaptic potentials in these terminals compared to their low-output counterparts. Other factors, however, need to be considered to fully account for the physiological differences in synaptic strength among the four muscles.

In this same motor unit there is structural evidence for the exocytotic release of dense-core vesicles exclusively at synapses (Fig. 11) (Patel and Govind 1997b). The primary evidence is the appearance of dense cores in the synaptic cleft accompanied by indentations of the presynaptic or postsynaptic membrane. In its simplest form, this structure consists of an Ω-shaped figure of the presynaptic membrane enclosing one dense core denoting release of a single dense-core vesicle. A larger indentation of the presynaptic membrane enclosing several dense cores denotes multiple release. A more complex form of multiple release is demonstrated where the presynaptic membrane is normal but the postsynaptic membrane is elaborated into a sac projecting into the muscle granular sarcoplasm and filled with dense cores (Fig. 12). The postsynaptic sac in some instances is compressed into a thin, finger-like extension, which lacks dense cores and, at its distal end, is separated into small cisternae, suggesting a mechanism for membrane recycling (Fig. 11). Profiles depicting single and multiple release of dense core vesicles occur more frequently at high-output terminals (cv2 and cv3) compared to their low-output counterparts (cpv7a and gm5a). The many multiple release figures closely adjacent to the active zones for fast transmitter release suggests a possible modulatory role for dense-core vesicles in synaptic transmission. Moreover, the modulatory effects of dense core vesicles appear to be long lasting as implied by the postsynaptic sacs that may permit prolonged release of the contents of their dense cores into the synaptic cleft. This observation is in keeping with the functional role of these stomach muscles, which is to be continuously active for long periods of time.

Other very active muscles, although used intermittently, are those of the swimming paddle, as blue crabs are beautiful swimmers, combining agility with endurance. Hence, the single excitor axon to the opener muscle in the swimming paddle

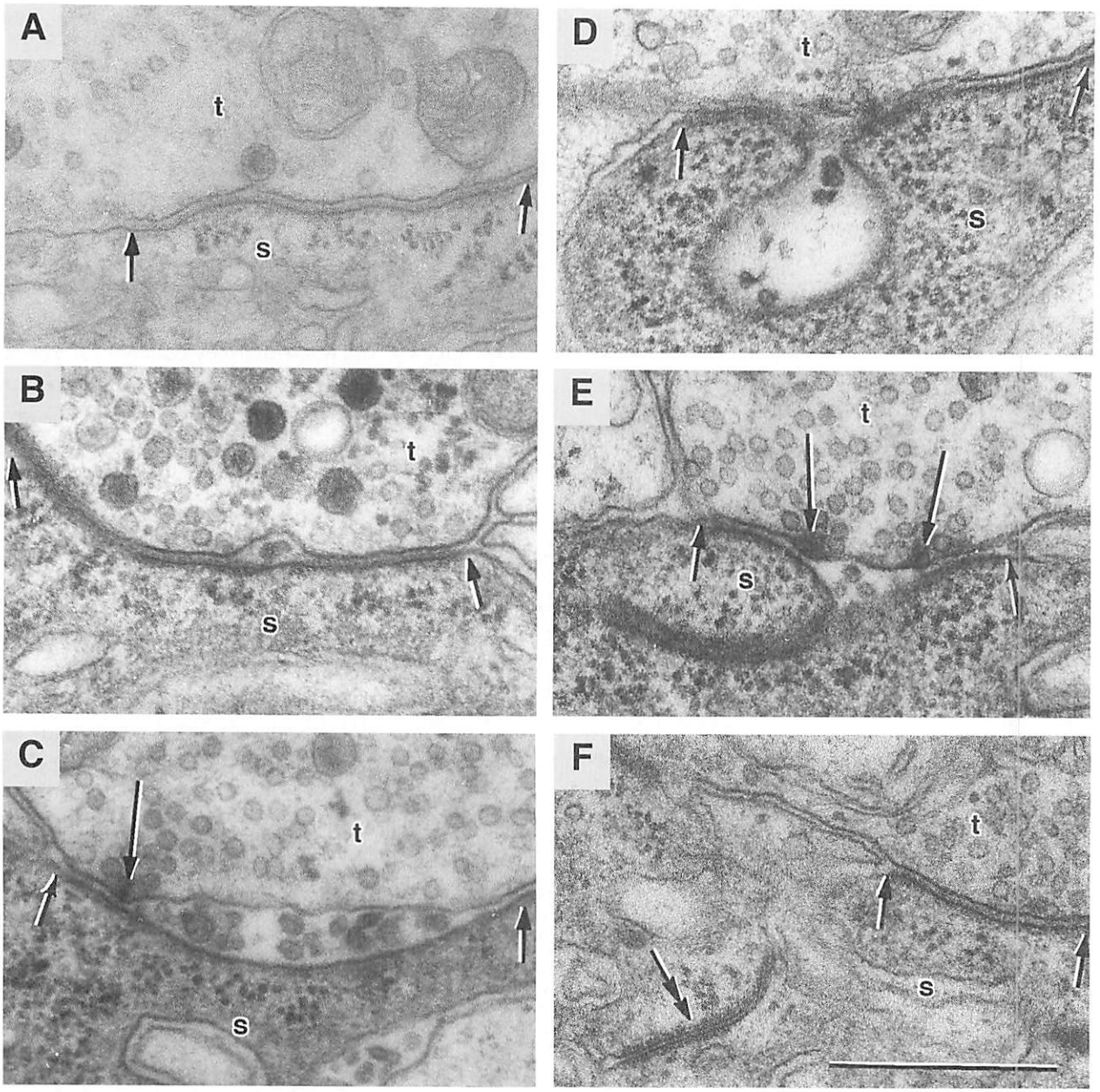

Figure 11. Exocytosis of dense core vesicles at neuromuscular synapses of blue crab stomach muscle cv2. Each panel shows a nerve terminal [t] populated with clear synaptic vesicles and some dense core vesicles making synaptic contact (between small arrows) with the muscle membrane in areas of granular sarcoplasm [s]. (A) Initial fusion of dense core vesicle to presynaptic membrane. (B) Infolding of presynaptic membrane enclosing a dense core, presumably via exocytosis of a single dense core vesicle. (C) Synapse with a presynaptic dense bar (long arrow) has an enlarged cleft containing several dense cores indicative of multiple exocytosis of dense core vesicles. (D) Synapse with the postsynaptic membrane forming a large sac containing several dense cores. (E) Synapse with two presynaptic dense bars (long arrows) between which the enlarged cleft contains several dense cores. The postsynaptic membrane extends as a slender finger-like extension into the muscle granular sarcoplasm. (F) A slender folded membranous structure (double arrowhead) in the granular sarcoplasm immediately adjacent to a synaptic contact resembles the postsynaptic finger-like extension in the previous micrograph. Bar: 0.5 μm. From Patel and Govind (1997b)

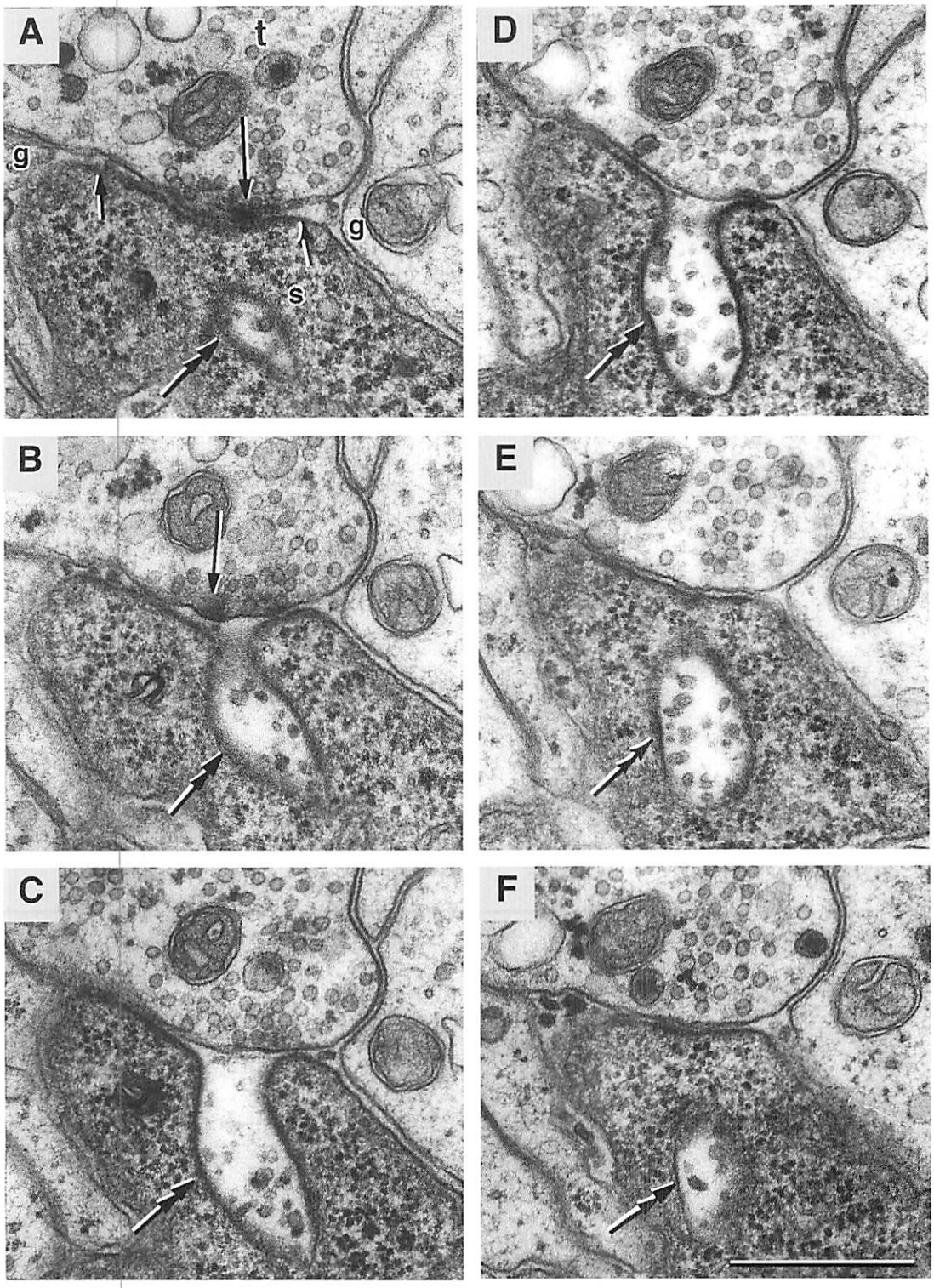

Figure 12. Serial micrographs depicting bulk exocytosis of dense core vesicles in excitatory nerve terminals in a blue crab stomach muscle. (A) Nerve terminal [t] embedded in the granular sarcoplasm [s] of muscle cv2 shows a synaptic contact (between small arrows) delimited by glial [g] tissue. The postsynaptic membrane has a very prominent invagination (double arrowhead), which is filled with many dense cores. This invagination appears as a small pouch in (A), connects to the postsynaptic membrane in (B), (C), and (D), and again appears as a pouch in (E) and (F). Note the dense bars (long arrows) in (A) and (B) lying directly above the invagination. Bar: 0.5 μm. From Patel and Govind (1997b).

branches more profusely and more richly innervates individual muscle fibers compared to its homolog in the walking leg (Honsa and Govind 2002). Moreover, its nerve terminals devote a substantial percentage of their volume to energy substrates (21%), a volume similar to terminals of the highly active stomach motoneurons (Patel and Govind 1997a; Sharman et al. 2000). However, unlike terminals of the stomach where mitochondria are the sole energy substrate, in the paddle opener terminals there is a mixture of mitochondria (12%) and glycogen granules (9%) (Fig. 14A) (Honsa and Govind 2002). Because glycogen provides a much more rapid source of energy than mitochondria, the enriched glycogen content of the paddle opener terminals appears to be an adaptation for the much higher firing frequencies of the swimming motoneurons (50-100 Hz) (Wood and Derby 1995), compared to those of the stomach neurons (5-10 Hz) (Selverston and Moulins 1987).

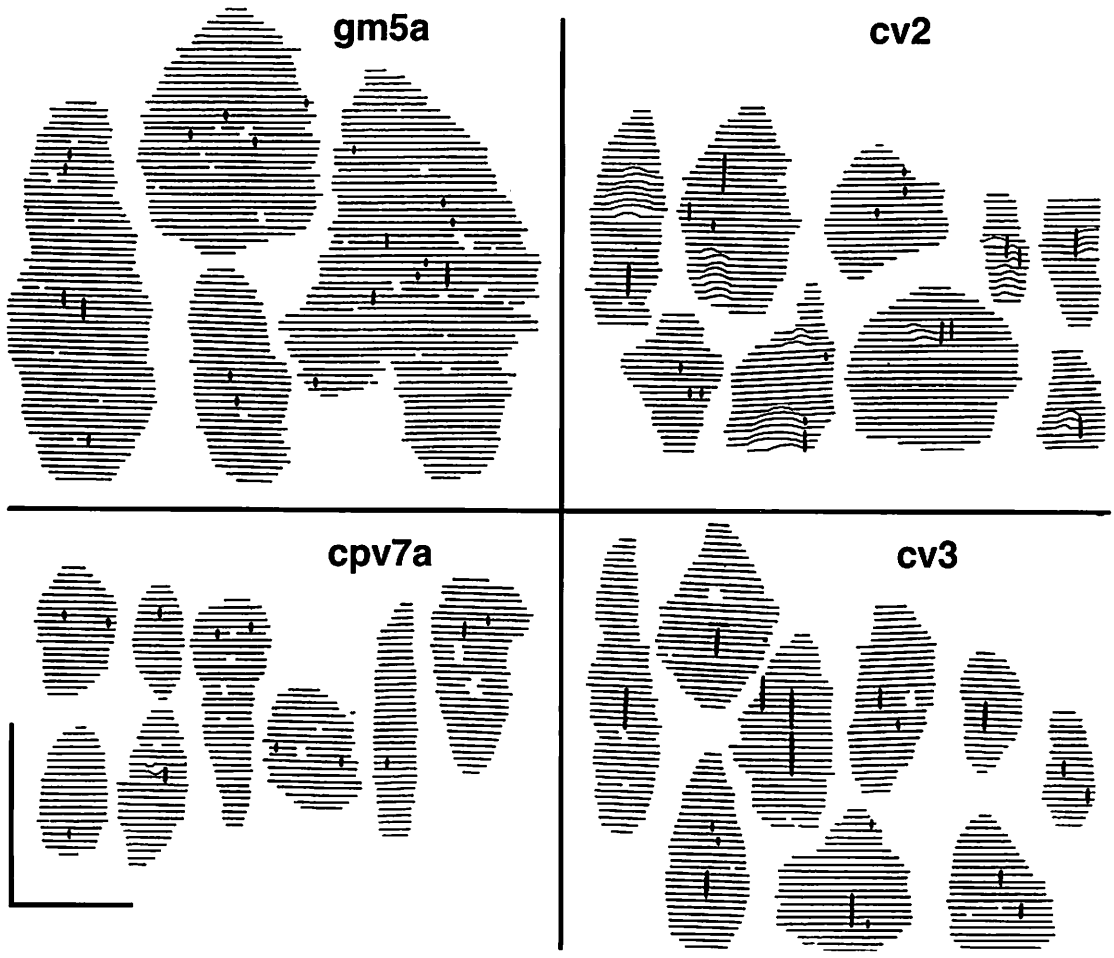

Figure 13. Two-dimensional representation of selected synapses from blue crab stomach muscles [gm5a] and [cpv7a] as low-output types, and [cv2] and [cv3] as high-output types. Each horizontal line represents a thin section and the thicker vertical lines represent dense bars that traverse one or more consecutive thin sections. White spaces represent perforations and the curved horizontal lines, most prevalent in [cv2] synapses, represent outfoldings of the postsynaptic membrane. High-output synapses [cv2, cv3] are characterized by longer and more closely-spaced dense bars compared to low-output synapses [gm5a, cpv7a]. Horizontal and vertical bars: 2 μm. From Patel and Govind (1997a).

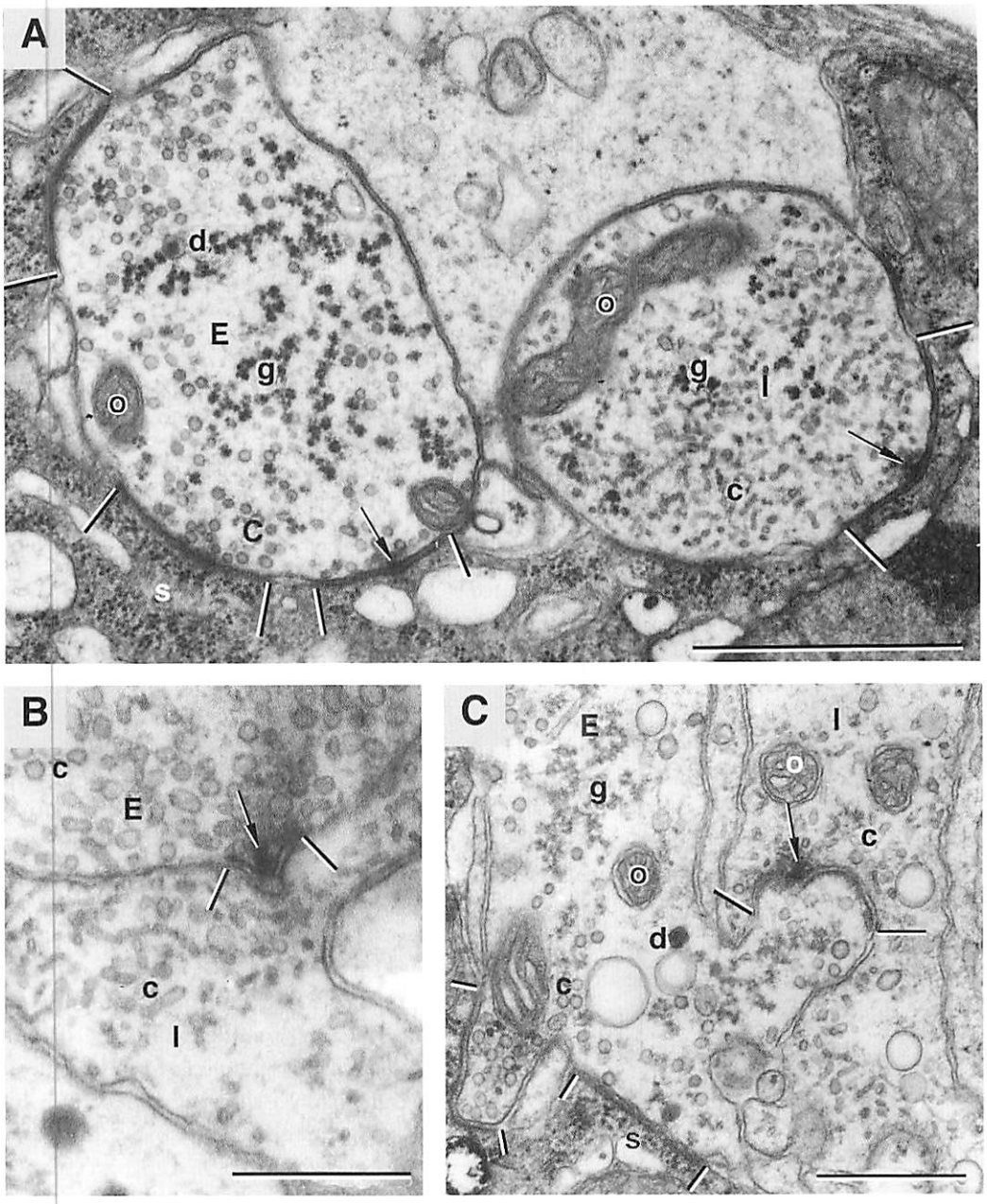

Figure 14. Neuromuscular and axo-axonal synapses in blue crab swimming paddle opener muscle. (A) Neighboring excitatory [E] and inhibitory [I] nerve terminals recognized respectively by their spherical and elliptical synaptic vesicles [c] also display a few dense core vesicles [d], mitochondria [o], and glycogen granules [g]. Synaptic contacts (between bars) recognized by densely stained, opposing membranes appear adjacent to muscle granular sarcoplasm[s]. At these synapses, presynaptic dense bars (arrows) with clustered synaptic vesicles denote an active zone. (B) An axo-axonal synaptic contact (between bars) complete with an active zone dense bar (arrow) from an excitor [E] onto an inhibitor [I] terminal; terminals are recognized respectively by their spherical and elliptical synaptic vesicles [c]. (C) An axo-axonal synaptic contact (between bars) from an inhibitor [I] onto an excitor [E] terminal; terminals are recognized, respectively, by their elliptical and spherical synaptic vesicles [c]. This synaptic contact, extending through 10 thin sections with several active zone dense bars (arrow), is strategically located on a small branch of the excitor axon where presynaptic inhibition would effectively cut off this region of the excitatory innervation. Note excitatory neuromuscular synaptic contacts (between small bars) adjacent to muscle granular sarcoplasm [s], mitochondria [o], and glycogen granules [g]. Bars: 1 μm in (A), 0.5 μm in (B), (C). From Honsa and Govind (2002).

Another unique feature of the excitor axon to the swimming paddle opener muscle is that it makes synaptic contact with the inhibitor axon (Fig. 14B) (Honsa and Govind 2002). These axo-axonal synapses making up only 4% of the excitor synapses (the rest are onto muscle fibers) are strategically located at bottlenecks of the inhibitor axon where they would be maximally effective in regulating local regions of the inhibitor axon. Thus, differentiation of the slow excitor axon to the paddle opener muscle entails not only regulating synaptic strength onto the target muscle by varying synaptic structure and function as outlined above for the stomach axons, but also in regulating local regions of the antagonistic inhibitor axon. Hence, these excitor to inhibitor synapses may play an unusual role in extending the functional range of motoneurons.

Inhibitory Axon

The classical scheme for motor supply to the decapod limb has a common inhibitor to all the limb muscles (Atwood 1976). The accessory flexor muscle in the merus of thoracic limbs follows this scheme in that both heads of this muscle receive a single inhibitory axon (Fig. 15) (Govind and Wiens 1985; Wiens and Govind 1985). In the distal head of the accessory flexor muscle, the inhibitor exerts significant effects only in a very restricted region, where the effect is powerful enough to completely overwhelm the excitor. At these sites the inhibitory synapses show considerable facilitation and summation.

The specific inhibitor axon to the swimming paddle opener muscle also exerts a powerful effect via two pathways, judging from structural evidence (Honsa and Govind 2002). One route is via its neuromuscular synapses (Fig. 14A) that serve to reduce or eliminate depolarization of the muscle fiber, i.e., postsynaptic inhibition. The other route is via synaptic contacts with the excitor axon that serve to reduce transmitter release from the excitor axon onto the muscle fiber, i.e., presynaptic inhibition (Fig. 14C). These inhibitor to excitor synapses constitute a substantial percentage (36%) of the total

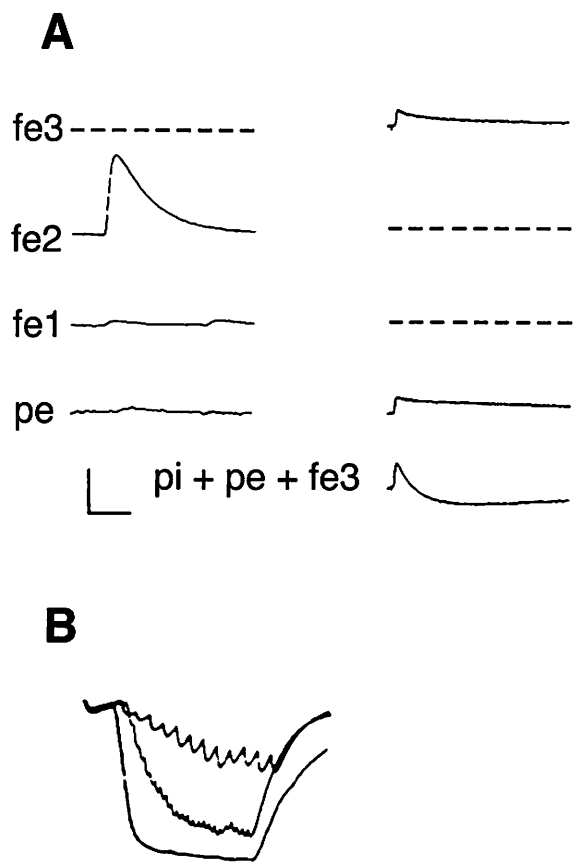

Figure 15. Excitatory and inhibitory innervation of the distal accessory flexor muscle of blue crab limb. (A) Postsynaptic potentials from two muscle fibers (left and right panels) showing innervation by four excitatory axons, three from the main flexor nerve [fe1, fe2, fe3] and one from the proximal accessory flexor nerve [pe]. An inhibitory axon in the proximal nerve [pi] strongly inhibits the fiber in the right panel, slowly overcoming the summed depolarization due to excitatory axons [pe] and [fe3] to produce a net hyperpolarization when all three axons are activated simultaneously. (B) Inhibitory postsynaptic potentials from a fiber showing facilitation (increase in size of individual responses) and temporal summation (increase in size of total response) with stimulation of the [pi] axon at 4, 10, and 20 Hz. Vertical bar: (A) left traces – 2 mV for [pe], 4 mV for [fe]; (A) right traces – 2 mV. (B) 4 mV. Horizontal bar: (A) left traces – 20 msec; (A) right traces – 100 msec. (B) 1 sec. From Wiens and Govind (1985).

synapses formed by the inhibitor axon, suggesting pronounced presynaptic inhibition that is more likely to rapidly and effectively decouple the opener muscle from the stretcher muscle in the adjoining segment; both muscles are innervated by the same excitor axon (Govind and Atwood 1982). Such decoupling will allow for the rapid and separate activation of these two muscles during swimming. It is also interesting to note that inhibitiory nerve terminals to the paddle opener muscle, like their excitor counterparts, exhibit a high volume (17%) of energy substrate which is differentiated into mitochondria (8%) and glycogen granules (9%), the former to support the prolonged firing of the swimming motoneurons and the latter to support their rapid rate of firing (Wood and Derby 1995).

Crustacean stomach muscles have been regarded as receiving exclusively excitatory innervation (Maynard 1972; Govind et al. 1975). However, electron microscopic examination of the stomach pyloric muscles in blue crabs revealed nerve terminals with either spherical synaptic vesicles indicative of an excitatory axon, or elliptical synaptic vesicles indicative of an inhibitory axon (Fig. 16) (Sharman et al. 2000). Synaptic vesicles assume these characteristic shapes when fixed with glutaraldehyde and osmium, and these shapes provide a reliable means for distinguishing excitatory from inhibitory axons (Uchizono 1967; Atwood and Morin 1970). In several blue crab pyloric muscles, including p2 and p11 to p14, the vesicle shape index (the ratio of major to minor diameter) for the excitatory axon is close to spherical at 1.2, but distinctly elliptical for the inhibitory axon at 1.9 (Sharman et al. 2000). Apart from the distinctive shape of their synaptic vesicles, the inhibitory nerve terminals resemble their excitatory counterparts in making synaptic contact with the muscle membrane, at which contacts there are distinct presynaptic dense bars representing active zones for transmitter release (Fig. 16). However, inhibitory innervation in these muscles is slightly less pervasive than excitatory innervation. Whether this

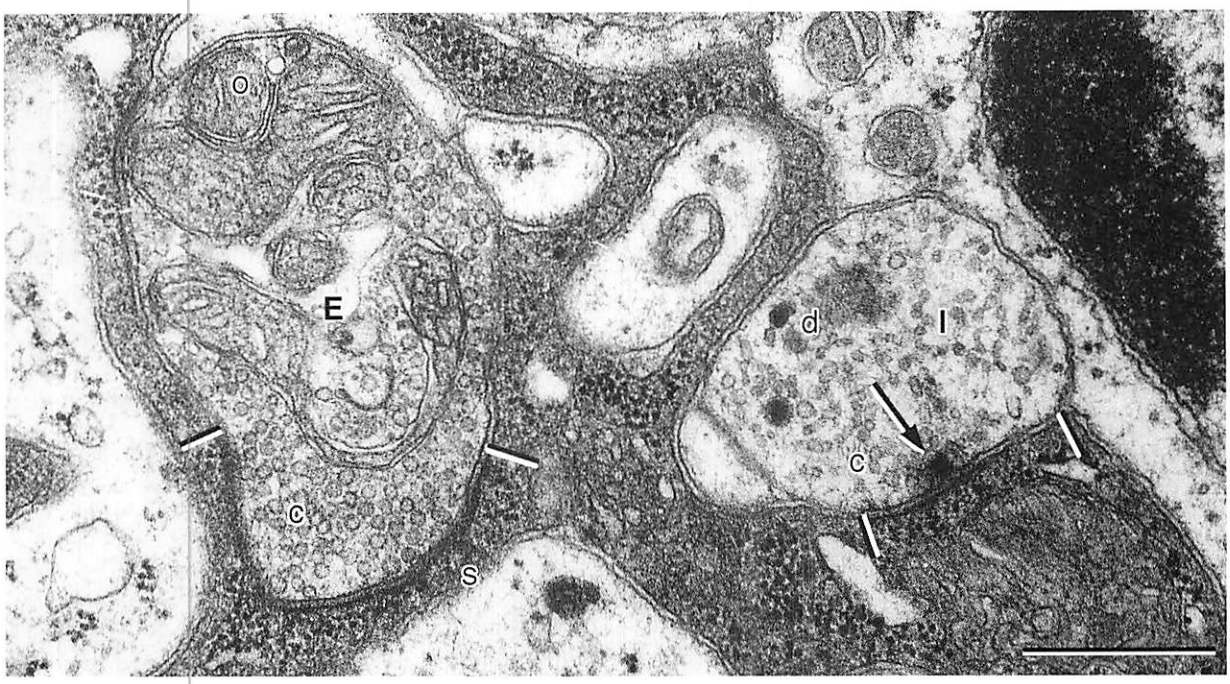

Figure 16. Excitatory [E] and inhibitory [I] nerve terminals in blue crab stomach pyloric muscle p12 characterized by clear [c] synaptic vesicles that are spherical and elliptical in [E] and [I], respectively. Terminals make synaptic contact (between bars) with muscle membrane in areas of granular sarcoplasm [s]. The [I] synapse shows a presynaptic dense bar (arrow). A few dense [d] core vesicles and mitochondria [o] are also visible. Bar: 0.5 μm. From Sharman et al. (2000).

inhibitory innervation derives from common or specific neurons is unknown, although it clearly provides another avenue for fine control of muscle contraction, hitherto unsuspected in the stomach muscles.

Putative Neuromodulatory Axon

A third type of terminal in the stomach pyloric muscle p14, based on its dense core vesicles, has been tentatively identified as a putative neuromodulatory terminal (Fig. 17) (Sharman et al. 2000). Here the dense core vesicles, unlike their counterparts in the excitatory and inhibitory terminals, are significantly larger and have eccentrically located dense cores. More strikingly, these unusual dense core vesicles constitute 47% terminal volume, whereas clear vesicles make up only 7%. The mitochondrial content at 6% is markedly less than that of excitatory and inhibitory terminals at 11 to 25%. This unusual dense core vesicle composition is present in long serially-sectioned lengths of terminals, suggesting a separate axon rather than regional variation in either excitatory or inhibitory axons.

Also supporting the thesis of a separate neuromodulatory axon is the finding of synaptic contact with muscle membrane and the docking and exocytosis of dense core vesicles (Fig. 17) (Sharman et al. 2000). Indeed, synaptic contact with both excitatory and inhibitory terminals by the neuromodulatory axon shows that its target includes not only the muscle, but the motor axons themselves. Thus, the neuromodulatory axon provides a mechanism for delivering precise amounts of slow transmitters to selected targets, thereby regulating muscle contraction. This mechanism makes the transfer function of the motor patterns to the pyloric muscles in crabs as complex as mechanisms for generating and modulating the motor patterns themselves in the stomatogastric ganglion.

Innervation of Muscles

Innervation is known for relatively few muscles, with the exception of the intrinsic foregut muscles where 32 muscles are supplied by approximately 15 excitor neurons (Table 1) (Govind et al. 1975). Most stomach muscles receive a single excitor neuron that is shared among two to four separate muscles, making fine control of these muscles reside largely in axonal firing patterns and differentiation of neuromuscular synapses (see above). A few pyloric muscles receive two to three axons, adding another level of control for muscle contraction. Additional levels of control of muscle contractions are provided by an inhibitor and a putative neuromodulator axon, making these the most highly regulated muscles.

Among the appendages, the antennular muscles appear to be very simply innervated (Table 2) (Roye 1994), whereas the claw closer shows the typical decapod pattern (Govind and Blundon 1985). The bipartite accessory flexor muscle shows the usual decapod pattern of a single excitor and a single common inhibitor to the proximal head but an unusual pattern in the distal head with the single private excitor coupled with three others from the parent flexor muscle for a total of four excitors; it also receives the common inhibitor (Govind and Wiens 1985; Wiens and Govind 1985). The four groups of basal muscles of the swimming paddle listed as receiving one to two excitors (White and Spirito 1973) may be an underestimate because one of these, the promotor muscle, is associated with seven motoneurons (Blight and Llinas 1980). Homologous muscles in another swimming crab *Portunus sanguinolentus* are innervated by several excitors (Hoyle 1973). Finally, the opener muscle in the swimming paddle exhibits the typical decapod pattern of a lone excitor and a specific inhibitor axon (Table 2) (Honsa and Govind 2002).

SENSORY NEURONS

Organization

Blue crabs respond to sensory stimuli via highly differentiated cells, most of which have their somata located at the periphery. These sensory neurons are bipolar, with the distally directed dendrite associated with transduction and proximally directed axons conducting spikes to the ganglion. A few sensory cells have centrally located somata. The dendritic

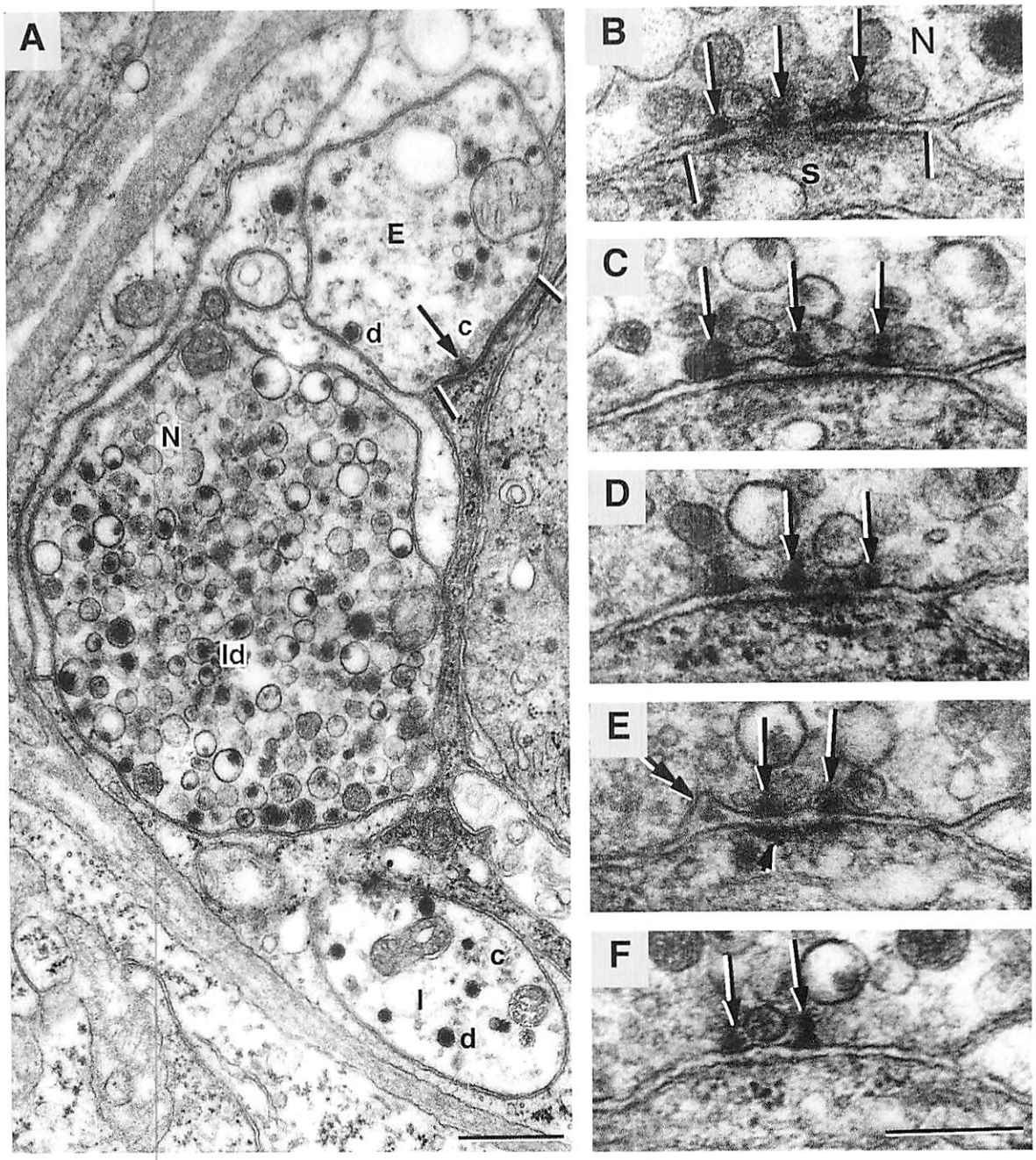

Figure 17. (A) Three adjacent nerve terminal profiles in blue crab stomach pyloric muscle p14 representing excitatory [E] and inhibitory [I] terminals with small, clear [c] synaptic vesicles that are spherical and elliptical in [E] and [I] respectively, and a neuromodulatory [N] terminal with predominantly large dense and dense core [ld] vesicles. The excitatory terminal has a long synapse (between bars) with a presynaptic dense bar (arrow). (B), (C), (D), (E), and (F) Five consecutive thin serial sections of a neuromodulatory [N] terminal in blue crab pyloric muscle p14 showing a synaptic contact (between bars) with muscle granular sarcoplasm [s]. Typical synaptic features include presynaptic dense bars (arrows), prominent postsynaptic density (arrowhead), and an infolding of the presynaptic membrane with an enclosed dense core (double arrowhead in E) indicative of exocytosis. Bars: 0.5 μm in (A); 0.25 μm in (B), (C), (D), (E), (F). From Sharman et al. (2000).

processes are usually embedded in supporting structures that serve to gather and amplify the stimuli. Sensory structures for receiving mechanical and chemical stimuli in blue crabs are reviewed below.

Mechanoreceptors

Thoracic-coxal Muscle Receptor Organ

Unlike other sensory receptors in decapod crustaceans, the thoracic-coxal receptor is unusual in that its soma is located in the ganglion and its sensory axon conducts signals without action potentials (Bush 1976). Because of its non-impulsive signal transmission, this receptor has been the focus of an extensive biophysical and physiological study in the fifth pereopods or swimming paddles of blue crabs (Blight and Llinas 1980). Here it is located within the medial branch of the large promotor muscle and consists of a separate muscle strand that originates in the exoskeletal rod of the sternite and inserts on the coxa, along with the parent promotor muscle (Fig. 18). The muscle receptor strand is innervated by two motor axons and by two sensory axons referred to as S- and T-fibers. The T-fiber in the ganglion appears as a large-diameter neurite filled with synaptic vesicles and making synaptic contact with numerous small profiles, presumably of promotor motoneurons.

Stretching of the receptor strand will activate the T-fiber, resulting in depolarization that propagates decrementally to the central terminations/dendrites; this is known as non-impulsive conduction. The T-fiber axon is therefore adapted for long distance decremental conduction by having a length constant of up to 60 mm, as well as compensatory mechanisms for the large electrical capacitance of the membrane which would distort the signal (Blight and Llinas 1980). This depolarization appears to be driven by movement of both sodium and calcium ions. Neurites of the T-fiber respond to the depolarization with transmitter release onto neurites of promotor motoneurons with short synaptic delay (1.4 msec), signifying a monosynaptic connection. Transmission at this synapse has a sigmoid form similar to that found at the squid *Loligo pealei* giant synapse. However, unlike the squid giant axon

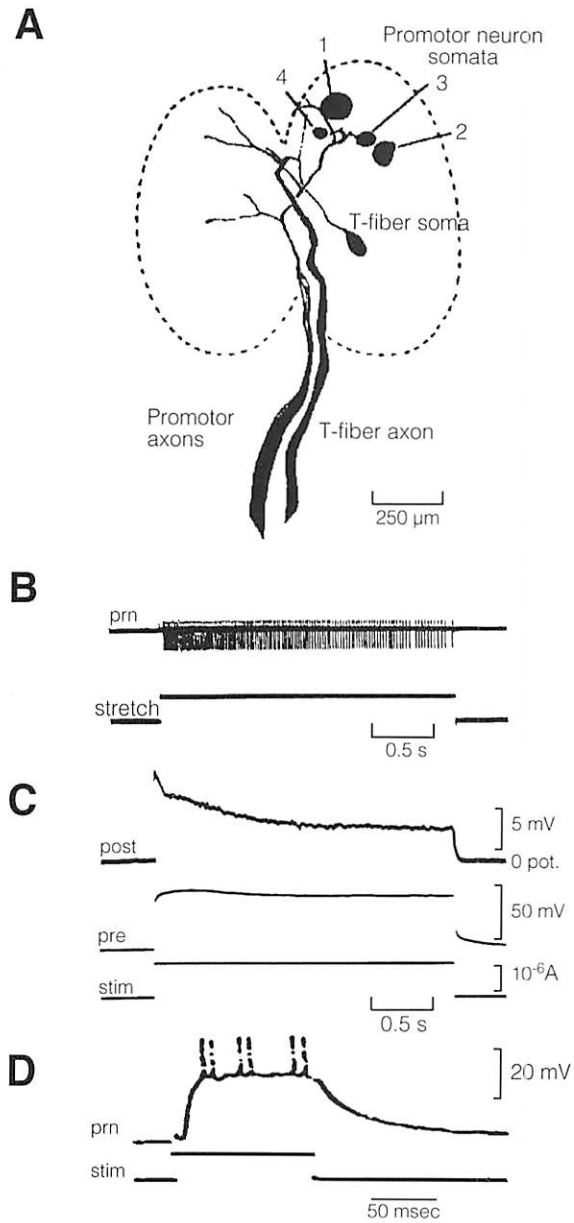

Figure 18. (A) Relationship of stretch neuron T-fiber to four promotor motoneurons [1-4] in the walking leg III and IV neuropil area of the ventral nerve cord in blue crab. (B) Stretching of the receptor muscle (lower trace) evokes sustained firing which shows adaptation in one of the promotor motoneurons recorded from the promotor nerve [prn]. (C) Injection of current in the T-fiber [stim] depolarizes it [pre] and gives rise to a junctional potential [post] in one of the motoneurons. (D) Current injection [stim] into the T-fiber synaptically depolarizes a promotor motoneuron [prn], resulting in spikes. From Blight and Llinas (1980).

synapse which is phasic and depletes its transmitter stores rapidly (Llinas et al. 1976), the T-fiber synapse is tonic and shows little if any depletion of its transmitter stores (Blight and Llinas 1980). Neither is there any sign of habituation or facilitation in keeping with its tonic nature. The set point of this synapse for reflex action is most likely regulated by the receptor muscle by adjusting the tension on the T-fiber endings.

Stretching the receptor strand triggers the promotor motoneurons to fire a train of spikes that show frequency adaptation (Fig. 18) (Blight and Llinas 1980), most likely due to transmitter depletion. This reflex is mimicked at the synaptic level by the EPSP amplitude in a promotor motoneuron in response to depolarization of the T-fiber. This similarity is also seen with sinusoidal depolarization of the T-fiber which more closely resembles the natural signal.

Apodeme Tension Receptors

Receptors monitoring tension of the walking leg opener (Tryba and Hartman 1997) and closer (Hartman 1985) muscles are found at the distal end of the apodeme (Fig. 19). They are comprised of relatively large 25 to 60 μm bipolar cells, numbering 25 to 35 in the closer apodeme and 9 to 15 in the opener apodeme. The distal dendritic ends of these cells are inserted through the hypocuticle into the endocutile and lie in series with the muscle. The proximally directed axons join to form a nerve from which spikes can be recorded, denoting activity of the sensory cells. Receptors are not spontaneously active nor do they respond to passive muscle stretch or unloaded isotonic contraction. However, isotonic contraction with loading or isometric contraction causes firing, confirming the receptors' function as series tension receptors. Contractile force is monitored via both firing frequency and the recruitment of additional units (Fig. 19). Indeed, firing rate closely parallels the rate of change of isometric force, demonstrating that these receptors more closely monitor changes in isometric force rather than total force. Such feedback to the central nervous system would be necessary for reflexes involved in stance, walking, and manipulation.

Short Hair Sensilla of Antennule

Each of the four short hair sensilla on the proximal segments of the antennules consists of a tapered shaft covered with unbranched hairs on all except the inner surface (Fig. 20) (Roye and Dillaman 1982). These sensilla do not respond to waterborne vibrations but to movements of the antennules, with the most anterior sensillum sensitive to antero-ventral deflection and the other three sensilla to postero-ventral deflection. Hence, these sensilla may function as external proprioceptors, and because of their location may act to regulate movements of the proximal and medial segments of the antennule. Innervating each sensillum is a cluster of two large and one small bipolar neurons with their distal processes directed towards the cuticular opening and their proximal processes as axons travelling in antennular nerve bundle IIIc (Roye 1986). In the cerebral ganglion, these axons have either a simple projection pattern of a single ipsilateral tuft to the median antennular neuropil or a complex projection pattern of tufts to ipsi- and contra-lateral median antennular neuropils as well as branches to two lateral antennular neuropils. Input to the median antennular neuropil suggests connections to interneurons, whereas input to the lateral antennular neuropil suggests connections to withdrawal motoneurons as they project to this area.

Statolith Sensilla of Statocysts

The statocysts at the base of the antennule are equilibrium organs operating via the movement of fluid in vertical and horizontal canals that stimulate three groups of mechanosensory sensilla (free hook, thread, and statolith sensilla). The statolith consists of two concentric rows of sensilla (Fig. 21) (Cate and Roye 1997). These sensilla are characterized by siliceous statoconia bound to the filamentous setules, thus creating a single mass that responds to acceleration of fluid in the canal. Each sensillum is innervated by a bipolar cell that projects bilaterally to the median antennular neuropil (Fig. 22), a region where neurites of the antennular withdrawal interneurons also project. Hence stimulation of the nerve carrying the statolith sensilla evokes spikes in

the withdrawal interneurons that in turn activate motoneurons and result in the reflex withdrawal of the antennules (Fig. 22).

Thread sensilla of the statocyst respond to directional rotation by firing their sensory axons, as well as those of higher order axons (Roye 1972). Because rotation of statocysts is accompanied by phasic movements of the thoracic limbs, the thread hairs are implicated in this reflex.

Chemoreceptors

Aesthetasc sensilla of antennules are olfactory sensilla, arranged in a dense tuft on the outer flagel-

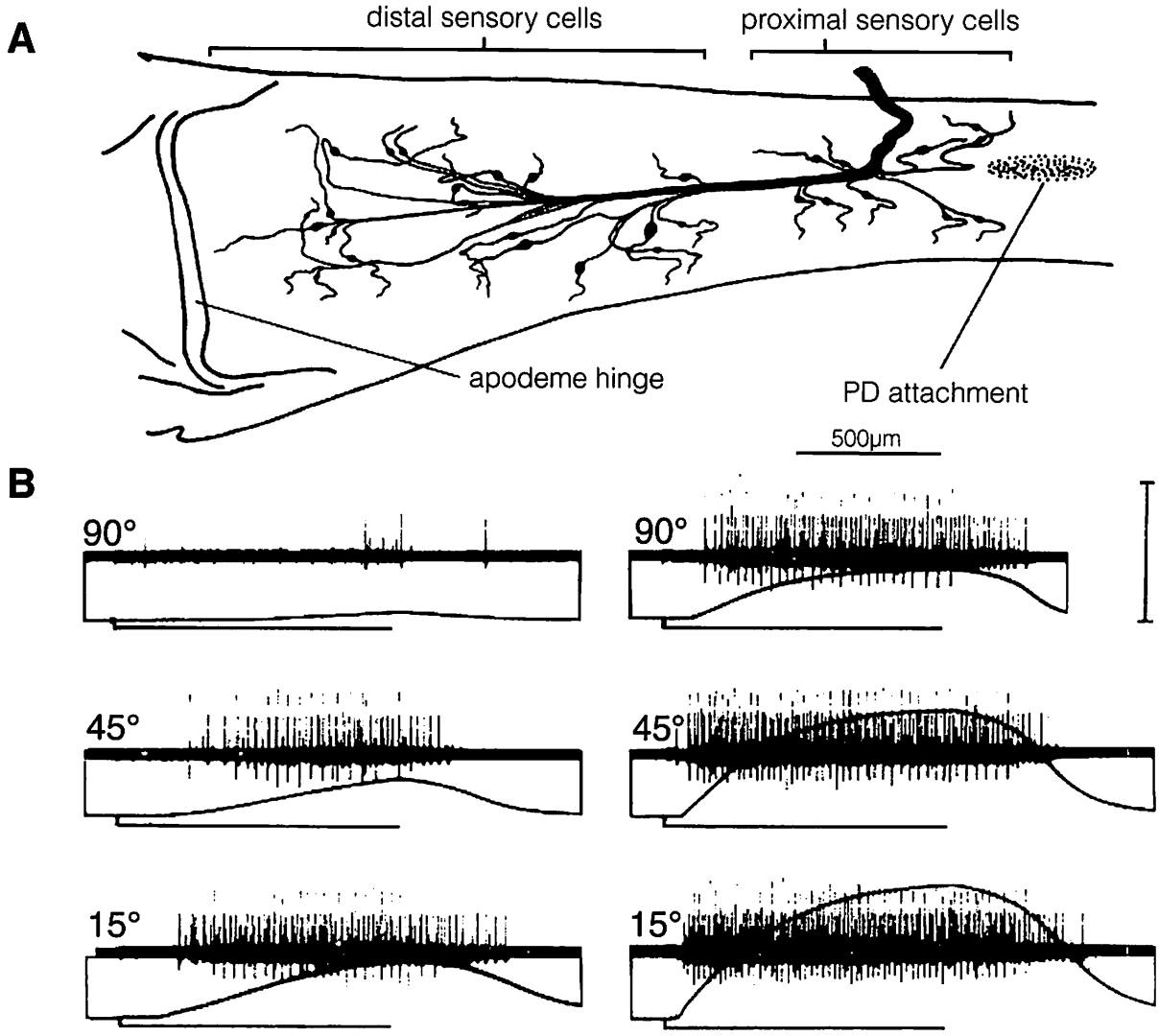

Figure 19. (A) Apodeme tension receptor in the closer muscle of the walking leg of a blue crab composed of proximal and distal groups of many bipolar sensory cells embedded in the apodeme between the hinge and attachment of the propus-dactylus [PD] organ. (B) Extracellular spike recordings (upper traces) from the closer muscle apodeme sensory nerve in response to increasing isometric tension (middle traces) of the closer muscle elicited via stimulation for 2 sec (standard lower traces) of its motor nerve. The nerve was stimulated at 40 Hz (left panels) and 100 Hz (right panels) while the dactyl was held at increasingly smaller angles to position the muscle from flaccid to rest length. From Hartman (1985).

lum of the antennule (Gleeson 1982). Each sensillum is innervated by approximately 100 bipolar sensory cells, each of which gives rise to a distal dendrite that projects into the aesthetasc (Fig. 23) (Gleeson et al. 1996). The dendrite gives rise to two cilia that subsequently subdivide into approximately 10 branches, making a total of over 1000 processes that project into the lumen of a sensillum. Most of these processes are simple. Very small outer dendritic processes are supported by a single microtubule and

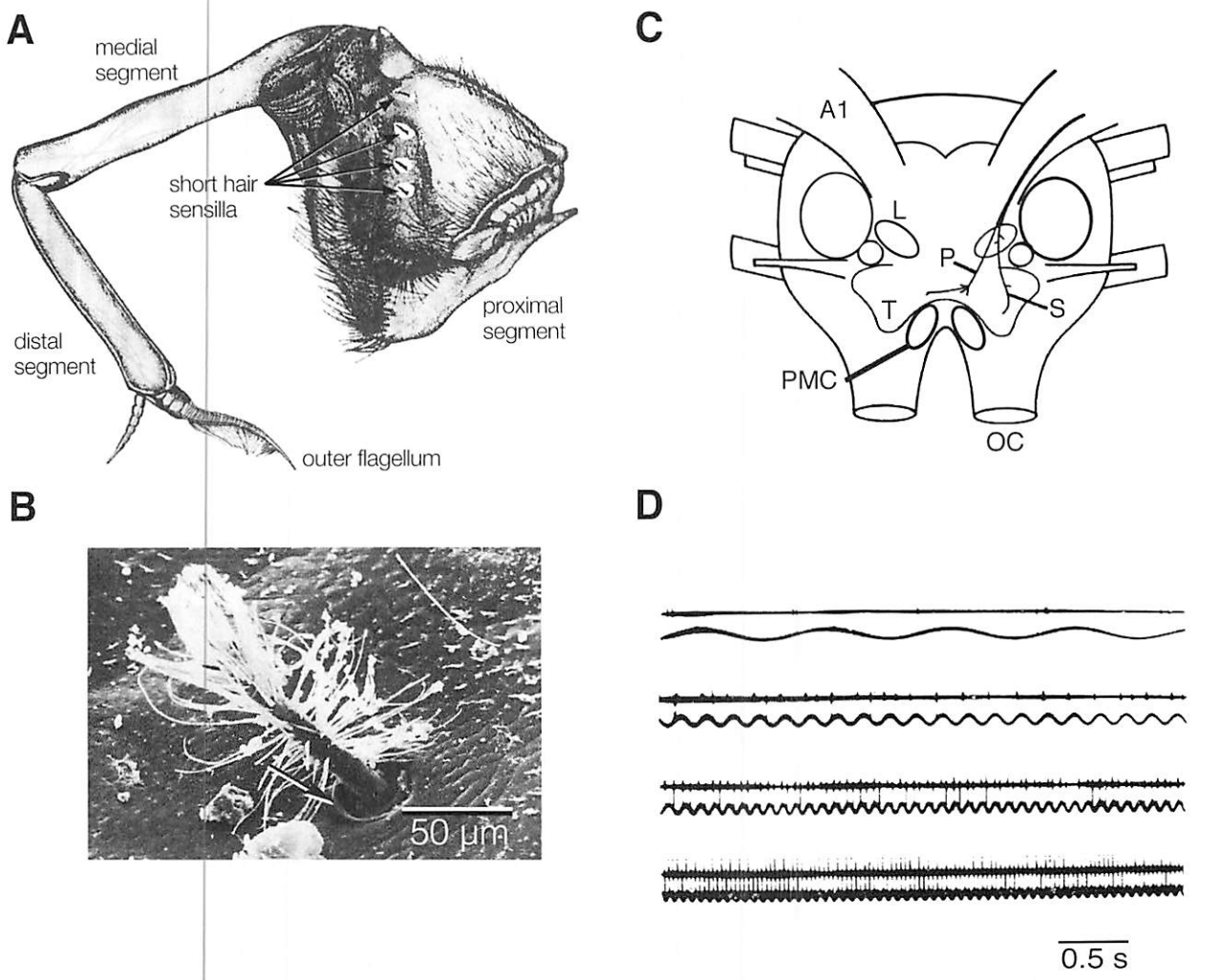

Figure 20. (A) Four short hair sensilla on the proximal segment of the antennule of blue crab. (B) Each sensilla consists of a single setule-laden shaft in a circular pit. (C) Central projection pattern of a type 1B afferent fiber that enters the cerebral ganglion via the antennular nerve [A1] and then gives rise to a primary [P] and secondary [S] neurite. The primary neurite branches anterior to the posteromedial cell tract [PMC] and then crosses over to branch in the corresponding contralateral area; the secondary neurite has initial branches in the lateral antennular neuropil [L] and final branches in the tegumentary [T] neuropil. (D) Extracellular spikes (upper traces) from cerebral ganglion nerve IIIC during sinusoidal oscillation (lower traces) of a single short hair sensillum. At low frequency oscillations, a single cell fires (small spikes), while at higher frequencies two additional cells fire (large downward and upward deflecting spikes). From Roye and Dillaman (1982); Roye (1986, 1994).

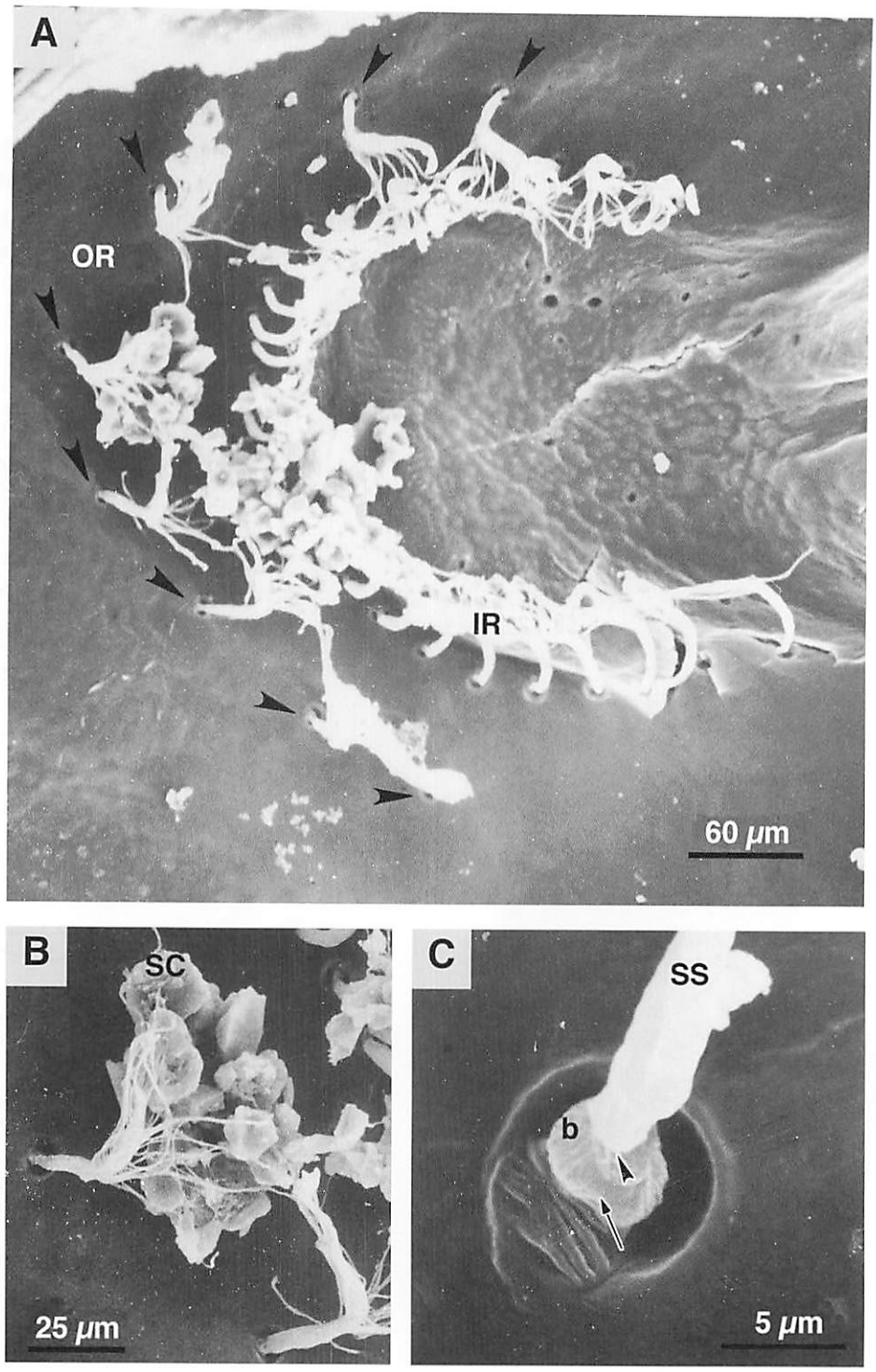

Figure 21. (A) Scanning electron micrograph of inner [IR] and outer [OR] row of blue crab statolith sensilla on ventral floor of statocyst. Arrowheads indicate single outer row sensilla. (B) A single outer row sensillum with its filaments decorated with statoconia [sc]. (C) The shaft [ss] of a statolith sensillum has a fulcrum (arrowhead) on an expanded bulb [b] covered with vertical folds except for a smooth tooth portion (arrow) in line with the fulcrum. From Cate and Roye (1997).

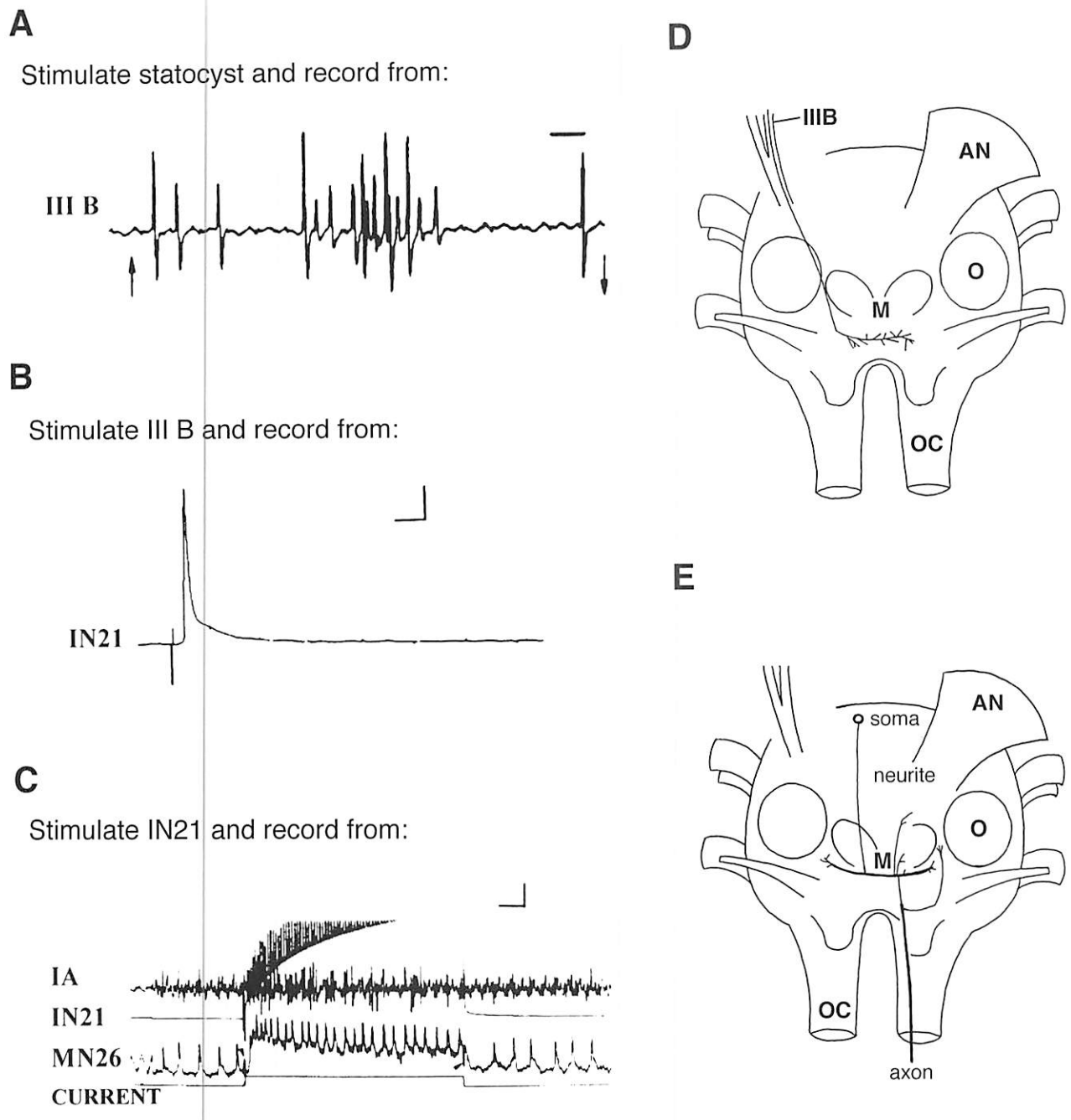

Figure 22. Physiology and morphology of blue crab statolith sensilla. (A) Directional movement of the statolith (between arrows) elicits firing in its axon recorded from sensory nerve [IIIB]. (B) A single stimulus to nerve IIIB results in a spike recorded intracellularly from interneuron 21 [IN21]. (C) Depolarization of [IN21] with current activates withdrawal motoneuron [MN26] with sustained firing of spikes recorded intracellulary from its neurite [MN26] and extracellularly from its motor nerve [1A]. (D) The axon of a single outer row statolith sensillum traveling in nerve [IIIB] forms dendritic branching in the median antennular neuropil [M] of the cerebral ganglion. Antennular nerve [AN], olfactory neuropil [O], oesophageal connective [OC]. (E) Morphology of interneuron 21 with its anteriorly located soma and a single neurite that projects dendrites in the median antennular neuropil [M] overlapping with those of the statolith sensillum, before exiting as an axon via the oesophageal connective [OC].Vertical bars: 10 mV in (B); 2 mV and 2 nA in (C). Horizontal bars: 10 msec in (A); 5 msec in (B); 20 msec in (C). From Cate and Roye (1997).

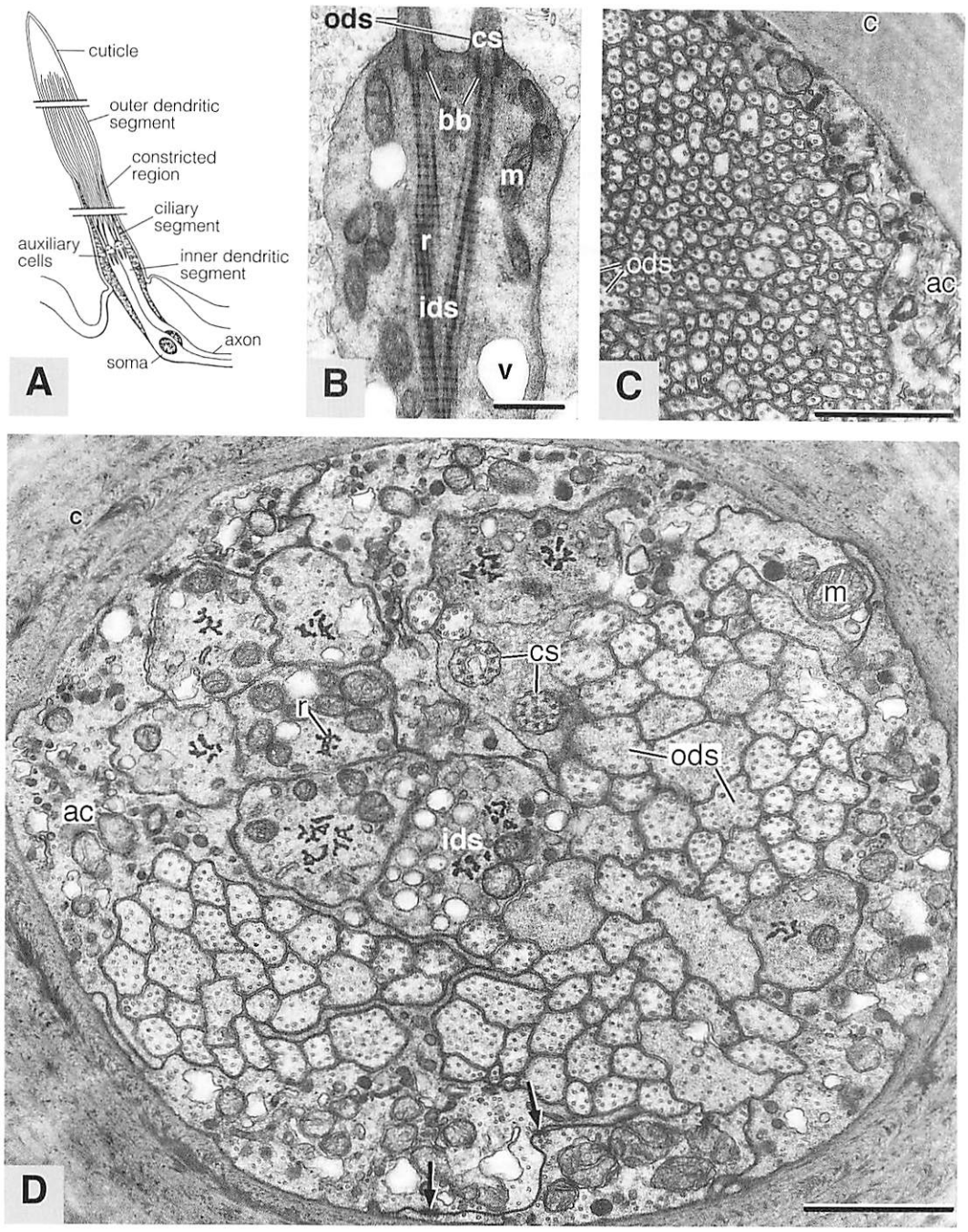

Figure 23. (A) Olfactory sensillum of blue crab depicting only two of about 40-160 sensory neurons innervating a single aesthetasc. Each neuron consists of a single inner dendritic segment that projects from the soma and forms two cilia. These cilia branch profusely to form the outer distal segment where transduction occurs in the aesthetasc. (B) Longitudinal view of transitional zone between inner [ids] and outer [ods] dendritic segments. The inner dendritic segment is supported by rootlets [r] that end in basal bodies [bb]. Originating from the paired basal bodies are ciliary segments [cs] that give rise to the outer dendritic segments. Mitochondria [m]. (C) Cross-section of outer dendritic segment [ods] with numerous branches, most with a single flagellum. Accessory cell [ac]; cuticle [c]. (D) An oblique section within the transitional zone showing inner [ids] and outer [ods] dendritic segments and their connecting ciliary segments [cs]. Ensheathing the dendrites are auxiliary cells [ac] connected via desmosomes (arrows). Cuticle [c]; mitochondria [m]; rootlets [r]. Bars: 0.5 μm in (B); 0.1 μm in (C), (D). From Gleeson et al. (1996).

are separated from the external environment by a thin permeable cuticle. Olfaction occurs primarily in these outer dendritic processes, although details of the mechanism are unknown. The outer dendrites show considerable plasticity in adjusting their length to the prevailing salinity: increasing as freshwater-acclimated crabs are moved to more saline conditions and decreasing as seawater crabs are moved to increasingly freshwater conditions. These length changes occur within a couple of days and may reflect differences in maintaining their effectiveness under variable salinities. In other words, these changes in dendrite length alter the responsiveness of the cells to chemicals. These chemicals may include both pheromones (Gleeson 1982) and food-associated odors (Cate et al. 1999).

INTERNEURONS

Broadly defined as neurons with processes only within the ganglia, relatively few interneurons have been studied in blue crabs. One such group is the interneurons controlling antennule withdrawal (Roye et al. 2000). These are represented by four of the largest axons in the oesophageal connective. The somata of these interneurons originate in the anterior cluster of the cerebral ganglion and give rise to relatively long primary neurites from which arise secondary and tertiary neurites that form extensive branching in several neuropilar regions of the ganglion (Fig. 24). Depolarization of these giant axons evokes withdrawal of the ipsilateral antennule, presumably due to synaptic activation of withdrawal motoneurons. Stimulation of the short hair sensilla of the antennules also elicits withdrawal of the antennule, although such withdrawal occurs independent of interneuronal activity, implying that these interneurons are sufficient but not necessary for antennule withdrawal. These withdrawal interneurons also respond to depolarization of the sensory nerve of statolith sensilla, denoting a strong sensory input for eliciting antennule withdrawal (Fig. 22) (Cate and Roye 1997).

The morphology of interneurons in the blue crab nervous system has been deduced by their immunoreactivity to dopamine (Wood et al. 1995) and proctolin (Wood et al. 1996) in an attempt to find structural correlates for the influence of these neuromodulators on the rhythmic behavior of the swimming paddles. The highly modified swimming paddles have distinctive rhythmic beating patterns for sideways and backwards swimming (Spirito 1972), and also have a third pattern associated with courtship display in males (Wood and Derby 1995). Stimulated by pheromones, the male stands erect on its walking legs with outstretched chelae and rhythmically beats the third maxilliped and the swimming paddle. The latter beats in a rhythmical up and down manner, rotating its most distal segment in the upstroke when the paddle is held erect over the body. Application of a number of chemicals and stimulation of interneurons in the oesophageal connectives suggests the existence of a basic rhythm of the swimming paddle, which is reconfigured to a courtship mode in the presence of proctolin, dopamine, and octopamine (Wood 1995; Wood et al. 1995). The propensity for courtship display in male blue crabs is also modulated hormonally by factors in the sinus gland-X organ complex, an endocrine gland in the eyestalk (Gleeson 1991).

In the cerebral ganglion, dopamine immunoreactivity is located in the form of both fibers and cell bodies (Fig. 25) (Wood and Derby 1996). Cell bodies are also located in the oesophageal ganglion. Dopamine immunoreactive fibers occur in the connectives where descending fibers would qualify as candidate interneurons for involvement in courtship display posture. Dopamine staining of fibers and cell bodies is seen in the compressed ventral nerve cord, where at least one pair of cell bodies stains in the suboesophageal segment and each of the thoracic segments.

Proctolin immunoreactive fibers occur in the optic ganglia and the cerebral ganglia where bilaterally paired somata are also present (Fig. 26) (Wood et al. 1996). A large cluster of cells (250) stain for this peptide in the suboesophageal region of the ventral nerve cord, similar in position to a group of C cells regarded as neurosecretory in crabs (Maynard 1961). The neuritic morphology of these cells varies, with the neurites projecting ipsi- and contra-laterally as well as anteriorly and posteriorly.

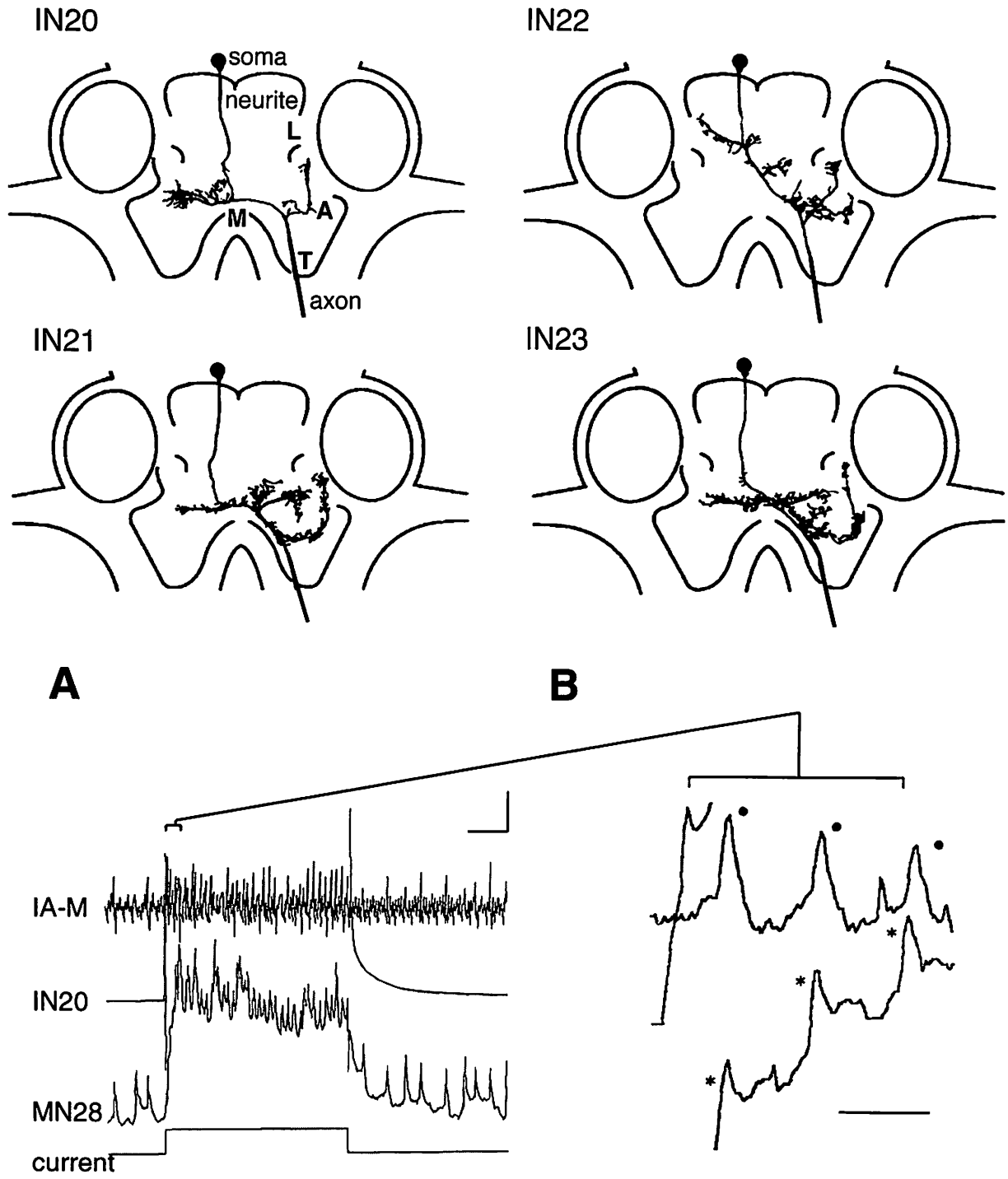

Figure 24. Morphology of four type-1 interneurons [IN20 to IN23] of blue crab, each with the somata in the anterior cluster of the cerebral ganglion and the axon exiting in the contralateral oesophageal connective. Neurites of these interneurons project in several neuropils including antennal [A], lateral antennular [L], median antennular [M], and tegumentary [T]. Physiology of these interneurons as seen (A) when interneuron 20 [IN20] is depolarized (current pulse) evoking a burst of postsynaptic potentials in motoneuron 28 [MN28] which is matched to extracellularly recorded spikes in nerve [IA-M]. In an expanded segment of the recording (B), postsynaptic potentials (asterisks) in [MN28] are matched 1: 1 to spikes (dots) in nerve [IA-M]. Vertical bar in (A): 60 nA for current; 3 mV for [MN28]; 12 mV for [IN20]. Horizontal bar: 80 ms in (A); 5 ms in (B). From Roye et al. (2000).

SUMMARY

Neurobiological research in blue crabs has been opportunistic, focusing on the appendages (antennules, maxillipeds, chelae, walking limbs, and swimming paddles) and the foregut. The antennules have come under study for the neural circuitry underlying their defensive withdrawal behavior. This has provided details of the structure and physiology of the movement-sensitive sensilla, the motoneurons, and the interneurons. Study of the olfactory aesthetasc of the antennules provides new insight into sensory plasticity as the dendrites rapidly adjust their length according to enviromental salinity. Differences in biomechanics of the paired asymmetric (crusher and cutter) chelae and the relative effectiveness of the homologous motoneurons result in the use by the crab of these chelae for crushing and tearing, respectively. The closer muscles of these dimorphic claws, however, are similar, and they have a broad range of sarcomere lengths, all >6 μm and therefore of the slow type. In the walking limb the minute distal accessory flexor muscle, comprised of slow fibers, receives a private excitor, as well as excitors of the parent flexor muscle, resulting in superinnervation. The swimming paddles are modified thoracic limbs with a highly extended range of motion and large surface area. They are powered by large basal muscles with regionally distributed fast and slow fibers (based on myofibrillar ATPase activities) and abundant mitochondria (based on NADH-diaphorase activities). The principal mode of swimming is sideways, although occasionally blue crabs swim backwards, and males wave their paddles in courtship display. Modification of a basic motor pattern appears to underlie these different swimming modes. A stretch receptor situated within the promotor swimming muscle has a large axon that conducts without action potentials. This depolarization at its central terminations triggers chemical transmitter release onto motoneurons, permitting an examination of pre- and post-synaptic events underlying synaptic transmission. Finally, the foregut of blue crabs with its rhythmic movements of the gastric mill and pyloric filter allows study of how motor

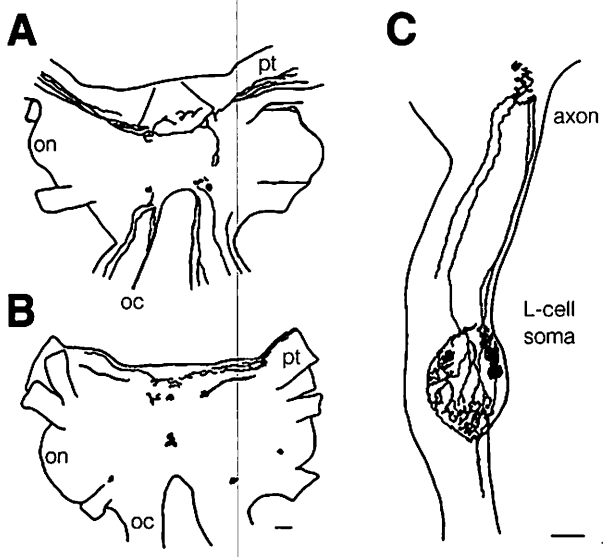

Figure 25. (A) and (B) Dorsal and ventral views of the blue crab cerebral ganglion showing distribution of dopamine immunoreactive fibers and cell bodies in relation to the oesophageal connective [oc], olfactory neuropil [on], and protocerebral tract [pt]. (C) Dopamine immunoreactive fibers and cell bodies in the oesophageal ganglion, including an L-cell with an anterior projecting axon that loops in the cerebral ganglion, returns to the oesophageal ganglion, and projects beyond it. Bars: 250 μm in (A), (B); 50 μm in (C). From Wood and Derby (1996).

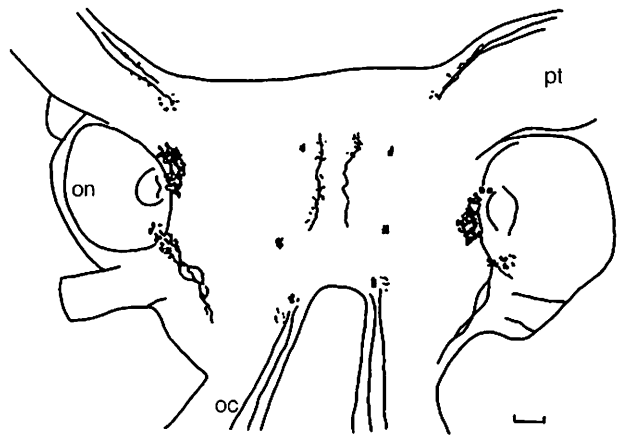

Figure 26. Distribution of proctolin immunoreactive fibers and cell bodies (single or clustered) in the female blue crab in relation to the oesophageal connective [oc], olfactory neuropil [on], and protocerebral tract [pt]. Bar: 250 μm. From Wood et al. (1996).

patterns are translated at the periphery. Because a large number of fast and slow muscles (based on sarcomere lengths and actin:myosin ratios) are innervated by few motoneurons, the neuromuscular synapses of individual excitatory motoneurons are highly differentiated within a muscle and among muscles. Inhibitory axons to the muscles provide a second level of control, while neuromodulatory axons add a third level to control both excitatory and inhibitory innervation. A high degree of differentiation epitomizes the muscles and neurons of blue crabs and invites further exploration.

ACKNOWLEDGMENTS

I thank Joanne Pearce for continuing research and academic support, Rosalind Coulthard for preparing illustrations, and three anonymous reviewers for helpful insights. Financial support for our explorations on blue crab neuromuscular systems reported in this review and for the review itself was generously provided by the Natural Sciences and Engineering Research Council of Canada.

REFERENCES

Atwood, H.L. 1973. An attempt to account for the diversity of crustacean muscle. American Zoologist 13:357-378.

Atwood, H.L. 1976. Organization and synaptic physiology of crustacean neuromuscular systems. Progress in Neurobiology 7:291-391.

Atwood, H.L. 1982. Synapses and neurotransmitters. Pages 105-150 in D.E. Bliss, H.L. Atwood, and D.C. Sandeman (eds.). The Biology of Crustacea. Volume 3. Neurobiology: Structure and Function. Academic Press, New York.

Atwood, H.L. and R.L. Cooper. 1996. Synaptic diversity and differentiation: crustacean neuromuscular junctions. Invertebrate Neuroscience 1:291-307.

Atwood, H.L., C.K. Govind and S.S. Jahromi. 1977. Excitatory synapses of blue crab gastric mill muscles. Cell and Tissue Research 177:145-158.

Atwood, H.L., C.K. Govind and I. Kwan. 1978. Nonhomogenous excitatory synapses of a crab stomach muscle. Journal of Neurobiology 9:17-28.

Atwood, H.L. and W.A. Morin. 1970. Neuromuscular and axo-axonal synapses of the crayfish opener muscle. Journal of Ultrastructural Research 32:351-369.

Atwood, H.L. and J.M. Wojtowicz. 1986. Short-term and long-term plasticity and physiological differentiation of crustacean motor synapses. International Review of Neurobiology 28:275-362.

Blight, A.R. and R. Llinas. 1980. The non-impulsive stretch-receptor complex of the crab: a study of depolarization-release coupling at a tonic sensorimotor synapse. Philosophical Transactions of the Royal Society London B Biological Sciences 290: 219-276.

Blundon, J.A. 1989. Effects of temperature and thermal history on neuromuscular properties of two crustacean species. Journal of Comparative Physiology B 158:689-696.

Blundon, J.A. and V.S. Kennedy. 1982. Mechanical and behavioral aspects of blue crab, *Callinectes sapidus* (Rathbun), predation on Chesapeake Bay bivalves. Journal of Experimental Marine Biology and Ecology 65:47-65.

Bush, B.M.H. 1976. Non-impulsive thoracic coxal receptors in crustaceans. Pages 115-151 in P.J. Mill (ed.). Structure and Function of Proprioceptors in the Invertebrates. Chapman and Hall, London.

Cate, H.S., R.A. Gleeson and C.D. Derby. 1999. Activity-dependent labeling of the olfactory organ of blue crabs suggests that pheromone-sensitive and food-odor sensitive receptor neurons are packaged together in aesthetasc sensilla. Chemical Senses 24:559 (Abstract).

Cate, H.S. and D.B. Roye. 1997. Ultrastructure and physiology of the outer row statolith sensilla of the blue crab *Callinectes sapidus*. Journal of Crustacean Biology 17:398-411.

Chapple, W.D. 1982. Muscle. Pages 151-184 in D.E. Bliss, H.L. Atwood and D.C. Sandeman (eds.). The Biology of Crustacea. Volume 3. Neurobiology: Structure and Function. Academic Press, New York.

Charlton, M.P. 1971. An electrophysiological analysis of maxilliped beating in the blue crab *Callinectes sapidus*. MSc thesis. McGill University, Montreal, Canada. 68 p.

Claiborne, B.J. and J. Ayers. 1987. Functional anatomy and behavior. Pages 9-29 in A.I. Selverston and M. Moulins (eds.). The Crustacean Stomatogastric System. Springer-Verlag, Heidelberg.

Cochran, D.M. 1935. The skeletal musculature of the blue

crab, *Callinectes sapidus* Rathbun. Smithsonian Miscellaneous Collections 92:1-76.

Gleeson, R.A. 1982. Morphological and behavioral identification of the sensory structures mediating pheromone reception in the blue crab, *Callinectes sapidus*. Biological Bulletin 163:162-171.

Gleeson, R.A. 1991. Intrinsic factors mediating pheromone communication in the blue crab, *Callinectes sapidus*. Pages 17-32 in R.T. Bauer and J.W. Martin (eds.). Crustacean Sexual Biology. Columbia University Press, New York.

Gleeson, R.A., L.M. McDowell and H.C. Aldrich. 1996. Structure of the aesthetasc (olfactory) sensilla of the blue crab, *Callinectes sapidus*: transformations as a function of salinity. Cell and Tissue Research 284:279-288.

Golding, D.W. and E. Bayraktaroglu. 1984. Exocytosis of secretory granules - a probable mechanism for the release of neuromodulator in invertebrate neuropiles. Experientia 40:1277-1280.

Govind, C.K. 1992. Claw asymmetry in lobsters: case study in developmental neuroethology. Journal of Neurobiology 23:63-74.

Govind, C.K. and H.L. Atwood. 1982. Neuromuscular systems. Pages 63-101 in D.E. Bliss, H.L. Atwood and D.C. Sandeman (eds.). The Biology of Crustacea. Volume 3. Neurobiology: Structure and Function. Academic Press, New York.

Govind, C.K., H.L. Atwood and D.M. Maynard. 1975. Innervation and neuromuscular physiology of intrinsic foregut muscles in the blue crab and spiny lobster. Journal of Comparative Physiology 96:185-204.

Govind, C.K. and J.A. Blundon. 1985. Form and function of the asymmetric chelae in blue crabs with normal and reversed handedness. Biological Bulletin 168: 321-331.

Govind, C.K. and C.J. Lingle. 1987. Neuromuscular organization and pharmacology. Pages 31-48 in A.I. Selverston and M. Moulins (eds.). The Crustacean Stomatogastric System. Springer-Verlag, Heidelberg.

Govind, C.K., D.E. Meiss, J. She and E. Yap-Chung. 1978. Fiber composition of the distal accessory flexor muscle in several crustaceans. Journal of Morphology 157:151-160.

Govind, C.K., J. Pearce, J.M. Wojtowicz and H.L. Atwood. 1994. "Strong" and "weak" synaptic differentiation in the crayfish opener muscle: structural correlates. Synapse 16:45-58.

Govind, C.K. and T.J. Wiens. 1985. Innervation of the limb accessory flexor muscles in several decapod crustaceans. I. Anatomy. Journal of Neurobiology 16:317-328.

Hajek, I., N. Chari, A. Bass and E. Gutmann. 1973. Differences in contractile and some biochemical properties between fast and slow abdominal muscles of the crayfish (*Astacus leptodactylus*). Physiologica Bohemslovia 22:603-612.

Hamilton, P.V. 1976. Predation on *Littorina irrorata* (Mollusca: Gastropoda) by *Callinectes sapidus* (Crustacea: Portunidae). Bulletin of Marine Science 26:403-409.

Hamilton, P.V., R.T. Nishimoto and J.G. Halusky. 1976. Cheliped laterality in *Callinectes sapidus* (Crustacea: Portunidae). Biological Bulletin 150:393-401.

Hartman, H.B. 1985. Tension receptors on the closer muscle apodeme in the walking legs of the blue crab, *Callinectes sapidus*. Journal of Comparative Physiology 157:355-362.

Hartnoll, R.G. 1971. The occurrence, methods, and significance of swimming in Brachyura. Animal Behavior 19:34-50.

Hawkins, W.E. and H.D. Howse. 1978. A light and electron microscope study of the cardiac ganglion of the blue crab *Callinectes sapidus* Rathbun. Transactions of the American Microscopical Society 97:363-380.

Honsa, J.K. and C.K. Govind. 2002. Structural definition of the neuromuscular system in the swimming-paddle opener muscle of blue crabs. Cell and Tissue Research 307:411-421.

Houlihan, D.F., C.K. Govind and A. El Haj. 1985. Energetics of swimming in *Callinectes sapidus* and walking in *Homarus americanus*. Comparative Biochemistry and Physiology 82A:267-279.

Hoyle, G. 1973. Correlated physiological and ultrastructural studies on specialized muscles. IIIb. Fine structure of the power-stroke muscle of the swimming leg of *Portunus sanguinolentus*. Journal of Experimental Zoology 185:97-110.

Hoyle, G. 1983. Muscles and their Neural Control. John Wiley and Sons, New York. 689 p.

Jahromi, S.S. and H.L. Atwood. 1969. Correlation of structure, speed of contraction, and total tension in fast and slow abdominal muscles of the lobster (*Homarus americanus*). Journal of Experimental Zoology 171:25-38.

Jahromi, S.S. and M.P. Charlton. 1979. Transverse sarcomere splitting: a possible means of longitudinal growth

in crab muscles. Journal of Cell Biology 80:736-742.

Jahromi, S.S. and C.K.Govind. 1976. Ultrastructural diversity in motor units of crustacean stomach muscles. Cell and Tissue Research 166:159-166.

Josephson, R.K. 1975. Extensive and intensive factors determining the performance of striated muscle. Journal of Experimental Zoology 194:135-154.

Lingle, C. 1980. The sensitivity of decapod foregut muscles to acetylcholine and glutamate. Journal of Comparative Physiology 138:187-199.

Llinas, R., I.Z. Steinberg and K.Walton. 1976. Presynaptic calcium currents and their relation to synaptic transmission: voltage clamp study in squid giant synapse and theoretical model for the calcium gate. Proceedings of the National Academy of Sciences USA 73:2918-2922.

Lnenicka, G.A. 1991. The role of activity in the development of phasic and tonic synaptic terminals. Annals of the New York Academy of Sciences 627:197-211.

Maynard, D.M. 1961. Thoracic neurosecretory structures in Brachyura. II. Secretory neurons. General and Comparative Endocrinology 1:237-263.

Maynard, D.M. 1972. Simpler networks. Annals of the New York Academy of Sciences 193:59-72.

Mykles D.L. 1985. Heterogeneity of myofibrillar proteins in lobster fast and slow muscles: variants of troponin, paramyosin, and myosin light chains comprise four distinct protein assemblages. Journal of Experimental Zoology 234:23-32.

Ogonowski, M.M. and F. Lang. 1979. Histochemical evidence for enzyme differences in crustacean fast and slow muscle. Journal of Experimental Zoology 207:143-151.

Patel, V. and C.K. Govind. 1997a. Structural-functional differences of a crab motoneuron to four stomach muscles. Journal of Neurocytology 26:389-398.

Patel, V. and C.K. Govind. 1997b. Synaptic exocytosis of dense-core vesicles in blue crab (*Callinectes sapidus*) stomach muscles. Cell and Tissue Research 289:517-526.

Read A.T. and C.K. Govind. 1997a. Claw transformation and regeneration in adult snapping shrimps: test of the inhibition hypothesis for maintaining bilateral asymmetry. Biological Bulletin 193:401-409.

Read A.T. and C.K. Govind. 1997b. Regeneration and sex-biased transformation of the sexually dimorphic pincer claw in adult snapping shrimps. Journal of Experimental Zoology 279:356-366.

Roye, D.B. 1972. Evoked activity in the nervous system of *Callinectes sapidus* following phasic excitation of the statocysts. Experientia 28:1307-1309.

Roye, D.B. 1979. The physiological basis for pitch-induced antennule movements in the blue crab, *Callinectes sapidus*. Comparative Biochemistry and Physiology 62A:475-484.

Roye, D.B. 1986. The central distribution of movement sensitive afferent fibers from the antennular short hair sensilla of *Callinectes sapidus*. Marine Behavior and Physiology 12:181-196.

Roye, D.B. 1989. Central arborization of motor neurons innervating the antennular proximal segment of *Callinectes sapidus* - proximal segment motoneurons. Marine Behavior and Physiology 14:101-114.

Roye, D.B. 1994. Antennular withdrawal motoneurons in the lateral antennular neuropil of *Callinectes sapidus*. Journal of Crustacean Biology 14:484-496.

Roye, D.B. and D.P. Bashor. 1991. Investigation of single antennular motoneurons in the lateral antennular neuropil of *Callinectes sapidus*. Journal of Crustacean Biology 11:185-200.

Roye, D.B. and R.M. Dillaman. 1982. Morphological and physiological characteristics of the antennular short hair sensilla of *Callinectes sapidus*. Marine Behavior and Physiology 9:59-71.

Roye, D.B., C.M. Kilroy, J.M. Doyle and L.E. Reuss. 2000. Decussating interneurons mediate antennular withdrawal in the blue crab, *Callinectes sapidus*. Journal of Crustacean Biology 20:603-613.

Schurmann, F.-W., R. Sandeman and D. Sandeman. 1991. Dense-core vesicles and non-synaptic exocytosis in the central body of the crayfish brain. Cell and Tissue Research 265:493-501.

Selverston, A.I. and F. Moulins. 1987. The Crustacean Stomatogastric System. Springer-Verlag, Berlin. 388 p.

Sharman, A., R. Hirji, J.T. Birmingham and C.K. Govind. 2000. Crab stomach muscles display not only excitatory but inhibitory and neuromodulatory nerve terminals. Journal of Comparative Neurology 425:70-81.

Silverman, H. and M.P. Charlton. 1980. A fast oxidative crustacean muscle: histochemical comparison with

other crustacean muscles. Journal of Experimental Zoology 211:267-273.

Spirito, C.P. 1972. An analysis of the swimming behavior of the portunid crab, *Callinectes sapidus*. Marine Behavior and Physiology 1:261-276.

Tisdale, A.D. and Y. Nakajima. 1976. Fine structure of synaptic vesicles in two types of nerve terminals in crayfish stretch receptor organs: influence of fixation methods. Journal of Comparative Neurology 165:369-386.

Tryba, A.K. and H.B. Hartman. 1997. Dynamic responses of series force receptors innervating the opener muscle apodeme in the blue crab, *Callinectes sapidus*. Journal of Comparative Physiology A 180:215-221.

Tse, F.W., C.K. Govind and H.L. Atwood. 1983. Diverse fiber composition of swimming muscles in the blue crab, *Callinectes sapidus*. Canadian Journal of Zoology 61:52-59.

Uchizono, K. 1967. Inhibitory synapses on the stretch receptor neurone of the crayfish. Nature 214:833-834.

Walrond, J.P., C.K. Govind and S.E. Huestis. 1993. Two structural adaptations for regulating transmitter release at lobster neuromuscular synapse. Journal of Neuroscience 13:4831-4845.

White, A.Q. and C.P. Spirito. 1973. Anatomy and physiology of the swimming musculature in the blue crab, *Callinectes sapidus*. Marine Behavior and Physiology 2:141-153.

Wiens, T.J. and C.K. Govind. 1985. Innervation of the limb accessory flexor muscles in several decapod crustaceans. II. Electrophysiology. Journal of Neurobiology 16:349-359.

Wiersma C.A.G. 1961. The neuromuscular system. Pages 191-240 in T.H. Waterman (ed.). The Physiology of Crustacea. Academic Press, New York.

Wood, D.E. 1995. Neuromodulation of rhythmic motor patterns in the blue crab *Callinectes sapidus* by amines and the peptide proctolin. Journal of Comparative Physiology A 177:335-349.

Wood, D.E. and C.D. Derby. 1995. Coordination and neuromuscular control of rhythmic behaviors in the blue crab, *Callinectes sapidus*. Journal of Comparative Physiology A 177:307-319.

Wood, D.E. and C.D. Derby. 1996. Distribution of dopamine-like immunoreactivity suggests a role for dopamine in the courtship display behavior of the blue crab, *Callinectes sapidus*. Cell and Tissue Research 285:321-330.

Wood, D.E., R.A. Gleeson and C.D. Derby. 1995. Modulation of behavior by biogenic amines and peptides in the blue crab, *Callinectes sapidus*. Journal of Comparative Physiology A 177:321-333.

Wood, D.E., M. Nishikawa and C.D. Derby. 1996. Proctolin-like immunoreactivity and identified neurosecretory cells as putative substrates for modulation of courtship display behavior in the blue crab, *Callinectes sapidus*. Journal of Comparative Neurology 368:153-163.

Young, R.E., J. Pearce and C.K. Govind. 1994. Establishment and maintenance of claw bilateral asymmetry in snapping shrimps. Journal of Experimental Zoology 296:319-326.

Chapter 5

The Functional Anatomy of the Circulatory System

IAIN J. MCGAW AND CARL L. REIBER

INTRODUCTION

There are a number of classical papers that describe the anatomy of the decapod crustacean circulatory system in detail. However, most of these articles were written at the beginning of the last century or the end of the previous century before the advent of modern imaging techniques allowed the detailed analysis of the circulatory system to be resolved (Haeckel 1857; Claus 1884; Bouvier 1891; Pearson 1908; Baumann 1921; Brody and Perkins 1930). A comprehensive study of the cardiovascular system of the blue crab *Callinectes sapidus* was carried out by Pyle and Cronin (1950), but these workers limited their descriptions to the major arterial systems, with only minimal coverage of the finer vasculature. We used two methods to map the entire circulatory system of *C. sapidus*: (1) injection of barium sulfate into the heart, followed by X-ray analysis and (2) injection of resin (Batson's Monomer) into the circulation, followed by soft tissue maceration and chitinous tissue removal with acid (McGaw and Reiber 2002). In this chapter we provide a detailed analysis of the anatomy of the circulatory system of *C. sapidus* and relate this to cardiovascular regulatory mechanisms, physiological behavior, and cardiovascular dynamics in decapod crustaceans.

A Synopsis of the Crustacean Circulatory System

The brachyuran crustacean circulatory system includes a single chambered heart that is suspended in a primary chamber, the pericardial sinus, by 11 suspensory ligaments (Maynard 1960). Hemolymph is pumped out into seven arteries (five arterial systems) (Figs. 1, 2, 3). Five arteries flow anteriorly: the anterior aorta, the paired anterolateral arteries, and the paired hepatic arteries. The small posterior aorta exits the heart posteriorly, and the largest artery, the sternal artery, exits the heart ventrally and divides thereafter to supply the limbs and mouthparts (Pearson 1908; Baumann 1921; Pyle and Cronin 1950; McLaughlin 1983). Each artery is valved at its origin (Alexandrowicz 1932) and opening or closing of the valves controls hemolymph flow into each arterial system. All arteries branch into smaller arteries and fine capillary-like vessels that ramify within the tissues. Arterial hemolymph perfuses the tissues at the level of the lacuna, where gas, nutrient, and waste exchange takes place.

Sandeman (1967) suggests that hemolymph is contained in a capillary-like network in portions of the circulatory system, which would make gas exchange in these areas similar to capillary exchange in vertebrate systems. Work by Abbott (1971) on the green crab *Carcinus maenas* suggests a unique type of blood channel analogous to capillaries, associated with the crab's nervous system. These capillaries are lined with glial cells and thus the vessel endothelium is of ectodermal origin yet is functionally a capillary exchange bed. Capillary-like structures have also been reported in the antennal glands of crayfish, and blue crabs appear to have similar structures (Miyawaki and Ukeshima 1967).

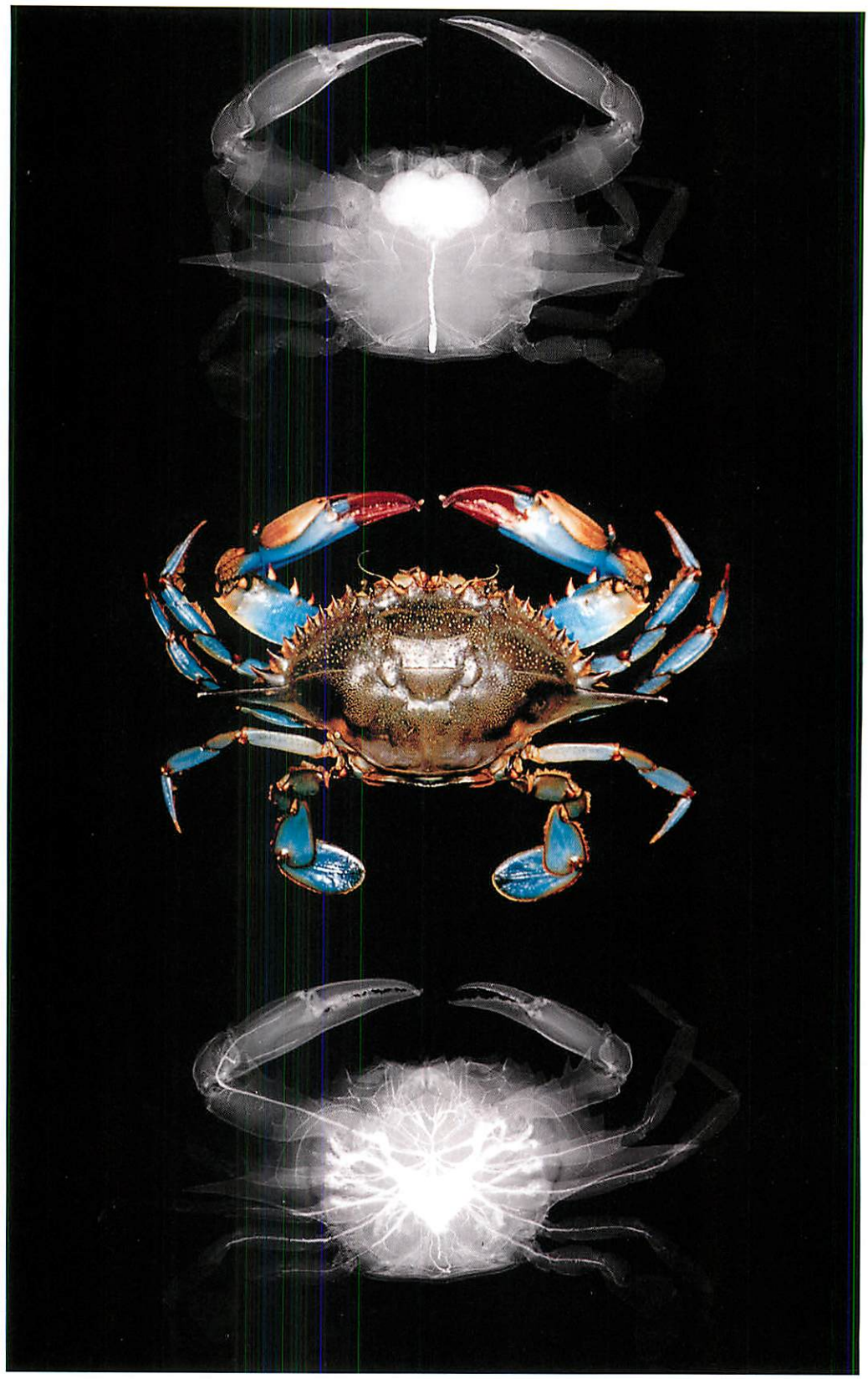

Figure 1. General form of the circulatory and digestive systems of *Callinectes sapidus*. The top figure shows the heart-shaped stomach region along with the midgut, obtained by X-raying the animal after a barium meal. The bottom image is an X-ray showing the heart and vasculature after injection with barium sulfate. From McGaw and Reiber (2002).

Decapod crustaceans lack a complete venous system. Specifically, hemolymph first drains into interstitial lacunae (small irregular spaces between tissues) and then into sinuses, which are large irregular inter-tissue spaces (Maynard 1960) that are often so poorly defined that they almost defy successful demonstration (Pyle and Cronin 1950). The hemolymph from these sinuses eventually collects in the large sternal or ventral thoracic sinus below the heart, which extends into five branchial sinuses. These empty into the infrabranchial sinus that extends along the posterior edges of the gills. From here, hemolymph flows into the gills by way of the afferent branchial veins and percolates through the lamellae where it is oxygenated. Hemolymph returns to the pericardial sinus via the branchiocardiac veins and then flows into the heart through three pairs of ostia (Maynard 1960; McLaughlin 1983). By definition, these veins differ from the sinuses because they are large, structurally distinct vessels that function solely as defined blood flow channels (Maynard 1960).

During the last decade, the physiology and control of the cardiovascular system has received extensive investigation (see McMahon and Burnett 1990; McGaw et al. 1994a; McMahon et al. 1997; McMahon 1999, 2001; Wilkens 1999). Cardiac parameters and hemolymph flow rates change in response to exercise (DeWachter and McMahon 1996a; McGaw and McMahon 1998), feeding (McGaw and Reiber

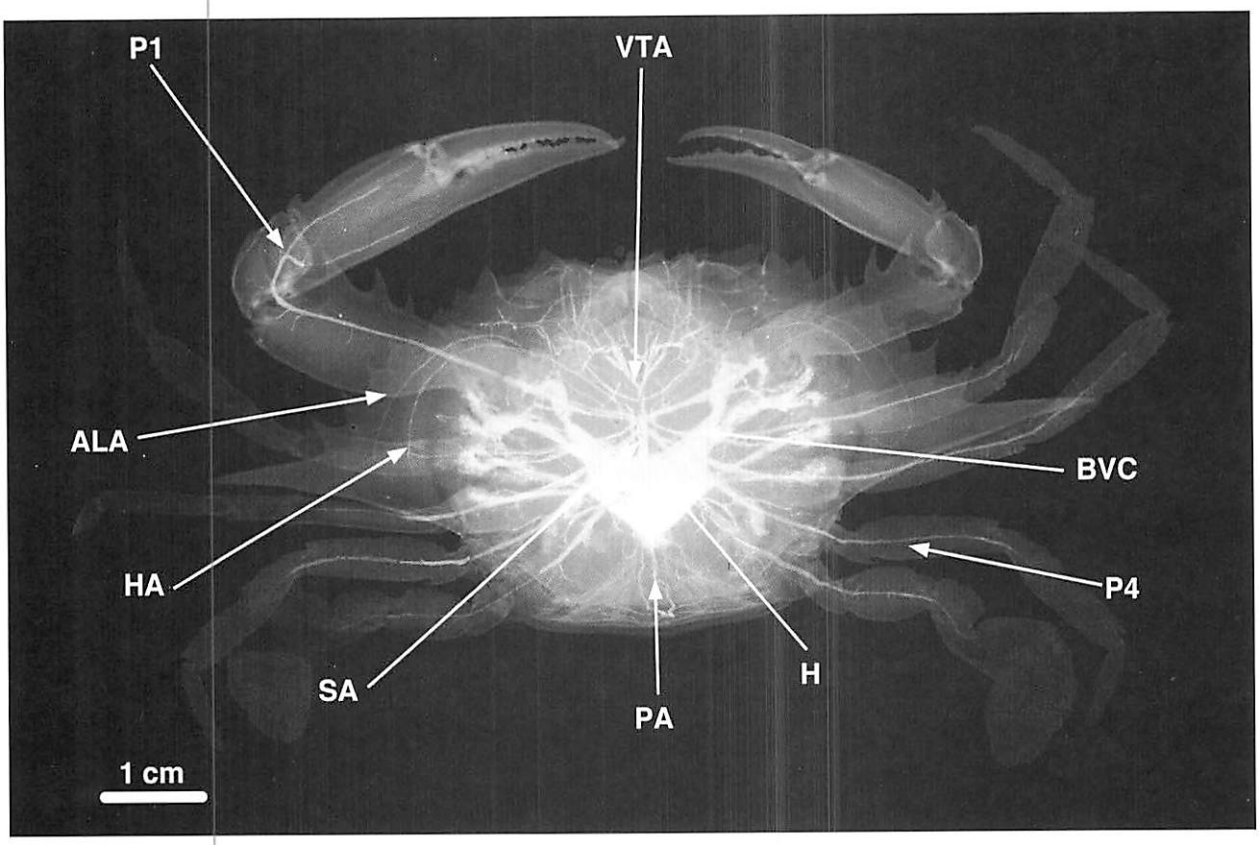

Figure 2. Dorsal view of the arterial system of *Callinectes sapidus* after injection of a suspension of barium sulfate into the pericardial sinus. The heart [H] and branchiocardiac veins [BCV] are clearly visible. The sternal artery [SA] exits ventrally and anteriorly before giving rise to the ventral thoracic artery [VTA], which splits and supplies hemolymph to the mouthparts, and the 5 pereopod arteries [P1-P5] (P1 and P4 labeled on figure). The small posterior aorta [PA] exits posteriorly and ventrally; the paired hepatic arteries [HA] and anterolateral arteries [ALA] exit from the anterior end of the heart. The anterior aorta was not seen in these preparations. From McGaw and Reiber (2002).

2000), hypoxia (Airriess and McMahon 1994; Reiber 1995, Reiber and McMahon 1998), emersion (Airriess and McMahon 1996), low salinity (McGaw and McMahon 1996; McGaw and Reiber 1998), and temperature change (DeWachter and McMahon 1996b). The system is now recognized as being relatively complex, with control mechanisms and pressures that rival some of the simple vertebrate closed systems (McMahon and Burnett 1990). In addition to modulation by environmental variables, a number of naturally occurring peptide and amine neurohormones modulate cardiac activity and differential hemolymph flow in intact crabs (Airriess and McMahon 1992; McGaw et al. 1994b, 1995; McGaw and McMahon 1995, 1997, 1999). These hormones act on the cardioarterial valves, the artery walls, central nervous system, or the cardiac muscle itself (Wiersma and Novitiski 1942; Wilkens et al. 1974).

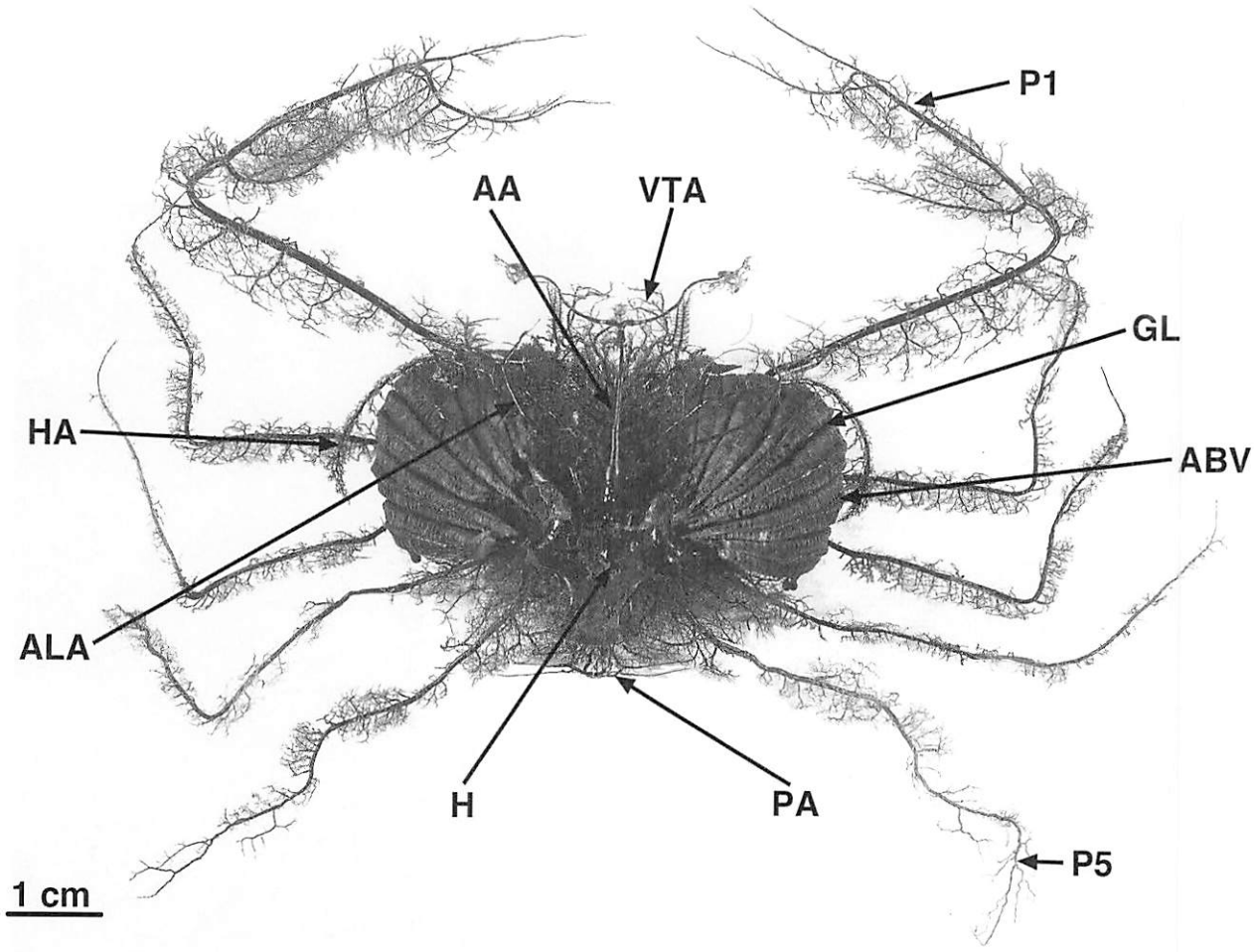

Figure 3. Dorsal view of a resin cast (made using Batson's Monomer No. 17) of the circulatory system of *Callinectes sapidus*; the branchiostegal circulation has been removed. The gills are intact and six afferent branchial veins [ABV] run between the gill lamellae [GL]. The heart and pericardial sinus [H] are situated slightly posterior to the midline of the carapace. The anterior aorta [AA], anterolateral arteries [ALA], and hepatic arteries [HA] branch off the anterior end of the heart. The posterior aorta [PA] exits posteriorly from the heart. Supplying hemolymph to the mouthparts and limbs respectively, the ventral thoracic arteries [VTA] and pereopod arteries [P1-P5] (P1 and P5 are labeled on figure) are branches of the sternal artery (not shown). From McGaw and Reiber (2002).

THE CIRCULATORY SYSTEM OF *CALLINECTES SAPIDUS*

The Heart

The heart lies on the dorsal part of the cephalothorax, just under the carapace, slightly posterior to the middle of the body, and directly above the midgut region. It lies inside the pericardial sinus and the whole structure is roughly pentagonal in shape (Fig. 4). The neurogenic myocardium of the crab heart is stimulated to contract by nerves from the cardiac ganglion that overlie and are embedded within the cardiac muscle. The cardiac ganglion serves as the pacemaker of the heart and regulator of myocardial contractile force (Maynard 1960). Cardiac ganglion output is influenced by cardioregulatory nerves (inhibitory and acceleratory fibers) that originate from the anterior ventral nerve cord and subesophageal ganglion (Wiersma and Novitiski 1942; Wilkens et al. 1974). Central neural integration of cardiac function appears to originate from command interneurons found in the circumesophageal ganglion that are able to cause tachycardia, bradycardia, and cardiac arrest (McMahon and Wilkens 1983).

Cardiac function may also be influenced by cardioactive hormones and neuropeptides released by specialized neurosecretory terminals of the pericardial organ. The pericardial organ lies in the pericardial cavity that completely surrounds the heart. It consists of nerve trunks, plexuses, and nerve endings. The site of release of cardioactive hormones is located directly upstream from the heart; the hormones enter the heart during diastole (Taylor 1982). Because all these neurosecretory products are released into the general circulation and because there are interactions between other components of the circulatory system, each substance that is released can potentially act at multiple sites other than the cardiac ganglion. These sites may include the myocardium, cardioarterial valves, and the central nervous system's regulatory center (Saver and Wilkens 1998). Additionally, both the ostia (paired filling inlets to the heart that are located dorsally, laterally, and ventrally on the heart) and cardioarterial valves appear to be innervated, thus enabling regulation of both filling and arterial perfusion.

Heart rate in *Callinectes sapidus* can be modulated by several environmental variables (see DeFur and Mangum 1979). However, one must be cautious when inferring an adaptive role from heart rate alone, because cardiac output and regional tissue perfusion may not be solely dependent on heart rate; changes in stroke volume of the heart or contraction/relaxation of the cardioarterial valves may play a significant role in determining cardiovascular dynamics (McGaw et al. 1994a).

The Arterial System

Seven arteries (five arterial systems) originate from the heart and subsequently branch to supply

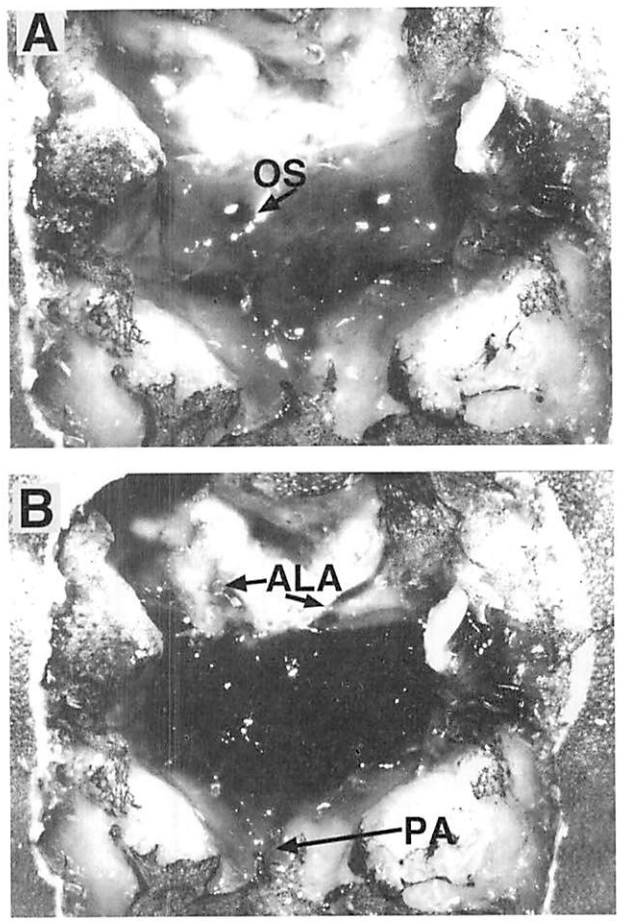

Figure 4. Photograph of the dye-injected heart of *Callinectes sapidus*, *in situ*, during (A) systole and (B) diastole, showing the ostia [OS], and the exit points of the anterolateral arteries [ALA] and posterior aorta [PA].

distinct regions of the body. Each of these is discussed in turn.

Anterior Aorta

The anterior aorta (AA) (previous authors have named it the ophthalmic artery, cephalic artery, dorsal median artery, median lateral artery, median aorta, median cephalic artery, or carotid artery) exits from the medial dorsal anterior aspect of the heart (Fig. 3) and is wider for the first third of its length. The functional significance of this tapered design is unclear, and it is not mentioned by Pyle and Cronin (1950) or in papers on other crab species (Pearson 1908; McLaughlin 1983; Airriess 1994; Davidson and Taylor 1995). The anterior aorta continues anteriorly over the gonads as well as the pyloric and cardiac stomachs, then dips ventrally towards the rostrum on the anterior edge of the carapace. It is the third largest artery in terms of diameter. Despite the anterior aorta's large diameter, hemolymph flow rates in this artery are relatively low. In *C. sapidus*, only 3 to 7% of the total cardiac output is delivered through this vessel (McGaw and Reiber 1998, 2000). By comparison, less than 1% of the cardiac output is pumped through the anterior aorta of the Dungeness crab *Cancer magister* (Airriess and McMahon 1994, 1996; McGaw et al. 1994a, b; McGaw and McMahon 1995, 1998, 1999). Hemolymph flow in this artery is characterized by regular periods of decreased flow or total cessation (McGaw et al. 1994a). In fact, in brachyuran crustaceans, this artery is only perfused heavily during periods of emersion (Airriess and McMahon 1996), acute exposure to low salinity (McGaw and Reiber 1998), and in response to the neurohormone octopamine (Airriess and McMahon 1992).

At the end of the anterior aorta is an enlarged region (Fig. 5A, B), the cor frontale (CF), which consists of tendons and two strips of striated muscle (Steinacker 1978). Although its exact function has not yet been defined, it is thought to act as an auxiliary heart, aiding hemolymph flow into the supraesophageal ganglion (brain) during periods of acardia (cessation of cardiac contraction) (Steinacker 1978; Davidson and Taylor 1995). The cor frontale may also behave as a variable elastic buffer by dampening pressure pulses to the cerebral vessels (Davidson and Taylor 1995).

Three arteries extend from the cor frontale: the cerebral artery and the paired optic arteries. The small cerebral artery (CA) branches anteriorly from the cor frontale and divides in two around the optic and oculomotor neuropiles, and numerous capillaries ramify throughout the supraesophageal ganglion (Haeckel 1857; Sandeman 1967). The paired optic arteries (OA) (also referred to as the ophthalmic arteries, or lateral ophthalmic arteries) exit at right angles to the anterior aorta and follow the anterior edge of the carapace (Fig. 5A); as their name suggests they supply hemolymph to the eyes. Each optic artery splits into smaller capillaries that ramify throughout the retina (Sandeman, 1967; Fig. 5B). There are also enlarged regions or lacunae around the position of the sinus gland and X-organ complex, organs that are involved with hormone production and that require a good blood supply to ensure effective hormone delivery to other areas of the body. One lateral optic artery (LOA) protrudes from each optic artery where it meets the eye (Fig. 5A). The lateral optic arteries are situated 180° relative to the optic arteries and run back towards the midline of the carapace, supplying hemolymph to the ventral flexor and dorsal extensor muscles of the eyes and antennae. Branches of these arteries may also supply the antennules. In freshly injected animals, the Batson's Monomer could be seen in the antennules; however, these fine vessels were lost during the tissue maceration process. In the crayfish *Astacus fluviatilis* (Baumann 1921) and the rock lobster *Jasus lalandii* (Paterson 1968), the eye muscles also receive a co-lateral hemolymph supply from the oculomotor arteries (Baumann 1921), which branch off the anterolateral arteries. However, this does not appear to be the case in brachyuran crustaceans (Pearson 1908; Pyle and Cronin 1950).

Anterolateral Arteries

The anterolateral arteries (ALA) (also referred to as the anterior lateral arteries, antennary arteries/aorta, lateral arteries, antennal artery, or lateral

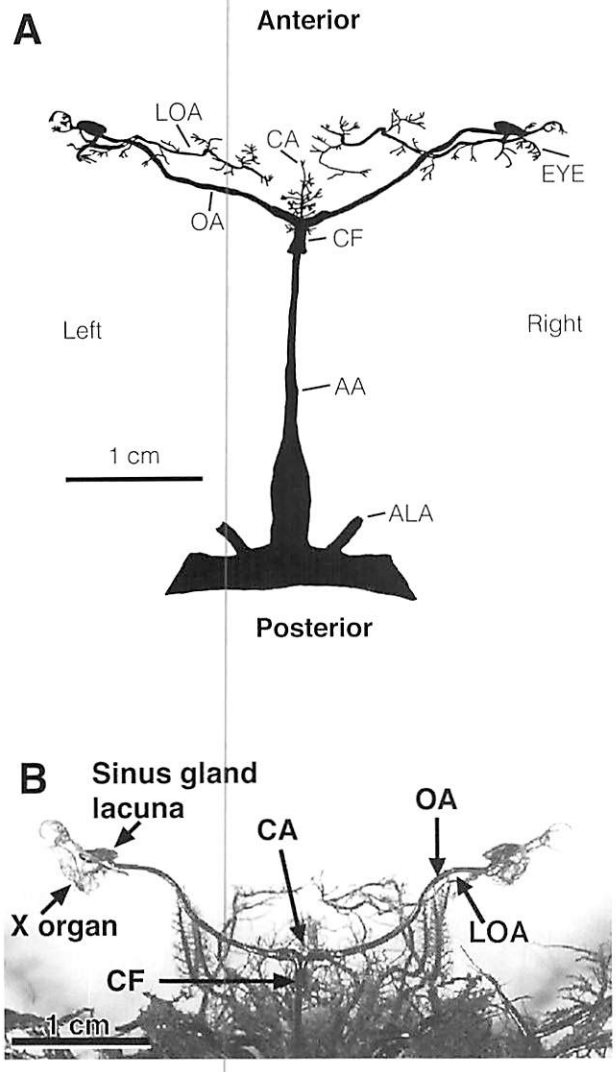

Figure 5. (A) Line drawing of the anterior aorta complex [AA] of *Callinectes sapidus* (dorsal view). The anterior aorta is enlarged at the end, forming the cor frontale [CF]. The small cerebral artery [CA] arises anteriorly from the cor frontale and the optic arteries [OA] exit laterally from this structure. The optic arteries perfuse the eyestalks. Smaller vessels, the lateral optic arteries [LOA], branch from the optic arteries to supply hemolymph to the antennules. Anterolateral artery [ALA]. (B) Enlarged view of a resin cast of eyestalks to show vessels ramifying the eye. The X-organ complex on the posterior face of the eye is heavily perfused and a small lacuna lies just below each sinus gland. Abbreviations as in (A). From McGaw and Reiber (2002).

cephalic arteries) extend dorsally and anteriorly from the heart at approximately a 40° angle, relative to the anterior aorta (Figs. 2, 3, 6), but are narrower in diameter than the anterior aorta. The first medial branch of the anterolateral artery is the cardiac stomach artery (CSA), which dips ventrally and anteriorly, passing through the gonads; additional branches leave the gonads and supply hemolymph to the pyloric and cardiac stomachs as well as the cardiopyloric muscles (Fig. 6). A second smaller branch also arises medially, but more anteriorly, from the main branch of the anterolateral artery; it progresses medially and anteriorly, but the course of this artery is more superficial than the cardiac stomach artery. This artery also supplies hemolymph to the gonads and we named this vessel the lesser gonadal artery (LGA).

The anterolateral artery continues its course and a large branch, the gonadal artery (GOA) (also referred to as the ovarian artery or spermatic artery), exits laterally at right angles to the main vessel, about two-thirds along its length. Almost immediately after branching off the anterolateral artery, the gonadal artery bends 90° anteriorly and runs parallel to the anterolateral artery, dorsal to the gonads, and supplies hemolymph to the gonads and the hypodermis of the cephalothorax. It then bends 90° laterally and extends out to the lateral surfaces of the cephalothorax; running superficially and dorsal to the hepatopancreas, the gonadal artery supplies hemolymph to this gland (Fig. 6). The gonadal artery bifurcates terminally, with one branch going laterally to the hypodermis of the lateral spine and the other continuing posteriorly around the distal dorsal edge of the hepatopancreas. A smaller lateral branch of the gonadal artery, the posterior hepatic artery (PHA), provides hemolymph to the posterior dorsal part of the hepatopancreas and carapace (Fig. 6).

Serving as a source for yet two more arteries, the main anterolateral artery continues anteriorly and superficially (dorsal to the gonads and hepatopancreas) towards the head region of the crab. As it passes the cardiac stomach, it dips down slightly and bifurcates. The medial branch is the antennal gland artery (AGA) (or antennary artery), which supplies hemolymph to the antennal gland and the antennae

(in the current preparations, the fine arteries in the antennae were lost). The outside branch is the mandibular artery (MA) (or external abductor mandibular artery, antennary artery), which supplies the external adductor muscles of the mandibles through a number of parallel sub-branches (Fig. 6). Other very fine vessels also branch along the length of the anterolateral artery, supplying hemolymph to the gonads, the hypodermis of the central cephalothorax, the posterior adductor muscle of the mandible, and the anterior parts of the branchiostegal circulation (Fig. 6).

The morphology of the blue crab's anterolateral artery is very uniform when compared with that of other crab species (Pearson 1908; Airriess 1994; Davidson and Taylor 1995). From measurements of the resin casts, only 2.7% of the hemolymph is contained in the anterolateral arteries; however, these arteries receive approximately 10% of the total cardiac output in *Callinectes sapidus* (McGaw and Reiber 1998, 2000) and 20% of the cardiac output in *Cancer magister* (McGaw and McMahon 1995, 1998, 1999). In *C. sapidus*, hemolymph flow increases in this artery during acute exposure to low salinity (McGaw and Reiber 1998) and during feeding (McGaw and Reiber 2000). In *C. magister*, hemolymph flow through the anterolateral artery decreases in response to the neurohormones proc-

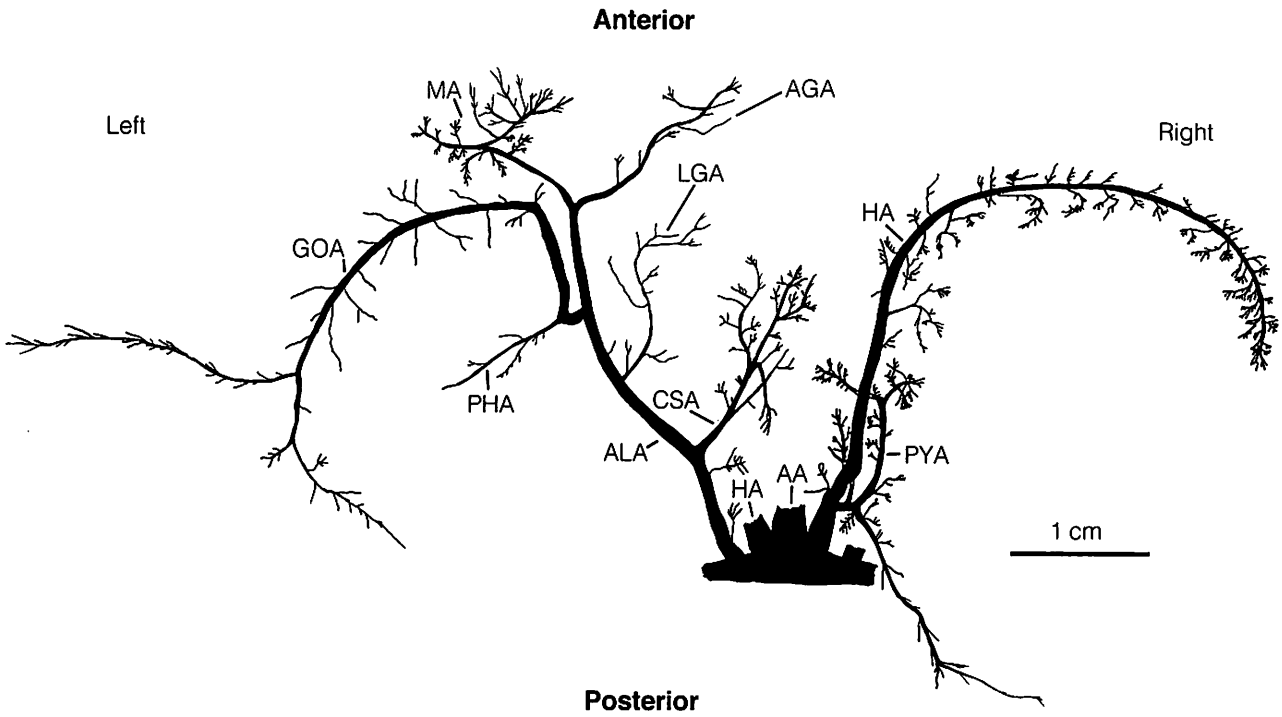

Figure 6. Line drawing of the paired anterolateral arteries [ALA] and hepatic arteries [HA] of *Callinectes sapidus* (only one of each pair shown). The cardiac stomach artery [CSA] and a smaller artery (lesser gonadal artery [LGA]) supplying hemolymph to the gonads branch off the inner surface of the anterolateral artery. At its end, the anterolateral artery splits into the mandibular artery [MA] and antennal gland artery [AGA]. The gonadal artery [GOA] exits at right angles from the outside of the anterolateral artery. This artery and its branch, the posterior hepatic artery [PHA], supply hemolymph to the gonads, hepatopancreas, and hypodermis. Smaller branches near the origin of the heart supply the branchiostegal circulation. The paired hepatic arteries perfuse the hepatopancreas and arise more ventrally than the ALAs, while the smaller pyloric hepatic artery [PYA] flows anteriorly under the stomach, along the midgut, and up and around the posterior edge of the hepatopancreas. Anterior aorta [AA]. From McGaw and Reiber (2002).

tolin (McGaw et al. 1994b) and F1 and F2 (McGaw and McMahon 1995), hypoxic exposure (Airriess and McMahon 1994), emersion (Airriess and McMahon 1996), and exposure to low salinity (McGaw and McMahon 1996). Conversely, hemolymph flow increases during activity (DeWachter and McMahon 1996a; McGaw and McMahon 1998) and in response to the neurohormone crustacean cardioactive peptide (CCAP) (McGaw et al. 1994b). When a physiological role is considered for some of these changes in flow through the anterolateral artery, the direction and magnitude often does not change as expected. The anterolateral artery has many sub-branches that lead to specific organs (Fig. 6) and pulsed-Doppler flowmeter recordings have been made on the first part of the main artery as it exits the heart. The vascular resistance of the arteries can be changed by various neurohormones, thus modulating blood flow to peripheral regions (Wilkens 1997; Wilkens et al. 1997). Therefore the changes that occur at the base of the artery may not necessarily reflect the perfusion levels of each individual branch of the anterolateral artery and its associated organs.

Hepatic Arteries

The paired hepatic arteries (HA) (also referred to as the lateral arteries) arise anteriorly and ventrally from the heart at about a 10° angle relative to the anterior aorta (Fig. 6). These arteries are depicted as very small vessels in portunid crabs (McLaughlin 1983), the rock lobster (Paterson 1968), crayfish species (Baumann 1921; Reiber 1994), and the shrimp *Caridina laevis* (Pillai 1963). However, in *Callinectes sapidus* they are greater in diameter than the anterolateral arteries (Figs. 2, 3, 6; Pyle and Cronin 1950). They are also the second largest arteries in terms of diameter in the Dungeness crab (Airriess 1994), the edible crab *Cancer pagurus* (Pearson 1908), and the New Zealand paddle crab *Ovalipes catharus* (Davidson and Taylor 1995). Almost immediately, these arteries dip ventrally under the stomach and laterally into the hepatopancreas (Fig. 6). Each hepatic artery gives off many capillary-like vessels that ramify profusely within the hepatopancreas. In *C. pagurus* (Pearson 1908) and *C. magister* (Airriess 1994), the main hepatic artery has two large branches that, when viewed from a dorsal aspect, lie posterior to the anterolateral arteries. However, in *C. sapidus* the hepatic artery is a single branch and it lies much closer to the anterolateral arteries when viewed dorsally (Figs. 2, 3, 6). The hepatopancreas of *C. sapidus* is smaller than that of cancrid crabs, accounting for the single instead of doubled branched system.

A small lateral branch, the pyloric hepatic artery (PYA), exits each hepatic artery soon after it leaves the heart and is much larger than previously described for *Callinectes sapidus* (Pyle and Cronin 1950). This vessel bifurcates almost immediately: one branch curves anteriorly under the pyloric and cardiac stomachs, and the midgut caeca, supplying hemolymph to these tissues; the other branch issues posteriorly, running along the midgut before turning dorsally around the posterior ventral margin of the hepatopancreas (Fig. 6).

When hemolymph flow was measured in the hepatic arteries with internal Doppler probes, hemolymph flow rates in these arteries were very uniform (McGaw and McMahon 1995, 1998, 1999; McGaw and Reiber 1998, 2000). The arteries receive 15 to 20% of the cardiac output in *Callinectes sapidus* (McGaw and Reiber 1998, 2000) and 25 to 30% of cardiac output in *Cancer magister* (McGaw and McMahon 1995, 1998, 1999). Flow rates decrease in response to perfusion of high concentrations of the neurohormones F1 and F2 (McGaw and McMahon 1995) and gamma aminobutyric acid (GABA) (McGaw and McMahon 1999); they increase during periods of feeding and subsequent digestion (McGaw and Reiber 2000).

Posterior Aorta

The posterior aorta (PA) (also referred to as the superior abdominal artery/aorta or dorsal abdominal artery) (Figs. 2, 3, 7) is a narrow-diameter vessel that leaves the posterior ventral side of the heart. In all brachyuran crustaceans (including *Callinectes sapidus*), the posterior aorta is the smallest-diameter artery (Fig. 7; Pearson 1908; Pyle and Cronin 1950).

Estimates from corrosion casts show that it holds 0.8% of the blood and receives only 1 to 3% of total cardiac output (McGaw and McMahon 1995, 1998, 1999; McGaw and Reiber 1998, 2000). In anomuran crustaceans, the posterior aorta is larger, receiving 12.3% of cardiac output in the red swamp crayfish *Procambarus clarkii* (Reiber 1994; Reiber et al. 1992) and 20.7% of the total cardiac output in the American lobster *Homarus americanus* (Reiber et al. 1997). It supplies the well-developed musculature of the abdomen (Baumann 1921; Pillai 1963; Paterson 1968). As the posterior aorta exits the heart of *C. sapidus*, two fine arteries branch at right angles and dip ventrally under the pericardial cavity to supply hemolymph to the posterior edge of the gonads, midgut, and possibly some of the promotor muscles of the pereopods (Fig. 7). A second pair of branches, the posterior lateral arteries (PLA), arises at 45° (from the posterior aorta) over the posterior midgut caecum. These coil through the posterior midgut caecum, dipping ventrally and anteriorly around the end of the midgut to anastamose with the inferior abdominal artery (IAA, Fig. 7). Two side branches exit the posterior lateral arteries, descending beneath the edges of the crab body and around the periphery of the posterior midgut caecum (Fig. 7).

The posterior aorta itself descends through the abdomen and there are regular branches off the posterior aorta that supply the tissues of the abdomen. The posterior aorta joins the inferior abdominal artery in the area of the second abdominal segment. It continues along the hindgut, but soon after bifur-

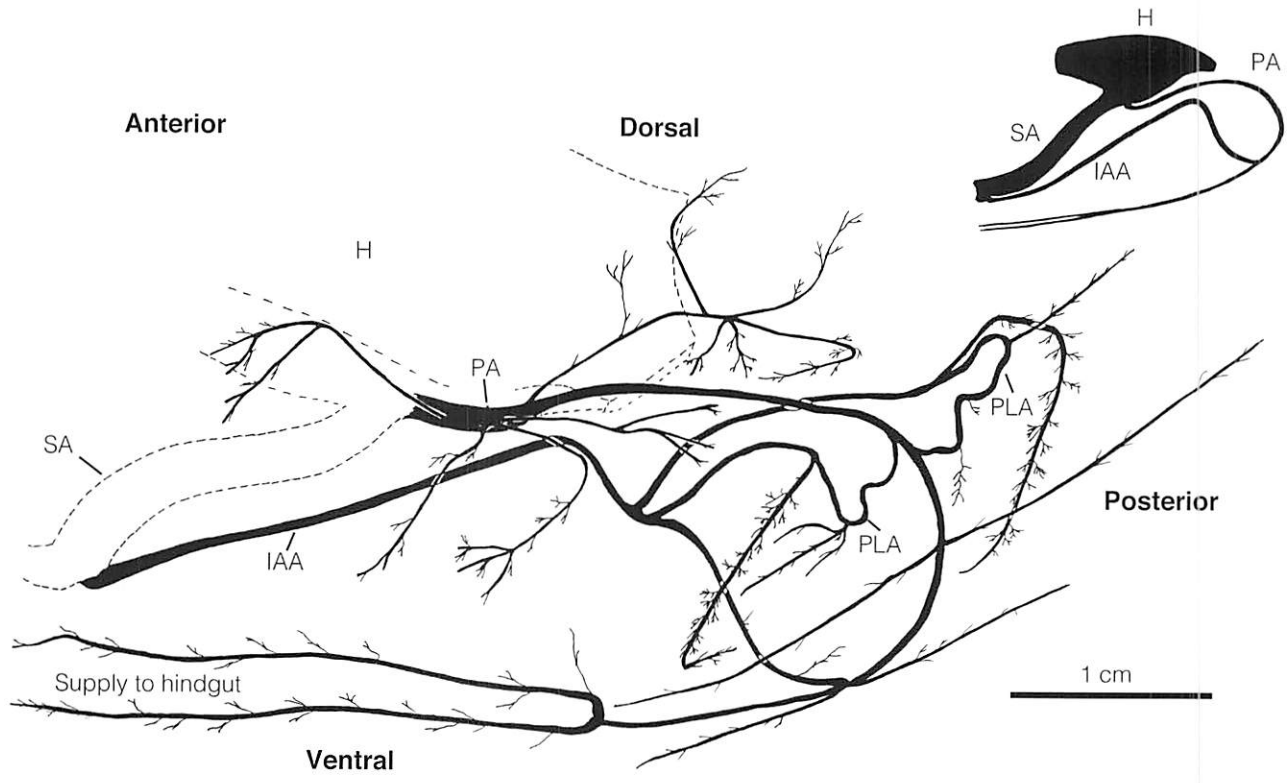

Figure 7. Line drawing of the posterior aorta complex of *Callinectes sapidus*, from an oblique dorso-lateral aspect (inset shows orientation). The posterior aorta [PA] exits posteriorly and ventrally from the heart [H, larger dashed line] near the origin of the sternal artery [SA, smaller dashed line]. The posterior aorta's course continues posteriorly towards the abdomen until it curves ventrally, supplying hemolymph to the tissues of the abdomen and hindgut. A number of small arteries arise from the posterior aorta. The largest are the posterior lateral arteries [PLA], which exit at right angles to the main artery. The inferior abdominal artery [IAA] exits from the end of the sternal artery and anastomoses with the posterior lateral arteries and posterior aorta. From McGaw and Reiber (2002).

cates, traversing either side of the hindgut to the anus in the telson and giving off many smaller branches to the tissues of the rectum and abdomen (Fig. 7). The co-lateral supply of hemolymph to the abdomen and hindgut by the posterior aorta, posterior lateral arteries, and inferior abdominal artery may help maintain hemolymph flow to these tissues when flow in either artery becomes occluded by movement of the abdomen or the presence of food in the hindgut.

Despite its being closely associated with the hindgut and posterior midgut caeca, there is no increase in flow in the posterior aorta during digestive processes (McGaw and Reiber 2000). However, flow does increase in the posterior aorta of *Cancer magister* during short-term low-salinity exposure (McGaw and McMahon 1996); this increase is due to extension of the abdomen, a behavioral adaptation that may enhance low-salinity survival (McGaw et al. 1999). Hemolymph flow also increases in this species in response to perfusion of the hormone proctolin (McGaw et al. 1994b). Hemolymph flow rates in *C. magister* also decrease in response to the FMRFamide-related peptides F1 and F2 (McGaw and McMahon 1995) during exposure to hypoxic water (Airriess and McMahon 1994) and emersion (Airriess and McMahon 1996), and during periods of activity (DeWachter and McMahon 1996a).

Sternal Artery

Exiting from the ventral surface of the heart close to the posterior aorta, the sternal artery (SA) (also referred to as the sternal aorta, descending artery, or main artery) is the largest in the circulatory system. According to corrosion casts, about 87% of the hemolymph is contained within the sternal artery and its associated branches and it receives 50 to 80% of the total cardiac output (McGaw and McMahon 1995, 1998, 1999; McGaw and Reiber 1998, 2000); it follows that changes in flow through this artery have the greatest effect on cardiac output (McGaw et al. 1994a). Likewise, in the sand crab *Portunus pelagicus* (Gribble and Reynolds 1993), the sternal artery complex receives over 90% of the cardiac output. In *Callinectes sapidus* the artery's course is directly ventral (Fig. 7). It passes on the right side of the midgut, after which it continues ventrally, until it turns anteriorly and passes through the fused thoracic ganglia. It ends at a point in the thorax above the telson and splits into two vessels: the inferior abdominal artery, which turns posteriorly, and the ventral thoracic artery, which proceeds anteriorly. There is disagreement as to whether its course is essentially vertical (McLaughlin 1983), or more anterior, ending at a point above the telson, which has been reported here for *C. sapidus*, and for other crustaceans (Pearson 1908; Airriess 1994). The sternal artery is valved at its origin, but control of blood flow into the peripheral regions served by the ventral thoracic artery is probably influenced by changes in down-stream resistance, possibly under control of neurohormones from the pericardial organs (Wilkens 1997; Wilkens et al. 1997).

Inferior Abdominal Artery

The inferior abdominal artery (IAA) (also referred to as the ventral abdominal artery or posterior ventral abdominal artery) exits from the end of the sternal artery (Fig. 7) and proceeds posteriorly and dorsally, following the sternal artery and the first part of the posterior aorta. It then passes ventrally through the abdomen along the hindgut and joins the posterior aorta in the region of the second abdominal segment. It supplies hemolymph to the hindgut and muscles of the abdomen.

Ventral Thoracic Artery

The ventral thoracic artery (VTA) (also known as the thoracic artery, sternal artery, or inferior thoracic artery) issues anteriorly from the sternal artery (Fig. 8) and is broadest at its origin with the sternal artery. Almost immediately it branches into seven vessels: three paired arteries that exit laterally and a smaller single artery that exits anteriorly (Fig. 8). The first pair of arteries (P3) exits laterally and posteriorly, providing hemolymph to the 3rd pair of pereopods; another branch (P4), which supplies hemolymph to the 4th pair of pereopods, arises from pereopod artery 3. Pereopod artery 4 in turn, gives off a branch (P5) that supplies the 5th swimming pereopods. The 2nd set of paired arteries (P2) exits from the ventral thoracic artery anterior to the first

pair (P3) and also flows laterally and posteriorly, taking hemolymph to the 2nd pair of pereopods (Fig. 8).

These pereopod arteries follow very similar plans: each artery extends into the tip of the dactyl and capillary-like vessels branch extensively along the entire length of each pereopod artery, supplying hemolymph to the muscles of the pereopods. The densities of these pereopod capillaries are greatest within the promotor, remotor, levator, and depressor muscles of the thoracic sterna; this area is highly vascularized (Fig. 9B). In the 5th pereopods, the vessel ramifies throughout the entire modified dactyl, known as the paddle (Fig 9A). These capillary-like structures are of much greater density than seen in the figures, but because of their delicacy they are easily lost in the corrosion casts during the maceration process. These muscles are shown to be more vascularized than previously described for *Callinectes sapidus* (Pyle and Cronin 1950) and other species of brachyuran Crustacea (Pearson 1908; Airriess 1994; Davidson and Taylor 1995). Because the blue crab is an active, fast-moving predator (Tagatz 1968), adequate blood flow to these muscles would be essential.

The first paired branches (P1) of the ventral thoracic artery exit laterally and anteriorly, supplying hemolymph to the chelae (Fig. 8). The main vessel traverses the coxa, basischium, merus, and carpus, giving off small branches at regular intervals. These branches divide among the muscles of that region (Fig. 9C). Three main branches supply hemolymph to the posterior extensor and anterior flexor muscles within the propodus (these muscles are used to open and close the chelae). The main vessel finally bifurcates at the dactyl, with each vessel extending to the very tips of the chelae (Fig. 9C). Each individual muscle fiber may be perfused by as many as seven or eight tiny vessels (Govind and Guchardi 1986). Such a complicated perfusion has been previously mentioned for *Callinectes sapidus* (Marcinek and LaBarbera 1994) and *Cancer pagurus* (Pearson 1908), but has not been shown clearly in figures.

On each pereopod artery, a smaller branch, the branchial artery (BA), arises on the superior surface (Fig. 10). However, this is still quite a large vessel. On pereopod arteries P1-P4, the branchial artery wraps around the base of the gills and appears to join the infrabranchial sinus; its course thereafter was not traceable in corrosion casts because it fused and was lost in the mass of the afferent and efferent branchial vessels. In pereopod 5, the branchial artery supplies hemolymph to the posterior parts of the branchiostegal circulation. The branchial artery supplies hemolymph to the gill tissues (Taylor and Greenaway 1979, 1984), but it is possible that this artery could act as a shunt, by-passing the muscle mass of the walking legs.

The final vessel exiting the ventral abdominal artery is a single artery of smaller diameter than the pereopod arteries that flows anteriorly, giving off three pairs of arteries along its course (Figs. 8, 9B). The first paired arteries (M3) exit at about 50° relative to the main vessel and supply the third maxillipeds. One branch curves into the endopod (en3) and the other branch extends into the exopod of the third maxilliped (ex3), with smaller side branches perfusing the epipod (ep3) (Fig. 8). A second pair of vessels (M2) arises off the ventral thoracic artery anteriorly to the first pair and bifurcates. The lower branch supplies the exopod and merus of the second maxilliped (exm2); the upper branch supplies the exopod of the first maxilliped (ex1) (Fig. 8). At the anterior end of the ventral thoracic artery is a final pair of arteries (M1) that bifurcate repeatedly. The upper branches extend to the mandibles (mdb), nearly meeting along the midline. The smaller lower branches supply the first and second maxillae (mx12), and very fine vessels also radiate out to the scaphognathite (scp) (preserved on only one side of cast: Fig. 8).

Hemolymph flow to the legs, chelae, and mouthparts via the sternal artery increases during activity (DeWachter and McMahon 1996a; McGaw and McMahon 1998), as well as during feeding and digestion (McGaw and Reiber 2000). Large increases in flow also occur in the sternal artery during exposure to hypoxic water (Airriess and McMahon 1994) and infusion of proctolin (McGaw et al. 1994b); however, reasons for these changes are

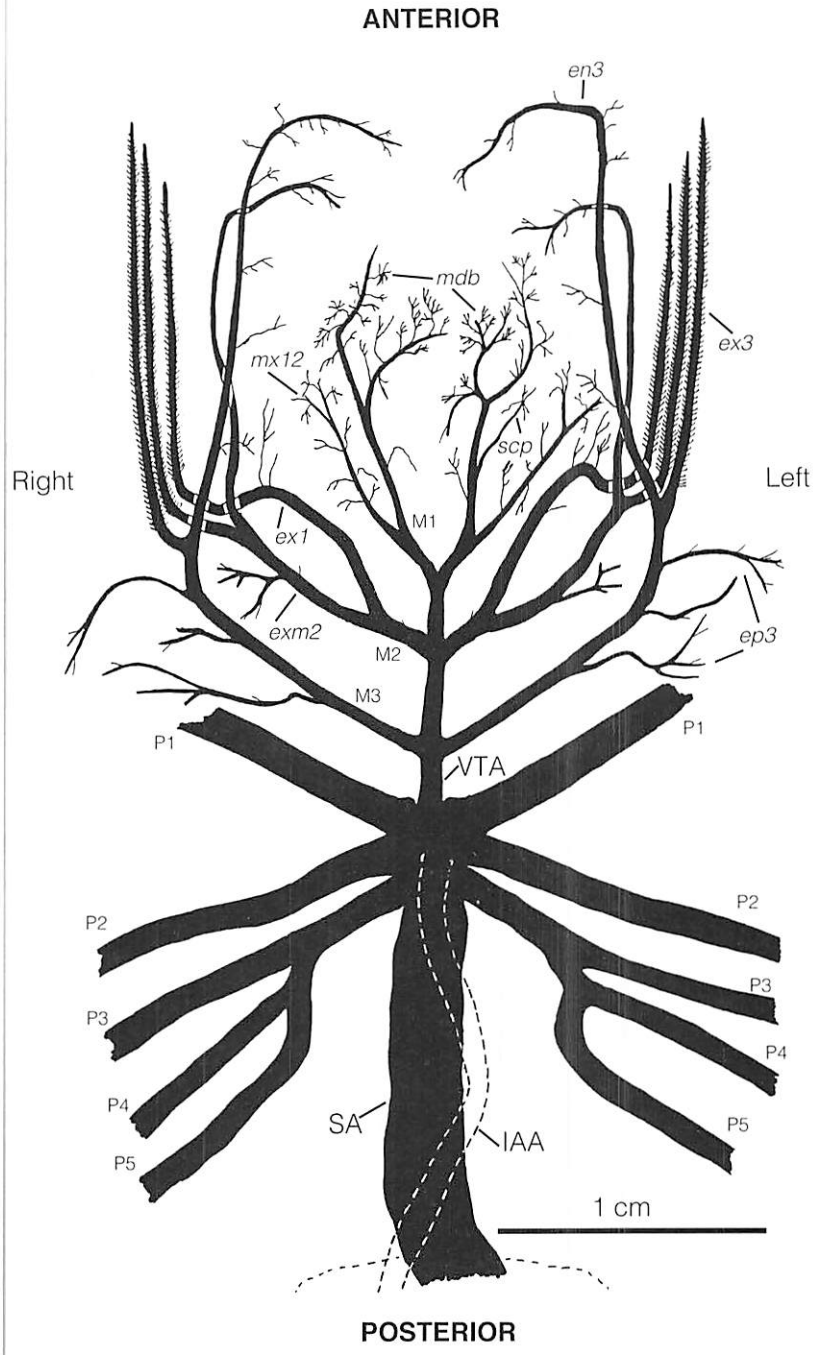

Figure 8. Line drawing (ventral view) of the major branches of the ventral thoracic artery [VTA] of *Callinectes sapidus*. The ventral thoracic extends from the anterior end of the sternal artery [SA]. Three paired branches split to supply hemolymph to the limbs [P1-P5]. The ventral thoracic artery continues its course anteriorly and splits into three pairs of branches [M1-M3] that supply hemolymph to the mouthparts. Branches of M3 supply hemolymph to the epipod [*ep3*], exopod [*ex3*], and endopod [*en3*] of the third maxilliped. The lower branch of M2 supplies hemolymph to the exopod and merus of the second maxilliped [*exm2*], while the upper branch perfuses the exopod of the first maxilliped [*ex1*]. At the end of the ventral thoracic artery, M1 bifurcates. The upper branches supply the mandibles [*mdb*] and the lower branches supply hemolymph to the first and second maxillae [*mx12*]. A smaller artery (preserved on only one side of the cast) supplies hemolymph to the scaphognathite [*scp*]. Inferior abdominal artery [IAA]. From McGaw and Reiber (2002).

unclear. Hemolymph flow decreases in the sternal artery during infusion of the FMRFamide-related peptides F1 and F2 (McGaw and McMahon 1995), as well as SchistoFLRFamide and leucomyosuppressin (McGaw and McMahon 1999). Differences in flow rates occur in *Callinectes sapidus* and *Cancer magister* during exposure to low salinity; flow increases in the former species (McGaw and Reiber 1998) and decreases in the latter (McGaw and McMahon 1996). These differences may be because *Callinectes sapidus* remains active in low salinity whereas *Cancer magister* adopts an isolation-type response, becoming quiescent and slowing ventilation of the branchial chambers (McGaw et al. 1999).

The Venous System

Sinuses

In crustaceans, the arterial blood collects in sinuses before flowing through the gills and back to the heart. There is disagreement in the literature about how anatomically well-defined these sinuses are. Pyle and Cronin (1950) report that many of the sinuses of *Callinectes sapidus* are so ill-defined that they almost defy successful demonstration. We propose that all sinuses are discrete channels rather than arbitrary spaces between organs, and that their form is determined by the boundaries of specific organs or muscles. However, under abnormally high pressures such as those generated during infusion of Batson's Monomer, the sinuses may be blown apart, thus exaggerating their form and interpretation (Davidson and Taylor 1995). In the present study, most of the sinuses appeared as a fine veneer between or covering the vessels; however, because of their delicate form, some were lost from the corrosion casts during the tissue maceration process. The fact that all areas of the arterial system were perfused, including the return channels, the gills, and branchiostegal sinuses (Fig. 3), suggests that ours is a complete cast; thus the representation of the sinuses is probably accurate.

The direction of hemolymph flow through the sinuses is as follows: hemolymph from the hepatic sinus and eye sinuses drains into a dorsal sinus (Pearson 1908) while hemolymph from the pereopods

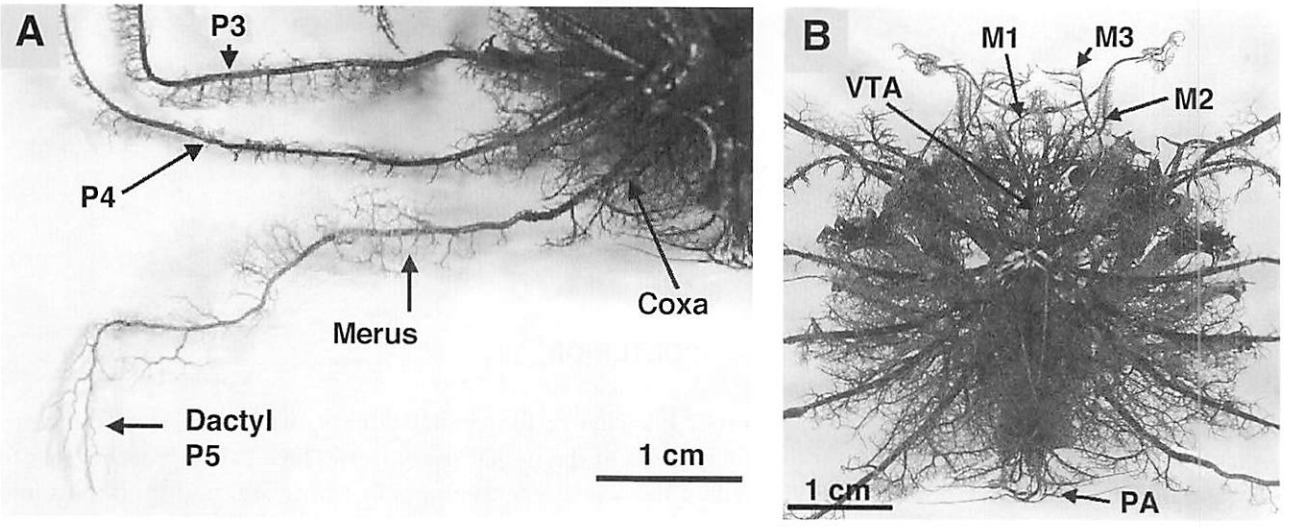

Figure 9. (A) Enlarged view of pereopods 3, 4, and 5 [P3, P4, and P5] of *Callinectes sapidus*, showing capillaries perfusing the musculature of each segmental region. The artery in P5 extends into the dactyl; its capillaries extend to the edges of the swimming paddle. (B) Enlarged ventral view of *Callinectes sapidus* focuses on the capillary mass that supplies the promotor, remotor, levator, and depressor muscles of the thoracic sterna. The ventral thoracic artery [VTA] exits anteriorly, giving rise to the arteries that supply hemolymph to the maxillipeds and mandibles [M1 to M3]. Posterior aorta [PA]. From McGaw and Reiber (2002).

drains through tube-like sinuses running longitudinally along the limbs (Davidson and Taylor 1995). Classical anatomical studies show that all sinuses eventually drain into a sternal or ventral thoracic sinus below the heart (e.g., Pearson 1908). The sternal sinus radiates out between the muscles of the thoracic sterna as the branchial sinuses. These then fuse with the infrabranchial sinus that runs along the posterior edge of the gills (Pearson 1908; Fig. 10). From here, hemolymph flows through the gill lamellae via the afferent and efferent branchial veins, which are distinguished from sinuses by having a definite shape and which function as return channels for blood (Maynard 1960). Oxygenated blood is returned to the heart by three pairs of branchiocardiac veins that empty into the pericardial sinus (Figs. 2, 3).

An alternative, dorsal venous return route via the branchiostegal circulation (Fig. 11) has been demonstrated (Taylor and Greenaway 1984; Farrelly and Greenaway 1987; Greenaway and Farrelly 1990; Taylor and Taylor 1992). Changes in the distribution of venous return between the branchial and branchiostegal circulations have been shown in the arid zone crab *Holthusiana transversa*, although precise estimations of the portioning have not been made in any crab (Taylor and Greenaway 1984; Taylor and Taylor 1992). The branchiostegal circulation of *Callinectes sapidus* appears as a fine mesh-work of lacunae that covers the posterior dorsal surface of the branchial chamber and extends over the pericardial cavity (Fig. 11). It is supplied with hemolymph (in part) by fine branches from the anterolateral arteries. However, the main hemolymph supply to the branchiostegal circulation is venous and comes from the dorsal and eye sinuses (Taylor and Greenaway 1984; Greenaway and Farrelly 1990; Taylor and Taylor 1992). Hemolymph returns to the pericardial cavity by way of lateral collecting vessels (Fig. 10).

The branchiostegal circulation is well developed in terrestrial crabs (Taylor and Greenaway 1979) and amphibious species (Greenaway and Farrelly 1990; Greenaway et al. 1996) where it is used for aerial gas exchange. The branchiostegal circulation of *Call-*

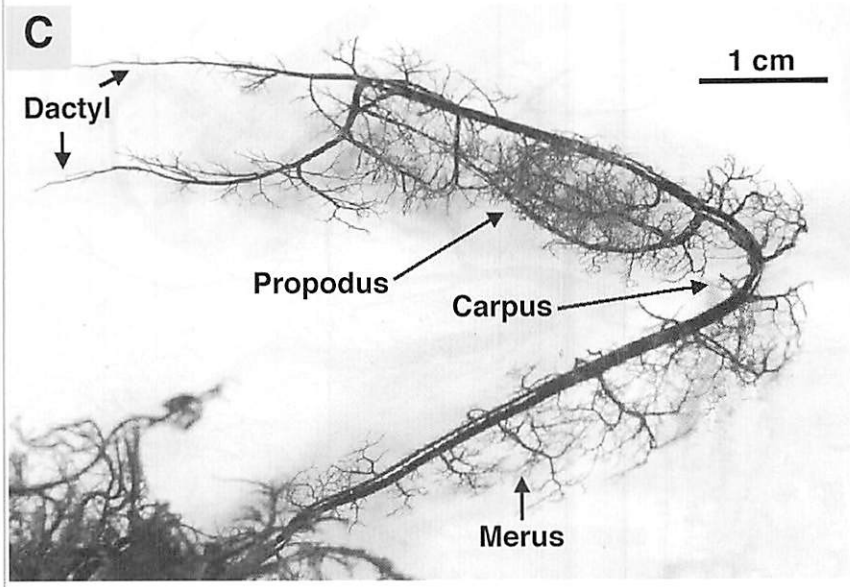

Figure 9 (continued). (C) Enlarged view of pereopod artery 1 [P1], which supplies hemolymph to the right chelae. Smaller arteries branch off the main vessel to supply the muscles of the chelae. In the propodus region, three branches supply hemolymph to the posterior extensor and anterior flexor muscles. Pereopod artery 1 finally bifurcates at the dactyl, with each vessel extending to the tips of the chelae. From McGaw and Reiber (2002).

inectes sapidus is similar to that of *Ovalipes catharus*, which is also a fully aquatic species (Davidson and Taylor 1995). In both species, its role is unclear, but it may be used for oxygen extraction during periods of reversed ventilation (Davidson and Taylor 1995).

Gill Vessels

Hemolymph collects in the infrabranchial sinus (IBS) at the base of the gill. From there it flows along the afferent branchial vein (ABV) that supplies individual lamellae (GL) (Fig. 10, 12A, B). Individual lamellae are separated at their margins by small spacing nodules that promote water circulation and increase gas exchange (Fig. 12; Taylor and Taylor 1992). Perfusion occurs in a counter-current orientation with ventilatory water flow, maximizing exchange capability (Burggren et al. 1974). Observations of a living lamella (made with a light microscope at 100x magnification) show that hemolymph flow is unidirectional, through the marginal canal along the anterior edge and through many fine lacunae within the lamellar hemocoel, thus providing an extensive surface area of exchange with inflowing water (Fig. 12B).

Hemolymph is directed through the gill lamellae via trabecular cells (TB), which extend to the midline of the lamellae (Fig. 12C) and provide lacunar channels through which hemolymph flows (Johnson 1980). Transmission electron microscopy shows that the lacunae come into close contact with the branchial epithelium, which is rich in mitochondria (Fig. 12C). After passing through the lamellae, hemolymph flows through the efferent

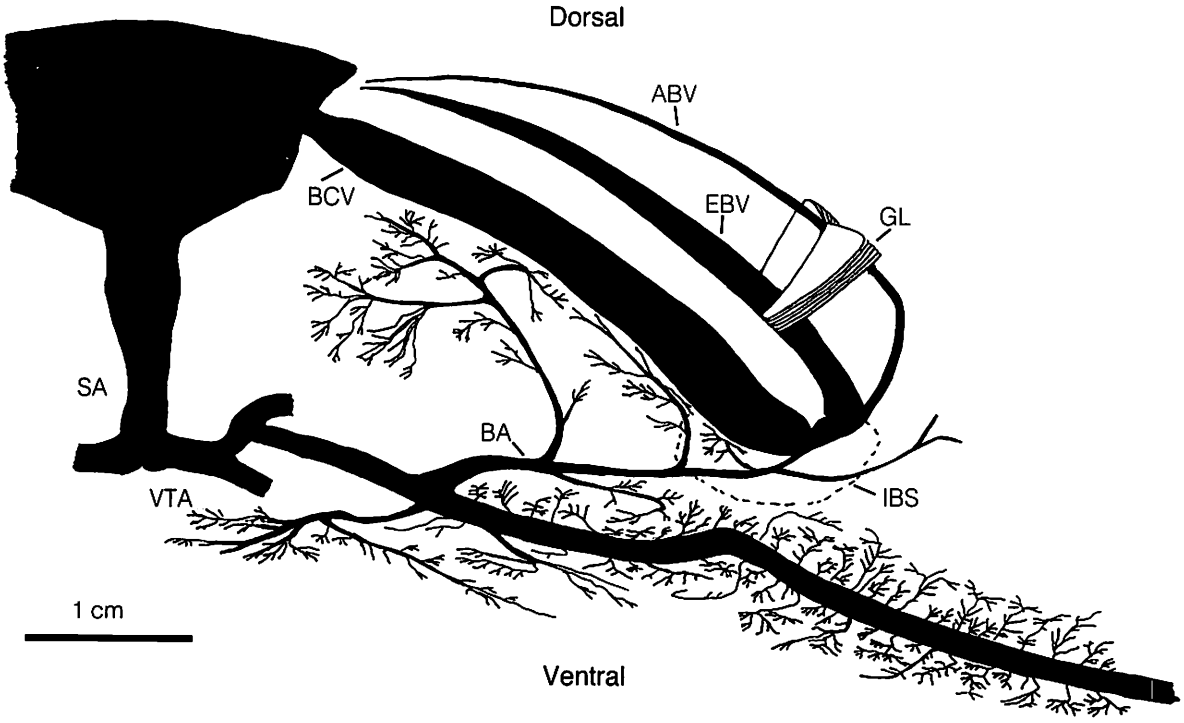

Figure 10. Line drawing of circulation within the gills of *Callinectes sapidus* (lateral view). The branchial artery [BA] exits from the anterior surface of each pereopod artery and supplies hemolymph to the exterior basal region of the gills. Hemolymph drains from the infrabranchial sinus [IBS, dashed line] at the base of each gill and flows along the afferent branchial vein [ABV], over the gill lamellae [GL], and along the efferent branchial vein [EBV], and is returned to the heart via the branchiocardiac veins [BCV]. Sternal artery [SA]; ventral thoracic artery [VTA]. From McGaw and Reiber (2002).

branchial vein (EBV) and continues into the branchiocardiac veins (BCV) (or branchiocardiac sinus, branchiopericardial veins). From there it drains into the pericardial sinus and back into the heart through the ostia (Greenaway and Farrelly 1984) (Figs. 3, 4, 10).

Regulation of blood flow through the gills is thought to occur via the efferent septum (valve), which acts as a variable resistance element in the efferent channels (Taylor and Taylor 1986; 1992). In isolated gill preparations, resistance has been shown to change in response to injections of a variety of neurohormones, which might allow regulation of flow through individual lamellae as well as the entire gill (Taylor et al. 1995).

CONCLUSIONS AND FUTURE DIRECTIONS

Cardiovascular performance and regulatory abilities in blue crabs should prove to be quite high and complex, given the activity patterns exhibited by this animal. We have shown that the circulatory system of *Callinectes sapidus* is more complex and more tightly regulated than usually described. All areas of the body are highly perfused by arteries, arterioles, and fine capillary-like vessels. The presence of sinuses, rather than a complete venous return system, defines the system as an open circulatory system. However, the terms open and closed are ambiguous. The systems of cladoceran, anostracan,

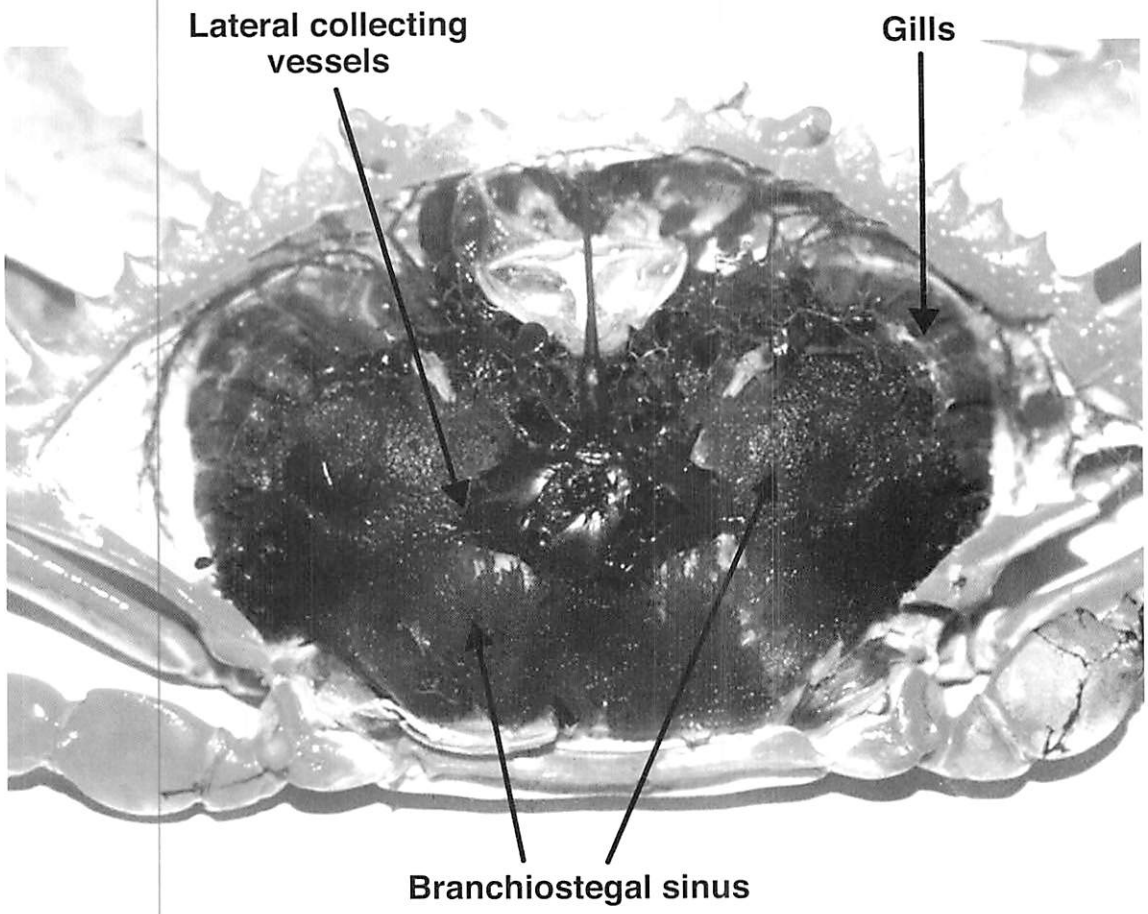

Figure 11. Dorsal view of a resin cast showing the branchiostegal circulation of *Callinectes sapidus*. The lattice work of sinuses extends over the posterior dorsal branchial chamber. Hemolymph drains back into the pericardial sinus via the lateral collecting vessels. From McGaw and Reiber (2002).

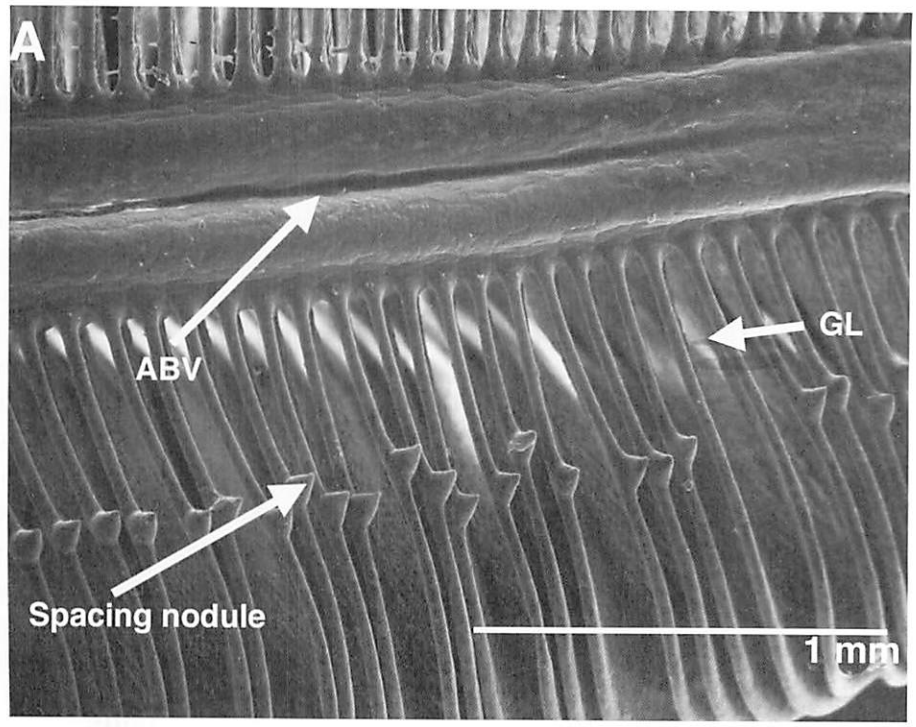

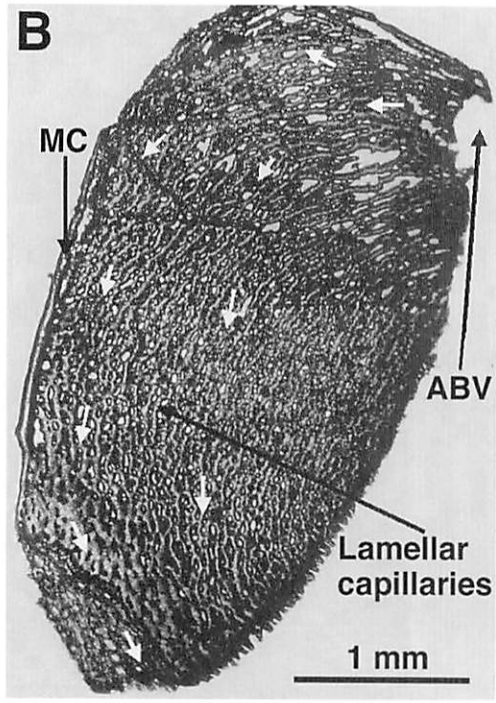

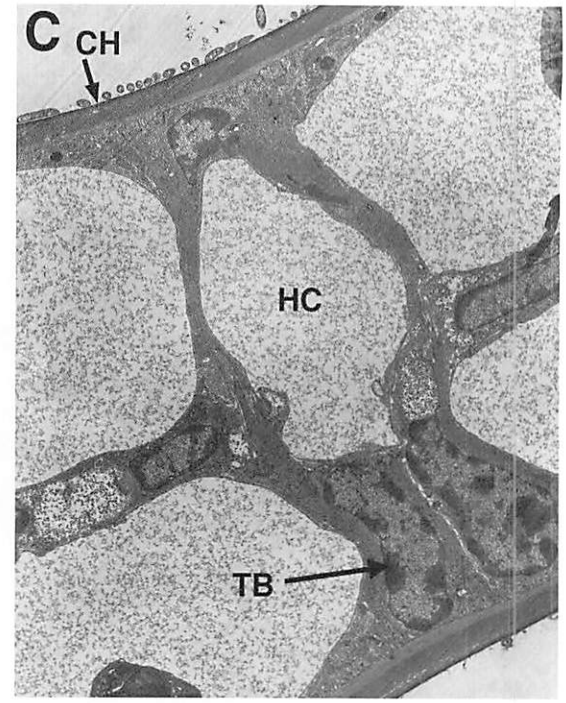

Figure 12.(A) Scanning electron micrograph of *Callinectes sapidus* gills (150x) to show arrangement of lamellae [GL] along the afferent branchial vein [ABV] and spacing nodules. (B) Resin cast of an individual lamella (light microscope, 100x) showing the regions where the lamella is attached to the afferent branchial vessel [ABV] and the marginal canal [MC], and the capillary network of the lamellae. White arrows indicate the direction of hemolymph flow. (C) Electron micrograph (9,900x) of a transverse section of a lamella of *Callinectes sapidus*, showing trabecular cells [TB], hemolymph channels [HC], and chitinous exchange surface of lamellae [CH]. From McGaw and Reiber (2002).

calanoid, and cirriped crustaceans (Maynard 1960; McLaughlin 1983) are definitely classed as open, because they lack the discrete vessels of the decapod crustaceans. The decapod crustacean system, however, is far more complex, with hydrostatic pressures that rival those of some lower vertebrate systems (McMahon and Burnett 1990) and neurohormonal control mechanisms that allow fine regulation of cardiac function and regional hemolymph flow (reviewed in McGaw and McMahon 1999).

Our study suggests that there may be room for a third category of circulatory system, one that would define the decapod crustacean circulatory system as "partially closed" rather than open. This proposal invites further investigation into whether the decapod crustacean circulatory system has a two fluid-compartment system (intracellular and hemolymph), or a more vertebrate-like three-fluid- compartment system (intracellular, interstitial, and blood).

Because the vascular system of the blue crab (and decapods in general) is recognized for its complexities, further examinations of the local or central regulatory capabilities of regional blood flow should also support the regulatory comparisons made between decapods and lower vertebrates. J.L. Wilkens (University of Calgary, Alberta, pers. comm.) has suggested that perfusion of the abdominal segments in lobster or crayfish may be regulated via valve-like structures located at the entrance to each segmental vessel. Active control of these valves has yet to be established (Davidson et al. 1998). Perfusion of tissues regulated at the local level by metabolic feedback mechanisms (intrinsic factors) also has yet to be established. However, Stegen and Grieshaber (2001) have shown that adenosine has strong effects on cardiac performance and hemolymph velocities in the American lobster. Hypoxic conditions have also been shown to modulate local blood flow in decapods (Reiber 1994; Reiber et al. 1997).

The complex nature of decapod crustacean cardiovascular functions should not come as a surprise given their long evolutionary history and diverse adaptive radiations, filling niches occupied by many amphibians, reptiles, and even mammals. The highly cited and reproduced diagram of McLaughlin (1980) should now be modified to reflect our current understanding of the circulatory system of the blue crab and to include some of the subtle yet significant newly identified anatomical details (Fig. 13; see also Fig. 14).

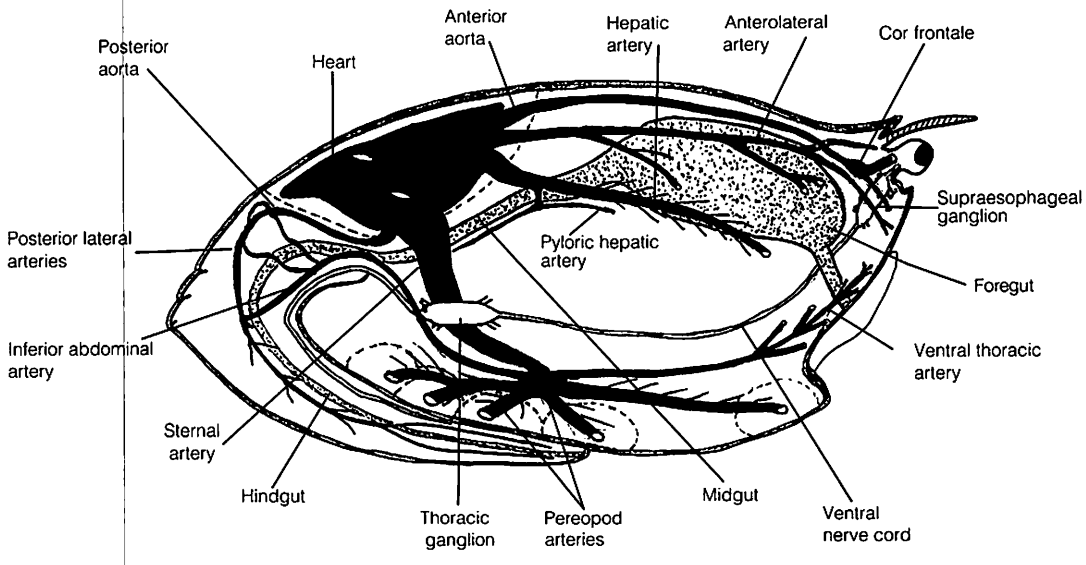

Figure 13. Line drawing of the arterial system of the blue crab from a lateral aspect, modified with permission from the drawing of McLaughlin (1980). The five dashed ovoid shapes in the ventral region represent the five pereopods and the dashed region around the heart is the pericardial sinus region.

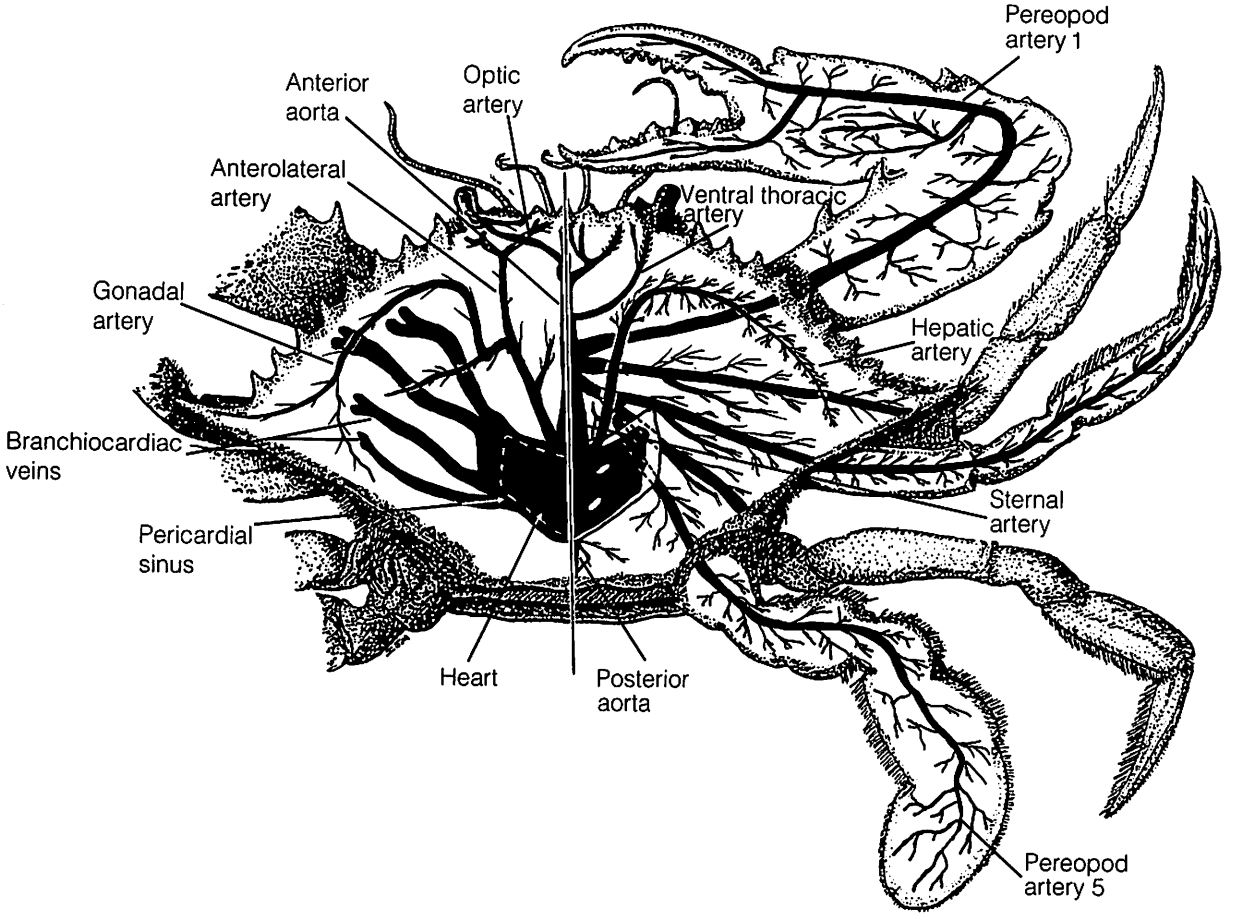

Figure 14. Line drawing of the arterial system of *Callinectes sapidus* from a dorsal aspect showing the superficial arteries (left side) and deep arterial systems (right side).

ACKNOWLEDGMENTS

We thank Dr. Patrick Apfel and Ray Goldsworthy (Department of Radiography, UNLV) for their assistance with X-ray technology and John Litty (Information Technology, UNLV) for photographic expertise. A portion of this research was supported by NSF grant IBN-98874534 (C.L.R.).

REFERENCES

Abbott, N.J. 1971. The organization of the cerebral ganglion in the shore crab, *Carcinus maenas*. II. The relation of intracerebral blood vessels to other brain elements. Zeitschrift für Zellforschung und Mikroskopische Anatomie 120:401-419.

Airriess, C.N. 1994. The control of the cardiovascular system of *Cancer magister*. Doctoral dissertation, University of Calgary, Alberta, Canada. 252 p.

Airriess, C.N. and B.R. McMahon. 1992. Aminergic modulation of circulatory performance in the crab *Cancer magister*. Pages 123-131 in R.B. Hill, K. Kuwasawa, B.R. McMahon and T. Kuramoto (eds.). Phylogenetic Models in Functional Coupling of the CNS and the Cardiovascular System. Comparative Physiology Volume 11. Karger, Basel, Switzerland.

Airriess, C.N. and B.R. McMahon. 1994. Cardiovascular adaptations enhance tolerance of environmental hypoxia in the crab *Cancer magister*. Journal of Experimental Biology 190:23-41.

Airriess, C.N and B.R. McMahon. 1996. Short-term emersion affects cardiac function and regional

haemolymph distribution in the crab *Cancer magister*. Journal of Experimental Biology 199:569-578.

Alexandrowicz, J.S. 1932. The innervation of the heart of the Crustacea. I. Decapoda. Quarterly Journal of Microscopic Science 75:181-249.

Baumann, H. 1921. Das GefaBsystem von *Astacus fluviatilis* (*Potamobius astacus*). Zeitschrift fuer Wissenschaftliche Zoologie 118:246-342.

Bouvier, E.L. 1891. Recherches anatomiques sur le systeme arterial des Crustaces Decapodes. Annals des Science Naturelles. Zoology et biologie animale II. Series (7) 9:197-282.

Brody, M.S. and E.B. Perkins. 1930. The arterial system of *Palaemonetes*. Journal of Morphology 50:127-142.

Brown, S.K. and D.N. Sherwood. 1981. Vascularization of the crayfish abdominal nerve cord. Journal of Comparative Physiology 143:93-101.

Burggren, W.W., B.R. McMahon and J.W. Costerton. 1974. Branchial water and blood-flow patterns and structure of the gill of the crayfish *Procambarus clarkii*. Canadian Journal of Zoology 52:1511-1518.

Claus, C. 1884. Zur kenntnis der kreislauforgane der Schizopoden und Decapoden. Arbeiten aus den zoologischen Instituten der Universität Wien und der zoologischen Station in Triest 5:271-318.

Davidson, G.M. and H.H. Taylor. 1995. Ventilatory and vascular routes in a sand burying swimming crab, *Ovalipes catharus* (White, 1843) (Brachyura, Portunidae). Journal of Crustacean Biology 15:605-624.

Davidson, G.W., J.L. Wilkens and P. Lovell. 1998. Neural control of the lateral abdominal arterial valves in the lobster *Homarus americanus*. Biological Bulletin 194: 72-82.

DeFur, P.L. and C.P. Mangum. 1979. The effects of environmental variables on the heart rates of invertebrates. Comparative Biochemistry and Physiology 62A:283-294.

DeWachter, B. and B.R. McMahon. 1996a. Haemolymph flow distribution, cardiac performance and ventilation during moderate walking activity in *Cancer magister* (Dana) (Decapoda, Crustacea). Journal of Experimental Biology 199:627-633.

DeWachter, B. and B.R. McMahon. 1996b. Temperature effects on heart performance and regional haemolymph flow in the crab *Cancer magister*. Comparative Biochemistry and Physiology 114A:27-33

Farrelly, C. and P. Greenaway. 1987. The morphology and vasculature of the lungs and gills of the soldier crab, *Mictyris longicarpus*. Journal of Morphology 193:285-304.

Govind, C.K. and J. Guchardi. 1986. Vascularization of a lobster muscle. Journal of Morphology 188:327-333.

Greenaway, P. and C. Farrelly. 1984. The venous system of the terrestrial crab *Ocypode cordimanus* (Desmarest 1825) with particular reference to the vasculature of the lungs. Journal of Morphology 181:133-142.

Greenaway, P. and C. Farrelly. 1990. Vasculature of the gas exchange organs in air breathing brachyurans. Physiological Zoology 63:117-139.

Greenaway, P., S. Morris, B.R. McMahon, C.A. Farrelly and K.L. Gallagher. 1996. Air breathing by the purple shore crab *Hemigrapsus nudus* (Dana). I. Morphology, behaviour and respiratory gas exchange. Physiological Zoology 69:785-805.

Gribble, N. and K. Reynolds. 1993. Use of angiography to outline the cardiovascular anatomy of the sand crab *Portunus pelagicus*. Journal of Crustacean Biology 13:627-637.

Haeckel, E. 1857. Über die Gewebe des Flusskrebses. Archiv für Anatomie, Physiologie, und wissenschaftliche Medizin (Berlin) 24:469-568.

Johnson, P.T. 1980. Histology of the Blue Crab, *Callinectes sapidus*. A Model for the Decapoda. Praeger Scientific, New York. 440 p.

Marcinek, D. and M. LaBarbera. 1994. Quantitative branching geometry of the vascular system of the blue crab, *Callinectes sapidus* (Arthropoda, Crustacea): A test of Murray's law in an open circulatory system. Biological Bulletin 186:124-133.

Maynard, D.M. 1960. Circulation and heart function. Pages 161-226 in T.H. Waterman (ed.). The Physiology of Crustacea, Volume 1. Academic Press, New York.

McGaw, I.J., C.N. Airriess and B.R. McMahon. 1994a. Patterns of haemolymph-flow variation in decapod crustaceans. Marine Biology 121:53-60.

McGaw I.J., C.N. Airriess and B.R. McMahon. 1994b. Peptidergic modulation of cardiovascular dynamics in the Dungeness crab *Cancer magister*. Journal of Comparative Physiology B 164:103-111.

McGaw, I.J. and B.R. McMahon. 1995. The FMRFamide-related peptides F1 and F2 alter hemolymph distribution and cardiac output in the crab *Cancer magister*. Biological Bulletin 188:186-196.

McGaw, I.J. and B.R. McMahon. 1996. Cardiovascular responses resulting from variation in external salinity

in the Dungeness crab *Cancer magister*. Physiological Zoology 69:1384-1401.

McGaw, I.J. and B.R. McMahon. 1997. Blood glucose and its control in Cancrid crabs. Arizona-Nevada Academy of Science 32:14 (Abstract).

McGaw, I.J. and B.R. McMahon. 1998. Endogenous rhythms of haemolymph flow and cardiac performance in the crab *Cancer magister*. Journal of Experimental Marine Biology and Ecology 224:127-142.

McGaw, I.J. and B.R. McMahon. 1999. Actions of putative cardioinhibitory substances on the *in vivo* decapod crustacean cardiovascular system. Journal of Crustacean Biology 19:435-449.

McGaw, I.J. and C.L. Reiber. 1998. Circulatory modification in the blue crab *Callinectes sapidus* during exposure and acclimation to low salinity. Comparative Biochemistry and Physiology 121A:67-76.

McGaw, I.J. and C.L. Reiber. 2000. Integrated physiological responses to feeding in the blue crab *Callinectes sapidus*. Journal of Experimental Biology 203:359-368.

McGaw, I.J. and C.L. Reiber. 2002. Cardiovascular system of the blue crab *Callinectes sapidus*. Journal of Morphology 251:1-21.

McGaw, I.J., C.L. Reiber and J.A. Guadagnoli. 1999. Behavioral physiology of four crab species in low salinity. Biological Bulletin 196:163-176.

McGaw, I.J., J.L. Wilkens., B.R. McMahon and C.N. Airriess. 1995. Crustacean cardioexcitatory peptides may inhibit the heart *in vivo*. Journal of Experimental Biology 198:2547-2550.

McLaughlin, P.A. 1980. Comparative Morphology of Recent Crustacea. W.H. Freeman and Company, San Francisco. 177 p.

McLaughlin, P.A. 1983. Internal Anatomy. Pages 1-52 in L.H. Mantel (ed.). Internal Anatomy and Physiological Regulation, Volume 5. The Biology of Crustacea. Academic Press, New York.

McMahon, B.R. 1999. Intrinsic and extrinsic influences on cardiac rhythms in crustaceans. Comparative Biochemistry and Physiology 124A:539-547.

McMahon, B.R. 2001. Control of cardiovascular function and its evolution in Crustacea. Journal of Experimental Biology 204:923-932.

McMahon, B.R and L.E. Burnett. 1990. The crustacean open circulatory system: A reexamination. Physiological Zoology 63:35-71.

McMahon, B.R. and J.L. Wilkens. 1983. Ventilation, perfusion, and oxygen uptake. Pages 289-372 in L.H. Mantel (ed.). Internal Anatomy and Physiological Regulation, Volume 5. The Biology of Crustacea. Academic Press, New York.

McMahon, B.R., J.L. Wilkens. and P.J.S. Smith. 1997. Invertebrate circulatory systems. Pages 931-1008 in A. Dantzler (ed.). Handbook of Physiology, Section 13. American Physiological Society. Oxford University Press, New York.

Miyawaki, M. and A. Ukeshima. 1967. On the ultrastructure of the antennal gland epithelium of the crayfish, *Procambarus clarkii*. Kumamoto Journal of Science B 8:59-73.

Paterson, N.F. 1968. The anatomy of the cape rock lobster *Jasus lalandii* (H. Milne Edwards). Annals of the South African Museum 51:1-232.

Pearson, J. 1908. *Cancer*. Liverpool Marine Biology Committee Memoirs XVI:1-209 + 13 plates.

Pillai, R.S. 1963. The circulatory system of *Caridina laevis* Heller. Crustaceana 8:66-74.

Pyle, R. and E. Cronin. 1950. The general anatomy of the blue crab *Callinectes sapidus* Rathbun. Maryland Board of Natural Resources Publication 87. Solomons Island, Maryland. 40 p.

Reiber, C.L. 1994. The hemodynamics of *Procambarus clarkii*. Physiological Zoology 67: 449-467.

Reiber, C.L. 1995. Physiological adaptations of crayfish to the hypoxic environment. American Zoologist 35:1-11.

Reiber, C.L and B.R. McMahon. 1998. The effects of progressive hypoxia on the crustacean cardiovascular system: a comparison of the freshwater crayfish, *Procambarus clarkii* and the lobster, *Homarus americanus*. Journal of Comparative Physiology 168B:168-176.

Reiber, C.L., B.R. McMahon and W.W. Burggren. 1992. Redistribution of cardiac output in response to hypoxia: a comparison of the freshwater crayfish, *Procambarus clarkii* and the lobster, *Homarus americanus*. Pages 22-28 in R.B. Hill, K. Kuwasawa, B.R. McMahon and T. Kuramoto (eds.). Phylogenetic Models in Functional Coupling of the CNS and the Cardiovascular System. Comparative Physiology Volume 11. Karger, Basel, Switzerland.

Reiber, C.L., B.R. McMahon and W.W. Burggren. 1997. Cardiovascular functions in two Macruran decapod crustaceans (*Procambarus clarkii* and *Homarus americanus*) during periods of inactivity, tail flexion and

cardiorespiratory pauses. Journal of Experimental Biology 200:1103-1113.

Sandeman, D.C. 1967. The vascular circulation in the brain, optic lobes and thoracic ganglion of the crab *Carcinus*. Proceedings of the Royal Society of London B 168:82-90.

Saver, M.A. and J.L. Wilkens. 1998. Comparison of the effects of five hormones on intact and open heart cardiac ganglionic output and myocardial contractility in the shore crab *Carcinus maenas*. Comparative Biochemistry and Physiology 120A:301-310.

Stegen, E. and M.K. Grieshaber. 2001. Adenosine increases ventilation rate, cardiac performance and haemolymph velocity in the American lobster *Homarus americanus*. Journal of Experimental Biology 204:947-957.

Steinacker, A. 1978. The anatomy of the decapod crustacean auxiliary heart. Biological Bulletin 154:497-507.

Tagatz, M.E. 1968. Biology of the blue crab, *Callinectes sapidus* Rathbun, in the St. Johns River, Florida. Fishery Bulletin 67:17-33.

Taylor, E.W. 1982. Control and co-ordination of ventilation and circulation in crustaceans: Responses to hypoxia and exercise. Journal of Experimental Biology 100:289-319.

Taylor, H.H, L.E. Burnett, K. Krajniak, W.W. Burggren and C.L. Reiber. 1995. Vasomotor responses in crab gills. Physiological Zoology 68:66 (Abstract).

Taylor, H.H. and P. Greenaway. 1979. The structure of the gills and lungs of the arid zone crab *Holthusiana* (*Austrothelphusa*) *transversa* (Brachyura, Sundathelphusidae) including observations on arterial vessels within the gills. Journal of Zoology 189:359-384.

Taylor, H.H and P. Greenaway. 1984. The role of the gills and branchiostegites in gas exchange in a bimodally air breathing crab *Holthusiana transversa*: Evidence for a facultative change in the distribution of the respiratory circulation. Journal of Experimental Biology 111:103-121.

Taylor, H.H. and E.W. Taylor. 1986. Observations of valve-like structures and evidence for rectification of flow in the gill lamellae of the crab *Carcinus maenas*. Zoomorphology 106:1-11.

Taylor, H.H and E.W. Taylor. 1992. Gills and lungs: The exchange of gases and ions. Pages 203-293 in F.W. Harrison and A.G. Humes (eds.). Microscopic Anatomy of the Invertebrates, Volume 10. Wiley Liss, New York.

Wiersma, C.A.G. and E. Novitiski. 1942. The mechanism of the nervous regulation of the crayfish heart. Journal of Experimental Biology 19:255-265.

Wilkens, J.L. 1997. Possible mechanisms of control of vascular resistance in the lobster *Homarus americanus*. Journal of Experimental Biology 200:487-493.

Wilkens, J.L. 1999. The control of cardiac rhythmicity and of blood distribution in crustaceans. Comparative Biochemistry and Physiology 124A:531-538.

Wilkens, J.L., G.M. Davidson and M.J. Cavey. 1997. Vascular peripheral resistance and compliance in the lobster *Homarus americanus*. Journal of Experimental Biology 200:477-485.

Wilkens, J.L., L.A. Wilkens, and B.R. McMahon. 1974. Central control of cardiac and scaphognathite pacemakers in the crab, *Cancer magister*. Journal of Comparative Physiology 90:89-104.

Chapter 6

Molting and Growth

STEVEN G. SMITH AND ERNEST S. CHANG

INTRODUCTION

The problem of how to increase body size, or grow, is a challenge for animals with rigid external skeletons. Perhaps the most straightforward solution is to increase the size of the hard outer shell and soft inner tissues concurrently, the approach taken by clams and sea urchins, for instance. Crustaceans are much more peculiar: an animal sheds its external shell, develops a new larger shell, increases the size of its internal body tissues to fill the new shell, and then molts again. For the blue crab *Callinectes sapidus* and other crustaceans with thick, heavily calcified outer shells, this growth process places individuals in a precarious situation immediately after molting. When animals lose their external skeletons, they are less able to eat, move, or fend off attackers, and their exposed soft bodies become easy targets for a host of predators. In addition, the considerable time and much of the energy invested in developing the outer shell are simply lost when the shell is discarded onto the seafloor at molting. Perhaps these risks and costs are the price of increased mobility of crabs and lobsters compared to clams and sea urchins. Our intent in this chapter, however, is not to speculate on why but rather to describe how the molting process occurs in blue crabs and related decapod crustaceans.

Maybe because of its peculiarity, molting or ecdysis has long fascinated crustacean biologists (Réaumer 1712, in Drach 1939). Early investigators of the life history of crabs and lobsters viewed molting as a short "interruption" in an animal's normal routine of searching for food, seeking shelter, etc. As was discovered through subsequent research, ecdysis is a remarkable physiological feat, and individuals spend a large proportion of their time between molts either recovering from or preparing for a molt event (Drach 1939; Passano 1960a). The perception of molting thus shifted from a brief interruption to a more encompassing "cycle" of physiological and biochemical events. Many aspects of a crab's or lobster's physiology and ecology, including respiration, feeding, and habitat preference, change at various points in this cycle that spans two molt events. The blue crab molt cycle thus serves as the underlying context for many of the topics discussed in subsequent chapters of this volume.

The crustacean molting process has also thwarted efforts to develop mathematical functions that accurately depict growth of an individual over its lifetime (Cobb and Caddy 1989). Traditional length-age growth models, such as the von Bertalanffy (1938) or Richards (1959) functions, describe growth as a continuous process and require length-at-age data for model fitting. These functions are readily applicable to many fish species because growth of individuals occurs in a continuous fashion and absolute age can be determined with relative ease by counting growth rings laid down on certain bony parts such as scales, fin rays, or otoliths (ear bones). This class of length-age functions may not be well-suited for modeling crustacean growth. One problem is that growth occurs discontinuously as a

series of discrete increases in length as an animal molts. A second problem concerns the practical difficulties in accurately determining the age of individual crustaceans. For example, the ageing technique most widely used for fish, examination of calcified structures, is not applicable to crustaceans because these structures are lost when the exoskeleton is shed at each molt. The inability to quantitatively describe growth has obscured our understanding of crustacean population dynamics in general, in turn making it difficult to construct sustainable harvest policies for blue crabs and other economically valuable decapod crustaceans (see Fogarty and Lipcius, Chapter 16).

In this chapter, we examine blue crab growth from a molt-process perspective. There are two main aspects of molting with respect to growth: (1) the time between molts and (2) the size increase at molting. We begin our examination with a description of the blue crab molt cycle and aspects of its hormonal and environmental control. Our intent in these sections is to gain an understanding of how various factors, biological and environmental, may influence molting processes. We next explore the issue of determinate versus indeterminate growth (i.e., the existence of a terminal instar) from physiological and demographic points of view. We then construct mathematical models that describe growth in length and weight of blue crabs over their life span, building upon our biological and environmental understanding of the molting process. Data from published empirical studies are used to estimate growth model parameters. We conclude by highlighting several areas of future research on molting and growth that would greatly improve our understanding of blue crab ecology and resource management.

THE MOLT CYCLE

The period between two molting events is commonly described in terms of a cycle tracing changes in the exoskeleton (or cuticle) between sheddings (Fig. 1). Drach (1939) divided the molt cycle into a series of stages associated with specific cuticular events from just after ecdysis (postmolt stages A, B, and C_{1-3}), through an interim period (intermolt stage C_4), to the period leading up to a subsequent ecdysis (premolt stage D). This staging method and subsequent variations (Passano 1960a; Drach and Tchernigovtzeff 1967) have been used to describe the molt cycle of blue crabs (Johnson 1980; Mangum 1985; Freeman et al. 1987) and many other decapods (see Adelung 1971; Berry 1971; Aiken 1980; O'Halloran and O'Dor 1988). Practical criteria developed by Mangum (1985) and Freeman et al. (1987) for rapid, non-destructive determination of molt stages of live, postlarval blue crabs are listed in Table 1.

Stage C_4 Integument

The crustacean integument has two main parts, an inner permanent hypodermis and an outer cuticle that is periodically shed (Fig. 1). At intermolt stage C_4, all layers of the cuticle are present: the thin outer epicuticle, composed of tanned lipoprotein and calcium carbonate ($CaCO_3$); the exocuticle, composed of tanned chitin-protein fibers and $CaCO_3$; the endocuticle, the thickest layer composed of untanned chitin-protein fibers and $CaCO_3$; and the innermost membranous layer, composed of chitin and protein but no calcium. The hypodermis is comprised of three principal layers. The outer epithelial cells, arranged one cell thick, form the layer in contact with the cuticle. The inner epithelial cells form the innermost layer, also one cell thick. In between is the connective tissue layer that consists of lipoprotein and pigment cells, oval reserve cells, and blood sinuses with hemocytes. Detailed accounts of the microstructure of decapod integumentary layers are given by Green and Neff (1972) and Roer and Dillaman (1984).

During progression of the molt cycle, both organic and mineral constituents of the cuticle are formed by the outer epithelial cells of the hypodermis. An important feature of the integument not shown in Fig. 1 are the pore canals, cytoplasmic extensions of the outer epithelial cells that run vertically through the layers of the cuticle. These pore canals are numerous, e.g., 950,000 mm^{-2} in the por-

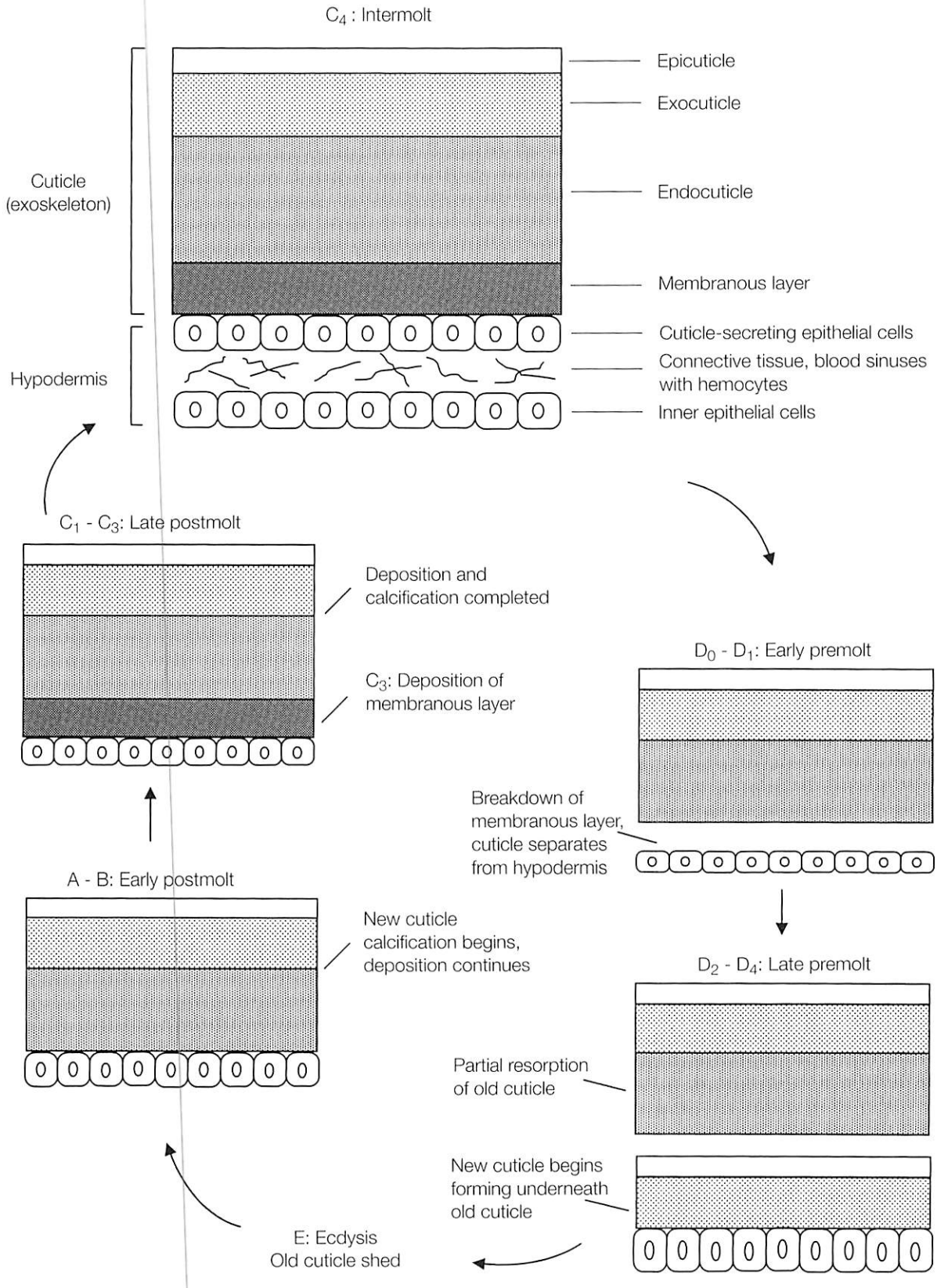

Figure 1. Conceptual diagram of the progression of changes occurring in the crustacean exoskeleton during stages of the molt cycle. Adapted from Roer and Dillaman (1984).

Table 1. Description of blue crab molt stages, modified from Passano (1960a), Johnson (1980), Mangum (1985), Freeman et al. (1987), and Hines and Young-Williams (in review), with supplemental information on body water percent from Haefner (1964) and Cameron and Wood (1985). Percent water and duration are approximate mean values.

Stage	Local name	Staging criteria	Locomotor activity	Feeding	Water %	Duration of stage %
Early postmolt					85	5
A_1	Softshell	No tangible rigidity in carapace; chelae soft and not functional	None, slight	None		
A_2	Softshell	Carapace soft with leathery, rough texture; chelae same as in A_1	Limited	None		
B_1	Papershell	Carapace soft but brittle; chelae beginning to harden and functional	Considerable	None		
B_2	None	Carapace hard at margins, mostly soft over dorsal surface; chelae hard	Full	Begins		
Late postmolt	Hardshell, or green sign		Full	Yes	70-80	25
C_1		Carapace hard; exocuticle thicker than endocuticle				
C_2-C_3		Carapace hard; endocuticle thicker than exocuticle				
Intermolt C_4	Green sign	Carapace hard; membranous layer present; color of dactyl (paddle) of fifth pereopod (swimming leg) uniformly greenish	Full	Yes	60-65	45
Early premolt			Full	Yes	60-65	15
D_0	Early white sign	Clear space begins to form along ventral rim of swim paddle				
D_1	Mid-white sign	White colored edge of swim paddle clearly visible				

Table 1, continued.

Stage	Local name	Staging criteria	Locomotor activity	Feeding	Water %	Duration of stage %
Late premolt					>60	10
D_2	Late white sign	Same as D_1	Full	Reduced		
D_3	Pink sign	Distinctive pink colored band forms along swim paddle edge	Reduced	None		
D_4	Red sign peeler	Dark red band forms along margin of swim paddle; ecdysial sutures about to break	None	None	Rise	
Ecdysis E	Buster, shedder	Ecdysial sutures open immediately ventral and anteroventral to lateral spines; animal emerging from shell	None	None	Rapid rise	<1

tunid *Carcinus maenas* (Roer 1980), keeping the hypodermis in close contact with all layers of the cuticle. Roer and Dillaman (1984) thus suggest that the cuticle should be considered living tissue.

Premolt

At the onset of premolt (stage D_0), solation (breakdown) of the membranous layer occurs, resulting in apolysis, the separation of the cuticle from the hypodermis (Fig. 1). The pore canals are severed during this process (Green and Neff 1972). Concurrently, the outer epithelial cells increase in height and complexity, and during stage D_1 these cells secrete the organic matrix of the new epicuticle (Roer and Dillaman 1984).

In *C. sapidus*, about 50% of the organic matrix in the separated cuticle is resorbed during late premolt stages D_2-D_4. In contrast, there is almost no resorption of $CaCO_3$ (Cameron and Wood 1985). The outer epithelial cells of the hypodermis attain maximum height and complexity, and begin secreting the organic matrix of the new exocuticle underneath the old exoskeleton (Fig. 1). Although portions of the new cuticle are formed before molting, the hardening processes of calcification and protein tanning occur, for the most part, after ecdysis. The one exception is that the epicuticle is tanned during premolt (Roer and Dillaman 1984). Premolt stages generally correspond to readily distinguishable "peeler" categories used in the softshell crab industry (Table 1; Fig. 2, right panels). A more refined method for determining premolt stages of decapods is based on the process of setagenesis, i.e., the development of setae or hair-like structures, in the cuticle of the scaphognathite, the appendage that pumps water across the gills (Aiken 1973). Application of this technique to blue crabs (Hines and Young-Williams, in review) is illustrated in Fig. 2 (left panels).

Descriptions of crab and lobster premolt behavior indicate that the overriding trait is for an individual to seek an isolated location in which to undergo ecdysis (Tamm and Cobb 1976; MacDiarmid 1989). Field studies of *C. sapidus* have shown that premolt crabs move into shallow, vegetated areas offering some protection from predators during molting

(Hines et al. 1987; deFur et al. 1988; Shirley et al. 1990; Wolcott and Hines 1990). Both feeding and locomotory movement activities are curtailed during late premolt, and by stage D_4 crabs have stopped eating and moving altogether (Table 1).

Distinct changes in physiology accompany these behavioral shifts. Although movement, an activity with a high tissue oxygen (O_2) demand, ceases at stage D_4, there is no corresponding reduction in ventilation, the active pumping of water across the gills that facilitates O_2 uptake into the hemolymph (i.e., blood). The resulting increase in blood O_2 levels leads to increases in blood HCO_3^- (bicarbonate), ammonia excretion, and pH (Mangum 1992). Concurrent with this rise in blood alkalinity is an increase in monovalent ion uptake, as evidenced by an increase in the activity of the transport enzyme Na^+/K^+-ATPase in the gills (Towle and Mangum 1985; Cameron 1989). These events are followed by osmotic water influx, which begins at a slow rate in stage D_4 crabs in the hours before molting. The conclusion of stage D_4 is marked by a rapid rise in water uptake, creating an intense build-up of internal hydrostatic pressure, the force of which breaks open the old cuticle along the ecdysial sutures (Neufeld and Cameron 1994).

Ecdysis

Molt stage E encompasses the actual events involved in shedding the old exoskeleton, a process termed exuviation. A detailed description of *C. sapidus* exuviation is provided in Fig. 3. The rapid uptake of water that began in late postmolt continues through ecdysis. The resulting high internal hydrostatic pressure provides the skeletal support that enables the animal to emerge from the old cuticle (Mangum 1992; Neufeld and Cameron 1994). For blue crabs, the whole process of exuviation is usually completed in a matter of minutes (Churchill 1919; Cameron 1985a).

Early Postmolt

A crab enters molt stage A_1 when it has completely cast off its old exoskeleton. The new cuticle is visibly wrinkled at this point (Cameron 1985a). The rapid uptake of water, which began in stage D_4, continues for up to several hours after ecdysis. Drinking accounts for two-thirds of the net water entering the blood space of blue crabs during this rapid uptake period, with osmotic uptake through the gills accounting for the remaining one-third (Neufeld and Cameron 1994). The net influx of water

Figure 2. (Opposite page) Setagenesis of the scaphognathite ("gill bailer") and swim paddle coloration during the molt cycle. Pairs of photos show cuticular and setal development of the scaphognathite (left) and coloration of the distal edge of the merus of the swim paddle (fifth pereopod) (right) during molt cycle progression from intermolt (C) through premolt (D_0-D_4) and ecdysis (E). (From Hines and Young-Williams, in review.) Letters with number subscripts follow the cuticular development stages of Drach (1939) and Aiken (1973) for other decapods, and are applied here (left side) to blue crabs for the transparent scaphognathite seen through a dissecting microscope. Color and stage names (right side) follow watermen's convention of the Chesapeake soft crab industry. C: intermolt; epidermis is closely adhered to the cuticle and bases of the setae (unlabeled arrow), with no sign of reorganization or retraction. Labeled arrows indicate seta components. (Note that apparent striations often seen in the epidermis are not new setae forming.) Green sign: hard crab; color of swim paddle is uniformly greenish, without discontinuity at edge (arrow). D_0: first stage of premolt; epidermis retracted from cuticle, progressively forming clear space (arrow). Early white sign: transition from green sign to white sign; development of white edge along margin of swim paddle (arrow). D_1: early setagenesis; maximal epidermal retraction, with epidermis characterized by invagination of papillae at sites of future setae (arrow) (note rough appearance of edge of epidermis); setal shaft formation progressing, but proximal ends not yet well-defined (dashed double arrow). Mid-white sign: white colored edge of swim paddle clearly visible (arrow).

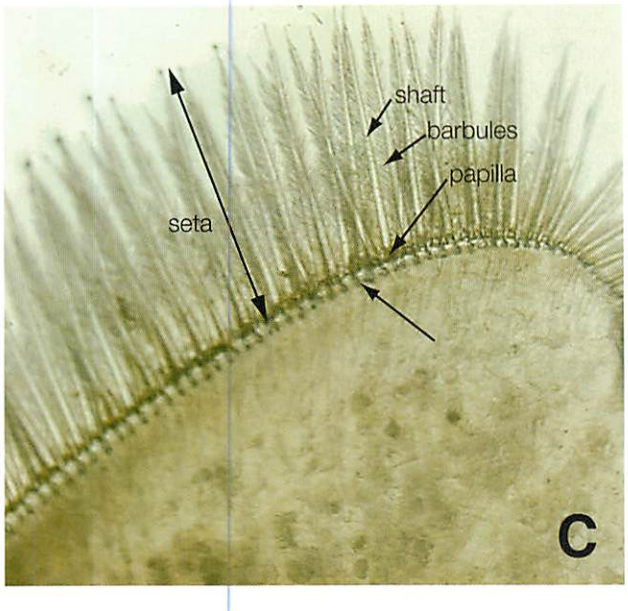
shaft
barbules
papilla
seta
C

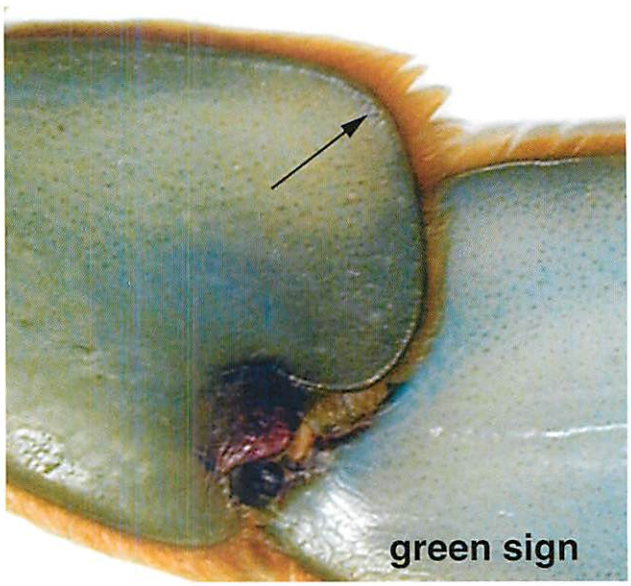
green sign

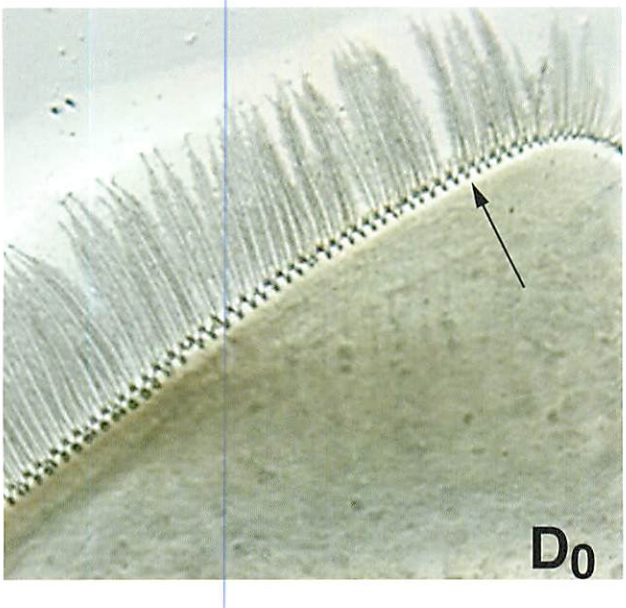
D0

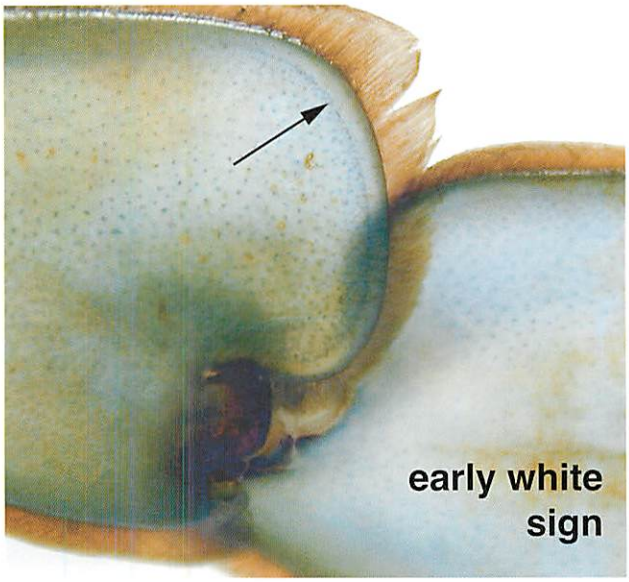
early white
sign

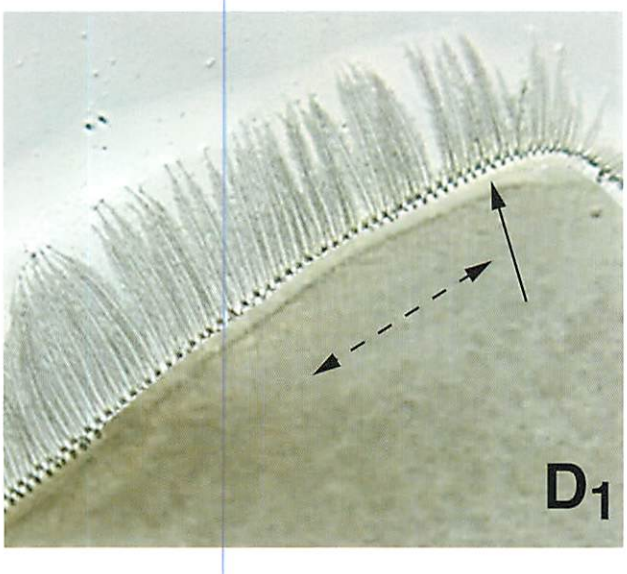
D1

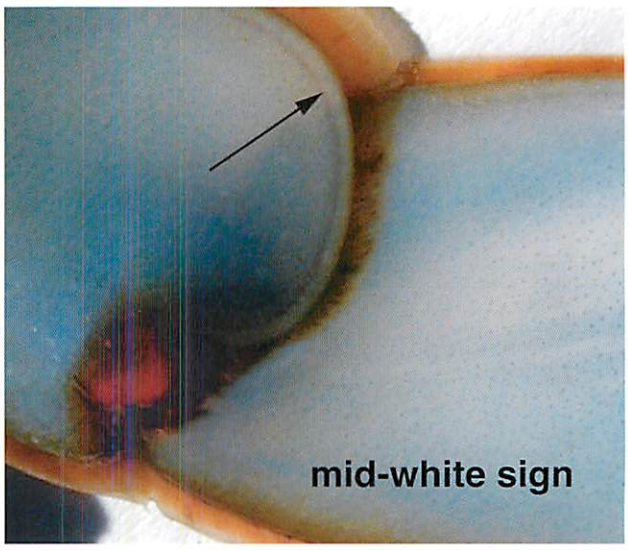
mid-white sign

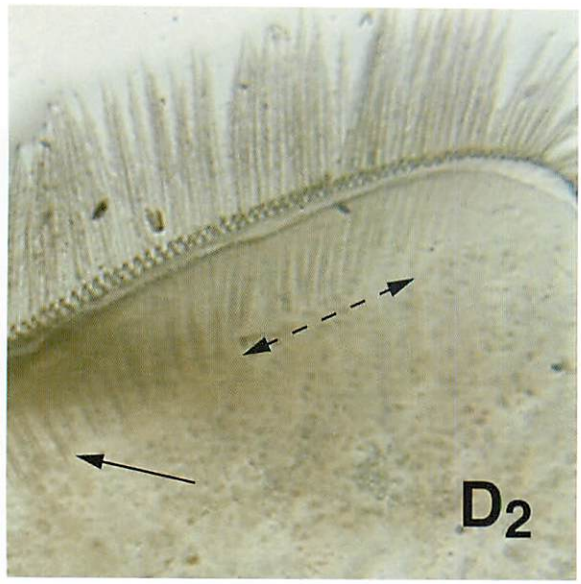
D2

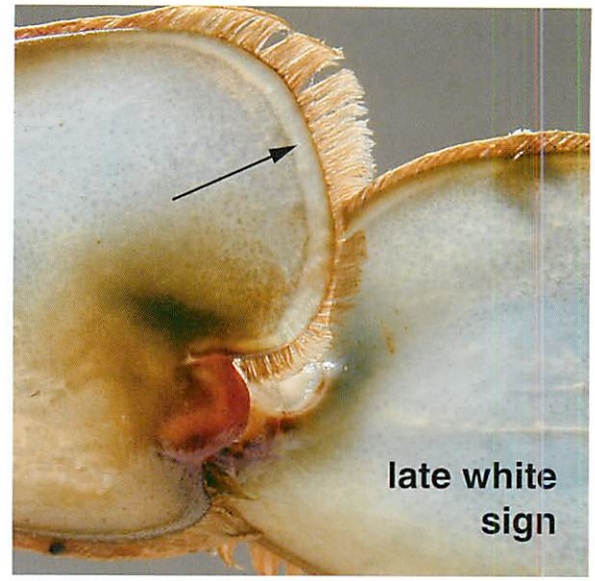
late white
sign

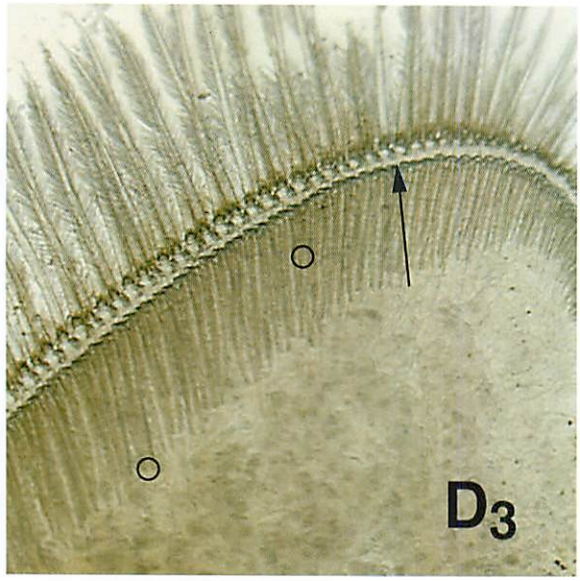
D3

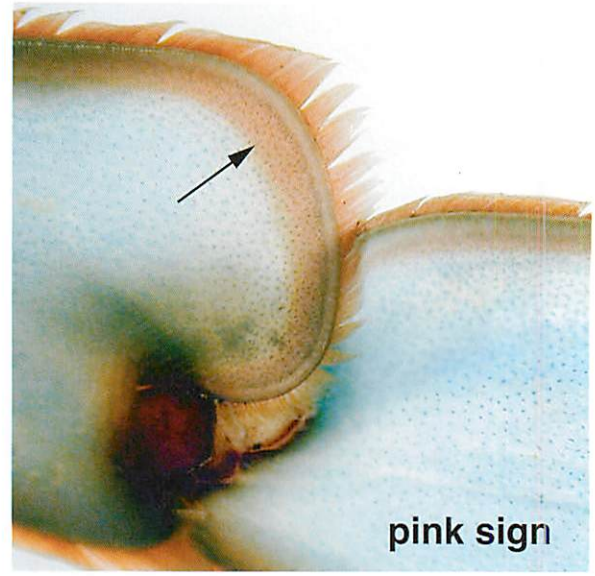
pink sign

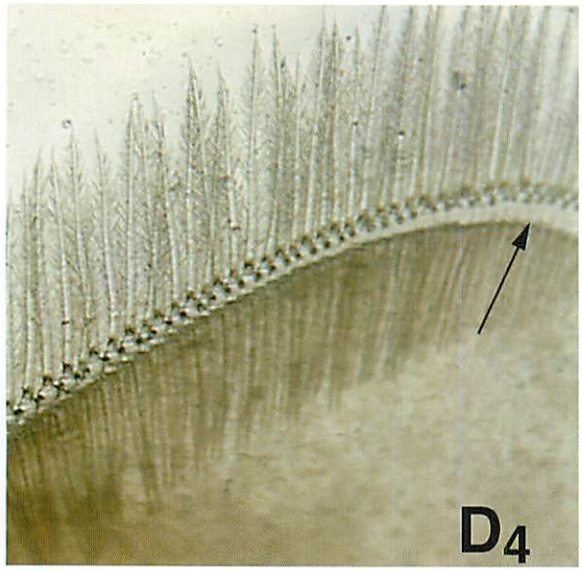
D4

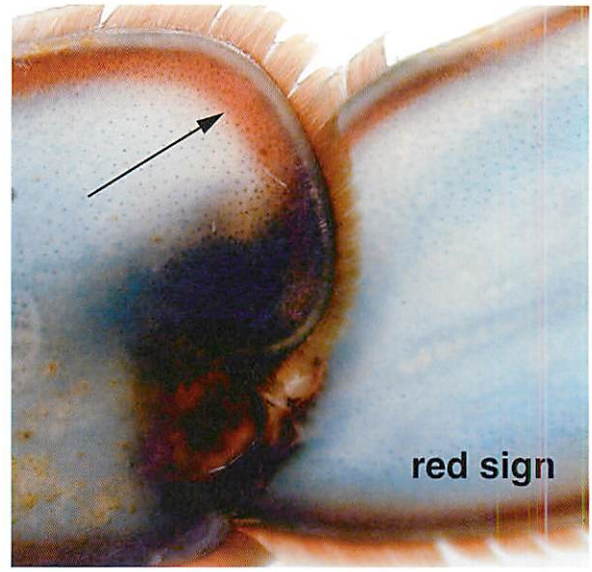
red sign

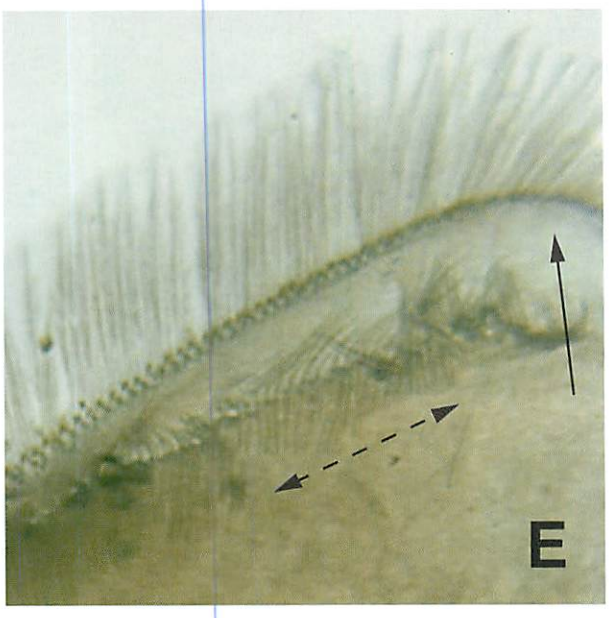

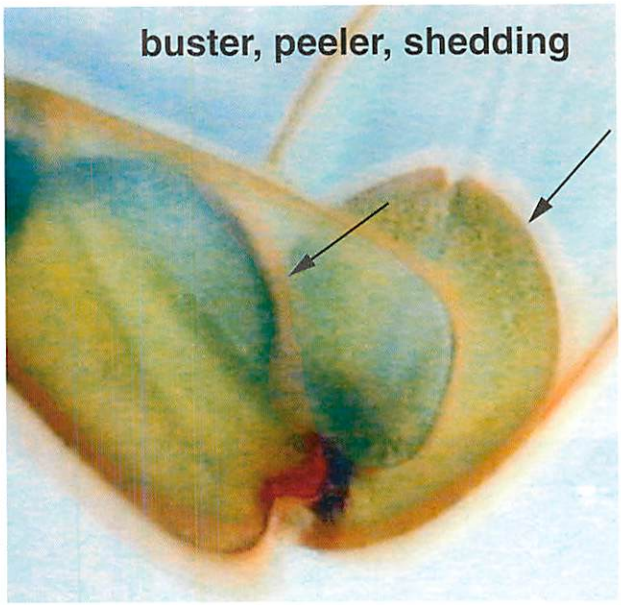

increases blood pressure to over five times normal intermolt levels, and this internal force expands the new cuticle until it becomes taut (Cameron 1989; Mangum 1992). Net water uptake and the resulting net increases in carapace width and body weight are complete by 1 to 2 h after exuviation. These new body dimensions remain constant until the next molt event (Haefner 1964; Neufeld and Cameron 1994).

Whole body calcium of blue crabs is near zero just after exuviation, indicating that Ca^{2+} is not stored in non-cuticular tissues before molting (Cameron and Wood 1985). In contrast to terrestrial species, premolt storage of calcium in soft tissues is not critical because Ca^{2+} is readily available in the external seawater medium (Greenaway 1985). Interestingly, calcification of the new cuticle in *C. sapidus* does not begin until water uptake and subsequent expansion of the exoskeleton is complete or nearly so (Cameron and Wood 1985). This delay is perhaps related to basic mechanical properties of the cuticle. The capacity for elongation is at a maximum in cuticle comprised of chitin and protein but no $CaCO_3$. Cuticle elongation capacity greatly diminishes as $CaCO_3$ content increases (Dendinger and Alterman 1983).

Figure 2, continued. (Opposite page and above) D_2: mid-setagenesis; setal shafts invaginated to maximum length (dashed double arrow) and visible along full length as double lines, but proximal ends are bifurcated (arrow) and pointed instead of blunt. Late white sign: white colored edge of swim paddle clearly visible (arrow). D_3: advanced setagenesis; shafts of setae appear blunt at proximal end (left circle) and with thick walls (right circle) as barbules become well formed and folded along the shaft; edge of new cuticle often appears scalloped (arrow), indicating folds or ripples before swelling begins. Pink sign: ready to molt; distinctive pink colored band forms along the swim paddle edge (arrow). D_4: setagenesis complete; tips of fully formed setae start to extend at surface of new cuticle (arrow), and scalloping disappears as swelling begins. Red sign: short duration transition stage continuous with "busting" as epimeral sutures begin to break; dark red band along margin of swim paddle (arrow). E: ecdysis; structures begin to pull out of exuvium (arrow), and swelling causes setae to evert, like fingers on a glove (dashed double arrow). Buster, peeler, shedding: molting; swim paddle (arrows) is pulled out of the shell. Photographs by A.C. Young-Williams and description by A.H. Hines, Smithsonian Environmental Research Center, Edgewater, Maryland.

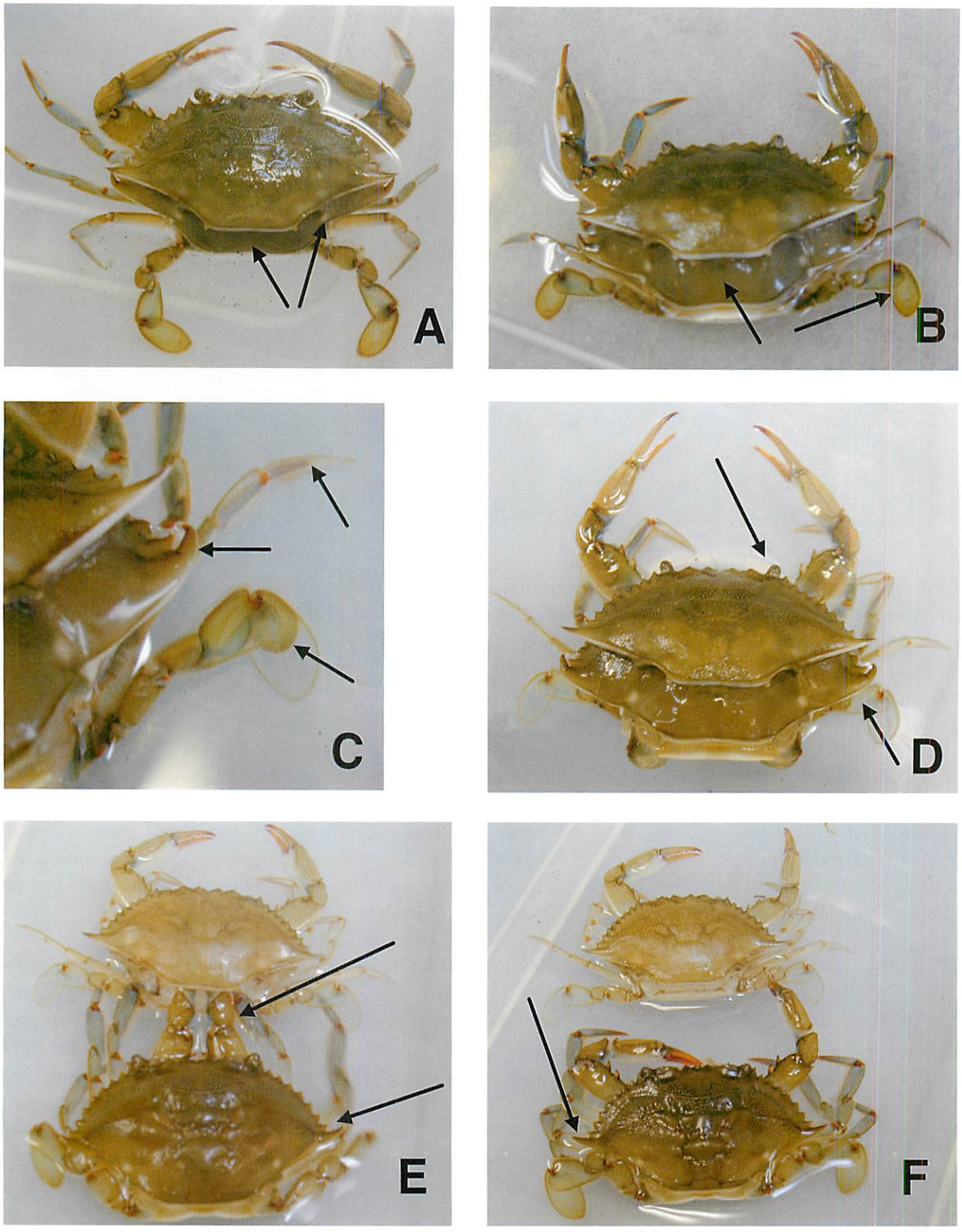
A
B
C
D
E
F

Calcification of the epicuticle and exocuticle and tanning of the exocuticle proteins begin in stages A_1-A_2. Calcium carbonate formation proceeds by the reaction

$$Ca^{2+} + HCO_3^- = CaCO_3 + H^+. \quad (1)$$

Calcium and bicarbonate ions from seawater enter the hemolymph through the gills, and are subsequently deposited in the cuticle via the outer epithelial cells, including the pore canals (Roer and Dillaman 1984; Cameron 1985b; Cameron and Wood 1985). In *C. sapidus*, uptake of Ca^{2+} and concomitant excretion of H^+ occur at extremely high rates compared to other decapods (Vigh and Dendinger 1982; Greenaway 1983; Cameron and Wood 1985). Uptake of Ca^{2+} across the gills appears to be largely passive, whereas Ca^{2+} is actively transported from the outer epithelial cells into the layers of the cuticle (Cameron 1989). Mouthparts, the gastric mill, walking legs, and other strategic regions of the exoskeleton are calcified first (Greenaway 1985).

During postmolt stages A_1-A_2, before any appreciable hardening of the exoskeleton, blue crabs are especially vulnerable to attack and injury from other animals, including other blue crabs. Softshell blue crabs (Table 1) are also in a precarious situation from a physiological perspective (Mangum 1992). In addition to undergoing a five-fold increase in blood pressure, a stage A_1-A_2 crab experiences a decrease in ventilation because the scaphognathite only works at about 50% capacity when it is soft. Fortunately, O_2 from seawater can enter the blood directly through the uncalcified postmolt cuticle. Crabs also undergo some amount of anaerobic respiration at this time; however, this produces lactic acid as a by-product, which acidifies the blood. The production of H^+ during $CaCO_3$ formation (equation 1) also contributes to a decrease in blood pH. The net increase in blood alkalinity during late premolt counterbalances this early postmolt acidosis. These mechanisms for sustaining respiration and blood acid-base balance are instrumental in enabling a crab to survive ecdysis and early postmolt. Mangum (1992) has noted that blue crabs survive this stressful period, in part, by reverting to primitive forms of skeletal support (i.e., hydrostatic; Taylor and Kier 2003) and respiration (i.e., subcutaneous).

Endocuticle secretion by the outer epithelial cells begins in stage B_1 (Fig. 1; Johnson 1980). Organic matrix formation and calcification occur simultaneously for this cuticle layer. Calcification also continues in the epicuticle and exocuticle (Roer and Dillaman 1984). A crab's ability to move progressively increases with this exoskeleton hardening. In stage B_2, blue crabs attain full locomotory movement ability and also begin to feed (Table 1).

Figure 3. (Opposite page) Ecdysis of a blue crab photographed in shallow water in the laboratory over about 30 minutes. (A) Suture lines rupture along the posterior (left arrow) and posterior-lateral (right arrow) margins of the carapace as the crab takes in water and swells. (B) Further swelling occurs and the dorsal carapace lifts off (left arrow). The crab begins to move its legs, but the legs have not yet begun to withdraw (right arrow). (C) With further leg movement the legs begin to withdraw from the exuvium, which is evident for the right fourth walking leg (top arrow) and right fifth leg (swim paddle) (bottom arrow). The swelling crab is not yet turgid, as indicated by the flopping lateral spine (middle arrow). (D) Withdrawal of walking legs is nearly complete (bottom arrow) and claws are progressing, but withdrawal of eyestalks (top arrow), foregut, and gills is not yet underway. (E) Crab extends chelae straight (top arrow) and pulls out of exuvium. The crab continues to swell but is not yet fully turgid, as lateral spines are still not fully extended (bottom arrow). (F) Ecdysis is complete, with complete swelling and extended lateral spines (arrow), but the early postmolt crab is still very soft as tanning of its new cuticle is underway. Note that the new instar is about 25% larger in carapace width than the exuvium, but much larger in volume. Photographs by A.C. Young-Williams and description by A.H. Hines, Smithsonian Environmental Research Center, Edgewater, Maryland.

Late Postmolt and Intermolt

Molt stage C includes late postmolt (C_1-C_3) and intermolt (C_4). Endocuticle deposition continues during late postmolt stages C_1-C_2, and is completed in stage C_3 (Roer and Dillaman 1984). Feeding and movement return to intermolt levels during this period (Table 1). Substantial growth of internal soft tissues occurs. Blue crabs are approximately 85% water and 15% dry tissue by weight immediately after ecdysis (Haefner 1964; Cameron and Wood 1985). Dry tissue content increases to about 30% of animal wet weight by the end of postmolt. Secretion of the membranous layer marks the completion of the new exoskeleton and the end of postmolt stage C_3 (Roer and Dillaman 1984). Although all layers of the cuticle are complete, internal tissue growth continues during intermolt stage C_4. Dry tissue content eventually reaches a maximum of 35 to 40% of animal weight (Haefner 1964; Cameron and Wood 1985).

Molting Processes, Cycle Stages, and Animal Size

The basic aspects of cycle progression through postmolt, intermolt, premolt, and ecdysis apply to all decapod life stages that undergo molting, which include larvae as well as juveniles and adults (Aiken 1980; Sasaki 1984). Distinct molt stages have even been identified in decapod embryos, as it appears that the process of embryonic development involves one to several molts that occur within the egg (Lachaise and Hoffmann 1982; Goudeau et al. 1990; Helluy and Beltz 1991). The main phase of somatic growth, and thus the majority of molting, occurs from postlarval settlement through the juvenile life stage. The rate of increase in body size tends to slow down as individuals enter the adult life stage and begin to produce offspring.

The time between molts, one main component of the molting process, is the duration of one complete circuit through the molt cycle. During the main juvenile growth phase, blue crabs remain in stage C_4 for nearly one-half of the total molt cycle period. The remaining cycle time is almost evenly divided between premolt (D_0-D_4) and postmolt (A_1-C_3) stages (Freeman et al. 1987; Table 1). A general property of decapods during the somatic growth phase is that actual cycle durations progressively increase with increasing animal size (Passano 1960a; Smith 1997); however, the average proportion of time spent in each molt stage appears to remain fairly constant irrespective of size (Adelung 1971; Aiken 1980; Freeman et al. 1987). The second main component of the molting process, the size increase at molting (i.e., molt increment), seems to be linked to the events of new cuticle formation and elongation that occur from late premolt through early postmolt. This process is also affected by animal size. In blue crabs, molt increments tend to increase as animal size increases during the juvenile growth phase (Churchill 1919; Gray and Newcombe 1938).

ENDOCRINE CONTROL

Much of the information about the endocrine regulation of molting in crustaceans has been obtained from species of decapods other than blue crabs. However, it is reasonable to assume that the generalities are applicable to blue crabs as well. For this reason, we will not limit this discussion solely to blue crabs.

Isolation and Characterization of the Molting Hormone

Using the classical endocrinological methods of ligation, extirpation, and implantation of suspected glands, Kopec (1922) first hypothesized that arthropod molting was regulated by hormones. The study required the development of various chromatographic techniques and the accumulation of large amounts of starting material before the first molting hormone was isolated and characterized. From several hundreds of kilograms of moth pupae, the steroid hormone ecdysone was isolated (Butenandt and Karlson 1954).

The structure of insect ecdysone was subsequently determined to be 2ß,3ß,14α,22R,25-pentahydroxy-5ß-cholest-7-en-6-one (Karlson et al. 1965; Huber and Hoppe 1965; Fig. 4). Shortly

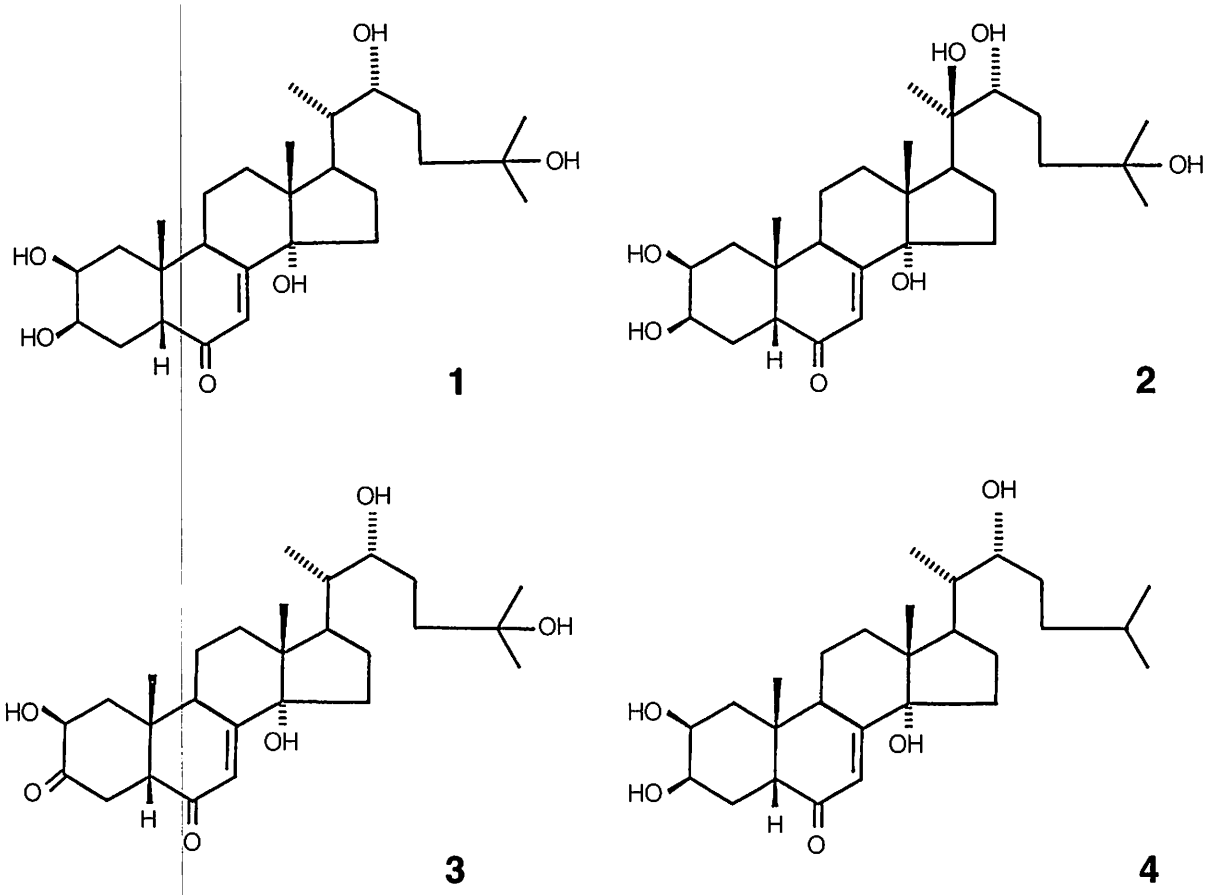

Figure 4. Structures of (1) ecdysone, (2) 20-hydroxyecdysone, (3) 3-dehydroecdysone, and (4) 25-deoxyecdysone.

thereafter, Horn and his colleagues (Hampshire and Horn 1966; Horn et al. 1966) isolated and determined the structure of a related steroid hormone, 20-hydroxyecdysone (Fig. 4) from the rock lobster *Jasus lalandei*. Although the hormone was originally called crustecdysone or ecdysterone, Horn's group demonstrated the identity of 20-hydroxyecdysone as the principal active form of the molting hormone from both insect and crustacean sources. In most species examined, it appears that ecdysone is the prohormone secreted by the Y-organ and it is hydroxylated by target tissues to 20-hydroxyecdysone (Chang and O'Connor 1978). There are exceptions to this paradigm, however, as described below. Although 20-hydroxyecdysone appears to be the predominant molting hormone in all decapod species examined to date, other ecdysteroids (steroids structurally related to 20-hydroxyecdysone that have molting hormone activity) have been characterized in hemolymph and tissues of various species. These other ecdysteroids include ecdysone; ponasterone A (25-deoxy-20-hydroxyecdysone); inokosterone (25-deoxy-20,26-dihydroxyecdysone); makisterone A (24-methyl-20-hydroxyecdysone); 20,26-dihydroxyecdysone; and 2-deoxyecdysone (for reviews, see Spindler et al. 1980; Skinner 1985; Watson et al. 1989; Chang 1993). Comparisons in the absolute concentrations of the different ecdysteroids between species are difficult to make due to different detection methods and the lack of standardization in the molt stage of the donor animals. Table 2 lists some of the ecdysteroid isolation and quantification data obtained from blue crabs.

Classical morphological observations and endocrinological experiments (Gabe 1953; Echalier 1959) indicated that the molting gland in the crab

Table 2. Quantification of ecdysteroids in *C. sapidus*.

Source	Method[1]	Type of ecdysteroid found	Concentration (ng g^{-1})
whole body[a]	MS	inokosterone	0-20
		makisterone A	0-24
		20-hydroxyecdysone	0-280
whole body (female)[b]	RIA	?	5-90
whole body (male)[b]	RIA	?	5-55
hemolymph (female)[b]	RIA	?	2-38[2]
hemolymph (male)[b]	RIA	?	2-50[2]
ovaries[b]	RIA	?	1.1-2.9
embryos[c]	HPLC, MS, RIA	ponasterone A	?
Y-organs[d]	RIA	?	11[3]

[a] Faux et al. 1969.
[b] Soumoff and Skinner 1983.
[c] McCarthy 1979.
[d] Schoettker and Gist 1990.

[1] Abbreviations: HPLC = high-performance liquid chromatography; MS = mass spectroscopy; RIA = radioimmunoassay.

[2] ng ml^{-1}

[3] ng mg^{-1} of Y-organ protein during the first 9 h in vitro.

C. maenas was the thoracic Y-organ. In crabs, the Y-organs are spheroidal glands located ventrally and anteriorly in the gill chambers. Organ culture experiments using Y-organs from the crabs *Cancer antennarius* and *Pachygrapsus crassipes* resulted in the characterization of ecdysone as the primary secretory product of the Y-organ (Chang and O'Connor 1977). Analogous results were obtained from the crayfish *Orconectes limosus* (Keller and Schmid 1979). In vitro cultures of blue crab Y-organs confirmed that these glands secrete ecdysteroids (Schoettker and Gist 1990). Neither the identification of the specific secretory product of the Y-organ nor the primary circulating ecdysteroid in the hemolymph have been reported for *C. sapidus*.

Recent data have revealed that there are other ecdysteroids secreted by the Y-organs in some crab species. These ecdysteroids include 3-dehydroecdysone (Fig. 4) from *C. antennarius* (Spaziani et al. 1989) and 25-deoxyecdysone (Fig. 4) from *C. maenas* (Lachaise et al. 1989; see review by Watson et al. 1989). It is apparent that much more comparative research must be conducted on the determination of the types and ratios of the different ecdysteroids secreted by the Y-organs from various species.

Regulation of the Molting Gland

The concentration of the molting hormone fluctuates dramatically during the molt cycle and these changes mediate the various biochemical and physiological processes that occur during the cycle. At postmolt, just after ecdysis, the molting hormone titer is negligible or may show a slight rise (Figs. 5 and 6; Soumoff and Skinner 1983). Low, relatively constant levels are observed during intermolt. There is an increase in ecdysteroids above intermolt levels

that is indicative of the premolt stage. A high level of the hormone followed by a precipitous drop is observed just before ecdysis.

It appears that alterations in the rate of synthesis or secretion of ecdysone by the Y-organ may be the predominant means of controlling circulating ecdysteroids. Partial evidence for this is the observation that the secretory rate of ecdysteroids by Y-organs in vitro is correlated with the amount of circulating ecdysteroids observed in the hemolymph of *P. crassipes*. Just before the substage of premolt in which the highest concentration of ecdysteroids was observed in the hemolymph, explanted Y-organs were found to secrete the greatest amount of ecdysone (Chang and O'Connor 1978). Whether this phenomenon is true for *C. sapidus* is unknown.

Removal of both stalked eyes of the fiddler crab *Uca pugilator* resulted in a shortening of the intermolt period (duration of molt cycle or molt interval; not to be confused with the intermolt stage) (Zeleny 1905). This observation lead to the postulation of an endocrine factor present in the eyestalks that normally inhibits molting — a molt-inhibiting hormone (MIH). Detailed microscopical examinations resulted in the description of a neurohemal organ in the eyestalk of several decapod crustaceans (Bliss and Welsh 1952; Passano 1953). This neurohemal organ is called the sinus gland and serves as a storage site for neurosecretory products. It consists of the enlarged endings of a group of neurosecretory neurons collectively called the X-organ (Hanström 1939). The shortened intermolt period of eyestalk-ablated decapods is likely due to a rapid elevation in the concentration of circulating ecdysteroids, which is a result of X-organ/sinus gland removal (Chang et al. 1976; Chang 1993; Fig. 6).

The demonstration of decreased ecdysteroid titers in eyestalk-ablated crabs that have been injected with eyestalk extracts (Hopkins 1982; Keller and O'Connor 1982) lends additional support to the paradigm of the MIH–Y-organ molt-controlling axis. Further evidence of this hypothesis was provided by Gersch et al. (1980), who demonstrated that if crayfish *O. limosus* were initially injected with sinus gland extracts, the subsequent culture of the crayfish Y-organs resulted in a decreased production

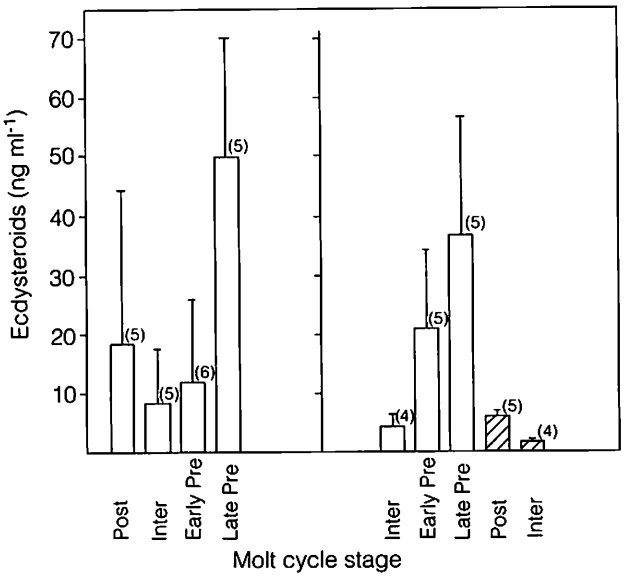

Figure 5. Ecdysteroid concentrations (means ± S.D.) in the hemolymph of male (left) and female (right) blue crabs during the course of the molt cycle. Numbers are crabs assayed. Hatched bars represent mature females. Data are presented as 20-hydroxyecdysone equivalents. Redrawn from Soumoff and Skinner (1983).

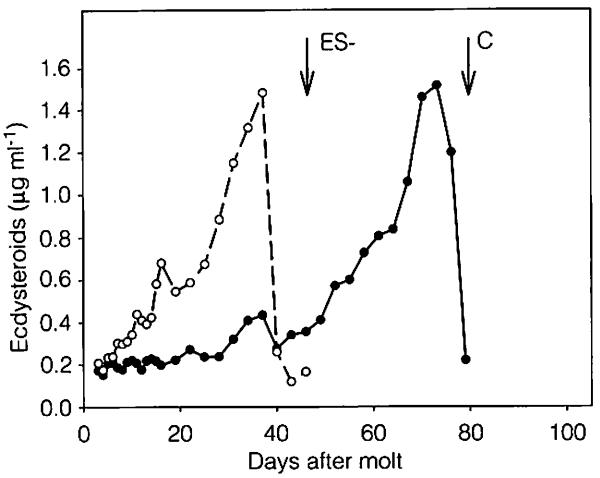

Figure 6. Hemolymph ecdysteroids from an intact (solid circles) Dungeness crab (*Cancer magister*) compared to a crab of the same age and molt stage that had its eyestalks removed 3 days after molt (open circles). Arrows indicate time of molt of the crab without eyestalks (ES-) and of the control (C) crab. Ecdysteroids were determined by radioimmunoassay. From Chang (1993). Reprinted with permission from the Annual Review of Entomology, Volume 38, copyright 1993 by Annual Reviews, www.annualreviews.org.

of ecdysone compared to control-injected animals. Subsequent experiments also demonstrated the ability of crab sinus glands to inhibit ecdysteroid secretion by the Y-organ (Soumoff and O'Connor 1982; Mattson and Spaziani 1985; Schoettker and Gist 1990). In vitro secretion of ecdysone by crab Y-organs could be inhibited when cultured with either conditioned medium that had previously been incubated with explanted sinus glands or by the addition of eyestalk extracts (Fig. 7).

Additional evidence of the inhibitory role of MIH was shown by Lee et al. (1998) and Watson et al. (2001b). Using a cDNA probe to *C. sapidus* MIH, they demonstrated that the amount of MIH mRNA in the eyestalk neural ganglia was negatively correlated with the hemolymph concentration of ecdysteroids, e.g., there were low levels of MIH mRNA in the eyestalk during premolt. However, Chung and Webster (2003) have recently reported data indicating that not only do circulating levels of MIH vary during the course of the molt cycle, but that the sensitivity of the Y-organ cells to MIH may also vary.

Molt-inhibiting hormone is a member of a novel neuropeptide family, representatives of which have to date only been found in arthropods. This is a fascinating neuropeptide family because its members regulate such diverse functions as molting, reproduction, and metabolism. There has been a flurry of recent publications about members of this peptide family (for reviews see Chang 1993; De Kleijn and Van Herp 1995; Webster 1998; Watson et al. 2001b; Böcking et al. 2002). These studies used lobsters *Homarus americanus*, shrimp and prawns (*Litopenaeus* spp., *Marsupenaeus japonicus*, *Metapenaeus ensis*, and *Macrobrachium rosenbergii*), crayfish (*O. limosus* and *Procambarus* spp.), isopods *Armadillidium vulgare*, locusts *Schistocerca gregaria*, and several crabs. For the purposes of this review, we will restrict our discussion primarily to members of this hormone family found in crabs.

The first crab MIH was characterized from *C. maenas* (Webster 1991). Its amino acid sequence was determined via Edman degradation sequencing methods (Fig. 8). It has 78 amino acid residues with six cysteines and unblocked N- and C-termini. With the use of PCR techniques, a cDNA encoding the complete precursor of MIH from *C. maenas* was isolated and sequenced. The precursor consists of a 35-amino acid residue signal peptide and the 78-amino acid mature MIH (Klein et al. 1993). Molt-inhibiting hormone peptides were also isolated or characterized from *C. sapidus* (Lee et al. 1995), *Cancer pagurus* (Chung et al. 1996), and *Cancer magister* (Umphrey et al. 1998).

Watson's laboratory has worked extensively on *C. sapidus* MIH. In addition to the molecular probes mentioned above, they have developed MIH anti-

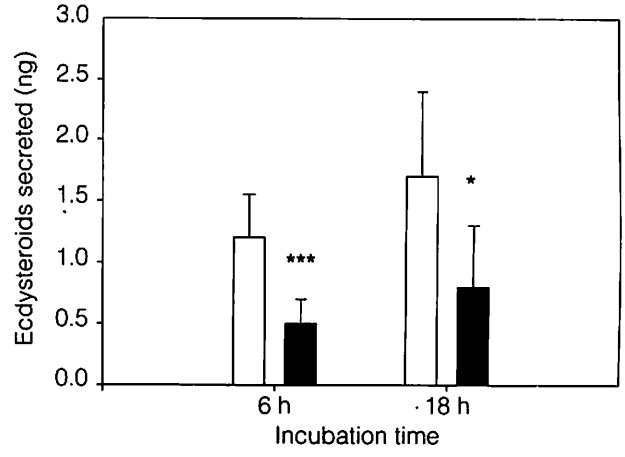

Figure 7. Sinus gland extract inhibition of ecdysteroid secretion by Y-organs. Each Y-organ from *Cancer magister* was cut into 8 pieces to decrease variability. Two pieces of each organ served as its own control. Each piece was preincubated in sterile lobster saline for 30 min and then placed into 0.5 ml of Medium 199 containing fetal bovine serum (10%), penicillin-G (12.5 U ml^{-1}), and streptomycin sulfate (12.5 µg ml^{-1}) in a 24-well tissue culture plate (Corning). Sinus gland extracts from *C. magister* were prepared in sterile lobster saline and added to the wells in a volume of 5 µl. Y-organ pieces were incubated for 6 or 18 h with continuous agitation at 16°C with (black bars) or without (open bars) sinus gland extracts (0.5 gland equivalents). Medium (50 µl) was removed from each well and assayed for ecdysteroids using radioimmunoassay. Data are expressed as means (± S.D.) of ecdysteroids secreted per Y-organ piece. Eight Y-organs were used for the experiment. Asterisks indicate significance at $p<0.05$ (*) or $p<0.001$ (***) (Tamone and Chang, unpublished).

	1										11									21					
Canm-MIH	R	V	I	N	D	D	C	P	N	L	I	G	N	R	D	L	Y	K	R	V	E	W	I	C	E	D
Cap-MIH	R	V	I	N	D	D	C	P	N	L	I	G	N	R	D	L	Y	K	K	V	E	W	I	C	E	D
Cap-MOIH-1	R	R	I	N	N	D	C	Q	N	F	I	G	N	R	A	M	Y	E	K	V	D	W	I	C	K	D
Cap-MOIH-2	R	R	I	N	N	D	C	Q	N	F	I	G	N	R	A	M	Y	E	K	V	D	W	I	C	K	D
Carm-CHH	pE	I	Y	D	T	S	C	K	G	V		Y	D	R	A	L	F	N	D	L	E	H	V	C	D	D
Carm-MIH	R	V	I	N	D	E	C	P	N	L	I	G	N	R	D	L	Y	K	K	V	E	W	I	C	E	D
Cas-MIH	R	V	I	N	D	D	C	P	N	L	I	G	N	R	D	L	Y	K	K	V	E	W	I	C	D	D
Lie-MOIH	pE	I	F	D	P	S	C	K	G	L		Y	D	R	G	L	F	S	D	L	E	H	V	C	K	D

					31										41										51	
Canm-MIH	C	S	N	I	F	R	N	T	G	M	A	T	L	C	R	K	N	C	F	F	N	E	D	F	L	W
Cap-MIH	C	S	N	I	F	R	N	T	G	M	A	T	L	C	R	K	N	C	F	F	N	E	D	F	L	W
Cap-MOIH-1	C	A	N	I	F	R	K	D	G	L	L	N	N	C	R	S	N	C	F	Y	N	T	E	F	L	W
Cap-MOIH-2	C	A	N	I	F	R	Q	D	G	L	L	N	N	C	R	S	N	C	F	Y	N	T	E	F	L	W
Carm-CHH	C	Y	N	L	Y	R	T	S	Y	V	A	S	A	C	R	S	N	C	Y	S	N	L	V	F	R	Q
Carm-MIH	C	S	N	I	F	R	K	T	G	M	A	S	L	C	R	R	N	C	F	F	N	E	D	F	V	W
Cas-MIH	C	A	N	I	Y	R	S	T	G	M	A	S	L	C	R	K	D	C	F	F	N	E	D	F	L	W
Lie-MOIH	C	Y	N	L	Y	R	N	P	Q	V	T	S	A	C	R	V	N	C	Y	S	N	R	V	F	R	Q

								61									71							
Canm-MIH	C	V	Y	A	T	E	R	T	E	E	M	S	Q	L	R	Q	W	V	G	I	L	G	A	G	R	E
Cap-MIH	C	V	Y	A	T	E	R	T	E	E	M	S	Q	L	R	Q	W	V	G	I	L	G	A	G	R	E
Cap-MOIH-1	C	I	D	A	T	E	N	T	R	N	K	E	Q	L	E	Q	W	A	A	I	L	G	A	G	W	N
Cap-MOIH-2	C	I	D	A	T	E	N	T	R	N	K	E	Q	L	E	Q	W	A	A	I	L	G	A	G	W	N
Carm-CHH	C	M	D	D	L	L	M	M	D	E	F	D	Q	Y	A	R	K	V	Q	M	V_{NH2}					
Carm-MIH	C	V	H	A	T	E	R	S	E	E	L	R	D	L	E	E	W	V	G	I	L	G	A	G	R	D
Cas-MIH	C	V	R	A	T	E	R	S	E	D	L	A	Q	L	K	Q	W	V	T	I	L	G	A	G	R	I
Lie-MOIH	C	M	E	D	L	L	L	M	E	D	F	D	K	Y	A	R	A	I	Q	T	V_{NH2}					

Figure 8. Amino acid sequences of the CHH/MIH/MOIH/VIH family of neuropeptides from crabs: *Cancer magister* molt-inhibiting hormone (Canm-MIH; Umphrey et al. 1998), *Cancer pagurus* MIH (Cap-MIH; Chung et al. 1996), *C. pagurus* mandibular organ-inhibiting hormones (Cap-MOIH-1, Cap-MOIH-2; Wainwright et al. 1996), *Carcinus maenas* crustacean hyperglycemic hormone (Carm-CHH; Kegel et al. 1989), *C. maenas* MIH (Carm-MIH; Webster 1991; Klein et al. 1993), *Callinectes sapidus* MIH (Cas-MIH; Lee et al. 1995), and *Libinia emarginata* MOIH (Lie-MOIH; Liu et al. 1997).

sera (Watson et al. 2001a; Lee and Watson 2002a) and reported progress on the production of recombinant MIH (Lee and Watson 2002b). Elucidation of the physiological action of MIH upon the Y-organ will be aided by the availability of large quantities of MIH.

Crustacean hyperglycemic hormone (CHH) is a member of the same neuropeptide family as MIH. It contains a high degree of homology with MIH. It has been isolated and characterized from the crab *C. maenas* (Kegel et al. 1989; Weidemann et al. 1989). In contrast to considerable accumulated knowledge on the structure of CHH, its localization in neurosecretory structures, and its activities in several bioassays, relatively little is known of the physiological role of CHH in vivo. One important role of CHH is the maintenance of glucose homeostasis. In the crayfish *O. limosus*, sinus gland removal that left the remainder of the eyestalk neural tissue and vision intact clearly demonstrated the hormone is responsible for maintaining the normal glucose level and for a circadian rhythm in blood glucose (Hamann 1974). Hyperglycemia is commonly observed under a variety of stressful conditions, and there is considerable indirect evidence to suggest that this stress hyperglycemia is caused by the release of CHH (for reviews see Kleinholz and Keller 1979 and Keller and Sedlmeier 1988). For example, under hypoxia, glucose may be released by CHH from carbohydrate stores to serve as a substrate for glycolysis and lactate formation, as is typical for anaerobiosis of decapod crustaceans.

Another important function of CHH has recently been documented in *C. maenas*. Chung et al. (1999) observed a dramatic rise in the late premolt concentration of CHH compared to intermolt

values (over 100-fold). This surge in CHH regulates the massive ion and water uptake during ecdysis and mediates the swelling necessary for successful ecdysis. The source of this premolt CHH was shown to be paraneurones located in the fore- and hindgut (Webster et al. 2000).

Other members of this same peptide family are the neuropeptides from the crabs *C. pagurus* (Wainwright et al. 1996) and *Libinia emarginata* (Liu et al. 1997). These hormones inhibit the mandibular organ (and hence are called mandibular organ-inhibiting hormones; MOIH). The mandibular organ and its secretory product are discussed in more detail below.

Yet another member of this novel neuropeptide hormone family is the vitellogenesis-inhibiting hormone (VIH) from *H. americanus* (Soyez et al. 1991). This peptide was isolated with the use of a heterologous assay involving the inhibition of yolk synthesis in eyestalk-ablated shrimp *Palaemonetes varians*. An analogous VIH has not yet been characterized from any crab species.

It is clear that members of the MIH/CHH/MOIH/VIH neuropeptide family are closely related and regulate the major physiological processes of crabs and other crustaceans. Recent data on the genomic organization of these peptides indicate that this peptide family can be divided into two subgroups (see Böcking et al. 2002 for review). Peptides belonging to the CHH subgroup are encoded by exons that include a translated CHH-precursor related peptide (CPRP). This CPRP is cleaved from the CHH prohormone to produce mature CHH. Genes coding for peptides belonging to the MIH/MOIH/VIH subgroup do not code for a CPRP.

There are various degrees of biological cross-reactivity between those peptides that have been assayed in intra- or interspecific comparisons. We believe that these hormones may have physiological relevance beyond the process implied by the names given to these peptides by researchers. For example, MIH may have distinct roles in crab physiology other than solely inhibiting the molt via repression of the Y-organ.

Methyl Farnesoate

The mandibular organ produces a sesquiterpenoid related to the insect juvenile hormone (Fig. 9). This related compound is methyl farnesoate (MF; Fig. 9), and was initially isolated from *L. emarginata* (Laufer et al. 1987). It was further determined that the secretory source of MF was the mandibular organ. Analogous data were obtained from the crabs *Cancer borealis* and *C. maenas* and other decapods (Borst et al. 1987).

Methyl farnesoate may have several different effects on crustacean development and reproduction (for review see Homola and Chang 1997). It has been shown to have an effect upon the duration of the molt cycle. When added to the water in which lobster larvae were cultured (Borst et al. 1987), there was a small yet significant increase in the time to metamorphosis compared to control larvae. These observations are consistent with the hypothesis that MF is acting as a crustacean juvenile hormone in that it promotes the retention of juvenile characteristics. There were, however, no significant changes in the morphology of the larval lobsters.

Manipulations involving the mandibular organ can alter the intermolt period. Yudin et al. (1980) observed that implantation of blue crab mandibular organs into white shrimp *Litopenaeus setiferus* resulted in shortened intermolt periods accompanied by more frequent molting (Table 3). The molt stimulation was not due to ecdysteroid secretion by the mandibular organ. Tamone and Chang (1993) observed that application of MF increases the synthesis and/or secretion of ecdysteroids by the Y-organ. Y-organs from *C. magister* were incubated with various concentrations of MF. In the presence of MF, the organs secreted more ecdysteroids into the medium after a 24-h incubation when compared to controls. The magnitude of this stimulation increased with higher concentrations of MF and increasing incubation times. Consistent results were observed in lobster larvae cultured in water containing MF. At various times, the larvae were extracted for ecdysteroids and assayed using an ecdysteroid radioimmunoassay. After 48 h, the larvae incubated with exogenous MF had significantly higher levels

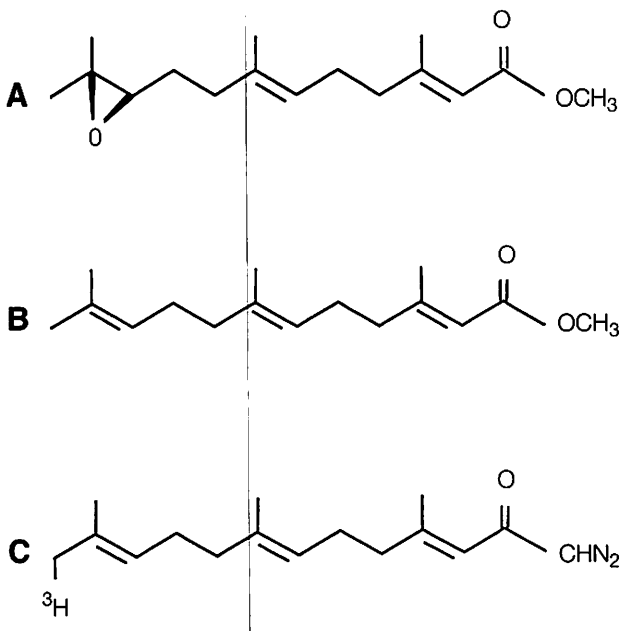

Figure 9. Structures of: (A) Juvenile hormone III. (B) Methyl farnesoate. (C) [^{3}H]-farnesyl diazomethyl ketone.

of ecdysteroids compared to control larvae (Chang et al. 1993).

Hemolymph MF binding proteins have been characterized in the few crustacean species examined. Prestwich et al. (1990) characterized a 40 kDa protein in the hemolymph of *H. americanus* that bound a photoaffinity analog of MF (farnesyl diazomethyl ketone, FDK; Ujváry and Prestwich 1990; Fig. 9). Binding of [^{3}H]-FDK was prevented in the presence of excess unlabeled MF. Methyl farnesoate binding proteins were also observed in the hemolymph of shrimp *Sicyonia ingentis* (Chang et al. 1992), crayfish *Procambarus clarkii* (King et al. 1995) and crabs (*L. emarginata*, Li and Borst 1991; *C. magister*, Tamone and Chang 1993).

Regeneration

Decapods have an amazing ability to regenerate limbs, and crabs have been the primary experimental animals for research in this area. The topic has been extensively reviewed by Skinner (1985) and Hopkins (1988). Wound closure occurs immediately proximal to the site of limb loss (autotomy plane) due to the extension of a connective tissue septum (Emmel 1910). In minutes, blood cells start to migrate to the site of the wound and a scab forms. Within hours to days, multipotent cells migrate to the site and mitosis and differentiation of a regenerating limb bud begin. Depending upon when limb loss occurred during the molt cycle, a fully formed, albeit often smaller, limb will unfold at the subsequent molt.

Skinner (1985) observed that both the time that autotomy (self-induced leg loss) occurred during the molt cycle and the number of limbs autotomized affected the duration of the intermolt period. Using the crab *Gecarcinus lateralis*, she observed that loss (and hence initiation of regeneration) of five or more limbs during the intermolt stage resulted in a shortened intermolt period. Loss of two or more limbs during early premolt lengthened the intermolt period. This has led to the postulation of an endocrine factor that is synthesized/released upon multiple limb autotomy in anecdysis (intermolt) and that

Table 3. Effect of *C. sapidus* mandibular gland implants on the molt cycle of white shrimp *Litopenaeus setiferus*. Control A: unmanipulated; Control B: jabbed with a needle; Control C: crab muscle implants; Experimental: implanted with crab mandibular glands (from Yudin et al. 1980). (n = sample size.)

Variable	Control A	Control B	Control C	Experimental
n	11	11	20	26
total number of molts	9	10	12	35[1]
mean intermolt period (d)	87.6	76.5	70.6	32.2[1]

[1] Significantly different from all controls at $p<0.05$.

shortens the intermolt period. This factor is called limb autotomy factor-anecdysial (LAF_{an}) (Holland and Skinner 1976; Skinner 1985). The other postulated factor, which is thought to be responsible for the proecdysial (premolt) lengthening of the intermolt period, is called limb autotomy factor-proecdysial (LAF_{pro}). Little is known about the chemical nature of these hypothesized factors, though LAF_{pro} is likely a peptide (Yu et al. 2002).

Regenerated limbs can be induced in heterotopic sites. For example, implantation of claw tissue of the crab *Cancer gracilis* into the stump of a recently autotomized walking leg can give rise to a regenerated claw (Kao and Chang 1996). In other experiments, one eyestalk of a crab *Cancer jordani* was removed and claw tissue was implanted into the eye socket. Occasionally a complete claw was able to differentiate in the heterotopic site (Kao and Chang 1997). The chemical natures of the morphogens involved in these unusual examples of regeneration are unknown.

Conceptual Model

The X-organ – Y-organ endocrine control system for molting is illustrated in Fig. 10A. This system regulates the transition from intermolt to premolt (Fig. 1), and thus plays a direct role in determining the duration of the molt cycle. As described above, animals spend the majority of time between molts in intermolt stage C_4 (Table 1). Empirical growth studies for *C. sapidus* and other decapods have found that the duration of stage C_4 varies widely among study animals of similar sizes, whereas durations of postmolt and premolt stages exhibit little individual variability (Berry 1971; Hopkins 1982; Freeman et al. 1987; O'Halloran and O'Dor 1988; Rahman and Subramoniam 1989). This observation indicates that most of the variability in the intermolt period can be attributed to stage C_4. The source of this variability has been further pinpointed to the transition between the intermolt and premolt stages of the molt cycle. Aiken's (1973) detailed investigation of the premolt stage of *H. americanus* recorded transition times from stages C_4 to D_3 for individual lobsters. Some lobsters steadily progressed through these stages with no pause, while others initially progressed part way through stage D_0 and then remained there for several weeks to several months before continuing through stages D_1 to D_3. This delay period, described by Aiken (1973) as a "development plateau," occurred in stage D_0 (the early phase of apolysis) in *H. americanus* and appears to occur either in the latter portion of stage C_4 or early stage D_0 in other species (Aiken 1980; Hopkins 1982). The duration of Aiken's (1973) "development plateau" appears directly linked to the MIH-controlled inhibition period of stages C_4 or D_0, or both, preceding stage D_1.

The connection between MIH and intermolt period variability has been further elucidated from results of eyestalk ablation studies. The intermolt period was shorter on average and often less variable for ablated versus unablated animals (Freeman et al. 1983; Radhakrishnan and Vijayakumaran 1984; Molyneaux and Shirley 1988; Koshio et al. 1989). Stage C_4 animals that underwent the ablation procedure proceeded immediately into premolt and ultimately molted sooner than stage C_4 control animals with intact eyestalks (Bückmann and Adelung 1964; Cheung 1969; Rao et al. 1973; Pradeille-Rouquette 1976; Rahman and Subramoniam 1989). Similar experiments on control and ablated premolt (stages D_1-D_4) animals yielded no difference in subsequent molting times (Rahman and Subramoniam 1989). Eliminating MIH thus seems to eliminate the intermolt-premolt delay period from the molt cycle, reducing the duration of stage C_4 (Sochasky et al. 1973; Aiken and Waddy 1976), but does not appear to either eliminate or affect the durations of other cycle stages (Adelung 1971; Aiken 1980).

Taken together, these results on various aspects of molt cycle biology indicate that cycle stages can be grouped into two distinct time phases, a physiologically required phase and a variable phase (Smith 1997). The required phase (solid lines, Fig. 10B) begins with the initiation of premolt by increased production of ecdysone or other ecdysteroids by the Y-organ, and continues through the sequential cascade of physiological and biochemical events comprising the premolt, ecdysial, and postmolt stages

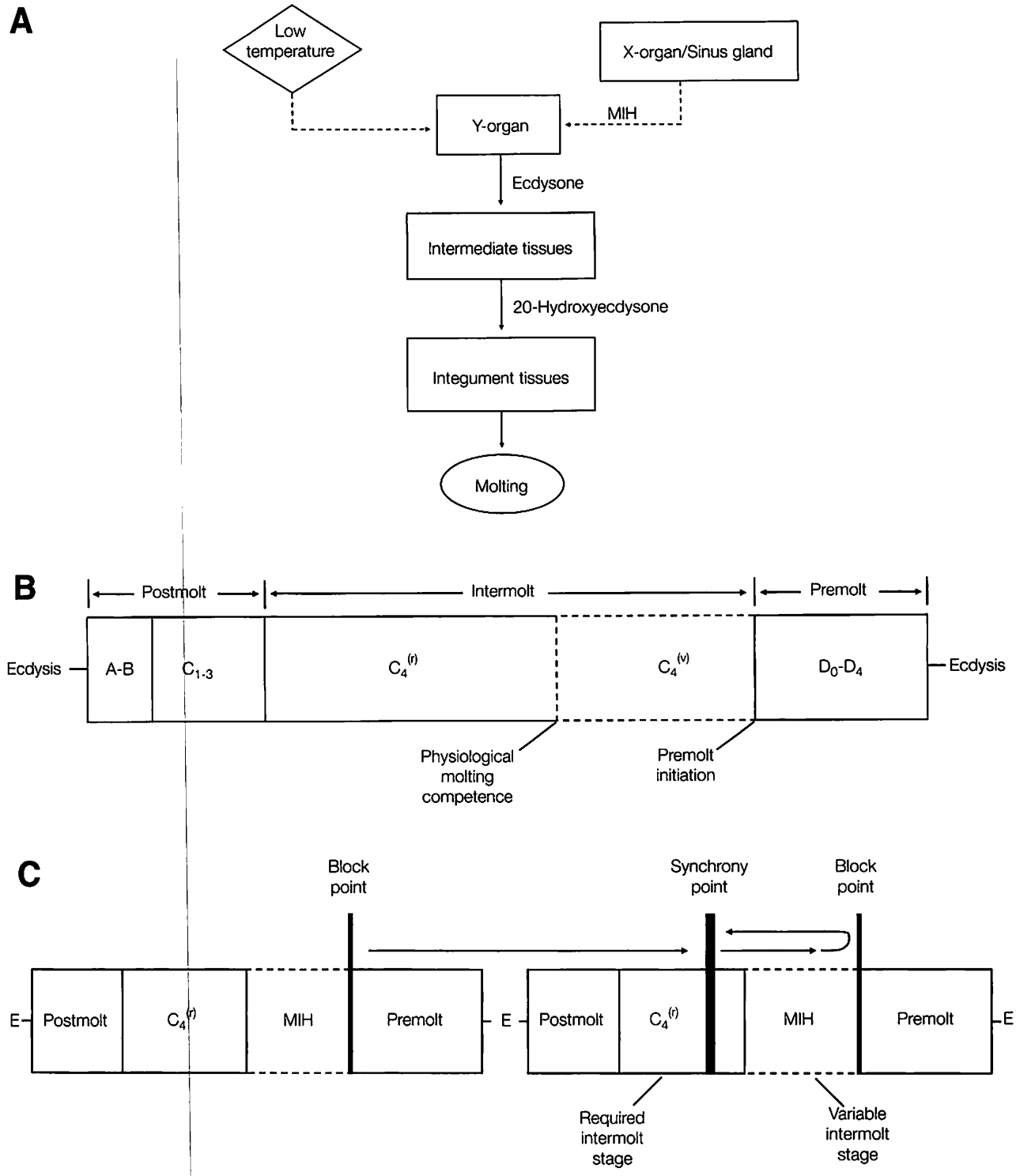

Figure 10. (A) Simple conceptual diagram of hormonal and temperature control of the molt cycle. Solid lines represent stimulation pathways; dashed lines represent inhibition pathways; MIH is molt-inhibiting hormone. (B) Conceptual model of relative durations of molt stages illustrating required (solid lines) and variable (dashed lines) phases of the molt cycle. (C) Conceptual model of environmental molting inhibition showing two consecutive molt cycles (E is ecdysis) and associated low-temperature block and synchrony points. Solid lines denote physiologically required cycle stages; dashed lines denote variable cycle stages under the control of MIH.

depicted in Fig. 1. This phase ends after internal tissue growth is completed in intermolt stage C_4 at the point where animals acquire the physiological capability to start another circuit through the molt cycle. This event can be termed the attainment of physiological molting competence. The variable phase (dashed lines, Fig. 10B) is the time period under MIH control between the attainment of molting competence and premolt initiation. This phase corresponds to the time period that is eliminated by eyestalk ablation. As illustrated in the conceptual model of Fig. 10B, stage C_4 contains portions of the required phase ($C_4^{(r)}$) and all of the variable phase ($C_4^{(v)}$). Although not shown in Fig. 10B, stage D_0 also appears to contain portions of the required and variable phases in some cases.

ENVIRONMENTAL CONTROL

In the preceding sections we have mainly discussed endogenous factors (e.g., animal size, endocrine system) that influence decapod crustacean molting processes. We now turn our attention to environmental or exogenous factors that affect molting and growth of decapods in general, and of blue crabs in particular. We specifically focus on the effects of environmental variables such as temperature on the two principal molting processes: (1) the time between molts, or intermolt period, and (2) the increase in length (e.g., carapace width) at molting, or molt increment. Note that intermolt period in this context denotes the overall duration between two ecdysial events rather than the specific duration of molt stage C_4.

Temperature

Temperature exerts a profound influence on many growth processes of cold-blooded organisms (i.e., ectotherms), including egg-to-adult emergence times for insects (Curry and Feldman 1987), instar durations of planktonic crustaceans (Kurata 1962; McLaren 1963), and intermolt periods of crabs and lobsters (Smith 1997). Plots of these various types of development times against temperature generally exhibit a decreasing exponential or hyperbolic relationship (Fig. 11A). Intermolt periods in *C. sapidus* are shorter at higher temperatures and longer at lower temperatures (Tagatz 1968b; Fig. 11C). While intermolt period is also influenced by animal size, the general effect of temperature is the same for all sizes. Expressing development in reciprocal time units (i.e., d^{-1}) yields a linearly increasing relationship with temperature (Fig. 11B). Fig. 11B is commonly termed the "development rate" function in contrast to the "development time" function of Fig. 11A (Curry and Feldman 1987). The corresponding development rate plot of the *C. sapidus* intermolt period data of Fig. 11C is shown in Fig. 11D. Viewed from this perspective, development rate, or the rate of progression through the molt cycle, increases with increasing temperature and is faster overall for comparatively smaller crabs.

Note that the linear property of the development rate-temperature response illustrated in Fig. 11B only holds for temperatures between an organism's T_{min} and T_{max} physiological temperature thresholds. These thresholds generally lie within lethal tolerance limits but demarcate temperatures coinciding with abrupt changes in the development rate response. Results from Leffler's (1972) growth study indicate that T_{max} is 34°C or slightly higher for *C. sapidus*. Properly acclimated blue crabs can survive up to 37 to 40°C (Tagatz 1969; Chung and Strawn 1984; Lewis and Roer 1988). As shown in Fig. 11B, T_{min} is the x-intercept of the linear development rate function. Development rate-temperature relationships for *C. sapidus* differ among size classes but appear to converge on a similar T_{min} value (Fig. 11D). A first-order approximation of T_{min} for *C. sapidus* can be obtained by averaging the x-intercepts of development rate functions fit to separate size classes. This procedure yields a T_{min} value of 8.9°C (Fig. 11D). Blue crabs are able to withstand temperatures down to at least 0°C (Tagatz 1969).

The average intermolt period of decapods of a given size is usually shortest at the upper temperature threshold T_{max} (Figs. 11A and B). The general response to temperatures above T_{max} is an increase in intermolt period (Chittleborough 1975; Smale 1978) and a corresponding decrease in development rate (Smith 1997). This high temperature effect on

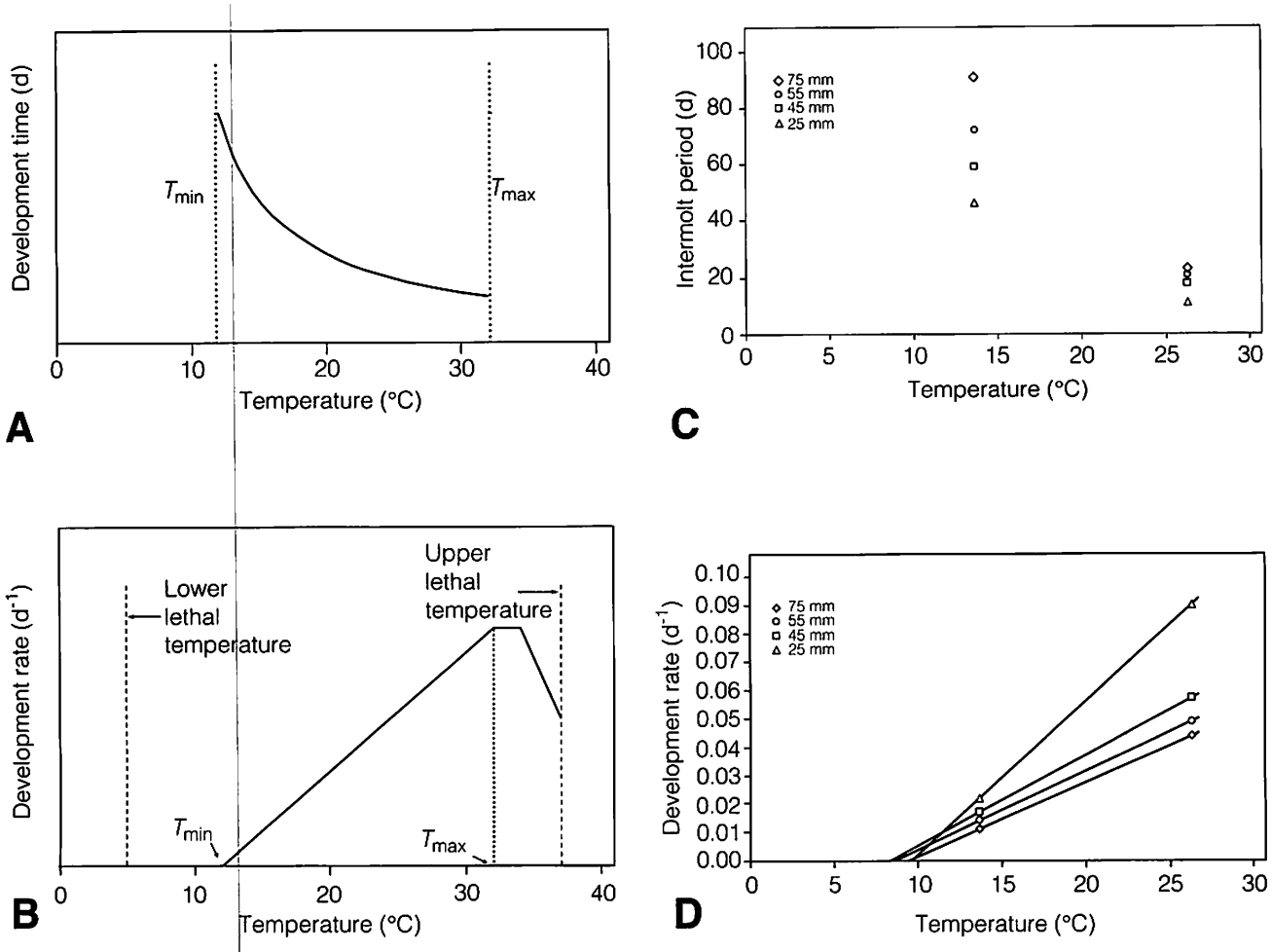

Figure 11. Conceptual temperature response functions for ectotherm (A) development time (e.g., intermolt period) and (B) development rate. Minimum (T_{min}) and maximum (T_{max}) physiological temperature thresholds are indicated in (A) and (B). Corresponding (C) average intermolt period-temperature and (D) average development rate-temperature plots for selected carapace width classes of blue crabs (data source: Tagatz 1968b).

intermolt period has not been studied for *C. sapidus*. In contrast to intermolt period, the average molt increment of blue crabs of a given size seems to remain relatively constant at temperatures between T_{min} and T_{max}, but appears to decrease at high temperatures in the vicinity of T_{max} (Tagatz 1968b; Leffler 1972). The general lack of a temperature effect on molt increment except at high temperatures at or above T_{max} has been observed in other decapods as well (Hartnoll 1982).

It has long been recognized that during the coldest periods of the year molting may stop altogether in crabs, e.g., *C. sapidus* (Churchill 1919), and lobsters, e.g., *H. americanus* (Templeman 1936), living in temperate regions. Hiatt (1948), in his classic study of the shore crab *P. crassipes*, termed this cessation of molting the "period of inhibited ecdysis"; it is sometimes referred to more specifically as a "winter anecdysis" (Orensanz and Gallucci 1988). The winter non-molting season for blue crabs appears to be associated with the minimum temperature threshold T_{min}. Molting inhibition was observed in South Carolina (Archambault et al. 1990) and Chesapeake Bay (Churchill 1919; Van Engel 1958;

Havens and McConaugha 1990) where the lowest average winter temperatures were at or below the estimated *C. sapidus* T_{min} of 8.9°C. In contrast, average winter temperatures remained above 8.9°C in Florida (Tagatz 1968b) and Mississippi Sound (Perry 1975) where year-round molting was observed.

Several studies have examined the effects of below-threshold temperatures on decapod molt cycle physiology. Experiments on *H. americanus* (Aiken and Waddy 1976) and fiddler crab *Uca pugnax* (Passano 1960b) found that low temperatures inhibit progression through the molt cycle at the intermolt-premolt transition step. This is the same point in the cycle that is blocked by the inhibition hormone MIH (Fig. 10A). This low-temperature block of premolt initiation occurred in *U. pugnax* after removal of eyestalks and thus the X-organ/sinus gland complex (Passano 1960b), indicating that temperature inhibition of the molt cycle is independent of MIH inhibition (Fig. 10A). Long-term experiments found that *H. americanus* individuals maintained at below-threshold temperatures of 5°C remained at intermolt stages C_4 to D_0 for periods up to 3 years, only progressing to premolt when temperatures were increased above T_{min} (Aiken 1980).

An interesting feature of the *H. americanus* experiments (Aiken and Waddy 1976) was that lobsters already in the premolt phase when temperatures were decreased below T_{min} were not prevented from molting, and continued through the postmolt and intermolt phases of the following molt cycle under below-threshold conditions. Experiments with *H. americanus* eyestalk-ablated and non-ablated individuals (Aiken and Waddy 1976) demonstrated that MIH inhibitory control resumed after low-temperature inhibition was removed. A conceptual model of molt cycle progression in response to below-threshold temperatures is shown in Fig. 10C (Smith 1997). During a low-temperature inhibition period, animals appear to progress to a specific point in molt stage $C_4^{(r)}$ ("synchrony point," Fig. 10C) regardless of their molt stage when the inhibition occurs. An interesting aspect of this conceptual model is that animals in the MIH-controlled $C_4^{(v)}$ stage at the time of temperature inhibition are not only prevented from entering premolt, but also must repeat some portions of intermolt stage C_4 after the temperature inhibition is removed. When temperatures rise above T_{min}, molt cycle progression begins from the synchrony point for all individuals in a population. This model explains the phenomenon of "synchronous molting" that has been observed in *C. sapidus* populations in spring after the winter nonmolting season (Bishop et al. 1983; Havens and McConaugha 1990).

Nutrition

There is very little quantitative information concerning the effect of nutrition on aspects of *C. sapidus* molting (Winget et al. 1976; Millikin et al. 1980; Millikin and Williams 1984). Studies on other decapod species, however, have shown that quality and quantity of food provided to captive animals influence intermolt period and molt increment in the expected manner: decreased nutrition results in longer intermolt periods and smaller molt increments, and increased nutrition has the opposite effect (Adelung 1971; Aiken 1980; Hartnoll 1982). The effect on intermolt period can be dramatic. Chittleborough's (1975) experiments on the lobster *Panulirus cygnus* demonstrated that reducing feeding frequency from once per day to once per week nearly doubled average intermolt period, a comparable effect to lowering temperature from 26° to 20°C in this species. These somewhat intuitive influences of nutrition on molting processes may offer at least one clue to the meaning of "physiological molting competence" (Fig. 10B). Blue crabs do not appear to progress from intermolt stage C_4 into premolt until they have decreased body water content to 60 to 65%, and have thus amassed enough dry tissue to account for 35 to 40% of their total weight (Table 1). It follows that a drop in food consumption, particularly during molt stages B_2 to C_4, would slow this net accumulation of dry tissue, lengthening the overall intermolt period. The extent to which nutrition affects growth of blue crabs in the wild, however, is unknown.

Salinity

The influence of salinity on decapod molting processes is much more subtle compared to the effects of temperature, nutrition, and animal size. Moreover, these effects are usually only observed at salinity extremes. The general response is a decrease in molt increment or an increase in intermolt period at very low or very high salinities, or both (Hartnoll 1982). Data for *C. sapidus* more or less support these observed trends. Tagatz (1968b) detected a small yet significant decrease in molt increment in blue crabs maintained in freshwater (<1 salinity[1]) compared to those held at higher salinities (mean 18). There was no effect on intermolt period, however. Tagatz's (1968b) growth study is notable in that sample size exceeded 2,000 observations and the experimental design controlled for temperature and animal size. Several small-scale experiments (e.g., low number of observations, varying animal sizes) reported no differences in molt increment among blue crabs maintained at salinities ranging from 2 to 30 (Haefner 1964; Haefner and Shuster 1964; Neufeld and Cameron 1994). Studies of the effect of salinity on blue crab respiration corroborate the results of Tagatz (1968b) to some degree. Consumption of O_2 showed a marked increase at salinities below 15 to 20 (King 1965; Findley et al. 1978), suggesting that blue crabs expend more energy in lower vs. higher salinity environments. From a bioenergetics perspective (Jobling 1994), an increase in the standard respiration rate at low salinities could negatively affect growth rate, i.e., effect a decrease in molt increment and/or increase in intermolt period.

Other Factors

Additional environmental or exogenous factors that have been shown to affect decapod molting processes are mostly artifacts of holding animals in captivity. Insufficient aquaria space, poor water quality, etc., can result in longer intermolt periods and reduced molt increments (Van Olst and Carlberg 1978; Mohamedeen and Hartnoll 1989; Smith 1997). Some of these adverse aspects of captivity seem to influence growth secondarily by affecting food consumption (Aiken 1980).

With respect to *C. sapidus*, there has been a long-held belief that the timing of ecdysial events is associated with phases of the moon (Churchill 1919). For example, the spring pulse in soft crab production, i.e., "synchronous molt," observed in temperate regions is thought to occur on or near the full moon. As described above, the phenomenon of synchronous molting appears to be a function of temperature alone. There will no doubt be a correlation between molting activity and moon phase for some time period after the spring rise in temperature (Ryer et al. 1990; Steele and Bert 1994), but correlation does not imply causation in this case. Churchill (1919) investigated the hypothesis of lunar control of molting over eighty years ago. He conducted growth experiments on blue crabs held in field enclosures, and thus subject to natural environmental conditions. Crabs molted in each lunar phase with almost equal frequency. Churchill (1919) concluded:

> No evidence whatever exists for the belief that the moon has any effect upon the molting of the crab, and the matter may be dismissed as of a class with all folklore superstitions concerned with the supposed relation between the moon and mundane affairs, such as the weather, gardening, and the like.

Quantitative examination of blue crab molt processes, presented below, supports this conclusion.

GROWTH FORMAT: DETERMINATE OR INDETERMINATE?

Crustaceans exhibit two different growth formats, determinate and indeterminate (Hartnoll 1982). In species with determinate growth, individuals progress through a series of molts until they

[1] Salinity is presented as a pure ratio with no dimensions or units, according to the Practical Salinity Scale (UNESCO 1985).

reach a final or terminal instar. Under an indeterminate growth format, individuals continue molting throughout their lifespan and do not possess a final molt stage. Examination of this aspect of growth for *C. sapidus* has largely centered on mature females, perhaps because of their distinct morphology (Kennedy and Cronin, Chapter 3) that enables them to be readily distinguished from male and immature female crabs. The conclusion by Churchill (1919) and later researchers (cf. Van Engel 1958) that *C. sapidus* females reach a terminal instar at the attainment of sexual maturity was mostly based on what they did not observe: evidence that adult females undergo ecdysis. Though circumstantial, this type of evidence should not be discounted. In Chesapeake Bay and many other regions, adult female blue crabs are subject to intense harvesting. As Abbe (1974) points out:

> Although millions of crabs have been handled annually over the past 90 years, only a very few adult females have been found showing any signs of preparation for an additional molt....

This type of evidence is unavailable for male blue crabs because it is not possible to separate adult males from juveniles by any readily identifiable morphological features. However, we do know that males attain sexual maturity at smaller sizes than females (Tagatz 1968a; Van Engel 1990), and males have been observed to molt again after reaching maturity (Van Engel 1958). But do males continue to molt and grow for their entire lifespan? Churchill (1919) conjectured that "there is no especial reason to suppose that the male molts indefinitely, in contradistinction to the female...." To gain further insight into the growth format of blue crabs, male as well as female, we examine the phenomenon of determinate growth from both physiological and demographic perspectives.

Physiological Aspects

There are two different endocrine scenarios for the occurrence of a terminal instar (Carlisle 1957; Skinner 1985; Fig. 10A). The first is physical degeneration of the Y-organ and the ensuing cessation in production of ecdysone. Because ecdysteroids are also involved in basic regenerative processes, terminal instar individuals of this type exhibit distinct morphological characteristics: lost appendages do not form limb buds and carapaces deteriorate to some extent (Carlisle 1957). Y-organ degeneration and these accompanying morphological features have been observed in some brachyuran species of the family Majidae (Skinner 1985). In the second scenario the Y-organ remains intact, but X-organ production of MIH at high concentrations continues indefinitely. Under this scenario, terminal instar individuals retain the ability to form regenerative limb buds and effect minor repairs to the carapace, and will even molt again if the X-organ is removed (Carlisle 1957; Cheung 1973). Cheung's (1973) experiments on the crab *Menippe mercenaria* add an interesting twist to the nature of X-organ terminal instar endocrine control. Eyestalk ablation induced molting in terminal instar individuals (>110 mm carapace width) if the operation was performed within 4 months after the terminal molt. Eyestalk ablation performed a year or more after the terminal molt did not induce molting, although these individuals were still able to form regenerative limb buds (Cheung 1973). These results suggest that the Y-organ can produce the necessary high quantities of ecdysone to initiate the molting process after a terminal molt, but this capacity diminishes over time.

Physiological evidence suggests that the scenario involving X-organ regulation of the terminal instar applies to *C. sapidus*. Large males (>140 mm carapace width) and mature females that lose an appendage form regenerative limb buds but do not enter into premolt (Ary et al. 1985). Mature females molt in response to eyestalk ablation (Havens and McConaugha 1990). Because terminal instar individuals retain the physiological capability of molting under this scenario, it is not surprising that field-captured *C. sapidus* adult females have been observed to enter premolt on rare occasions, most likely as a result of some physiological anomaly (Abbe 1974; Olmi 1984).

Demographic Aspects

The occurrence of a terminal molt implies the existence of a finite number of instars. Whether total

postlarval instar number is fixed or varies to some extent among individuals is unknown for *C. sapidus*. We can, however, narrow our focus to reproductively mature crabs. Figure 12 illustrates a method for estimating the potential number of adult instars (Smith 1997). Three types of information are used: (1) percent of mature individuals at carapace width classes (Fig. 12A, shaded dots) for females (left panel; Tagatz 1968a) and males (right panel; Van Engel 1990); (2) average molt increment (Fig. 12A, solid squares and lines) by premolt carapace width (CW) and sex (Gray and Newcombe 1938; Tagatz 1968b); and (3) sampling survey estimates of population size structure (Fig. 12B) by sex (Archambault et al. 1990). For females, average molt increment projections for premolt sizes corresponding to 10, 50, and 90% maturity levels are shown in Fig. 12A (left panel, solid squares and lines). These projections represent molt increments of crabs that are sexually immature before molting and reach maturity at the indicated "molt 1." Note that the percentage of crabs expected to molt to maturity at a given premolt size corresponds to the percentage of immature animals at that size. The projected upper size range of the first female adult instar (Fig. 12A, left panel) corresponds with the observed upper size range of females in the population (Fig. 12B, left panel). These results support the view that female blue crabs reach a terminal instar at the molt to maturity. The analysis shown in the right panels of Figs. 12A and 12B indicates that determinate growth occurs in *C. sapidus* males as well. Male crabs appear to possess two adult instars, in contrast to females. A limited number (≤3) of adult instars has also been observed in males and females of other

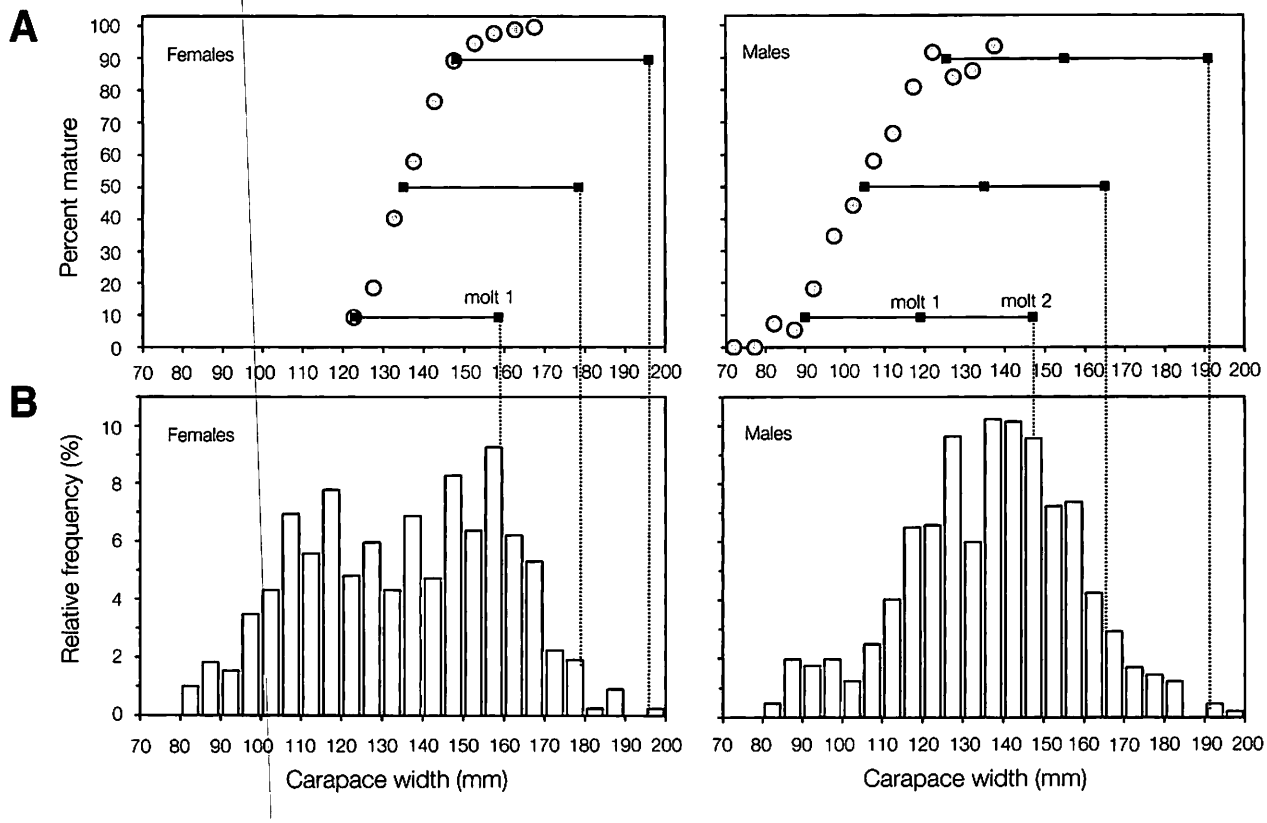

Figure 12. (A) Percent maturity-carapace width plots (shaded dots) for *C. sapidus* females (left panel; data source: Tagatz 1968a) and males (right panel; data source: Van Engel 1990). Solid squares and lines are average molt increment projections (data sources: Gray and Newcombe 1938; Tagatz 1968b) for premolt sizes corresponding to 10, 50, and 90% maturity levels. (B) Relative frequency histograms for *C. sapidus* carapace width from the field sampling study of Archambault et al. (1990) conducted in North Carolina. Data for females (left panel) and males (right panel) are August and September samples pooled over a 9-year study period.

brachyuran species, including the cancrids *C. magister* and *C. pagurus* (Orensanz and Gallucci 1988), geryonid *Chaceon maritae* (Melville-Smith 1989), and portunids *Portunus sanguinolentus* (Ryan 1967) and *Scylla serrata* (Robertson and Kruger 1994).

The length frequency histograms of Fig. 12B are from a fishery-independent trawl survey conducted on a blue crab population in North Carolina (Archambault et al. 1990). The steep decline in numbers from 155 to 200 mm CW and the absence of crabs >200 mm CW are strikingly similar features of blue crab size composition data reported for different types of surveys (e.g., fishery-independent, fishery-dependent) using different gears (e.g., trawls, crab pots) over a wide geographical range, including Texas (More 1969), Louisiana (Jaworksi 1972), Mississippi (Perry 1975), Florida (Steele and Bert 1994), Georgia (Palmer 1974), South Carolina (Eldridge and Waltz 1977), and Chesapeake Bay (Rothschild et al. 1992). Presumably, fishing intensity varied among the regions and time periods of these surveys. Molt increment data (Gray and Newcombe 1938; Tagatz 1968b) suggest that larger crabs would increase to sizes well above 200 mm CW should they molt again, yet individuals of these projected sizes are not observed in any appreciable numbers. It is common for one or two unusually large individuals to be observed in a large-scale population sampling survey. For example, Tagatz (1965) observed a 246 mm CW male and Archambault et al. (1990) observed a 254 mm CW female. These are expected postmolt sizes of crabs that were approximately 180 to 200 mm CW before molting.

There are at least two plausible explanations why 180 to 200 mm CW individuals might molt one more time. First, a small proportion of crabs are still sexually immature at large sizes, i.e., carapace widths at the 99% maturity level (Fig. 12A). Immature female crabs as large as 177 mm CW have been reported (Tagatz 1968a). These late-maturing individuals would be expected to reach their respective final adult instars at sizes well over 200 mm CW. Second, there are likely to be a few individuals that possess one additional adult instar (Abbe 1974; Olmi 1984). As described above, blue crabs retain the physiological capacity to molt for at least some period of time after reaching the terminal instar. Some sort of physiological abnormality in the endocrine system, e.g., an anomalous drop in MIH production at this instar, could result in an additional ecdysis.

Tag-recapture experiments provide some information on instar durations of large individuals that may have reached a final molt stage. Tagged large *C. sapidus* females and males have been recaptured 2 to 3 years later without molting in studies conducted on populations in North Carolina (Fischler 1965; Judy and Dudley 1970), Florida (Tagatz 1968a), Mississippi (Perry 1975), and Texas (More 1969). The longest observed tag-recapture time interval for both sexes, 3 years, represents a minimum estimate of the potential duration of the final adult instar. Empirical growth data place this potential duration time in demographic perspective. Average intermolt period for larger premolt animals (130 to 140 mm CW) was approximately 5 weeks under summer conditions, with a maximum of 11 weeks (Tagatz 1968b). It thus appears that large (>150 mm CW) male and female blue crabs have ample opportunity to molt again, but a variety of demographic evidence indicates that they do not. We will conclude our demographic examination of determinate growth in the mathematical modeling section below.

MATHEMATICAL DESCRIPTION

Mathematical models describing growth of an individual over its lifespan are fundamental building blocks of cohort-structured demographic models (Fogarty and Lipcius, Chapter 16). These models are of great utility in assessing and managing exploited populations of aquatic animals — fishes, crustaceans, molluscs, etc. — for sustainable harvests. Because these cohort-structured models incorporate basic dynamic processes of growth, survivorship, and reproduction, they are also invaluable tools for understanding the ecology of aquatic species at the population level.

Growth models focus on two aspects of the growth process:

$$\frac{dL}{da} \quad \text{and} \quad \frac{dW}{da},$$

or change in length L and change in weight W with respect to change in age a. A common strategy, which we follow in this chapter, is to first develop a length-age model and then describe weight-at-age via a weight-length relationship. In this context "length" refers to any accepted linear measure of size, usually carapace length for lobsters and anomuran crabs and carapace width for brachyuran crabs, including the blue crab. Table 4 provides a glossary of growth model variables, while Table 5 summarizes the principal data sources used in model development.

Growth in Length

Our approach to mathematically describing growth in length of an individual blue crab utilizes a molt-process model that separates crustacean growth into two main components, molt increment and intermolt period. Each of these molting processes (molt increment and intermolt period) is described by an independent set of predictive functions based on empirical data. These functions are ultimately linked together within a numerical modeling framework to depict lifespan growth in length. The ability to incorporate relevant features of our biological understanding of molting and growth described in the previous sections is a key attribute of this modeling approach.

Molt Increment

The main objective of a molt increment model is to predict how much a crab will increase in length at a given molt event. Our examination above suggested that molt increment is insensitive to environmental factors such as temperature and salinity except at extreme values (i.e., temperatures exceeding T_{max} or salinities less than 1) that would be encountered infrequently by individuals of a given population, e.g., blue crabs inhabiting Chesapeake Bay. Molt increment of blue crabs and other decapods does appear to be related to at least one endogenous factor, the size of an animal before molting (Gray and Newcombe 1938; Hartnoll 1982). A general mathematical model for molt increment predicts postmolt length as a function of premolt length

$$L_{i+1} = f(L_i) + \varepsilon, \qquad (2)$$

where L_{i+1} is length at instar i+1 (i.e., postmolt carapace width), L_i is premolt length, and ε is the model error term. Interestingly, this model was first applied by Gray and Newcombe (1938) in a study of blue crab growth. Its use was extended to other crustaceans in the classic studies of Hiatt (1948) and Kurata (1962) (see Botsford 1985 for historical review). The basic model-building steps (Neter et al. 1996) are: (1) identify an appropriate model form (i.e., linear, hyperbolic, etc.) for the function $f(L_i)$ describing the average relationship between postmolt and premolt length; (2) identify an appropriate probability density function for the error term ε; and (3) identify an estimation method (i.e., ordinary least-squares regression, nonlinear regression, etc.) appropriate for the combination of (1) and (2).

The mean postmolt-premolt carapace width relationship for blue crabs is examined in the data plots of Figs. 13A and 13B (open circles). These data were pooled from three different growth studies (Table 5), one targeting small crabs (L_i <30 mm CW) of both sexes (Newcombe et al. 1949b; Fig. 13A), and the other two (Gray and Newcombe 1938; Tagatz 1968b) targeting mostly larger crabs (L_i >30 mm) distinguished by sex (females in Fig. 13A, males in Fig. 13B). Although sample sizes were quite high in each of these studies (n>400; Table 5), data were reported (and thus plotted in Fig. 13) as size class mean values rather than actual observations. The mean relationship between postmolt and premolt CW appears fairly linear within certain ranges of L_i, but these linear trends are noticeably different among various premolt size ranges. Of particular note is the downward shift in the molt increment function for male crabs at L_i=100 mm (Fig. 13B). This shift seems to coincide with sexual maturation, a phenomenon of molt increment that has been observed in many crustaceans and that is often

Table 4. Glossary of variables for modeling blue crab growth.

Variable	Description	Units
a	Age	Days
a_r	Age at recruitment	Days
a_λ	Oldest age	Days
b_0, b_1	Parameters of weight-length function	Dimensionless
$f(y)$	Probability density function (PDF)	Dimensionless
i	Instar (postlarval molt number)	Number
i_m	Instar at first sexual maturity	Number
$IP(i)$	Within-season intermolt period of instar i	Days
$IP_{dd}(i)$	Within-season degree-day intermolt period	Degree-days
j	Observation subscript	Dimensionless
L	Animal length (carapace width)	mm
L_i	Length at instar i	mm
L_m	Length at first sexual maturity	mm
L_r	Length at recruitment	mm
L_λ	Length at oldest age	mm
$NMT(i)$	Number of molts to terminal instar from instar i	Number
t	Time	Day of year
t_{dd}	Degree-days at time t	Degree-days
t_i	Time at molting to instar i	Day of year
t_l	Time at low temperature molting inhibition	Day of year
t_r	Time at recruitment	Day of year
t_s	Time at start of molting season	Day of year
t_λ	Time at reaching oldest age	Day of year
t_Ω	Time at molting to terminal instar $i=\Omega$	Day of year
T	Water temperature	°C
T_{min}	Low temperature molting inhibition threshold	°C
T_{max}	High temperature physiological threshold	°C
W	Animal weight	g
W_i	Weight at instar i	g
α_0,α_1	Parameters of molt increment function	Dimensionless
β	Scale parameter of the shifted exponential PDF	Dimensionless
$\beta(L_i)$	Duration of molt cycle variable phase	Degree-days
β_0,β_1	Parameters of duration function $\beta(L_i)$	Dimensionless
γ	Shift parameter of the shifted exponential PDF	Dimensionless
$\gamma(L_i)$	Duration of molt cycle required phase	Degree-days
γ_0,γ_1	Parameters of duration function $\gamma(L_i)$	Dimensionless
ε	Model error term	Dimensionless
$\Lambda(t_k,t)$	Cumulative degree-days from time of precursor event k to time t	Degree-days
$\tau(t_i,t_{i+1})$	Between-season intermolt period	Days
$\tau(t_i,t_l)$	Duration between molting to instar i and low temperature molting inhibition	Days
$\tau(t_l,t_s)$	Duration of non-molting season	Days
$\tau(t_s,t_{i+1})$	Duration between start of molting season and molting to instar i+1	Days
$\tau_{dd}(t_s,t_{i+1})$	Degree-day duration between start of molting season and molting	Degree-days
$\tau(t_\Omega,t_\lambda)$	Terminal instar duration	Days
Ω	Terminal instar	Number

Table 5. Description of data sources used to model blue crab growth; CW is carapace width; n is sample size.

Growth process	Geographical location	Experimental conditions	Data format	Sex	Premolt CW range (mm)	n	Reference
Molt increment	Chesapeake Bay	Field enclosures	Size class means	F M	10-140 10-160	259 191	Gray and Newcombe 1938
Molt increment	Chesapeake Bay	Laboratory aquaria	Size class means	F, M	2-29	530	Newcombe et al. 1949b
Molt increment	St. Johns River, Florida	Field enclosures	Size class means	F M	20-140 20-140	1,211 1,026	Tagatz 1968b
Molt increment	Georgia	Laboratory aquaria	Observations[1]	F, M	35-65	177	Fitz and Wiegert 1991
Intermolt period	St. Johns River, Florida	Field enclosures; Temperature: summer mean, 26.3°C; winter mean, 13.7°C	Size class means	F M F, M	20-140 20-140 20-100	summer: 642 summer: 614 winter: 208	Tagatz 1968b
Intermolt period	Carolinas	Laboratory aquaria; Temperature: 23.5°C	Instar means	F, M	2-7	575	Millikin et al. 1980; Millikin and Williams 1984
Intermolt period	Georgia	Laboratory aquaria; Temperature: ambient, 17-29°C	Observations[1]	F, M	50-60	28	Fitz and Wiegert 1991
Weight-length	Chesapeake Bay	Field captured individuals	Size class means	F M	10-180 10-200	138 99	Newcombe et al. 1949a

[1] Original observations provided by H.C. Fitz (South Florida Water Management District, West Palm Beach, Florida.)

accompanied by abrupt shifts in allometry, e.g., relationships between carapace length and carapace width, chela length and carapace width, etc. (Hartnoll 1982). A similar shift in the molt increment function is not apparent in larger female crabs (Fig. 13A, L_i >30 mm), which stop molting after reaching the maturity instar. A peculiarity of these data is the apparent change in the postmolt-premolt CW relationship at $L_i = 30$ mm between smaller and larger crabs. It is unknown whether this shift in molt increment is due to some actual, yet-to-be-discovered biological process, or is perhaps attributable to a difference in experimental conditions (laboratory aquaria vs. field enclosures) between the growth studies targeting smaller and larger crabs (Table 5).

We follow Gray and Newcombe's (1938) strategy of modeling molt increment as a series of separate linear postmolt-premolt CW relationships for different life stages and sexes. The formal name for this type of model is "multi-phase" regression (Draper and Smith 1981). The statistical model for each linear segment is

$$L_{i+1,j} = \alpha_0 + \alpha_1 L_{i,j} + \varepsilon_j, \quad (3)$$

where α_0 and α_1 are the respective intercept and slope parameters, and ε_j is the error residual of the jth observation. An objective technique for locating the "change-point," or the point along the x-axis where a change in phase (i.e., shift) occurs, in molt

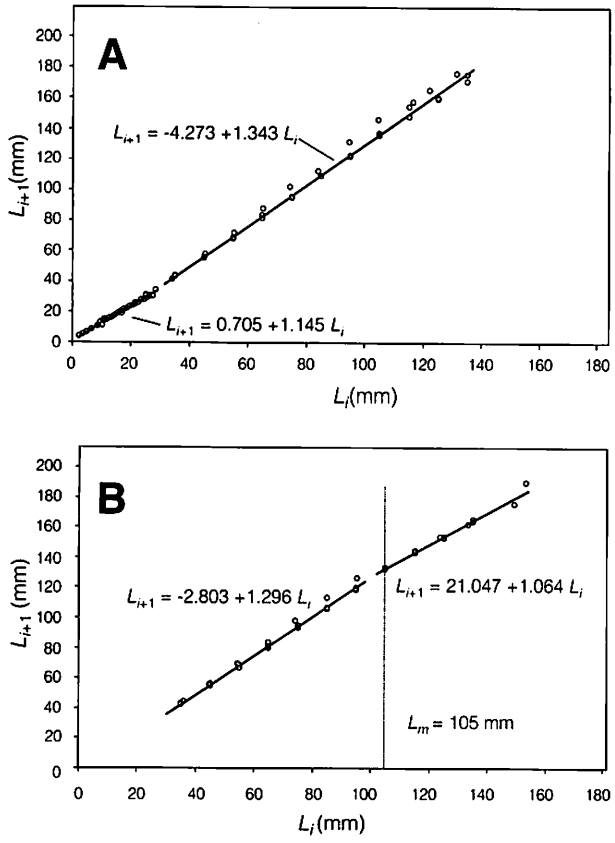

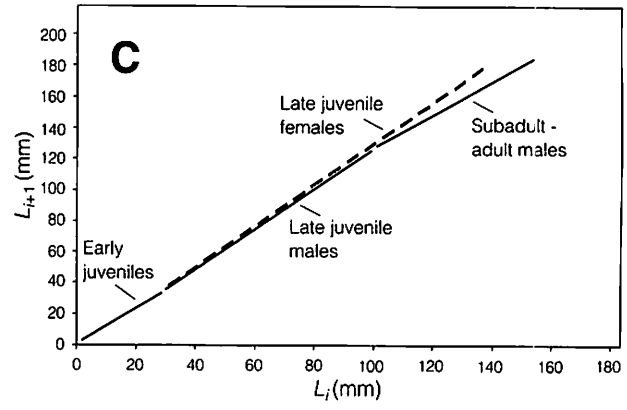

Figure 13. Blue crab molt increment functions (data sources: Gray and Newcombe 1938; Newcombe et al. 1949b; Tagatz 1968b; see Table 5 for description). (A) Postmolt-premolt carapace width data plots and fitted relationships for early juvenile males and females ($L_i \leq 30$ mm) and late juvenile females ($L_i > 30$ mm). (B) Data and fitted relationships for late juvenile males ($30 < L_i \leq 100$ mm) and subadult-adult males ($L_i > 100$ mm); the vertical dotted line denotes mean carapace width at sexual maturity (Van Engel 1990). (C) Summary of estimated functions by life stage and sex.

increment models is described in Somerton (1980). Identification of an appropriate probability density function for the error term of equation (3) is illustrated in Fig. 14, using data from the study of Fitz and Wiegert (1991). Original observations were graciously provided by H.C. Fitz (South Florida Water Management District, West Palm Beach, Florida). The postmolt-premolt CW plot for pooled female and male immature blue crabs is shown in Fig. 14A. Although the range of premolt L is narrow, the variance of L_{i+1} appears fairly constant over this interval of L_i. The frequency histogram of error residuals resulting from the ordinary least-squares (OLS) regression fit of equation (3) to these data is diagrammed in Fig. 14B. The residuals are symmetric and satisfy the Shapiro-Wilk test (Shapiro and Wilk 1965) for normality ($p > 0.05$). The normal $N(0,\sigma^2)$ distribution was thus selected as an appropriate error probability density function.

Molt increment model parameters (equation 3) were estimated using least-squares regression for the following life stage-sex groups (Figs. 13A, 13B; Table 6): early juvenile males and females ($L_i \leq 30$ mm CW); late juvenile females ($L_i > 30$ mm); late juvenile males ($30 < L_i \leq 100$ mm); and subadult-adult males ($L_i > 100$ mm). Size class means were weighted by the corresponding sample size. The fitted lines are plotted together in Fig. 13C. The molt increment functions for late juvenile females and late juvenile males appear nearly coincident. However, because the lines were estimated from mean values rather than observations, we are unable to conduct any formal statistical tests for differences among the various functions.

Intermolt Period

In this section we develop a model to predict intermolt period using observations of molt cycle duration obtained from animals held in captivity. Crustacean intermolt period can also be predicted "indirectly" in some cases using observations of molting frequency, or the number of molt events

occurring in a time period, as opposed to direct observations of durations between molt events. Data on molting frequency are usually obtained from tagging studies. A technical requirement is a tag that can be retained by an animal through one or more molts.

Two main approaches have been developed for estimating intermolt period from molt frequency data; however, neither approach is generally applicable to blue crab populations. One approach applies only to populations exhibiting asynchronous, i.e., year-round, molting (Munro 1983; Hoenig and Restrepo 1989; Millar and Hoenig 1997). A second approach is most readily applicable to crustacean populations with very short molting seasons during which individuals would be expected to molt either once or not at all (Hancock and Edwards 1967; Smith 1997). As described above, the situation for many blue crab populations lies somewhere in between these two conditions. Blue crabs in temperate regions exhibit distinct molting and nonmolting seasons, and the molting season is generally of sufficient duration (e.g., April to November in Chesapeake Bay) for pre-terminal instar crabs to complete at least several molt cycles.

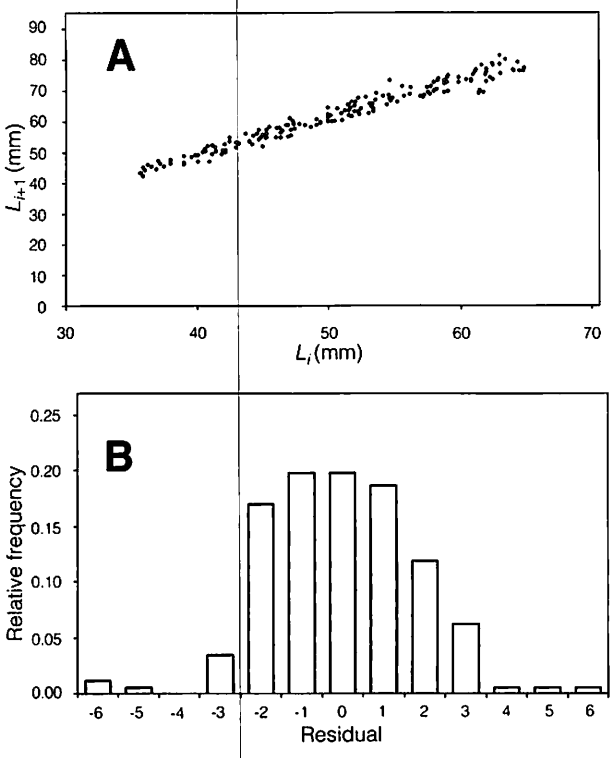

Figure 14. Examination of the error probability density function for the molt increment model (equation 3). (A) Plot of postmolt-premolt carapace width observations (L_i range 35-65 mm) from the study of Fitz and Wiegert (1991; see Table 5). (B) Corresponding frequency histogram of least-squares regression residuals.

In developing a predictive function for blue crab intermolt period, we draw upon several characteristics of molt cycle duration described in previous sections. As shown in Fig. 11, mean intermolt period is influenced by animal size and temperature. Temperature influence occurs in two distinct ways. First, temperature dictates the rate of molt cycle progression for crabs at a given size when temperature remains within the physiological thresholds T_{min} and T_{max} (Figs. 11B, 11D). Second, molt cycle progression is blocked when temperature drops below T_{min} (Fig. 10). Variation of intermolt period occurs at a specific stage in the molt cycle (C_4), and is linked to X-organ production of MIH. A general mathematical model incorporating these characteristics is

$$IP(i) = f(L_i, T) + \varepsilon, \qquad (4)$$

in which intermolt period (IP) of instar i is a function of both premolt length (L_i) and temperature (T), and variability of $IP(i)$ is accounted for in the error term ε. Practical application of equation (4) requires identification of (1) a specific mathematical function for describing average intermolt period with respect to size and temperature, and (2) an appropriate probability density function for the error distribution. In this section we focus development on a "within-season" intermolt period model that is valid when temperature remains between T_{min} and T_{max}. A model for predicting intermolt periods that span a winter inhibition season, termed the "between-season" IP model, is described in the following section.

Data plots from the growth study of Tagatz (1968b) indicate a linear relationship between intermolt period and premolt carapace width under uniform temperature conditions (Fig. 15A). These data also suggest that the intermolt period-length relationship is the same for male and female blue crabs,

Table 6. Molt-process growth model parameters for blue crabs.

Symbol	Description	Function/value	Units	Reference
t_r	Settlement date, 1st postlarval instar		Day of year	
	Early-, mid-, late-season in Chesapeake Bay;	Jul 15, Sep 15, Nov 15		van Montfrans et al. 1990
	mid-season in Louisiana	Jul 15		Estimated from spawning season (Adkins 1972) and larval development schedule (van Montfrans et al. 1990)
a_r	Age at settlement	0	Days	Model starting value
L_r	Carapace width, 1st postlarval instar	2.5	mm	Newcombe et al. 1949b; Millikin and Williams 1984
L_m	Mean carapace width at maturity		mm	
	Females	135		Tagatz 1968a; Figure 12A, left panel
	Males	105		Van Engel 1990; Figure 12A, right panel
L_{i+1}	Postmolt carapace width		mm	
	Early juveniles, both sexes, $L_i \leq 30$	$L_{i+1} = 0.705+1.145L_i$		Data sources: Gray and Newcombe 1938; Newcombe et al. 1949b; Tagatz 1968b
	Late juvenile females, $L_i > 30$	$L_{i+1} = -4.273+1.343L_i$		
	Late juvenile males, $30 < L_i \leq 100$	$L_{i+1} = -2.803+1.296L_i$		
	Subadult-adult males, $L_i > 100$	$L_{i+1} = 21.047+1.064L_i$		Estimation: Equation 3, Figure 13
T_{min}	Low temperature molting inhibition threshold	8.9	°C	Method: Curry and Feldman 1987 Data source: Tagatz 1968b Estimation: Figs. 11B and 11D
$IP_{dd}(i)$	Within-season intermolt period	$IP_{dd}(i) = \gamma(L_i)+\beta(L_i)$ $\gamma(L_i) = 43.5+1.74L_i$ $\beta(L_i) = 53.18+2.82L_i$	Degree-days	Method: Smith 1997 Data sources: Tagatz 1968b; Millikin and Williams 1984 Estimation: Equations 7-10, Figure 16C
$\tau_{dd}(t_s, t_{i+1})$	Duration between start of molting season and molting	$\tau_{dd}(t_s, t_{i+1}) = 0.25[\gamma(L_i)+\beta(L_i)] + \beta(L_i)$	Degree-days	Equations 18 and 19
$\tau(t_\Omega, t_\lambda)$	Terminal instar duration	3-4	Years	Data sources: Fischler 1965; Tagatz 1968a; More 1969; Judy and Dudley 1970; Perry 1975
$NMT(i_m)$	Number of molts to terminal instar from instar at first sexual maturity i_m		Number	Figure 12, Equation 21
	Females	0		
	Males	1		
W-L	Weight-length relationship		g	Data source: Newcombe et al. 1949a Estimation: Equation 24, Figure 20
	Females	$W = 0.000355L^{2.571}$		
	Males	$W = 0.000274L^{2.662}$		

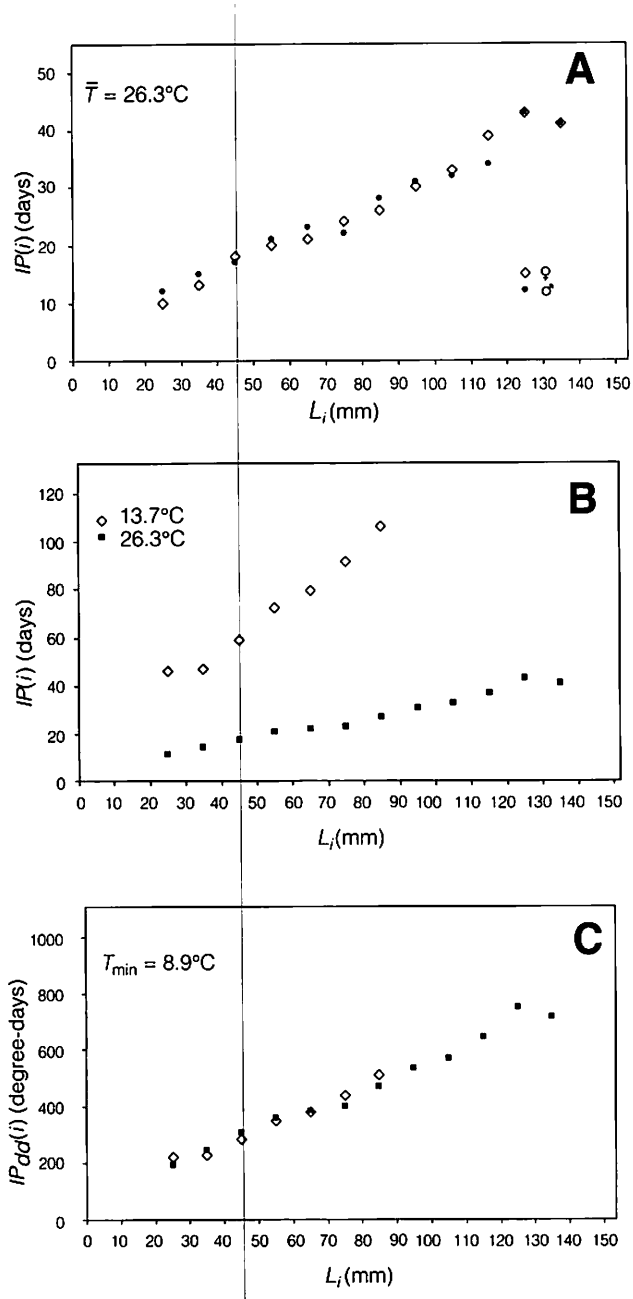

Figure 15. Examination of *C. sapidus* intermolt period as a function of size and temperature from the growth study of Tagatz (1968b). (A) Plots of intermolt period-length size class means for males (filled circles) and females (open diamonds) at summer temperature conditions. (B) Plots of intermolt period-length size class means (combined sexes) for summer (filled squares) and winter (open diamonds) temperature conditions. (C) Data plot from panel (B) after degree-day conversion of intermolt period time units.

and does not differ between reproductively immature (all females, males <100 mm) and mature (males >100 mm) individuals. At different uniform temperatures, the intermolt period-length relationship appears to remain linear but follows a separate function for each temperature regime (Fig. 15B).

A standard approach for incorporating temperature effects on the growth rate of ectotherms is the degree-day method (Curry and Feldman 1987). General application of this method to crab and lobster intermolt periods is detailed in Smith (1997). The basic premise of this approach is that the duration of a physiological process can be expressed as the cumulative sum of daily temperatures occurring through the time period. Applied to intermolt durations, this method essentially converts *IP* time units from "chronological" days (d) to "physiological" degree-days (dd). The number of degree-days in a single chronological day t is computed from the formula

$$t_{dd} = \begin{cases} \bar{T}(t) - T_{\min}, & \bar{T}(t) > T_{\min} \\ 0, & \bar{T}(t) \le T_{\min} \end{cases}, \qquad (5)$$

where $\bar{T}(t)$ is average water temperature for day t and $T_{\min}$ is the low temperature threshold below which molting does not occur. The data of Fig. 15B were converted to degree-day time units, and the resulting plot is shown in Fig. 15C. The separate uniform-temperature intermolt period-length relationships (Fig. 15B) reduce to a single linear relationship in terms of degree-days (Fig. 15C).

A probability density function for intermolt period needs to account for both the required and variable components of the molt cycle. The conceptual molt stage timeline diagram of Fig. 10B is redrawn in Fig. 16A in terms of the required and variable cycle phases. The sum of the durations of stages A to $C_4^{(r)}$ and D_0 to D_4, i.e., the entire required phase, yields the physiological minimum intermolt period. The range of *IP* observations will thus have a nonzero, positive lower bound. This lower bound is evident in the frequency histogram of Fig. 16B, computed from degree-day-adjusted *IP* observations for a single size class (50 to 60 mm CW) from the growth study of Fitz and Wiegert (1991; see Table 5). The pattern of *IP* variation is

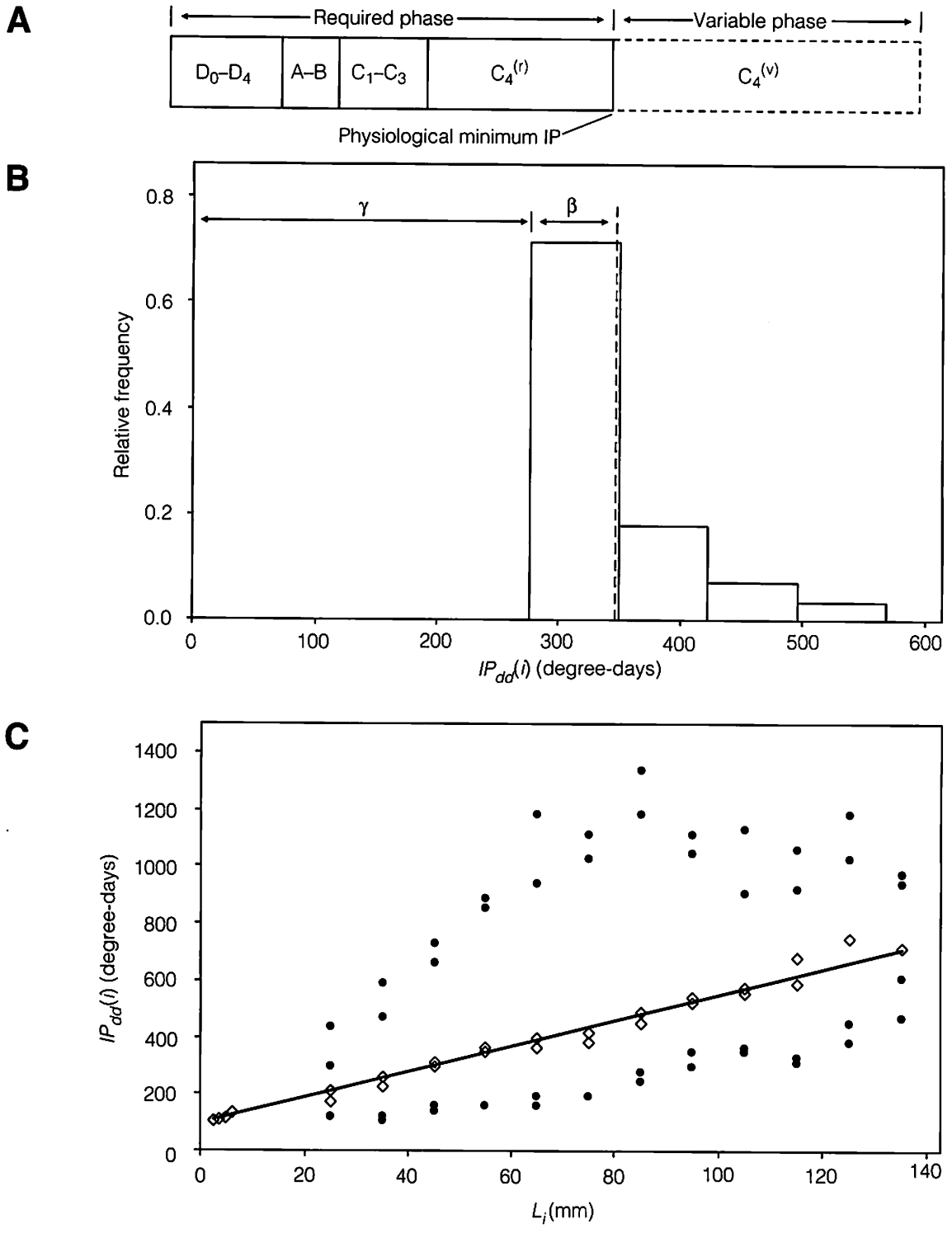

Figure 16. (A) Molt stage timeline diagram of Figure 10B redrawn with respect to the required and variable phases of the molt cycle. (B) Frequency histogram of intermolt period observations of blue crabs 50 to 60 mm carapace width from the study of Fitz and Wiegert (1991). Mean intermolt period is denoted by the vertical dashed line; γ and β are parameters of the shifted exponential probability density function (equation 6). (C) Plot of size class mean (open diamonds), minimum (lower solid circles) and maximum (upper solid circles) intermolt period-length values (data sources: Tagatz 1968b, Millikin and Williams 1984; see Table 5) and the corresponding maximum likelihood-fitted function (solid line; equation 7); estimated parameter values are provided in Table 6.

indicative of an asymmetric, non-normal probability density function in which the majority of observations occur near or below the size class mean (vertical dashed line). As shown in the data plot of Fig. 16C, values of mean intermolt period (open diamonds) are closer to minimum rather than maximum observations within size classes along the range of premolt length. The pattern of *IP* variation illustrated in Fig. 16B is characteristic of time-to-event duration data from many diverse fields of investigation. Some examples are service-to-failure times of electronic components in engineering reliability studies, survival times of patients after surgery in biomedical research, and interarrival times of bank customers in business queueing models (Law and Kelton 1991). Duration data are usually not normally distributed, but instead follow asymmetric distributions such as the exponential, gamma, or Weibull probability density functions (Kalbfleisch and Prentice 1980; Law and Kelton 1991). Variation of *IP* for *C. sapidus* and a number of other crab and lobster species conforms quite well to the shifted exponential distribution (Smith 1997), with probability density function

$$f(y) = \frac{1}{\beta} e^{-\frac{(y-\gamma)}{\beta}} \qquad (6)$$

for random variable y. The parameters γ and β of equation (6) have specific biological meaning with respect to crustacean intermolt period. The shift parameter γ represents the physiological minimum *IP*, and parameter β represents the mean duration of the variable cycle phase under MIH control (Figs. 16A and 16B). The overall mean intermolt period is the sum of these two parameters.

The probability density function of equation (6) is valid for a single size class. To extend it to incorporate premolt length L_i, we note that the data plot of Fig. 16C indicates the minimum intermolt period exhibits an increasing relationship with premolt length in the same fashion as the mean *IP*. The full predictive function for average intermolt period $IP_{dd}(i)$ can thus be expressed as

$$IP_{dd}(i) = \gamma(L_i) + \beta(L_i), \qquad (7)$$

where $\gamma(L_i)$ is a linear function

$$\gamma(L_i) = \gamma_0 + \gamma_1 L_i \qquad (8)$$

predicting the duration of the molt cycle required phase, and $\beta(L_i)$ is a linear function

$$\beta(L_i) = \beta_0 + \beta_1 L_i \qquad (9)$$

predicting the average duration of the molt cycle variable phase. Average intermolt period is thus predicted by the sum of two separate lines. The complete probability density function for *IP* is obtained by substituting $IP_{dd}(i)=y$, $\gamma(L_i)=\gamma$, and $\beta(L_i)=\beta$ in equation (6), yielding

$$f[IP_{dd}(i)] = \frac{1}{\beta_0 + \beta_1 L_i} e^{-\frac{IP_{dd}(i)-(\gamma_0+\gamma_1 L_i)}{\beta_0+\beta_1 L_i}} . \qquad (10)$$

Standard least-squares methods for parameter estimation are not appropriate when model error is distributed non-normally. A maximum likelihood procedure for estimating parameters γ_0, γ_1, β_0, and β_1 of equation (10) is developed in Smith (1997), along with computer algorithms for carrying out the estimation. This procedure was applied to the data of Fig. 16C, and the overall fitted intermolt period-length model (equation 7) is shown on the graph (solid line). Table 6 provides parameter estimates.

Molt-Process Length-Age Model

The basic construction of molt-process growth curves (Hiatt 1948) is simple. Premolt length L_i is used to predict the time when the next molt will occur via an intermolt period function (equation 4), and also the associated increase in length at this molt via a molt increment function (equation 2), resulting in postmolt length L_{i+1}. This procedure is repeated for L_{i+1} to predict the time and length increase of the subsequent molt, and so on. This modeling approach has been difficult to apply in practice, however, because intermolt period is very sensitive to changes in temperature, molting may be inhibited during winter in colder regions, and species may

possess a terminal instar after which molting does not occur for the remainder of an animal's lifespan. In this section we describe a general numerical modeling framework following Smith (1997), which incorporates these aspects of the crustacean molting process. We apply the model to describe the growth of *C. sapidus* in two geographical regions, Louisiana and Chesapeake Bay. As will be illustrated, two advantages of the molt-process growth model over continuous length-age functions (e.g., von Bertalanffy 1938 or Richards 1959) are that it realistically depicts the discontinuous nature of crustacean growth in length-at-age and it does not require explicit age data.

Much of the complexity of molt-process growth models entails the estimation of specific molting dates for each instar $i=1, 2,...,\Omega$, where $i=1$ is the first postlarval instar and $i=\Omega$ is the last instar for species with indeterminate growth or the terminal instar for species with determinate growth. For a given t_i, time (day of year) at molting to instar i, the date of the subsequent molt t_{i+1} is estimated by a 3-step procedure. Computational examples are provided in Table 7. The first step is to use the intermolt period function (equation 7) to predict the quantity $IP_{dd}(i)$, the expected degree-day duration of a molt cycle for a crab of length L_i. We will refer to this predicted value as the "target" degree-days needed for molting. Because molt-process growth curves are necessarily constructed in chronological time units (e.g., days, weeks, years), the actual calendar date of molting t_{i+1} will depend on the environmental temperature regime in effect from t_i to t_{i+1}. We introduce the general function $\Lambda(t_k,t)$ to represent the cumulative degree-days from the time of a precursor event k (e.g., molting) to time t, defined as

$$\Lambda(t_k,t)=\int_{t=t_k}^{t} t_{dd}\,dt, \tag{11}$$

where t_{dd} is the degree-days for day t (equation 5) and $dt=1$ day. For example, the cumulative degree-days for an intermolt period $IP_{dd}(i)$ are given by

$$IP_{dd}(i)=\Lambda(t_i,t_{i+1})=\int_{t=t_i}^{t_{i+1}} t_{dd}\,dt, \tag{12}$$

where t_i is the time (day) at molting to instar i and t_{i+1} is the time at molting to instar $i+1$. Step 2 entails using an input time series of water temperature $T(t)$ and equations (5) and (11) to compute $\Lambda(t_i, t)$, the cumulative degree-days from date t_i to subsequent date t. As shown in Table 7, numerical integration of equations (11) or (12) is carried out by summing t_{dd} over a range of calendar days t. Step 3 is to identify the calendar day t_{i+1} of molting that is expected to occur when the target degree-days have been accumulated, i.e., when $\Lambda(t_i,t) \geq IP_{dd}(i)$. The resulting intermolt period measured in chronological time units, $IP(i)$, is obtained from

$$IP(i)=\int_{t=t_i}^{t_{i+1}} t\,dt, \tag{13}$$

the cumulative calendar time from t_i to t_{i+1}.

At the time of molting to instar $i+1$, length L at instar $i+1$ is predicted from equation (3). Substituting L_{i+1} from equation (3) for L_i in equation (7) begins the procedure for estimating the time of the next molt, t_{i+1}. The iterative process is begun with input values for $L_r(a_r,t_r)$, the respective length, age, and molting date of the first postlarval instar $i=1$. Post-settlement age a at time t is computed by

$$a(t)=\int_{t=t_r}^{t} t\,dt, \tag{14}$$

thus enabling specification of $L(a,t)$, length at age and time.

The above procedure for estimating molting date t_{i+1} is valid as long as temperature $T(t)$ remains above the threshold T_{min} (equation 5). When $T(t)$ drops below T_{min}, progression through the molt cycle is physiologically blocked (Fig. 10). Time periods in which $T(t)$ remains above T_{min} constitute "molting seasons," which begin at time t_s, the date when the event $T(t)>T_{min}$ occurs. These seasons are spanned by periods of low temperature molt inhibition, which begin at time t_I, the date when the event $T(t)\leq T_{min}$ occurs. As illustrated in Fig. 17, between-season intermolt period, denoted as $\tau(t_i, t_{i+1})$, is estimated from three separate time segments

$$\tau(t_i,t_{i+1})=\tau(t_i,t_I)+\tau(t_I,t_s)+\tau(t_s,t_{i+1}), \tag{15}$$

Table 7. Example of computational worksheets for predicting the time t at molting to instar $i+1$ using the degree-day method (equations 5, 11, and 13) for a 10 mm blue crab under two different environmental temperature regimes. Parameters: L_i = 10 mm (premolt carapace width); $IP_{dd}(i)$ = 142.3 degree-days (equation 9, Table 6); T_{min} = 8.9°C (Table 6).

Case 1. Increasing temperature regime				Case 2. Decreasing temperature regime			
t (Day of year)	$T(t)$ (°C)	t_{dd} (Degree-days)	$\Lambda(t_i, t_{i+1})$ (Degree-days)	t (Day of year)	$T(t)$ (°C)	t_{dd} (Degree-days)	$\Lambda(t_i, t_{i+1})$ (Degree-days)
t_i = 180	—	0.0	0.0	t_i = 250	—	0.0	0.0
181	24.0	15.1	15.1	251	24.0	15.1	15.1
182	24.5	15.6	30.7	252	23.5	14.6	29.7
183	25.0	16.1	46.8	253	23.0	14.1	43.8
184	25.5	16.6	63.4	254	22.5	13.6	57.4
185	26.0	17.1	80.5	255	22.0	13.1	70.5
186	26.5	17.6	98.1	256	21.5	12.6	83.1
187	27.0	18.1	116.2	257	21.0	12.1	95.2
188	27.5	18.6	134.8	258	20.5	11.6	106.8
t_{i+1}=189	28.0	19.1	153.9	259	20.0	11.1	117.9
$IP(i)$ = 9 d			$\Lambda(t_i, t_{i+1}) \geq IP_{dd}(i)$	260	19.5	10.6	128.5
				261	19.0	10.1	138.6
				t_{i+1}=262	18.5	9.6	148.2
				$IP(i)$ = 12 d			$\Lambda(t_i, t_{i+1}) \geq IP_{dd}(i)$

where $\tau(t_i, t_I)$ is the duration from time at molting t_i to time of low temperature inhibition t_I, $\tau(t_I, t_s)$ is the duration of the low temperature inhibition period, and $\tau(t_s, t_{i+1})$ is the duration from the start of the molting season t_s to time at molting t_{i+1}. The first segment, duration $\tau(t_i, t_I)$, is given by

$$\tau(t_i, t_I) = \int_{t=t_i}^{t_I} t \, dt \qquad (16)$$

and is estimated from the procedure for within-season intermolt period using equations (5), (7), and (11) by substituting the time at molting t_{i+1} with the time at low temperature inhibition t_I. The second segment, duration of the low temperature inhibition period, is given by

$$\tau(t_I, t_s) = \int_{t=t_I}^{t_s} t \, dt \,, \qquad (17)$$

where $T(t) \leq T_{min}$ for all t.

The third segment, post-inhibition time $\tau(t_s, t_{i+1})$, is the duration from the synchrony point of molt stage $C_4^{(r)}$ to ecdysis (Fig. 10C), which involves a portion of the $C_4^{(r)}$ stage, the variable phase (stage $C_4^{(v)}$) under MIH control, and all premolt stages D_0 to D_4 (Fig. 17). This "season-to-molt" duration is similar to the within-season intermolt period except that it does not involve the entire required phase. However, the exact portion of stage $C_4^{(r)}$ of the within-season molt cycle (Fig. 10B) that is included in season-to-molt progressions (Fig. 17) is unknown,

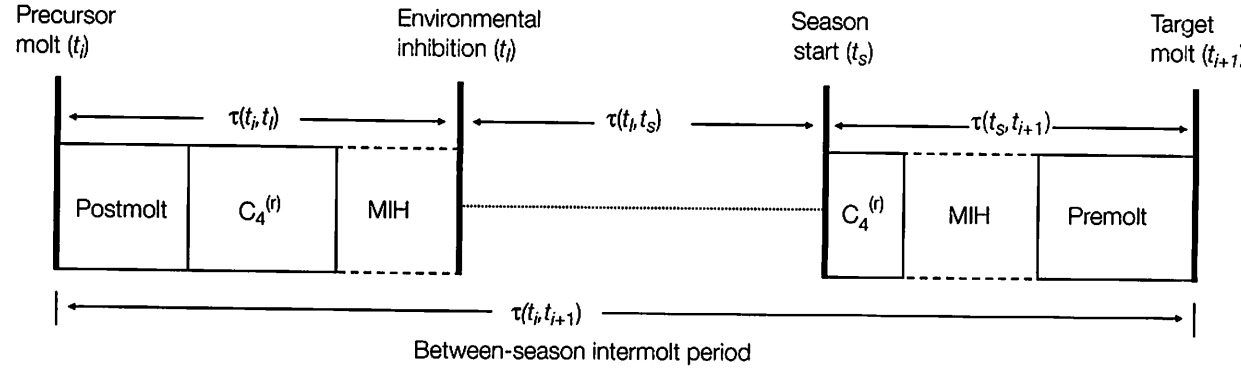

Figure 17. Conceptual diagram of model for between-season intermolt period, based on the low-temperature inhibition scenario depicted in Figure 10. The overall duration between molt events $[\tau(t_i, t_{i+1})]$ is the sum of pre-inhibition $[\tau(t_i, t_I)]$, inhibition period $[\tau(t_I, t_s)]$, and post-inhibition $[\tau(t_s, t_{i+1})]$ durations.

and it is also unclear whether the season-to-molt variable phase is coincident with the variable phase of within-season *IP*. Predicting the time at molting t_{i+1} after the start of a molting season t_s requires an additional degree-day function

$$\tau_{dd}(t_s,t_{i+1})=f(L_i) \qquad (18)$$

that we can infer to be analogous to equation (7) for within-season IP_{dd} (i), i.e., $f(L_i)$ is linear and observations of $\tau_{dd}(t_s,t_{i+1})$ follow a shifted exponential probability density function. Model-fitting of equation (18) requires observations of season-to-molt duration at premolt length obtained from empirical studies. These experiments would entail maintaining animals at below-T_{min} temperatures for sufficient time to allow molt cycles to synchronize at the $C_4^{(r)}$ stage. Temperatures would then be increased to above-T_{min} levels and the subsequent season-to-molt durations would be recorded for each individual. Experiments of this type have yet to be performed for *C. sapidus*, however. Drawing upon the observation that premolt stages of blue crabs account for about 25% of the average molt cycle duration (Table 1), we propose that equation (18) is reasonably approximated by

$$\tau_{dd}(t_s,t_{i+1})=0.25[\gamma(L_i)+\beta(L_i)]+\beta(L_i), \qquad (19)$$

where $\gamma(L_i)$ and $\beta(L_i)$ are the respective required and variable phase durations from the within-season *IP* function (equations 7-9). From equations (5) and (11), molting is expected to occur at day $t=t_{i+1}$ when cumulative degree days $\Lambda(t_s,t)$ reach or exceed the season-to-molt degree-days $\tau_{dd}(t_s,t_{i+1})$ predicted from equation (19). The chronological time duration $\tau(t_s, t_{i+1})$ is then computed from

$$\tau(t_s,t_{i+1}) = \int_{t=t_s}^{t_{i+1}} t \, dt . \qquad (20)$$

Parameterization of the numerical molt-process length-age model for *C. sapidus* males and females is documented in Table 6. Growth was modeled under annual temperature regimes approximating conditions in Louisiana and Chesapeake Bay (Fig. 18A). Chesapeake Bay temperatures are comparatively cooler throughout the year, and also drop below T_{min} during winter and early spring. The estimated mean postlarval settlement date in Louisiana (based on Adkins 1972 and van Montfrans et al. 1990; see Table 6), t_r=Jul 15 (Day of year 196), occurs during the middle of the summer high-temperature season, whereas in Chesapeake Bay mean settlement occurs after the summer peak during the temperature decline of early fall (t_r=Sep 15, Day of year 258; van Montfrans et al. 1990). Corresponding molt-process growth curves reflect these differences in settlement

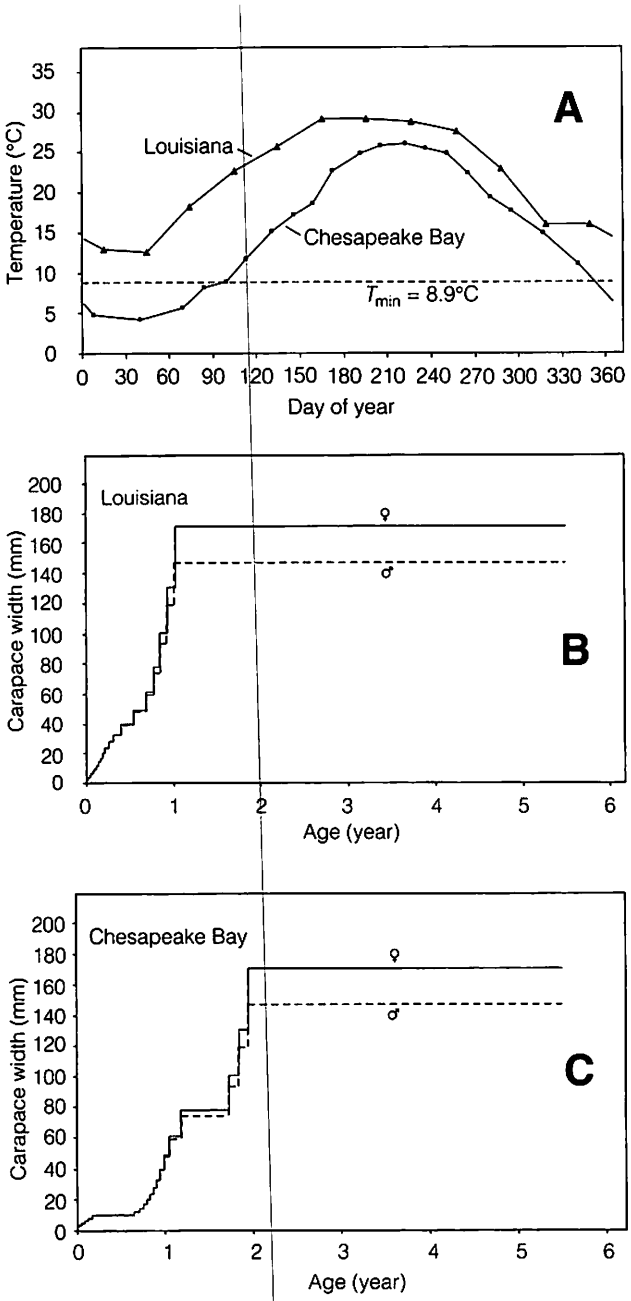

Figure 18. (A) Annual temperature regimes for Louisiana (triangles; data source: Adkins 1972) and Chesapeake Bay (squares; data source: U.S. Environmental Protection Agency, Chesapeake Bay Program, Annapolis, Maryland); dashed line denotes minimum physiological temperature threshold (T_{min}). (B-C) Molt-process length-age models for *C. sapidus* females (solid line) and males (dashed line) in (B) Louisiana and (C) Chesapeake Bay; model parameters are provided in Table 6.

time and temperature between the two regions. An "average" blue crab female or male in Louisiana is projected to become subject to capture in the hard crab fishery (L_c=127 mm CW) and attain sexual maturity (females, L_m=135 mm; males, L_m=105 mm) at an age of about 1 year (Fig. 18B). In Chesapeake Bay these events are projected to occur at about 2 years of age (Fig. 18C).

For species with indeterminate growth, iterative modeling of intermolt period and molt increment stops when the oldest age $a=a_\lambda$ is attained. Oldest age a_λ is usually unknown, but can be derived from the molt-process model by incorporating a "stopping rule" based on estimates of the length at oldest age L_λ (i.e., maximum average length). For species such as *C. sapidus* exhibiting determinate growth, iterative modeling stops at instar $i=\Omega$. Terminal instar number Ω is rarely known; however, a model stopping rule based on the number of instars after reaching L_m, length at attainment of sexual maturity, can be used to estimate $i=\Omega$ for many species (Smith 1997). We define the variable $NMT(i)$ as the number of molts from instar i to the terminal instar. Beginning from the maturity instar i_m, the quantity $NMT(i_m)$ is the number of adult instars minus one,

$$NMT(i_m)=\left(\sum_{i=i_m}^{i=\Omega} i\right)-1. \qquad (21)$$

During construction of the molt-process growth curve, the stopping rule using $NMT(i_m)$ is activated at the attainment of sexual maturity, i.e., when $L_i \geq L_m$. After each subsequent molt event, the equation

$$NMT(i+1)=NMT(i)-1 \qquad (22)$$

is employed until $NMT=0$, i.e., attainment of the terminal instar. The analysis of Fig. 12 indicates that *C. sapidus* females have one adult instar and that males have two adult instars, resulting in estimates of $NMT(i_m)=0$ for females and $NMT(i_m)=1$ for males (Table 6). The duration $\tau(t_\Omega,t_\lambda)$ between t_Ω, the time at molting to the terminal instar, and t_λ, the time at reaching the oldest age, provides the final time segment for the lifespan molt-process growth curve. Oldest age can then be estimated as $a_\lambda=a(t_\lambda)$ in

equation (14). Estimates of terminal instar duration $\tau(t_\Omega, t_\lambda)$ can be obtained empirically from tagging or captivity growth studies. Tagging studies for *C. sapidus* males and females suggest terminal instar durations of at least 3 to 4 years for both sexes (Table 6; Figs. 18B, 18C).

The Chesapeake Bay length-age model projections (Fig. 18C) are recast in terms of length at time t over a 3-year period in Fig. 19A. Also shown are growth curves with settlement dates reflecting the beginning (t_r=Jul 15) and ending (t_r=Nov 15) seasonal bounds of postlarval settlement for the recruit year class of blue crabs in Chesapeake Bay (van Montfrans et al. 1990). The difference in length among the early-, mid-, and late-season settlement cohorts at a given time is pronounced through the second winter. However, all settlement cohorts are projected to reach the terminal instar during the molting season between the second and third winters.

The model-projected wintertime ranges of carapace width from Fig. 19A are indicated (horizontal lines) on a graph of *C. sapidus* abundance-at-length in Fig. 19B estimated from a winter dredge survey in Chesapeake Bay (Rothschild et al. 1992). The growth model projection can assist in elucidating the wintertime size-age composition of Chesapeake Bay crabs from the numbers-at-size estimates. The age-0 recruit class (1st Winter, Fig. 19B) appears to include crabs <55 or 60 mm CW and exhibits modal peaks at 20 to 25 mm. The lower extent of the age-0 size range is uncertain because individuals become fully vulnerable to the dredge sampling gear at carapace widths >15 mm. The age-1 year class (2nd Winter) exhibits peak size modes at 100 to 110 mm CW with a lower bound at about 60 mm. The upper extent of the age-1 size range is obscured by overlap with the size range of the terminal instar, which begins at about 120 mm CW (Fig. 12). The analysis of Fig. 12 suggests that the majority of crabs reach the terminal instar at carapace widths ranging from 135 to 175 mm. The terminal instar size range includes multiple year classes comprised of mostly age 2 and older crabs (3rd+ Winter).

The field estimates of abundance-at-length (Fig. 19B) can in turn be used to evaluate the performance of the molt-process growth model. The mag-

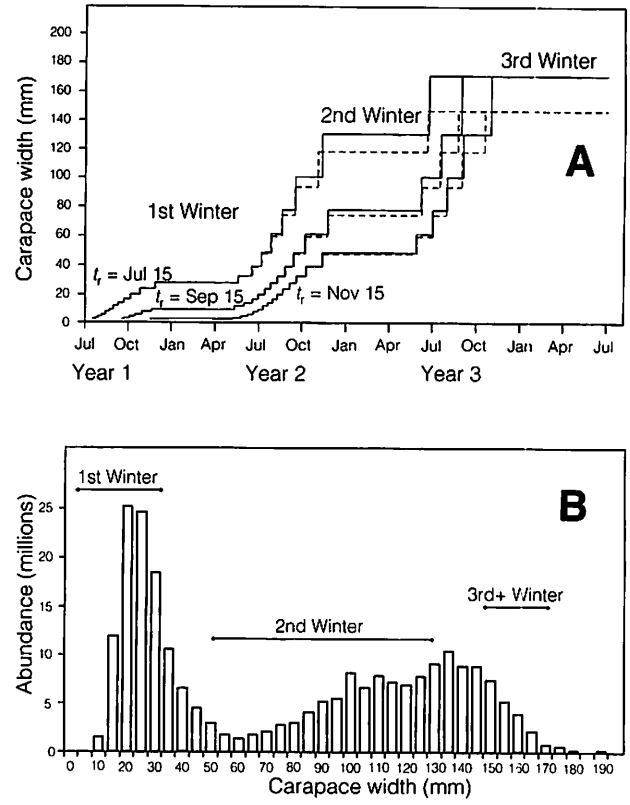

Figure 19. (A) Three-year molt-process growth model projections for Chesapeake Bay *C. sapidus* females (solid line) and males (dashed line) with early- (t_r=Jul 15), mid- (t_r=Sep 15), and late-season (t_r=Nov 15) postlarval settlement dates (Table 6). (B) *C. sapidus* abundance-at-size estimated from a dredge survey conducted in Chesapeake Bay during winter 1990-1991 (Rothschild et al. 1992); horizontal lines denote wintertime size ranges from the growth model projections of panel (A).

nitude of the range in size predicted by the model for the age-0 and age-1 year classes at the respective first and second winters matches well with that observed in the survey estimates. The upper bound of the model-projected size range for the age-0 year class, however, is somewhat lower than the upper bound of the age-0 size range inferred from the field survey. Likewise, the lower bound of the size range at the second winter is 50 mm CW according to the growth model compared to approximately 60 mm for the age-1 class observed in the survey. These discrepancies suggest that the model is predicting a somewhat slower rate of growth compared to the

rate observed in the population. As a performance check, the model was used to project the growth of a crab with initial size 20 mm CW, the peak mode at the first winter, over a 1-year period to the following winter. The projected ending size was 100 mm CW, the peak wintertime size mode of the age-1 year class. This projection suggests that the problem of slow growth in the model is confined to early instars with carapace widths <20 mm. Interestingly, this corresponds to the size range in which *C. sapidus* molt-process data are either very sparse (intermolt period, Fig. 16C) or somewhat suspect (molt increment, Fig. 13A).

The narrow size range predicted by the growth model for terminal instar crabs (3rd+ Winter, Fig. 19B) is largely a result of using a deterministic molt increment function in conjunction with a single constant size (L_m) demarcating sexually immature and mature individuals, the key variable that invokes the terminal instar stopping rule (equations 21 and 22). A more realistic representation of the terminal instar size range could be achieved by extending the model to incorporate variation in molt increment (Fig. 14) and length at maturity (Fig. 12).

Growth in Weight

A weight-age growth model can be obtained by converting predicted length values from a length-age model to values of weight using a weight-length relationship. There are a number of published accounts examining *C. sapidus* weight-carapace width relationships in different geographical regions, but most did not obtain observations of weight over the full range of length (e.g., Pullen and Trent 1970; Olmi and Bishop 1983; Cadman and Weinstein 1985). Size class means of weight-length from the study of Newcombe et al. (1949a; see Table 5) are plotted in Fig. 20A for males (crosses) and females (diamonds). These data have their own limitations as well, most notably the paucity of observations at intermediate carapace widths. However, this limitation is less problematic from a model-fitting standpoint than a lack of data at either end of the length range.

The data of Fig. 20A follow the general power relationship

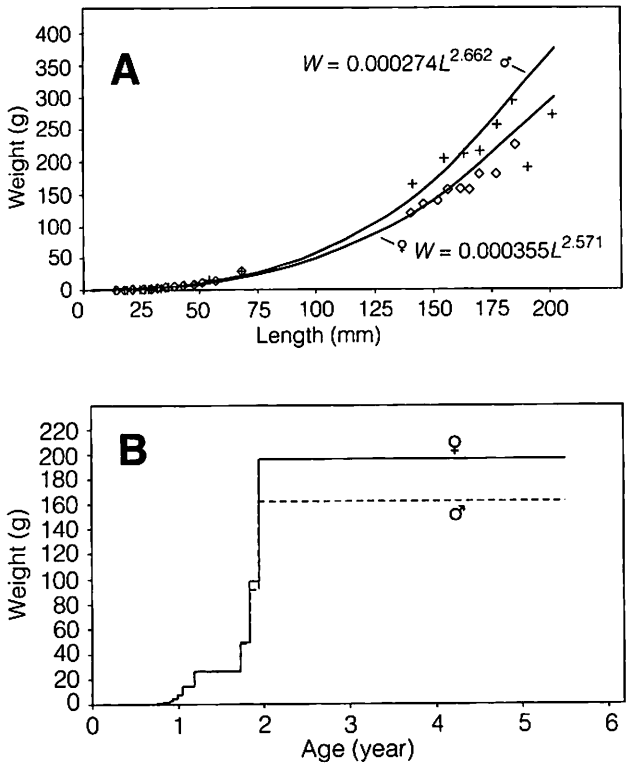

Figure 20. (A) Plot of *C. sapidus* weight (g)-length (mm carapace width) data and fitted relationships for males (crosses) and females (diamonds) from the study of Newcombe et al. (1949a; see Table 5). (B) Molt-process weight-at-age growth models for blue crab females (solid line) and males (dashed line) in Chesapeake Bay (mean settlement date t_r=Sep 15).

$$W_i(a,t)=b_0[L_i(a,t)]^{b_1}, \tag{23}$$

where b_0 and b_1 are model parameters. A common model for parameter estimation is obtained by transforming both sides of equation (23) using the natural logarithm function

$$\log_e W_j=\log_e b_0+b_1\log_e L_j+\varepsilon_j, \tag{24}$$

where $\log_e b_0$ and b_1 are the respective intercept and slope of a linear function and ε_j is the residual error of the jth observation. The choice of an appropriate estimation model (e.g., nonlinear or linear) and corresponding parameter estimation method (e.g., nonlinear regression or least-squares regression) hinges

on the error assumptions, however. An examination of these estimation issues pertaining to weight-length relationships is provided in Diaz et al. (2001). For the data from Newcombe et al. (1949a), which are in the form of size class means rather than observations, the error assumptions are not of much concern. We estimated the parameters of the linearized function (equation 24) for females and males separately using least-squares regression (Fig. 20A; Table 6). Size class means were weighted with the corresponding sample size. The divergence between the female and male fitted relationships is most apparent for adults (males, L_m=105 mm; females, L_m=135 mm). As discussed in Newcombe et al. (1949a), at larger sizes male blue crabs are heavier on average than females at a given carapace width. This finding has been observed in other blue crab weight-length studies as well (Pullen and Trent 1970; Olmi and Bishop 1983).

Molt-process weight-age curves for female and male blue crabs in Chesapeake Bay (mean settlement date t_r=Sep 15) are shown in Fig. 20B. These growth projections were obtained by converting the length-age curves of Fig. 18C into values of weight-at-age using the respective female and male weight-length relationships of Fig. 20A. The weight-age models for both sexes indicate that a 5- to 6-fold increase in weight is expected to occur during the last three molt events, and that weight nearly doubles during the terminal molt alone.

Biological Insights

A sound biological understanding of the molting process, particularly the interplay between hormonal and environmental control, was central to the development of a mathematical model of blue crab growth. In this section we highlight a few of the interesting biological insights gained from viewing the growth processes of blue crabs from a quantitative perspective.

There are clear differences between male and female blue crabs for many aspects of growth, including molt increment (Fig. 13), weight-length (Fig. 20A), and the number of adult instars (Fig. 12). The divergence between the sexes in the molt increment and weight-length functions is most apparent at sizes corresponding to the onset of gonadal development and maturation. A notable exception is intermolt period. The average relationship between intermolt period and length appears to be essentially the same for males and females, and there does not seem to be a noticeable change in the intermolt period function for male blue crabs at sexual maturity (Fig. 15A). Although the data for examining this issue are limited, the lack of change in the intermolt period-length relationship in response to sexual maturation has been observed in other decapods as well (Hartnoll 1982; Smith 1997).

Some aspects of the intermolt period-length function are worth noting. After degree-day adjustment, the mean relationship between intermolt period and premolt length is strongly linear, and the variance conforms quite well to the shifted exponential probability density function. The intermolt period-length data of Fig. 16C, which were principally obtained from crabs subjected to natural photoperiod and lunar cycles (Table 5), do not exhibit even the slightest hint of periodicity with respect to the mean or variance relationships as would be expected if some form of lunar control of molting were at work. The linearity of the average intermolt period-length relationship indicates that molt cycle duration increases at a constant rate of increasing premolt length. This is perhaps reflective of the general observation by investigators that although the overall molt cycle duration is progressively longer with increasing animal size, the proportion of the average time spent at each different molt stage remains constant irrespective of size (Adelung 1971; Aiken 1980; Freeman et al. 1987). The variance of intermolt period, in contrast, increases exponentially with increasing premolt length, a basic property of exponential-gamma probability density functions (Law and Kelton 1991). The intermolt period can be thought of as a stochastic time-to-event process (Kalbfleisch and Prentice 1980). The duration of the variable molt cycle phase (Fig. 10) appears somewhat analogous to the service-to-failure time of a device: the X-organ can be envisioned as an MIH-producing machine that is placed in service at the attainment of molting competence and then fails at the initiation of premolt. This would suggest that

high variability may be an inherent property of crustacean intermolt period. Empirical investigations support this view. As documented above, temperature and nutrition can greatly influence the mean intermolt period, but neither these nor any other discernable exogenous factors seem to have any effect on the underlying pattern of intermolt period variation (Aiken 1973; Hopkins 1982; Smith 1997).

According to the molt-process growth curves of Figs. 18B and 18C, blue crabs in Louisiana are expected to reach sexual maturity and enter the hard crab fishery around 1 year after settlement, whereas these events are expected to occur around 2 years post-settlement for blue crabs in Chesapeake Bay. These differences in growth schedules are likely to be substantial with respect to developing sustainable harvest policies for the two regions. Recall that the only differences in the growth model parameters for the two regions are the estimated mean settlement date (t_r) and the annual temperature regime (Fig. 18A). When viewed from a degree-day perspective, crabs in Louisiana and Chesapeake Bay would be expected to attain adulthood and harvestable size at roughly similar physiological times, i.e., cumulative degree-days post-settlement. For example, male blue crabs in Louisiana are expected to become subject to capture (L_c=127 mm CW) in 4,792 degree-days compared to 4,724 degree-days for males in Chesapeake Bay. Females are expected to reach this size in 4,206 degree-days in Louisiana and 4,385 degree-days in Chesapeake Bay.

A probabilistic perspective of physiological time gives further credence to determinate growth of *C. sapidus*. For higher-latitude regions where molting is inhibited during winter, the cumulative degree-days within the molting season is in effect an environmentally-imposed maximum intermolt period for all individuals in the population. A question arises concerning the issue of determinate growth: Do larger crabs have enough time to complete a full molt cycle during the molting season? In Chesapeake Bay there are 2,554 degree-days constituting the molting season according to the temperature regime of Fig. 18A. The average intermolt period of a 150 mm CW blue crab is estimated to be 781 degree-days (Fig. 16C, equation 7, Table 6). Using the cumulative distribution function for the shifted exponential probability density function, we estimate that 99.1% of 150 mm CW blue crabs would be expected to complete a full molt cycle in less than 2,554 degree-days. For crabs 200 mm CW, we would expect 97.0% to complete a molt cycle during the molting season. Bear in mind that these percentages would increase if we invoke the season-to-molt scenario (Fig. 17, equation 18). Thus, if growth were indeterminate, blue crabs of all sizes in Chesapeake Bay would be expected to molt at least once during the molting season, and the expected length of crabs at the final instar would be well in excess of the largest length ever observed for *C. sapidus* (254 mm CW, Archambault et al. 1990). Tagging studies conducted in lower-latitude regions where molting occurs year-round have documented intermolt periods of at least 3 years for both male and female blue crabs (Tagatz 1968a; More 1969; Perry 1975). Using the Louisiana temperature regime (Fig. 18A), 14,132 degree-days are estimated to accumulate over a 3-year period. Under the assumption of indeterminate growth, the probability that an intermolt period for a 150 mm CW crab would be equal to or longer than this quantity is estimated to be $p = 0.24 \times 10^{-12}$, i.e., highly unlikely. A striking feature of the molt-process growth curves shown in Figs. 18B and 18C, which presume determinate growth, is that *C. sapidus* females and males appear to spend two-thirds or more of their potential lifespan at the terminal instar after growth in length has been completed. In this aspect of population biology, blue crabs are more similar to humans than they are to fishes.

The difficulties in modeling crustacean growth have traditionally been attributed to the problem of age determination (Hancock 1977). The perception has been that obtaining explicit length-at-age data for crustaceans as is commonly done for fishes would facilitate estimation of continuous length-age functions (e.g., von Bertalanffy 1938 or Richards 1959) that are used to model the growth of fishes. The existence of a functional relationship between size and age forms the underlying basis of these standard continuous length-age models. Our analysis of blue crab molting and growth suggests that a

general predictive relationship of the form $L=f(a)$ is tenuous at best. At the terminal instar, the relationship between size and age is fully disassociated, e.g., blue crabs have the same length at 2 and 5 years post-settlement (Figs. 18B and 18C). For crabs subject to winter non-molting seasons, this disassociation between size and age also seems to occur during the main phase of growth before reaching the terminal instar. This phenomenon is inferred from Figs. 10C and 17, which illustrate the effects of below-threshold temperatures on molt cycle progression. Post-inhibition season-to-molt durations $[\tau(t_s,t_{i+1})]$ are not dependent on pre-inhibition $[\tau(t_i,t_l)]$ or inhibition $[\tau(t_l,t_s)]$ period durations (Fig. 17). Seasons of low-temperature molt inhibition thus effectively sever the functional relationship between intermolt period and length that exists under non-inhibiting temperature conditions (Fig. 16C) which, in turn, physiologically severs the relationship between size and age, regardless of whether age is measured in days or degree-days.

There is no question that techniques for direct ageing would be of great benefit for understanding certain aspects of blue crab stock dynamics, e.g., elucidating the age composition and estimating mortality rates for the terminal instar phase of a population. A promising methodology in this regard involves quantifying the accumulation of fluorescent pigments (lipofuscins) in neural tissues (brain and eyestalk) as a direct measure of physiological age (Ju et al. 1999). This approach circumvents the historical problem of attempting to age various calcified structures that are not retained through successive molts. With respect to constructing crustacean length-age models, however, explicit age data are of questionable utility. Knowing the age of an individual crab to even the exact day or degree-day does not necessarily enable reliable prediction of its size, and thus may provide little useful information for realistically modeling its growth.

FUTURE RESEARCH

We hope this chapter has illuminated some of the gains in our biological and mathematical understanding of blue crab molting and growth that have occurred in recent years. Research has largely focused on development of techniques — e.g., endocrinological, mathematical, statistical — for collecting information and constructing models. However, actual data on processes related to molting and growth are still limited. One example is low-temperature inhibition of molting. The ability to model both within-season and between-season intermolt period (equations 7 and 15) appears to be central to the biological realism of the molt-process growth model for blue crabs inhabiting higher-latitude regions such as Chesapeake Bay (Figs. 18C and 19A). Yet direct physiological evidence supporting the underlying conceptual model of a low-temperature block of Y-organ production of ecdysteroids (Fig. 10) is very sparse for decapod crustaceans (Passano 1960b; Aiken 1980) and does not exist for *C. sapidus* or any other portunid species. In addition, the estimate of the key threshold parameter T_{min} (Fig. 11) was based on intermolt period data from a single study (Tagatz 1968b) conducted in a single geographical location (St. Johns River, Florida) under experimental conditions in which variation of environmental temperature was not tightly controlled (Table 5).

A second example of limited data involves the functions of the molt-process growth model. Molt increment data have been obtained for blue crabs in two regions (Chesapeake Bay, northeastern Florida), within-season intermolt period data are from a single region (northeastern Florida), and data for the season-to-molt function (equation 18) are nonexistent (Tables 5 and 6). Large-scale studies of molt increment and intermolt period have generally focused on crabs larger than 20 mm CW, with much less emphasis placed on smaller individuals. Although crabs less than 20 mm CW account for a small proportion of the range of premolt size, approximately 50% of postlarval instars occur between 2 and 20 mm CW (Figs. 18B and 18C). A further limitation is that molt-process growth data at present are available in the form of size class means rather than actual observations. Consequently, while we are able to estimate parameters of the various functions, we are unable to perform any statistical inference on the parameters, e.g., comparing molt increment func-

tions among regions, or to incorporate parameter uncertainty into the molt-process growth model.

It is clear that a multitude of research topics could be pursued in furthering our understanding of blue crab molting and growth. We focus our recommendations for the direction of growth research over the next few years by outlining three research programs likely to lead to substantial improvements in the scientific basis for blue crab resource management, as well as an improved ecological understanding of the role of blue crabs in aquatic ecosystems.

The first and most pressing research program is designed to improve the empirical and physiological underpinnings of the molt-process growth model described above. The major elements of this program should ideally be carried out on blue crab populations in two or more higher-latitude regions where molting is inhibited during winter and in two or more lower-latitude regions where molting occurs year-round. The program entails three main phases. The objective of phase 1 is to elucidate the low-temperature molting inhibition threshold T_{min}. An initial estimate of T_{min} can be obtained by the procedure illustrated in Fig. 11D. Requisite data are intermolt period observations from a laboratory-based factorial experiment using crabs from at least four discrete carapace width classes that encompass the full range of premolt L, with the crabs maintained at four discrete temperatures well within the range of T_{min} and T_{max}. Validation of the estimated T_{min} involves a series of follow-on experiments tracking molt stage progression (e.g., Aiken and Waddy 1976; Aiken 1980) and ecdysteroid concentrations of crabs held at temperatures below and above the estimated threshold. A second more elaborate set of follow-on experiments (e.g., Passano 1960b) would examine whether low-temperature and MIH inhibition of molting are truly independent.

Once T_{min} has been robustly estimated and validated, phase 2 entails conducting laboratory growth studies to obtain data for the three principal functions of the molt-process growth model: molt increment (equation 3, Fig. 13), within-season intermolt period (equation 7, Fig. 16C), and season-to-molt duration (equation 18). The objective of these experiments is to obtain laboratory observations of molt increment and intermolt period that are representative of blue crabs in the wild. Recreating natural conditions as closely as possible in the laboratory environment with respect to food and other influential animal maintenance variables, such as habitat space and substrate, is a prudent and perhaps necessary strategy. In contrast, experiments carried out with aquaculture-oriented objectives — maintaining animals at unnaturally high temperatures and food quantities to enhance the rate of molting, but stocking aquaria at high density to reduce costs — may not yield data that are applicable for modeling molt-process growth of natural populations. Observations for each growth function will necessarily be obtained from post-settlement male and female blue crabs encompassing the entire range of premolt carapace width. It should be pointed out that the degree-day approach for modeling within-season intermolt period, once T_{min} is known, greatly relaxes the temperature requirements of the captivity environment for these experiments. Temperature need only be restricted within the T_{min} and T_{max} thresholds and recorded on a daily (or more frequent) basis by the investigator, i.e., temperature does not need to be tightly controlled at some fixed level. Season-to-molt experiments involve an additional first step that does require precise temperature control: crabs are held at a fixed temperature below T_{min} for 1 to 2 months to ensure that each animal has reached the low-temperature "synchrony point" in the molt cycle (Fig. 10C). Temperature is then gradually increased to above T_{min}, after which the temperature requirements are the same as for within-season intermolt period experiments.

Phase 3 is comprised of longer-term captivity experiments pertaining to determinate growth of blue crabs. Experimental individuals of both sexes are brought into captivity at some instar before undergoing sexual maturation, and then maintained until death. This procedure will enable direct observations of the number of adult instars and the duration of the terminal instar (measured in both days and degree-days). To gain a clearer understanding of the hormonal control of determinate growth, studies along the lines of Cheung (1973) using a subset of

these experimental crabs would examine the function of the Y-organ and X-organ during progression of the terminal instar.

The second research program is designed to address the impacts of salinity and food on blue crab growth. These aspects of growth are perhaps best examined within a bioenergetics modeling framework. This approach describes growth in terms of biological processes that account for metabolic energy gain (food consumption) and loss (respiration, egestion, and excretion) (Jobling 1994). Separate mathematical models describing each process (e.g., food consumption) as functions of animal size, temperature, salinity, etc., are combined to predict the overall change in weight of an organism through time (Kitchell et al. 1977; Luo and Brandt 1993). The benefits of this modeling approach go well beyond predicting weight-at-age. Explicit incorporation of key abiotic and biotic environmental factors as explanatory variables provides a window for understanding and modeling spatial and trophodynamic aspects of blue crab growth. Spatially-explicit bioenergetics models can be used to identify areas within an ecosystem where the expected "growth potential" of an individual crab is maximized, minimized, etc., and can thus provide very useful information to habitat managers (Brandt et al. 1992). Bioenergetics growth functions are fundamental components of models analyzing trophodynamic impacts, e.g., estimating the prey biomass on an annual basis required to support current population levels of blue crabs in Chesapeake Bay. Bioenergetics growth functions also form the basic building blocks of cohort-structured spatially dynamic predator-prey models (Ault et al. 1999) that can be used to quantitatively evaluate sustainable fishery harvest policies from a holistic, ecosystem-based perspective. For example, a demographic model of this type could potentially analyze not only direct fishing impacts on a given blue crab population but also indirect population effects due to habitat degradation and concurrent harvesting of important predator (e.g., striped bass *Morone saxatilis*) and prey (e.g., soft-shelled clam *Mya arenaria*) species.

Bioenergetics growth research entails two main phases. The first and most challenging phase is to extend the current modeling framework for continuously-growing fishes to discontinuously-growing crustaceans. For example, crab food consumption varies not only with variations in animal size and temperature as for fishes, but also according to molt stage (Table 1). Likewise, movement activity and thus respiration also varies with molt stage. Energy loss at molting when the old exoskeleton is discarded needs to be accounted for, as well as the suspension of molting and growth during cold winters. The eventual bioenergetics growth modeling framework for blue crabs will likely be some hybrid of fish bioenergetics models and crustacean molt-process models. The second phase involves conducting laboratory studies to obtain empirical data for estimating the various mathematical functions and parameters required for constructing bioenergetics growth models. These studies will necessarily include factorial experiments observing food consumption and standard respiration of individual blue crabs with respect to animal size, temperature, salinity, and molt stage.

Principal sources of data for the above two research programs are obtained from blue crabs held in captivity. However, the overall intent of both programs is to understand and model molting and growth of blue crabs in their natural environment. The third research program entails developing methodologies for obtaining at least some of the requisite growth data from individual blue crabs in the wild. Some promising headway has been made by studies employing creative uses of ultrasonic telemetry tags (see Wolcott and Hines 1990). These tags are currently undergoing rapid technological development (Arendt et al. 2001; Block et al. 2001), resulting in telemetry devices that are progressively smaller, lighter, and more sophisticated both in the types of information that can be obtained (e.g., continuous-time observations of animal spatial position, depth, water temperature, salinity, etc.) and in modes of data transmission (e.g., fixed-position buoy arrays, satellites, etc.). Research could be directed towards engineering telemetry devices that can relay information specific to crustacean molting and growth, such as the timing of ecdysis events together with hourly measurements of temperature and salinity

during the intermolt period. This type of study would necessarily be conducted in two phases, a laboratory research and development phase followed by a field implementation phase.

These research programs are likely to be challenging endeavors, and are intentionally designed to draw upon many diverse fields of expertise, including blue crab physiology and ecology, crustacean endocrinology and biochemistry, mathematical demography, statistics, applied marine physics and engineering, marine aquaria systems, etc. Each program also involves a mix of what might be characterized as "basic" and "applied" research elements. This chapter attests to the benefits of forming collaborative research partnerships to concurrently address basic and applied aspects of scientific problems. The recent gains in our understanding of blue crab molting and growth are a direct result of integrating basic and applied research results from many fields of study. It is our hope that scientists and funding agencies alike will recognize the utility of this research strategy. We are well aware of the practical difficulties involved in coordinating research efforts among a group of multidisciplinary investigators and of securing funding for programs with applied research components from agencies with a bent towards basic research and vice-versa. We are also highly confident that the potential gains in scientific understanding and benefits to the blue crab resource resulting from research programs such as those outlined above far outweigh these associated logistical nuisances.

ACKNOWLEDGMENTS

We thank A.H. "Tuck" Hines and Alicia C. Young-Williams for providing photographs and accompanying descriptions of premolt stages of the molt cycle and of the ecdysis process of blue crabs. We thank H.Carl Fitz for providing original data on blue crab growth. S.G.S.'s work has been supported by grants from University of Maryland Sea Grant (R/F-87-PD) and the Hudson River Foundation (HRF 008/98A). Some of the research described in this chapter was funded by grants to E.S.C. from the National, California, and Connecticut Sea Grant College Programs. The views expressed herein are those of the authors and do not necessarily reflect the views of NOAA or any of its sub-agencies. The U.S. Government is authorized to reproduce and distribute this chapter for governmental purposes. S.G.S. thanks Jiangang Luo and Natalia Zurcher for graphical assistance. E.S.C. thanks Sharon A. Chang for assistance in the preparation of this chapter. We thank the anonymous reviewers for their helpful comments.

REFERENCES

Abbe, G.R. 1974. Second terminal molt in an adult female blue crab, *Callinectes sapidus* Rathbun. Transactions of the American Fisheries Society 103:643-644.

Adelung, D. 1971. Untersuchungen zur Häutungsphysiologie der dekapoden Krebse am Beispiel der Strandkrabbe *Carcinus maenas*. Helgoländer Wissenschaftliche Meeresuntersuchungen 22:66-119.

Adkins, G. 1972. A study of the blue crab fishery in Louisiana. Louisiana Wildlife and Fisheries Commission, Technical Bulletin 3:1-57.

Aiken, D.E. 1973. Proecdysis, setal development, and molt prediction in the American lobster *(Homarus americanus)*. Journal of the Fisheries Research Board of Canada 30:1337-1344.

Aiken, D.E. 1980. Molting and growth. Pages 91-163 in J.S. Cobb and B.F. Phillips (eds.), The Biology and Management of Lobsters, Volume 1. Academic Press, New York.

Aiken, D.E. and S.L. Waddy. 1976. Controlling growth and reproduction in the American lobster. Proceedings of the World Mariculture Society 7:415-430.

Archambault, J.A., E.L. Wenner and J.D. Whitaker. 1990. Life history and abundance of blue crab, *Callinectes sapidus* Rathbun, at Charleston Harbor, South Carolina. Bulletin of Marine Science 46:145-158.

Arendt, M.D., J.A. Lucy and D.A. Evans. 2001. Diel and seasonal activity patterns of adult tautog, *Tautoga onitis*, in lower Chesapeake Bay, inferred from ultrasonic telemetry. Environmental Biology of Fishes 62:379-391.

Ary, R.D., Jr., C.K. Bartell, R.M. Grisoli and M.A. Poirrier. 1985. Morphological changes in regenerating

chelipeds of the blue crab *Callinectes sapidus* Rathbun as indicators of the progression of the molt cycle. Journal of Shellfish Research 5:1-8.

Ault, J.S., J. Luo, S.G. Smith, J.E. Serafy, J.D. Wang, R. Humston and G.A. Diaz. 1999. A spatial dynamic multistock production model. Canadian Journal of Fisheries and Aquatic Sciences 56(Supplement 1):4-25.

Berry, P.F. 1971. The biology of the spiny lobster *Panulirus homarus* (Linnaeus) off the east coast of southern Africa. Oceanographic Research Institute (Durban) Investigational Report 28:1-75.

Bishop, J.M., E.J. Olmi, III, J.D. Whitaker and G.M. Yianopoulos. 1983. Capture of blue crab peelers in South Carolina: an analysis of techniques. Transactions of the American Fisheries Society 112:60-70.

Bliss, D.E. and J.H. Welsh. 1952. The neurosecretory system of brachyuran Crustacea. Biological Bulletin 103:157-169.

Block, B.A., H. Dewar, S.B. Blackwell, T.D. Williams, E.D. Prince, C.J. Farwell, A. Boustany, S.L.H. Teo, A. Seitz, A. Walli and D. Fudge. 2001. Migratory movements, depth preferences, and thermal biology of Atlantic bluefin tuna. Science 293:1310-1314.

Böcking, D., H. Dircksen and R. Keller. 2002. The crustacean neuropeptides of the CHH/MIH/GIH family: structures and biological activities. Pages 84-97 in K. Wiese (ed.), The Crustacean Nervous System. Springer, Berlin.

Borst, D.W., H. Laufer, M. Landau, E.S. Chang, W.A. Hertz, F.C. Baker and D.A. Schooley. 1987. Methyl farnesoate (MF) and its role in crustacean reproduction and development. Insect Biochemistry 17:1123-1127.

Botsford, L.W. 1985. Models of growth. Pages 171-188 in A. Wenner (ed.). Crustacean Growth: Factors in Adult Growth. Crustacean Issues 3. A.A. Balkema, Rotterdam.

Brandt, S.B., D.M. Mason and E.V. Patrick. 1992. Spatially-explicit models of fish growth rate. Fisheries (Bethesda) 17:23-33.

Bückmann, D. and D. Adelung. 1964. Der Einfluss der Umweltfaktoren auf das Wachstum und den Häutungsrhythmus der Strandkrabbe *Carcinides maenas*. Helgoländer Wissenschaftliche Meeresuntersuchungen 10:91-103.

Butenandt, A. and P. Karlson. 1954. Über die Isolierung eines Metamorphose-Hormons der Insekten in Kristallisierter Form. Zeitschrift für Naturforschung 9B:389-391.

Cadman, L.R. and M.P. Weinstein. 1985. Size-weight relationships of postecdysial juvenile blue crabs (*Callinectes sapidus* Rathbun) from the lower Chesapeake Bay. Journal of Crustacean Biology 5:306-310.

Cameron, J.N. 1985a. Molting in the blue crab. Scientific American 252:102-109.

Cameron, J.N. 1985b. Post-moult calcification in the blue crab (*Callinectes sapidus*): relationships between apparent net H^+ excretion, calcium and bicarbonate. Journal of Experimental Biology 119:275-285.

Cameron, J.N. 1989. Post-moult calcification in the blue crab, *Callinectes sapidus:* timing and mechanism. Journal of Experimental Biology 143:285-304.

Cameron, J.N. and C.M. Wood. 1985. Apparent H+ excretion and carbon dioxide dynamics accompanying carapace mineralization in the blue crab (*Callinectes sapidus*) following moulting. Journal of Experimental Biology 114:187-196.

Carlisle, D.B. 1957. On the hormonal inhibition of moulting in decapod Crustacea. II. The terminal anecdysis in crabs. Journal of the Marine Biological Association of the United Kingdom 36:291-307.

Chang, E.S. 1993. Comparative endocrinology of molting and reproduction: insects and crustaceans. Annual Review of Entomology 38:161-180.

Chang, E.S., M.J. Bruce and S.L. Tamone. 1993. Regulation of crustacean molting: a multi-hormonal system. American Zoologist 33:324-329.

Chang, E.S., W.A. Hertz and G.D. Prestwich. 1992. Reproductive endocrinology of the shrimp *Sicyonia ingentis:* steroid, peptide, and terpenoid hormones. NOAA Technical Reports NMFS 106:1-6.

Chang, E.S. and J.D. O'Connor. 1977. Secretion of α-ecdysone by crab Y-organs in vitro. Proceedings of the National Academy of Sciences U.S.A. 74:615-618.

Chang, E.S. and J.D. O'Connor. 1978. In vitro secretion and hydroxylation of α-ecdysone as a function of the crustacean molt cycle. General and Comparative Endocrinology 36:151-160.

Chang, E.S., B.A. Sage and J.D. O'Connor. 1976. The qualitative and quantitative determinations of ecdysones in tissues of the crab, *Pachygrapsus crassipes*, following molt induction. General and Comparative Endocrinology 30:21-33.

Cheung, T.S. 1969. The environmental and hormonal control of growth and reproduction in the adult

female stone crab, *Menippe mercenaria* (Say). Biological Bulletin 136:327-346.

Cheung, T.S. 1973. Experiments on the simultaneous regeneration of claws in the aged male stone crab, *Menippe mercenaria* (Say), with special reference to the terminal molt. Bulletin of the Institute of Zoology Academia Sinica (Taipei) 12:1-11.

Chittleborough, R.G. 1975. Environmental factors affecting growth and survival of juvenile western rock lobsters *Panulirus longipes* (Milne-Edwards). Australian Journal of Marine and Freshwater Research 26:177-196.

Chung, J.S., H. Dircksen and S.G. Webster. 1999. A remarkable, precisely timed release of hyperglycemic hormone from endocrine cells in the gut is associated with ecdysis in the crab *Carcinus maenas*. Proceedings of the National Academy of Sciences U.S.A. 96:13103-13107.

Chung, J.S. and S.G. Webster. 2003. Moult cycle-related changes in biological activity of moult-inhibiting hormone (MIH) and crustacean hyperglycaemic hormone (CHH). European Journal of Biochemistry 270:3280-3288.

Chung, J.S., M.C. Wilkinson and S.G. Webster. 1996. Determination of the amino acid sequence of the moult-inhibiting hormone from the edible crab, *Cancer pagurus*. Neuropeptides 30:95-101.

Chung, K.S. and K. Strawn. 1984. Seasonal change in thermal tolerance of common estuarine crustaceans. Bulletin of the Japanese Society of Scientific Fisheries 50:451-456.

Churchill, E.P., Jr. 1919. Life history of the blue crab. Bulletin of the Bureau of Fisheries 36:91-128 + 9 plates.

Cobb, J.S. and J.F. Caddy. 1989. The population biology of decapods. Pages 327-374 in J.F. Caddy (ed.), Marine Invertebrate Fisheries: Their Assessment and Management. Wiley, New York.

Curry, G.L. and R.M. Feldman. 1987. Mathematical Foundations of Population Dynamics. Texas A&M University Press, College Station. 246 p.

deFur, P.L., D. Nusbaumer and R.J. Lewis. 1988. Physiological aspects of molting in blue crabs from the tidal fresh-water Potomac River, Virginia. Journal of Crustacean Biology 8:12-19.

De Kleijn, D.P.V. and F. Van Herp. 1995. Molecular biology of neurohormone precursors in the eyestalk of Crustacea. Comparative Biochemistry and Physiology 112B:573-579.

Dendinger, J.E. and A. Alterman. 1983. Mechanical properties in relation to chemical constituents of postmolt cuticle of the blue crab, *Callinectes sapidus*. Comparative Biochemistry and Physiology 75A:421-424.

Diaz, G.A., S.G. Smith, J.E. Serafy and J.S. Ault. 2001. Allometry of the growth of pink shrimp *Farfantepenaeus duorarum* in a subtropical bay. Transactions of the American Fisheries Society 130:328-335.

Drach, P. 1939. Mue et cycle d'intermue chez les crustacés décapodes. Annales de l'Institut Océanographique 19:103-391.

Drach, P. and C. Tchernigovtzeff. 1967. Sur la méthode de déterminacion des stades d'intermue et son application générale aux crustacés. Vie et Milieu 18A:595-610.

Draper, N. and H. Smith. 1981. Applied Regression Analysis, 2nd ed. Wiley, New York. 709 p.

Echalier, G. 1959. L'organe Y et le déterminisme de la croissance et de la mue chez *Carcinus maenas* (L.), Crustacé Décapode. Annales des Sciences Naturelles. Zoologie et Biologie Animale 12:1-59.

Eldridge, P.J. and W. Waltz. 1977. Observations on the commercial fishery for blue crabs *Callinectes sapidus* in estuaries in the southern half of South Carolina. South Carolina Marine Resources Center, Technical Report 21:1-35.

Emmel, V.E. 1910. A study of the differentiation of tissues in the regenerating crustacean limb. American Journal of Anatomy 10:109-156.

Faux, A., D.H.S. Horn and E.J. Middleton. 1969. Moulting hormones of a crab during ecdysis. Chemical Communications 1969:175-176.

Findley, A.M., B.W. Belisle and W.B. Stickle. 1978. Effects of salinity fluctuations on the respiration rate of the southern oyster drill *Thais haemastoma* and the blue crab *Callinectes sapidus*. Marine Biology 49:59-67.

Fischler, K.J. 1965. The use of catch-effort, catch-sampling, and tagging data to estimate a population of blue crabs. Transactions of the American Fisheries Society 94:287-310.

Fitz, H.C. and R.G. Wiegert. 1991. Tagging juvenile blue crabs, *Callinectes sapidus*, with microwire tags: retention, survival, and growth through multiple molts. Journal of Crustacean Biology 11:229-235.

Freeman, J.A., G. Kilgus, D. Laurendeau and H.M. Perry. 1987. Postmolt and intermolt molt cycle stages of *Callinectes sapidus*. Aquaculture 61:201-209.

Freeman, J.A., T.L. West and J.D. Costlow. 1983. Postlarval

growth in juvenile *Rhithropanopeus harrisii*. Biological Bulletin 165:409-415.

Gabe, M. 1953. Sur l'existence, chez quelques Crustacés Malacostracés, d'un organe comparable à la glande de la mue des Insectes. Comptes Rendus Hebdomadaires des Seances de l'Académie des Sciences 237:1111-1113.

Gersch, M., G.-A. Bohm and H. Eibisch. 1980. Die Wirkung des Hautungs-Hemmfaktors aus Sinusdrusen (molt inhibiting hormone-activity MIH) auf die Ecdysteroidproduktion aktivierter Y-Organe des Flusskebses *Orconectes limosus* (Crustacea, Decapoda). Zoologische Jahrbücher. Abteilung für Allgemeine Zoologie und Physiologie der Tiere 84:46-57.

Goudeau, M., F. Lachaise, G. Carpentier and B. Goxe. 1990. High titers of ecdysteroids are associated with the secretory process of embryonic envelopes in the European lobster. Tissue & Cell 22:269-281.

Gray, E.H. and C.L. Newcombe. 1938. Studies of moulting in *Callinectes sapidus* Rathbun. Growth 2:285-296.

Green, J.P. and M.R. Neff. 1972. A survey of the fine structure of the integument of the fiddler crab. Tissue & Cell 4:137-171.

Greenaway, P. 1983. Uptake of calcium at the postmoult stage by the marine crabs *Callinectes sapidus* and *Carcinus maenas*. Comparative Biochemistry and Physiology 75A:181-184.

Greenaway, P. 1985. Calcium balance and moulting in the Crustacea. Biological Reviews of the Cambridge Philosophical Society 60:425-454.

Haefner, P.A., Jr. 1964. Hemolymph calcium fluctuations as related to environmental salinity during ecdysis of the blue crab, *Callinectes sapidus* Rathbun. Physiological Zoology 37:247-258.

Haefner, P.A., Jr. and C.N. Shuster, Jr. 1964. Length increments during terminal molt of the female blue crab, *Callinectes sapidus*, in different salinity environments. Chesapeake Science 5:114-118.

Hamann, A. 1974. Die neuroendokrine Steuerung tagesrhythmischer Blutzuckerschwankungen durch die Sinusdrüse beim Flusskrebs. Journal of Comparative Physiology 89:197-214.

Hampshire, R. and D.H.S. Horn. 1966. Structure of crustecdysone, a crustacean moulting hormone. Chemical Communications 1966:37-38.

Hancock, D.A. 1977. Population ecology and growth. Australia Commonwealth Scientific and Industrial Research Organization Division of Fisheries and Oceanography Circular 7:279-286.

Hancock, D.A. and E. Edwards. 1967. Estimation of annual growth in the edible crab (*Cancer pagurus* L.). Journal du Conseil International pour l'Exploration de la Mer 31:246-264.

Hanström, B. 1939. Hormones in Invertebrates. Oxford University Press, London. 198 p.

Hartnoll, R.G. 1982. Growth. Pages 111-196 in L.G. Abele (ed.), The Biology of Crustacea, Volume 2. Academic Press, New York.

Havens, K.J. and J.R. McConaugha. 1990. Molting in the mature female blue crab, *Callinectes sapidus* Rathbun. Bulletin of Marine Science 46:37-47.

Helluy, S.M. and B.S. Beltz. 1991. Embryonic development of the American lobster (*Homarus americanus*): quantitative staging and characterization of an embryonic molt cycle. Biological Bulletin 180:355-371.

Hiatt, R.W. 1948. The biology of the lined shore crab, *Pachygrapsus crassipes* Randall. Pacific Science 2:135-213.

Hines, A.H., R.N. Lipcius and A.M. Haddon. 1987. Population dynamics and habitat partitioning by size, sex, and molt stage of blue crabs *Callinectes sapidus* in a subestuary of central Chesapeake Bay. Marine Ecology Progress Series 36:55-64.

Hines, A.H. and A.C. Young-Williams. (in review). Setal development and changing swim paddle coloration during premolt in the blue crab, *Callinectes sapidus*.

Hoenig, J.M. and V.R. Restrepo. 1989. Estimating the intermolt periods in asynchronously molting crustacean populations. Biometrics 45:71-82.

Holland, C. and D. Skinner. 1976. Interactions between molting and regeneration in the land crab. Biological Bulletin 150:222-240.

Homola, E. and E.S. Chang. 1997. Methyl farnesoate: crustacean juvenile hormone in search of functions. Comparative Biochemistry and Physiology 117B:347-356.

Hopkins, P.M. 1982. Effects of neurosecretory factors on in vivo levels of ecdysteroids in hemolymph of the fiddler crab, *Uca pugilator*. American Zoologist 22:938 (Abstract).

Hopkins, P.M. 1988. Control of regeneration in crustaceans. Pages 327-340 in H. Laufer and R.G.H. Downer (eds.), Endocrinology of Selected Invertebrate Types. Alan R. Liss, New York.

Horn, D.H.S., E.J. Middleton, J.A. Wunderlich and F. Hampshire. 1966. Identity of the moulting hor-

mones of insects and crustaceans. Chemical Communications 1966:339-340.

Huber, R. and W. Hoppe. 1965. Zur Chemie des Ecdysons. VII. Die Kristall- und Molekülstruktur Analyse des Insektenverpuppungshormons Ecdyson mit der automatisierten Faltmolekulmethode. Chemische Berichte 98:2403-2424.

Jaworski, E. 1972. The Blue Crab Fishery, Barataria Estuary, Louisiana. Louisiana State University Sea Grant, Baton Rouge. 112 p.

Jobling, M. 1994. Fish Bioenergetics. Chapman and Hall, New York. 328 p.

Johnson, P.T. 1980. Histology of the Blue Crab *Callinectes sapidus*. A Model for the Decapoda. Praeger, New York. 440 p.

Ju, S.-J., D.H. Secor and H.R. Harvey. 1999. Use of extractable lipofuscin for age determination of blue crab *Callinectes sapidus*. Marine Ecology Progress Series 185:171-179.

Judy, M.H. and D.L. Dudley. 1970. Movements of tagged blue crabs in North Carolina waters. Commercial Fisheries Review 32(11):29-35.

Kalbfleisch, J. and R. Prentice. 1980. The Statistical Analysis of Failure Time Data. Wiley, New York. 336 p.

Kao, H.-W. and E.S. Chang. 1996. Homeotic transformation of crab walking leg into claw by autotransplantation of claw tissue. Biological Bulletin 190:313-321.

Kao, H.-W. and E.S. Chang. 1997. Limb regeneration in the eye sockets of crabs. Biological Bulletin 193:393-400.

Karlson, P., H. Hoffmeister, H. Hummel, P. Hocks and G. Spiteller. 1965. Zur Chemie des Ecdysons. VI. Reaktionen des Ecdysonmolekuls. Chemische Berichte 98:2394-2402.

Kegel, G., B. Reichwein, S. Weese, G. Gaus, J. Peter-Katalinic and R. Keller. 1989. Amino acid sequence of the crustacean hyperglycemic hormone (CHH) from the shore crab, *Carcinus maenas*. FEBS Letters 255:10-14.

Keller, R. and J.D. O'Connor. 1982. Neuroendocrine regulation of ecdysteroid production in the crab *Pachygrapsus crassipes*. General and Comparative Endocrinology 46:384.

Keller, R. and E. Schmid. 1979. In vitro secretion of ecdysteroids by Y-organs and lack of secretion by mandibular organs of the crayfish following molt induction. Journal of Comparative Physiology 130:347-353.

Keller, R. and D. Sedlmeier. 1988. A metabolic hormone in crustaceans: the hyperglycemic neuropeptide. Pages 312-326 in H. Laufer and R.G.H. Downer (eds.), Endocrinology of Selected Invertebrate Types. Alan R. Liss, New York.

King, E.N. 1965. The oxygen consumption of intact crabs and excised gills as a function of decreased salinity. Comparative Biochemistry and Physiology 15:93-102.

King, L.E., Q. Ding, G.D. Prestwich and S.S. Tobe. 1995. The characterization of a haemolymph methyl farnesoate binding protein and the assessment of methyl farnesoate metabolism by the haemolymph and other tissues from *Procambarus clarkii*. Insect Biochemistry and Molecular Biology 25:495-501.

Kitchell, J.F., D.J. Stewart and D. Weininger. 1977. Applications of a bioenergetics model to yellow perch (*Perca flavescens*) and walleye (*Stizostedion vitreum vitreum*). Journal of the Fisheries Research Board of Canada 34:1922-1935.

Klein, J.M., S. Mangerich, D.P.V. de Kleijn, R. Keller and W.M. Weidemann. 1993. Molecular cloning of crustacean putative molt-inhibiting hormone (MIH) precursor. FEBS Letters 334:139-142.

Kleinholz, L.H. and R. Keller. 1979. Endocrine regulation in Crustacea. Pages 159-213 in E.J.W. Barrington (ed.), Hormones and Evolution, Volume 1. Academic Press, New York.

Kopec, S. 1922. Studies on the necessity of the brain for the inception of insect metamorphosis. Biological Bulletin 42:323-342.

Koshio, S., L.E. Haley and J.D. Castell. 1989. The effect of two temperatures and salinities on growth and survival of bilaterally eyestalk ablated and intact juvenile American lobsters, *Homarus americanus*, fed brine shrimp. Aquaculture 76:373-382.

Kurata, H. 1962. Studies on the age and growth of Crustacea. Bulletin of the Hokkaido Regional Fisheries Research Laboratory 24:1-115.

Lachaise, F., G. Carpentier, G. Somme, J. Colardeau and P. Beydon. 1989. Ecdysteroid synthesis by crab Y-organs. Journal of Experimental Zoology 252:283-292.

Lachaise, F. and J.A. Hoffmann. 1982. Ecdysteroids and embryonic development in the shore crab, *Carcinus maenas*. Hoppe-Seylor's Zeitschrift für Physiologische Chemie 363:1059-1067.

Laufer, H., D. Borst, F.C. Baker, C. Carrasco, M. Sinkus, C.C. Reuter, L.W. Tsai and D.A. Schooley. 1987.

Identification of a juvenile hormone-like compound in a crustacean. Science 235:202-205.

Law, A.M. and W.D. Kelton. 1991. Simulation Modeling and Analysis, 2nd ed. McGraw-Hill, New York. 672 p.

Lee, K.J., T.S. Elton, A.K. Bej, S.A. Watts and R.D. Watson. 1995. Molecular cloning of a cDNA encoding putative molt-inhibiting hormone from the blue crab, *Callinectes sapidus*. Biochemical and Biophysical Research Communications 209:1126-1131.

Lee, K.J. and R.D. Watson. 2002a. Antipeptide antibodies for detecting crab (*Callinectes sapidus*) molt-inhibiting hormone. Peptides 23:853-862.

Lee, K.J. and R.D. Watson. 2002b. Expression of crustacean (*Callinectes sapidus*) molt-inhibiting hormone in insect cells using recombinant baculovirus. Journal of Experimental Zoology 292:41-51.

Lee, K.J., R.D. Watson and R.D. Roer. 1998. Molt-inhibiting hormone mRNA levels and ecdysteroid titer during a molt cycle of the blue crab, *Callinectes sapidus*. Biochemical and Biophysical Research Communications 249:624-627.

Leffler, C.W. 1972. Some effects of temperature on the growth and metabolic rate of juvenile blue crabs, *Callinectes sapidus*, in the laboratory. Marine Biology 14:104-110.

Lewis, D.H. and R.D. Roer. 1988. Thermal preference in distribution of blue crabs, *Callinectes sapidus*, in a power plant cooling pond. Journal of Crustacean Biology 8:283-289.

Li, H. and D.W. Borst. 1991. Characterization of a methyl farnesoate binding protein in hemolymph from *Libinia emarginata*. General and Comparative Endocrinology 81: 335-342.

Liu, L., H. Laufer, Y.J. Wang and T. Hayes. 1997. A neurohormone regulating both methyl farnesoate synthesis and glucose metabolism in a crustacean. Biochemical and Biophysical Research Communications 237:694-701.

Luo, J. and S.B. Brandt. 1993. Bay anchovy *Anchoa mitchilli* production and consumption in mid-Chesapeake Bay based on a bioenergetics model and acoustic measures of fish abundance. Marine Ecology Progress Series 98:223-236.

MacDiarmid, A.B. 1989. Moulting and reproduction of the spiny lobster *Jasus edwardsii* (Decapoda: Palinuridae) in northern New Zealand. Marine Biology 103:303-310.

Mangum, C.P. 1985. Molting in the blue crab, *Callinectes sapidus*: a collaborative study of intermediary metabolism, respiration and cardiovascular function, and ion transport. Preface. Journal of Crustacean Biology 5:185-187.

Mangum, C. 1992. Physiological aspects of molting in the blue crab *Callinectes sapidus*. American Zoologist 32:459-469.

Mattson, M.P. and E. Spaziani. 1985. Characterization of molt-inhibiting hormone (MIH) action on crustacean Y-organ segments and dispersed cells in culture and a bioassay for MIH-activity. Journal of Experimental Zoology 236:93-101.

McCarthy, J.F. 1979. Ponasterone A: a new ecdysteroid from the embryos and serum of brachyuran crustaceans. Steroids 34:799-806.

McLaren, I.A. 1963. Effects of temperature on growth of zooplankton, and the adaptive value of vertical migration. Journal of the Fisheries Research Board of Canada 20:685-727.

Melville-Smith, R. 1989. A growth model for the deep-sea red crab (*Geryon maritae*) off South West Africa/Namibia (Decapoda, Brachyura). Crustaceana 56: 279-292.

Millar, R.B. and J.M. Hoenig. 1997. A generalized model for estimating periods of asynchronously molting insects and crustaceans from field or laboratory data. Journal of Agricultural, Biological, and Environmental Statistics 2:1-14.

Millikin, M.R., G.N. Biddle, T.C. Siewicki, A.R. Fortner and P.H. Fair. 1980. Effects of various levels of dietary protein on survival, molting frequency and growth of juvenile blue crabs (*Callinectes sapidus*). Aquaculture 19:149-161.

Millikin, M.R. and A.B. Williams. 1984. Synopsis of biological data on the blue crab, *Callinectes sapidus* Rathbun. NOAA Technical Report NMFS 1:1-39.

Mohamedeen, H. and R.G. Hartnoll. 1989. Larval and postlarval growth of individually reared specimens of the common shore crab *Carcinus maenas* (L.). Journal of Experimental Marine Biology and Ecology 134: 1-24.

Molyneaux, D.B. and T.C. Shirley. 1988. Molting and growth of eyestalk-ablated juvenile red king crabs, *Paralithodes camtschatica* (Crustacea: Lithodidae). Comparative Biochemistry and Physiology 91A: 245-251.

More, W.R. 1969. A contribution to the biology of the blue crab (*Callinectes sapidus* Rathbun) in Texas, with

a description of the fishery. Texas Parks and Wildlife Department, Technical Series 1:1-31.

Munro, J.L. 1983. The biology, ecology and bionomics of spiny lobsters (Palinuridae), spider crabs (Majidae) and other crustacean resources. ICLARM Studies and Reviews 7:206-222.

Neter, J., H.K. Kutner, C.J. Nachtsheim and W. Wasserman. 1996. Applied Linear Statistical Models, 4th ed. McGraw-Hill, New York. 1,408 p.

Neufeld, D.S. and J.N. Cameron. 1994. Mechanism of the net uptake of water in moulting blue crabs (*Callinectes sapidus*) acclimated to high and low salinities. Journal of Experimental Biology 188:11-23.

Newcombe, C.L., F. Campbell and A.M. Eckstine. 1949a. A study of the form and growth of the blue crab *Callinectes sapidus* Rathbun. Growth 13:71-96.

Newcombe, C.L., M.D. Sandoz and R. Rogers-Talbert. 1949b. Differential growth and moulting characteristics of the blue crab, *Callinectes sapidus* Rathbun. Journal of Experimental Zoology 110:113-152.

O'Halloran, M.J. and R.K. O'Dor. 1988. Molt cycle of male snow crabs, *Chionoecetes opilio*, from observations of external features, setal changes, and feeding behavior. Journal of Crustacean Biology 8:164-176.

Olmi, E.J., III. 1984. An adult female blue crab, *Callinectes sapidus* Rathbun (Decapoda, Portunidae), in proecdysis. Crustaceana 46:107-109.

Olmi, E.J., III and J.M. Bishop. 1983. Variations in total width-weight relationships of blue crabs, *Callinectes sapidus*, in relation to sex, maturity, molt stage, and carapace form. Journal of Crustacean Biology 3:575-581.

Orensanz, J.M. and V.F. Gallucci. 1988. Comparative study of postlarval life-history schedules in four sympatric species of *Cancer* (Decapoda: Brachyura: Cancridae). Journal of Crustacean Biology 8:187-220.

Palmer, B.A. 1974. Studies on the blue crab (*Callinectes sapidus*) in Georgia. Georgia Department of Natural Resources, Contribution Series 29:1-59.

Passano, L.M. 1953. Neurosecretory control of molting in crabs by the X-organ sinus gland complex. Physiologia Comparata et Oecologia 3:155-189.

Passano, L.M. 1960a. Molting and its control. Pages 473-536 in T. H. Waterman (ed.), The Physiology of Crustacea, Volume 1. Academic Press, New York.

Passano, L.M. 1960b. Low temperature blockage of molting in *Uca pugnax*. Biological Bulletin 118:129-136.

Perry, H.M. 1975. The blue crab fishery in Mississippi. Gulf Research Reports 5:39-57.

Pradeille-Rouquette, M. 1976. Influence de différents facteurs sur la croissance somatique de *Pachygrapsus marmoratus* (Fabricius) Crustacé Décapode. Cahiers de Biologie Marine 17:77-91.

Prestwich, G.D., M.J. Bruce, I. Ujvary and E.S. Chang. 1990. Binding proteins for methyl farnesoate in lobster tissues: detection by photoaffinity labeling. General and Comparative Endocrinology 80:232-237.

Pullen, E.J. and W.L. Trent. 1970. Carapace width-total weight relation of blue crabs from Galveston Bay, Texas. Transactions of the American Fisheries Society 99:795-798.

Radhakrishnan, E.V. and M. Vijayakumaran. 1984. Effect of eyestalk ablation in spiny lobster *Panulirus homarus* (Linnaeus): 1. On moulting and growth. Indian Journal of Fisheries 31:130-147.

Rahman, M.K. and T. Subramoniam. 1989. Molting and its control in the female sand lobster *Thenus orientalis* (Lund). Journal of Experimental Marine Biology and Ecology 128:105-115.

Rao, K.R., S.W. Fingerman and M. Fingerman. 1973. Effects of exogenous ecdysones on the molt cycles of fourth and fifth stage American lobsters, *Homarus americanus*. Comparative Biochemistry and Physiology 44A:1105-1120.

Réaumur R.-A.F. 1712. Sur les diverses reproductions qui se font dans les Écrevisses, les Omars, les Crabes, etc., et entre autres sur celles de leurs jambes et de leurs écailles. Mémoires de l'Academie Royale de Sciences, p. 226-245. Not seen; cited by Drach (1939).

Richards, F.J. 1959. A flexible growth function for empirical use. Journal of Experimental Botany 10:290-300.

Robertson, W.D. and A. Kruger. 1994. Size at maturity, mating and spawning in the portunid crab *Scylla serrata* (Forskal) in Natal, South Africa. Estuarine, Coastal and Shelf Science 39:185-200.

Roer, R.D. 1980. Mechanisms of resorption and deposition of calcium in the carapace of the crab *Carcinus maenas*. Journal of Experimental Biology 88:205-218.

Roer, R. and R. Dillaman. 1984. The structure and calcification of the crustacean cuticle. American Zoologist 24:893-909.

Rothschild, B.J., J.S. Ault, E.V. Patrick, C.I. Zhang, S.G. Smith, H. Li, T. Maurer, B. Daugherty, G. Davis, S. Endo and R. McGarvey. 1992. Assessment of the

Chesapeake Bay Blue Crab Stock. Final report to NOAA Chesapeake Bay Stock Assessment Committee. Reference number [UMCEES]CBL 092-082, University of Maryland Chesapeake Biological Laboratory, Solomons.

Ryan, E.P. 1967. The morphometry of sexually mature instars in the crab *Portunus sanguinolentus* (Herbst) (Brachyura: Portunidae). Marine Biological Association of India, Symposium Series 2:715-723.

Ryer, C.H., J. van Montfrans and R.J. Orth. 1990. Utilization of a seagrass meadow and tidal marsh creek by blue crabs *Callinectes sapidus*. II. Spatial and temporal patterns of molting. Bulletin of Marine Science 46:95-104.

Sasaki, G.C. 1984. Biochemical Changes Associated with Embryonic and Larval Development in the American Lobster *Homarus americanus* Milne-Edwards. Doctoral dissertation, Massachusetts Institute of Technology, Cambridge. 458 p.

Schoettker, P.J. and D.H. Gist. 1990. In vitro ecdysteroid production by Y-organs of the blue crab *Callinectes sapidus*. Journal of Crustacean Biology 10:487-491.

Shapiro, S.S. and M.B. Wilk. 1965. An analysis of variance test for normality (complete samples). Biometrika 52:591-611.

Shirley, M.A., A.H. Hines and T.G. Wolcott. 1990. Adaptive significance of habitat selection by molting adult blue crabs *Callinectes sapidus* (Rathbun) within a subestuary of central Chesapeake Bay. Journal of Experimental Marine Biology and Ecology 140:107-119.

Skinner, D.M. 1985. Molting and regeneration. Pages 43-146 in D.E. Bliss and L.H. Mantel (eds.), The Biology of Crustacea, Volume 9. Academic Press, New York.

Smale, M.J. 1978. Migration, growth and feeding in the Natal rock lobster *Panulirus homarus* (Linnaeus). Oceanographic Research Institute (Durban) Investigational Report 47:1-56.

Smith, S.G. 1997. Models of Crustacean Growth Dynamics. Doctoral dissertation, University of Maryland, College Park. 337 p.

Sochasky, J.B., D.E. Aiken and D.W. McLeese. 1973. Does eyestalk ablation accelerate molting in the lobster *Homarus americanus*? Journal of the Fisheries Research Board of Canada 30:1600-1603.

Somerton, D.A. 1980. Fitting straight lines to Hiatt growth diagrams: a re-evaluation. Journal du Conseil International pour l'Exploration de la Mer 39:15-19.

Soumoff, C. and J.D. O'Connor. 1982. Repression of Y-organ secretory activity by molt inhibiting hormone in the crab *Pachygrapsus crassipes*. General and Comparative Endocrinology 48:432-439.

Soumoff, C. and D.M. Skinner. 1983. Ecdysteroid titers during the molt cycle of the blue crab resemble those of other Crustacea. Biological Bulletin 165:321-329.

Soyez, D., J.P. Le Caer, P.Y. Noel and J. Rossier. 1991. Primary structure of two isoforms of the vitellogenesis inhibiting hormone from the lobster *Homarus americanus*. Neuropeptides 20:25-32.

Spaziani, E., R.D. Watson, M.P. Mattson and Z.-F. Chen. 1989. Ecdysteroid biosynthesis in the crustacean Y-organ and control by an eyestalk neuropeptide. Journal of Experimental Zoology 252:271-282.

Spindler, K.-D., R. Keller and J.D. O'Connor. 1980. The role of ecdysteroids in the crustacean molt cycle. Pages 247-280 in J.A. Hoffmann (ed.), Progress in Ecdysone Research. Elsevier/North-Holland, Amsterdam.

Steele, P. and T.M. Bert. 1994. Population ecology of the blue crab, *Callinectes sapidus* Rathbun, in a subtropical estuary: population structure, aspects of reproduction, and habitat partitioning. Florida Marine Research Publications 51:1-24.

Tagatz, M.E. 1965. The fishery for blue crabs in the St. Johns River, Florida, with special reference to fluctuation in yield between 1961 and 1962. U.S. Fish and Wildlife Service Special Scientific Report Fisheries 501:1-11.

Tagatz, M.E. 1968a. Biology of the blue crab, *Callinectes sapidus* Rathbun, in the St. Johns River, Florida. Fishery Bulletin 67:17-33.

Tagatz, M.E. 1968b. Growth of juvenile blue crabs, *Callinectes sapidus* Rathbun, in the St. Johns River, Florida. Fishery Bulletin 67:281-288.

Tagatz, M.E. 1969. Some relations of temperature acclimation and salinity to thermal tolerance of the blue crab, *Callinectes sapidus*. Transactions of the American Fisheries Society 98:713-716.

Tamm, G.R. and J.S. Cobb. 1976. Diel ecdysis rhythms in juvenile lobsters *Homarus americanus*. Journal of the Fisheries Research Board of Canada 33:819-821.

Tamone, S.L. and E.S. Chang. 1993. Methyl farnesoate

stimulates ecdysteroid secretion from crab Y-organs in vitro. General and Comparative Endocrinology 89:425-432.

Taylor, J.R.A. and W.M. Kier. 2003. Switching skeletons: hydrostatic support in molting crabs. Science 301:209-210.

Templeman, W. 1936. Local differences in the life history of the lobster (*Homarus americanus*) on the coast of the Maritime provinces of Canada. Journal of the Biological Board of Canada 2:41-88.

Towle, D.W. and C.P. Mangum. 1985. Ionic regulation and transport ATPase activities during the molt cycle in the blue crab *Callinectes sapidus*. Journal of Crustacean Biology 5:216-222.

Ujváry, I. and G.D. Prestwich. 1990. An efficient synthesis of the crustacean hormone [12-^{3}H]-methyl farnesoate and its photolabile analog [13-^{3}H]-farnesyl diazomethyl ketone. Journal of Labelled Compounds and Radiopharmaceuticals 28:167-174.

Umphrey, H.R., K.J. Lee, R.D. Watson and E. Spaziani. 1998. Molecular cloning of a cDNA encoding molt-inhibiting hormone of the crab, *Cancer magister*. Molecular and Cellular Endocrinology 136:145-149.

UNESCO. 1985. The International System of Units (SI) in Oceanography. Technical Paper in Marine Science 45. 124 p.

Van Engel, W.A. 1958. The blue crab and its fishery in Chesapeake Bay. Part 1 - reproduction, early development, growth, and migration. Commercial Fisheries Review 20(6):6-17.

Van Engel, W.A. 1990. Development of the reproductively functional form in the male blue crab, *Callinectes sapidus*. Bulletin of Marine Science 46:13-22.

van Montfrans, J., C.A. Peery and R.J. Orth. 1990. Daily, monthly and annual settlement patterns by *Callinectes sapidus* and *Neopanope sayi* megalopae on artificial collectors deployed in the York River, Virginia: 1985-1988. Bulletin of Marine Science 46:214-229.

Van Olst, J.C. and J.M. Carlberg. 1978. The effects of container size and transparency on growth and survival of lobsters cultured individually. Proceedings of the World Mariculture Society 9:469-479.

Vigh, D.A. and J.E. Dendinger. 1982. Temporal relationships of postmolt deposition of calcium, magnesium, chitin and protein in the cuticle of the Atlantic blue crab, *Callinectes sapidus* Rathbun. Comparative Biochemistry and Physiology 72A:365-369.

von Bertalanffy, L. 1938. A quantitative theory of organic growth (Inquiries on growth laws. II). Human Biology 10:181-213.

Wainwright, G., S.G. Webster, M.C. Wilkinson, J.S. Chung and H.H. Rees. 1996. Structure and significance of mandibular organ-inhibiting hormone in the crab, *Cancer pagurus*. Journal of Biological Chemistry 271:12749-12754.

Watson, R.D., K.J. Lee, K.J. Borders, H. Dircksen and K.Y. Lilly. 2001a. Molt-inhibiting hormone immunoreactive neurons in the eyestalk neuroendocrine system of the blue crab, *Callinectes sapidus*. Arthropod Structure and Development 30:69-76.

Watson, R.D., K.J. Lee, S. Qiu, M. Luo, H.R. Umphrey, R.D. Roer and E. Spaziani. 2001b. Molecular cloning, expression, and tissue distribution of crustacean molt-inhibiting hormone. American Zoologist 41:407-417.

Watson, R.D., E. Spaziani and W.E. Bollenbacher. 1989. Regulation of ecdysone biosynthesis in insects and crustaceans: a comparison. Pages 188-203 in J. Koolman (ed.), Ecdysone: From Chemistry to Mode of Action. Georg Thieme Verlag, Stuttgart.

Webster, S.G. 1991. Amino acid sequence of putative moult-inhibiting hormone from the crab *Carcinus maenas*. Proceedings of the Royal Society of London B 244:247-252.

Webster, S.G. 1998. Neuropeptides inhibiting growth and reproduction in crustaceans. Pages 33-52 in G.M. Coast and S.G. Webster (eds.), Recent Advances in Arthropod Endocrinology. Cambridge University Press, Cambridge.

Webster, S.G., H. Dircksen and J.S. Chung. 2000. Endocrine cells in the gut of the shore crab *Carcinus maenas* immunoreactive to crustacean hyperglycaemic hormone and its precursor-related peptide. Cell and Tissue Research 300:193-205.

Weidemann, W., J. Gromoll and R. Keller. 1989. Cloning and sequence analysis of cDNA for precursor of a crustacean hyperglycemic hormone. FEBS Letters 257:31-34.

Winget, R.R., C.E. Epifanio, T. Runnels and P. Austin. 1976. Effects of diet and temperature on growth and mortality of blue crab, *Callinectes sapidus*, maintained in a recirculating culture system. Proceedings of the National Shellfisheries Association 66:29-33.

Wolcott, T.G. and A.H. Hines. 1990. Ultrasonic telemetry of small-scale movements and microhabitat selection by molting blue crabs (*Callinectes sapidus*). Bulletin of Marine Science 46:83-94.

Yu X., E.S. Chang and D.L. Mykles. 2002. Characterization of limb autotomy factor-proecdysis (LAFpro), isolated from limb regenerates, that suspends molting in the land crab *Gecarcinus lateralis*. Biological Bulletin 202:204-212.

Yudin, A.I., R.A. Diener, W.H. Clark and E.S. Chang. 1980. Mandibular gland of the blue crab, *Callinectes sapidus*. Biological Bulletin 159:760-772.

Zeleny, C. 1905. Compensatory regulation. Journal of Experimental Zoology 2:1-102.